REFERENCE ONLY

UNIVERSITY OF LONDON THESIS

Degree	Year	Name of Author
PhD	2005	RAKIC, SONJA

y
inde
965

The role of p35/Cdk5 in the developing cerebral cortex

A thesis submitted to the University of London for the degree of Doctor of Philosophy

by

Sonja Rakić

Department of Anatomy and Developmental Biology
University College London
London WC1E 6BT
United Kingdom

August, 2005

ProQuest LLC
789 East Eisenhower Parkway
P.O. Box 1346
Ann Arbor, MI 48106-1346

ABSTRACT

This thesis has focussed on the role of cyclin-dependent kinase 5 (Cdk5) and its activator, p35, in controlling the proper formation of the cerebral cortex.

First, cortical layer formation in *p35* mutants was re-examined. Interestingly, the prenatal layer I (LI) seems wider, more cellular, and without a clear border with the cortical plate (CP) in these animals.

Second, interneuron arrangement in *p35* and *Cdk5* mutants was studied. Molecules, such as neuregulins (NRGs), which can bind to ErbB receptors and potentially signal through the p35/Cdk5 pathway, were also examined. Cortical interneurons express Cdk5, but Cdk5 is not active in developing forebrain in *p35* mutants. It appears that migration of cortical interneurons from the ganglionic eminence (GE) is a Cdk5-independent process. However, my results have suggested that: (i) radial inward migration of interneurons, from LI into the CP, might be a Cdk5-dependent mechanism; (ii) prenatal cortical interneurons and projection neurons do not communicate directly. Intriguingly, ErbB4 is highly expressed on the surface of migrating cortical interneurons. Two intracellular isoforms of the rat ErbB4 exist, with one having a unique tyrosine residue for binding PI3-kinase. I have shown that, although ErbB4 signalling is necessary for migration of cortical interneurons from the GE, this process could occur through a PI3K-independent mechanism. The hypothesis that the ErbB4 receptor signals via the Cdk5 pathway was also tested. I found that: (i) Roscovitine, a Cdk5 specific inhibitor, impairs the neuronal chemotactic response to NRG1β; (ii) Cdk5 phosphorylates ErbB4 threonine (1152) *in vitro*.

Third, splitting of the preplate layer (PPL) in *p35* mutants was studied. In these animals the PPL splits incompletely, which results in misplaced subplate neurons and *reeler*-like positioning of thalamocortical axons.

In summary, my experiments have provided novel information about some signalling molecules, and their receptors, that are involved in the migration of cortical neurons.

For my parents Radmila and Momčilo, sister Vera,

grandmother Milena Vukadinović

and Djordje Vukadinović in recognition of their

love, untiring support and belief in me

ACKNOWLEDGEMENTS

My sincere gratitude goes to my PhD supervisor, John Parnavelas, for accepting me into his lab, giving me support to freely explore neuroscience and providing encouragement when necessary.

I am most grateful to my friend Margareta (Meggie) Nikolić for giving me constant advice and support, academic or otherwise. She not only generously provided p35 mutants, but also introduced me to the world of biochemistry. My thanks also to members of Meggie's lab: Monisha Banerjee, Daniel Worth, Tom Jacobs, Arjune Sen and Frederic Causeret.

In addition, I would like to thank Zoltan Molnar for passing on his great expertise in the technique of axonal tracing.

I am grateful to present and former members of my lab, Mary Antypa, Melissa Barber, Anna Cariboni, Gaelle Friocourt, William Andrews, Anastasia Liapi, Bagirathy Nadarajah, Pavlos Alifragis and Colin Davis, all of whom taught me and cheered me up whenever I needed it.

Special thanks to Anna Cariboni and Roberto Maggi for sharing the GN11 cell line with me. I am deeply indebted also to Anastasia (Nadia) Liapi for the infinite patience, kindness and knowledge she provided at all times. Thanks also to Colin Davis, whom I supervised during his BSc; part of our mutual work is presented in chapter 5.

I am grateful to all the following from UCL who made my life as a PhD student much easier: Biological Services and Confocal Microscopy unit, Mark Turmaine, Ian Blaney, Steve Townsend, Helen Jefferson-Brown, Marg Glover, Mary Rahman, Lola Martinez, David Parkinson, Anna Droggiti and Ashwin Woodhoo.

Also, I spent wonderful years demonstrating human topographic anatomy with people from the UCL DR (dissection room). My special thanks to Paul O'Higgins, Ian Johnson, Sandra Martelli, Wendy, Derek and Darren.

Thanks to Rabinder Prinjha (NCS, Neurology & GI CEDD, H17 1124B, NFSP-North Third Avenue, Harlow, Essex) for kindly providing a mouse monoclonal antibody to Nogo-A (clone 6D5).

Additional thanks to Navin Parasram who assisted me with the statistics.

I would also like to thank Linda and John Hunt for their immense support and help.

Special thanks to Nada Zečević and Ana Milošević, who introduced me to neuroscience and to all great people from the Institute of Biological Research, Belgrade, where I took my first steps in research.

Thanks to Jelena Vasić, Maja Ivković, Maja Marinković, Maja Popadić, Ivana Petrović, Ljiljana Dimitrijević, Miljan Djordjević, Nebojša Ković, Vasići and Vasićoidi for their true friendship.

Above all I would like to thank David Hunt who has tirelessly assisted and encouraged me to complete my thesis. I am deeply grateful for his effort and dedication in teaching me the cloning technique from A to Z. Giving thanks is too little reward for all the help I have received from him.

During the course of my thesis I was supported by Departmental Studentship and Overseas Research Student Award.

TABLE OF CONTENTS

INDEX OF FIGURES

INDEX OF TABLES

CHAPTER 1

Introduction

In evolutionary terms, the cerebral cortex is the youngest part of the central nervous system (CNS) and in humans, it has become specialized to the extent that we have become 'wise men' (Homo sapiens). This 'cloak' of cells and fibres, intermingled and connected to the highest degree, determines our intelligence and personality, as well as how we sense, act, and control vital functions.

At present, the processes underlying the normal development of the cerebral cortex, such as neurogenesis, migration, and differentiation, are not well understood, which is mandatory before it will be possible to determine precisely how cortical formation can go wrong. Cell migration is an important developmental process, and it will be the subject of this thesis. The cytoskeleton, a network of protein filaments extending throughout the cytoplasm, is directly responsible for cell movements. Cyclin-dependent kinase 5 (Cdk5), among many molecules, controls cytoskeletal dynamics and organization, and plays an essential role in cerebral cortical formation.

CEREBRAL CORTEX (ADULT)

Cellular organization

Phylogenetically, the cerebral cortex is divided into neocortex and allocortex. The neocortex (also called isocortex) comprises more than 90% of the total cortical area. There are 2 principal cell types in the neocortex: projection neurons and local circuit neurons (otherwise known as interneurons). The cells of the neocortex are arranged in 6 layers (Fig.1-1C). Layers, from pia to white matter, are: I - molecular layer; II - external granular layer; III - external pyramidal layer; IV - internal granular layer; V - internal pyramidal layer; VI - multiform (polymorphic) layer. Less then 10 % of the total cortical area is allocortex, which consists of archicortex (hippocampal formation) and palleocortex (olfactory cortex). The allocortex is not a six-layered structure.

The neocortex is divided into areas, each having a unique cellular and laminar structure. This map of cortical areas was adapted after the cytoarchitectonic scheme proposed by Brodmann in the early part of the previous century (Brodmann, 1909). Brodmann's areas clearly show that anatomical differences relate to different functions. For example, in the motor cortex, layers II-V are dominated by large pyramidal cells to such a degree that individual layers cannot be delineated. Because of the apparent lack of stellate (granular) cells, the motor cortex is termed agranular. In contrast layers in primary sensory cortex are dominated by small stellate cells and pyramidal neurons. Thus, this type of cortex is known as granular cortex.

Brodmann's cytoarchitectonic areas form the basis for the functional areas defined by electrophysiology and fMRI. Indeed, the functional organization of the cortex, as determined by functional mapping studies, is such that each of the motor and sensory cortical areas is arranged hierarchically into primary, secondary and association areas. All functional areas are bilateral. However, symmetric areas do not have the same functional importance, as certain areas in one hemisphere dominate functionally over their counterparts in the other hemisphere. This phenomenon is called lateralization.

Projection neurons

Projection neurons, mostly pyramidal in shape, comprise 80-85% of all cortical neurons. They use the excitatory amino acid L-glutamate as a neurotransmitter. Projection neurons range in size from 10 micrometers in diameter to 70 micrometers for the giant pyramidal cells (*Betz cells*) of the motor cortex in humans. They are morphologically distinct, identified by their long apical dendrite that emanates from the apex of the pyramidal cell body and ascends vertically to the cortical surface, and by the basal dendrites that emerge from nearer the base of the cell soma and are directed horizontally. The apical dendrites of pyramidal cells are studded with spines that are the preferential sites for synaptic contacts (asymmetrical synapses). Projection neurons send long axons within the cortex, to the same or opposite hemisphere, or to various subcortical sites. Thus, pyramidal cells are the principal output neurons of the cortex.

Interneurons

GABA-containing interneurons are local circuit neurons that provide controlled inhibition to cortical projection cells. They constitute approximately 15-20% of the total population of cortical neurons (Meinecke and Peters, 1987;Hendry et al., 1987), and show diverse morphological, biochemical and physiological properties. A common feature for all cortical interneurons is that their short axons do not leave the cortex. Feldman and Peters (1978) have proposed a scheme of classification of cortical interneurons based on dendritic morphology, and described multipolar (or stellate), bitufted and bipolar types. A subpopulation of multipolar and bitufted neurons are known as chandelier cells. GABAergic interneurons also express different calcium-binding proteins (calbindin, calretinin, and parvalbumin), neuroendocrine peptides (somatostatin, neuropeptide Y, cholycystokinin, vasoactive intestinal peptide), and enzymes (nNOS and NADPH-diaphorase) (Parnavelas et al., 1989). Interneurons form symmetrical synapses with both pyramidal cells and other interneurons, with the exception of chandelier cells, which only form synapses with the axon initial segments of pyramidal cells (Parnavelas et al., 1989).

Cortical connections

The neurons residing in the upper layers (II-IV, **receptive** layers) receive inputs from subcortical regions, such as thalamus and other cortical neurons of the same or opposite hemisphere. In contrast, the majority of deep layer (V and VI, **efferent** layers) pyramidal neurons project to subcortical regions of the brain (e.g. thalamus, spinal cord) and thus, constitute the collective output system of the cortex.

Cortical afferents, arising predominantly in the thalamus (thalamocortical), terminate in layer IV and to some extent in layers I, III and VI; afferents from other cortical areas terminate predominantly in layers II and III. Cortical efferents (also called corticofugal projections) are divided into: a) corticothalamic, from layer VI, b) corticocortical, mainly from layers II and III, and c) corticosubcortical for striatum, superior colliculus, pons and spinal cord, from layer V. Corticocortical projections connect two hemispheres (commisural fibres: corpus callous, anterior and posterior commissures) or different areas within the same hemisphere (association fibres).

CEREBRAL CORTEX (DEVELOPMENT)

Models of cortical area patterning

It is a yet unsolved puzzle how the cerebral cortex is organized into highly specific functional maps. There are two extreme models that explain cortical map formation, the 'protomap' (Rakic, 1988) and 'protocortex' (O'Leary, 1989). In the 'protomap' model, the cerebral cortex is patterned as it is created, within its proliferative zones. A contrasting view, presented in the 'protocortex' model, favours the idea that initially the cortex is *tabula rasa* (Latin, "scraped tablet", though often translated "blank slate") and its regional identity is defined entirely by extrinsic signals along the thalamocortical fibres. Recent studies support mainly the 'protomap' model, since it has been found that basic cortical regionalization occurs before cortical connections are made, although there is evidence indicating that cortical input plays an important role in the fine tuning of cerebral cortical patterning.

Early cortical patterning

The prosencephalon, which includes the cerebral cortex, is derived from cells at the rostral margin of the neural plate (Rubenstein and Beachy, 1998). These cells are under the influence of signalling pathways that regulate dorsal-ventral (D-V), anterior-posterior (A-P) and medial-lateral (M-L) patterning. A few signalling molecules, released from discrete signalling centres, provide early positional information in the dorsal telencephalon. These signals organize the cerebral cortex in domains characterized by expression of particular transcription factors in the ventricular zone that will, in turn, control further cortical area subspecialization. For example, fibroblast growth factor 8 (FGF8) is secreted from the anterior signalling centre, which encompasses the anterior neural ridge and anteromedial telencephalon, and orchestrates the development of the A-P axis (Fukuchi-Shimogori and Grove, 2001).The transcription factors Emx2 and Pax6 are expressed along the A-P axis in the cortical ventricular zone at the early stage with gradual and opposing fashions: Emx2 is most abundant in caudomedial cortex, whereas Pax6 prevails in the rostrolateral cortex

(Bishop et al., 2000;Mallamaci et al., 2000b;Muzio and Mallamaci, 2003). COUP-TFI, similar to Emx2, exhibits high-caudal-to-low-rostral expression patterns across the neocortex throughout its development (Liu et al., 2000). The cortical hem, a second signalling centre, lies along the medial edge of the cortex and expresses multiple Wnt (2b, 3a, 5a, 7a; Grove et al., 1998) and BMP (bone morphogenic proteins; 2,4,6,7; Furuta et al., 1997) genes. WNT, and in particular Wnt3a (Lee et al., 2000b), and the canonical WNT signalling pathway (Galceran et al., 2000) are important in the formation of the hippocampus. BMP signals are also implicated in the development of the choroid plexus epithelium in the lateral ventricles (Hebert et al., 2002). Anti-hem, a potential third cortical signalling centre, located along the lateral margin of the developing cerebral cortex, produces various EGF family members such as TGFα, neuregulins 1,3, and secreted WNT antagonist sFrp2 (Kim et al., 2001). Sonic hedgehog (Shh) may be involved in patterning of the temporal cortical areas (Ragsdale and Grove, 2001).

Further specification into forebrain subdivisions involves other regulatory genes, and their expression pattern reveals discrete A-P (transverse) and D-V (longitudinal) boundaries suggestive of a segment-like organization of the prosencephalon. This has led to the 'prosomeric' model (Puelles and Rubenstein, 1993). A system of hierarchical gene expression is employed in the definition of discrete subdivisions of the prosencephalon and its derivatives. Accordingly, different genes are responsible for defining subpallium (e.g. Mash1, Dlx1/2, Ebf1, Nkx2.1, Lhx6), ventral pallium (e.g Dbx1), pallium (e.g. Pax6, Emx1/2, Ngn1/2, Tbr1), dorsal thalamus (e.g. Gbx2, Ngn2), cortical layers (e.g. Tbr1 - layer VI and subplate, during development; Otx1 - layers V and VI; Er81 - layer V; Rorβ - layer IV; Brb2 – layers II, IV, and V), and functional cortical areas (e.g. LAMP - limbic cortex; latexin - lateral cortex; H2z1 – somatosensory areas S1 and S2; Cad6 - somatosensory cortex; Cad8 - motor cortex). There are also 'proneural' genes, which encode transcription factors of basic helix-loop-helix class that act on neuroepithelial cells to define neuronal precursor fate. Neurogenin 1 and 2 induce cortical identity and define glutamatergic neurons. In contrast, Mash1 provides basal ganglia identity and specifies the formation of GABAergic neurons. Furthermore, projection neurons are fated to express e.g. Tbr1 and Emx1, while cortical interneurons are characterized by presence of e.g. Dlx genes and Lhx6 (reviewed by (Rubenstein et

al., 1999; Wilson and Rubenstein, 2000; Bertrand et al., 2002; O'Leary and Nakagawa, 2002; Grove and Fukuchi-Shimogori, 2003; Hevner et al., 2003a).

Cortical neurogenesis

Genesis of projection neurons takes place within two proliferative zones of the developing cortex. These neurons are produced predominantly in the ventricular zone, with some pyramidal neurons and postnatally generated glia arising in the subventricular zone (Tarabykin et al., 2001; Noctor et al., 2004). Neurogenesis of cortical interneurons occurs in the ventral telencephalic proliferative zones.

Neurogenesis gives rise to either neuronal precursors or postmitotic neurons, according to several modes of cell division during neurogenesis:

-symmetrical progenitor cell division: a pre-migratory process in which the pool of neuronal progenitors is expanded (i.e. one progenitor cell gives rise to two progenitor cells)

-asymmetrical progenitor division: a process in which the pool of progenitor cells is broadly maintained, whilst the pool of neurons is steadily expanded (i.e. one progenitor cell gives rise to one progenitor cell and one neuron)

-symmetrical terminal division: a process which depletes the pool of proliferating progenitor cells (i.e. one progenitor cell gives rise to two neurons)

Cortical cell death

The developing cortex requires a precise number of neurons in order to acquire its proper structure and connections. Interestingly, neurons are produced in excess and superfluous cells are eliminated by programmed cell death. Indeed, there are two types of programmed cell death during cortical development: target-independent and target-dependent. Target-independent programmed cell death occurs in the proliferative zones, and controls the neuronal progenitor pool (Blaschke et al., 1998). In contrast, target-dependent cell death takes place when neurons attempt to make connections, and compete with other neurons for limited quantities of target-derived growth factors, such as NGF (Levi-Montalcini and Hamburger, 1951; Cohen and Levi-Montalcini, 1957).

Terminology in the developing cerebral cortex

The developing mammalian neocortex is a multi-layered structure. Very often in the literature, the entire depth of the telencephalic wall is referred to as the developing cortex, and this thesis is not an exception. The basic terminology was established at the end of the 19th century by His (His, 1889). He distinguished proliferative germinal cells from migrating, postmitotic neuroblasts that move through a syncytial mass of spongioblasts. The final destination for migrating neuroblasts was termed the marginal layer. This inadequate terminology was corrected by the Boulder Committee (1970) which proposed more appropriate names for the developing cortical layers: ventricular zone; subventricular zone; intermediate zone; marginal zone; cortical plate. However, the terminology proposed by the Boulder Committee has since been revised. The ventricular zone is now often referred to as the neuroepithelial layer. The subplate zone, a transient cellular compartment first identified in the human foetal telencephalon (Kostovic and Rakic, 1980), has now received official recognition. Furthermore, the marginal zone was renamed by Marin-Padilla as the primordial plexiform layer in the period before the cortical plate emerges, and as layer I in the period following this event (Marin-Padilla, 1971). However, the primordial plexiform layer is now commonly termed the preplate layer (Rickmann et al., 1977; Stewart and Pearlman, 1987). The subpial granular layer (SGL) is a transient layer of cells immediately beneath the pia. It was first discovered in humans, where it is present from 11 to 29 gestational weeks (Brun, 1965; Rakic and Zecevic, 2003), but some groups have also described an SGL-like structure in rodents (Meyer et al., 2000).

Terminology used in this thesis

Preplate layer (PPL), layer I (LI), cortical plate layer (CP), subplate layer (SP), intermediate zone (IZ), subventricular zone (SVZ), ventricular zone (VZ) (Fig.1-1A,B).

PPL – The preplate layer is the earliest postmitotic cortical layer. Emerging CP cells split the PPL into layer I, which contains Reelin-secreting Cajal-Retzius (CR) cells, and the SP. PPL and its derivatives (LI and SP) are mostly transient structures, and play

important roles in proper cortical layering and precise formation of thalamocortical projections.

CP – The cortical plate gives rise to the future grey matter of the neocortex (layers II-VI). Layer formation occurs in a characteristic 'inside-out' pattern.

IZ – The intermediate zone gives rise to the adult white matter. During development, this zone contains axons, and is also a site of extensive neuronal migration (radial and tangential).

VZ, SVZ – The neuroepithelial cells of the cortical ventricular zone are the precursors of differentiated neurons. This pseudostratified layer boasts intense nuclear interkinetics, such that mitosis takes place at the surface of the ventricle, then the nucleus move up to replicate DNA; the process repeats. By comparison, the cortical SVZ gives rise to glia as well as neurons. However, both the cortical VZ and SVZ disappear (or undergo transformation to become the subependyma) in adulthood.

NEURON MIGRATION

Cell migration is a tightly regulated process that occurs in tissue during development, chemotaxis and wound healing. Cortical neurons migrate mostly in radial and tangential directions. Migrating neurons typically display bipolar morphology with a major leading process and a smaller trailing process. Defects in migration during human cortical development can lead to mental retardation, epilepsy (Gleeson and Walsh, 2000), schizophrenia (Church et al., 2002), autism and dyslexia (Peterson, 1995).

Neuron migration depends on the translation of extracellular cues into intracellular cytoskeletal responses. It is a complex process, and conceals several distinct phases. A neuron receives a motogenic and/or guidance factor first, and then extends the leading process. This is usually followed by the adhesion to the radial glia or extracellular matrix, translocation of the nucleus, retraction of the trailing process, and in the final phase detachment from the substrate of migration.

While motogenic factors stimulate random cell migration, guidance factors direct the neuron movement according to the gradient of certain chemicals in their environment (chemotaxis). Many guidance factors are also motogenic, and *vice versa*. The motogenic molecules are for instance (i) growth factors (epidermal growth factor – EGF; Threadgill et al., 1995; Caric et al., 2001; hepatocyte growth factor/scattered factor - HGF/SF; Powell et al., 2001; brain-derived neurotrophic factor - BDNF and neurotrophin-4, Behar et al., 1997) and (ii) neurotransmitters (GABA; Behar et al., 1996; glutamate; Komuro and Rakic, 1993; Behar et al., 1999). Migrating neurons sense directional cues (also called chemotropic) that are either membrane-bound or secreted. The guidance response to chemotropic factors can be either attractive or repulsive, and depends on the receptor type expressed on the migrating cells. Signalling molecules, most likely chemotropic, such as semaphorins (Raper, 2000), slits (Wong et al., 2002), netrins (Colamarino and Tessier-Lavigne, 1995), ephrins (Flanagan and Vanderhaeghen, 1998) have been implicated in controlling neuronal migration. There is a large overlap between guidance cues for neuron migration and guidance cues for axons, highlighting the similarity in the molecular basis of these guidance processes.

Extension (also called protrusion) of the leading process and the translocation of the nucleus (nucleokinesis) (Edmondson and Hatten, 1987) are two important steps underlying migration of neurons. Dynamic modifications of actin filaments and microtubules at the cell periphery are implicated in extension of the leading process as well as in retraction of the trailing process. A cell moves by first protruding the actin-based structures, namely lamellipodia and finger-like filopodia. The Rho family of small GTPases (RhoA, Rac1, Cdc42) controls the actin dynamics via a number of effector proteins, such as Cdk5 and Pak1 (Nikolic et al., 1998). There are several actin-binding proteins that take part in neuron migration (e.g. filamin1 and its interacting protein FILIP). Microtubules (MT), co-operate with actin and play a role in cell movements via MT-interacting proteins, such as microtubule-associated proteins (MAPs: MAP1B, doublecortin – Dcx, tau), motor proteins (dynein – mediates transport towards the MT minus end and kinesin – mediates transport towards the MT plus end), and others (e.g. kinases: FAK, or enzymes: non-catalytic subunit of platelet activating factor-acetylhydrolase, Pafah1b1 - also termed Lis1).

Nucleokinesis covers two events, first translocation of the centrosome towards the leading process, then movement of the nucleus in the direction of the centrosome.

Nucleokinesis has recently been described in both radially (see review Tsai and Gleeson, 2005) and tangentially (Bellion et al., 2005) migrating cortical neurons. Nucleokinesis critically depends on the microtubule network of the migrating neurons, in particular on perinuclear microtubules that link the microtubule organizing centre (MTOC) in the polarized centrosome with the nucleus. Perinuclear microtubules associate with microtubule motor dynein and other related molecules such as Lis1, Ndel1, Dcx and FAK kinase. Interestingly, Ndel1, FAK, and Dcx are all substrates of Cdk5 (Niethammer et al., 2000; Xie et al., 2003; Graham et al., 2004; Tanaka et al., 2004b; Xie and Tsai, 2004), indicating an important role for this kinase in nuclekinesis. Positioning of the centrosome in front of the nucleus and its translocation towards the leading process, which precedes nuclear translocation, is also an important part in nucleokinesis. It requires dynamic microtubules located in the leading neurite and a properly positioned centrosome. Molecules that promote polarization of the centrosome, such as mPar6α play important role in this process (Solecki et al., 2004). In neurons, disruption of nuclear translocation leads to defective neuronal migration (Solecki et al., 2004; Shu et al., 2004; Tanaka et al., 2004a).

Cell adhesion is an important component of neuron migration, and in general involves protein molecules at the surface of cells called cell adhesion molecules (CAMs). The extracellular domains of CAMs extend from the cell and bind to other cells (cell-to-cell adhesion) or extracellular matrix (ECM; cell-to-ECM adhesion) by binding to (i) other adhesion molecules of the same type (homophilic binding), (ii) binding to other adhesion molecules of a different type (heterophilic binding) or (iii) binding to an intermediary 'linker' which itself binds to other adhesion molecules. The intracellular domains of CAMs bind to the cytoskeletal proteins, in particular actin. Different families of CAMs have been implicated in cortical neuron migration, for instance cadherins (Kwon et al., 2000), intergrins (Schmid and Anton, 2003; Sanada et al., 2004; Schmid et al., 2005), and immunoglobulin superfamily (reviewed by Rougon and Hobert, 2003).

Origin and migration of cortical neurons

Generation of cortical projection neurons and interneurons occurs at different sites within the telencephalon. It is well established that projection neurons originate from the

dorsal telencephalon, while cortical interneurons come from the ventral telencephalon (Fig.1-2). Static (Golgi and electron microscopic) as well as more dynamic live-imaging studies show that cortical neurons display different modes of migration summarised in Table 1-1.

Origin and migration of cortical projection neurons

Cortical projection neurons originate from the local cortical proliferative zones, VZ and SVZ, by distinct patterns of division, asymmetrical and symmetrical, respectively (Noctor et al., 2004). They arise directly from radial glial cells (Malatesta et al., 2000; Miyata et al., 2001; Noctor et al., 2001; Tamamaki et al., 2001; Noctor et al., 2002).

Radial glia

Radial glial cells have a dual function during corticogenesis: they are neurogenic and act as a guidance substrate for migrating neurons. Radial glia cells have their soma in the VZ and a process that reaches the pial surface where it is attached to the basal membrane (Magini, 1888; Rakic, 1971; Rakic, 1972). For a long time it was thought that radial glia cells played merely a supporting role, as a scaffold, for radially migrating neurons (Rakic, 1971). It has been demonstrated that abnormalities in the development of radial glia lead to abnormal radial migration of neurons in cerebral cortex (Anton et al., 1997) and cerebellum (Rio et al., 1997). However, radial glial cells have been postulated to be neuronal progenitor cells (Malatesta et al., 2000; Miyata et al., 2001; Noctor et al., 2001; Tamamaki et al., 2001). Their eventual fate is of astrocyte lineage (Ramon y Cajal, 1911; Schmechel and Rakic, 1979).

Modes of migration

For the most part, cortical projection neurons reach their final destination by radial migration. In the neocortex, this process is comprised of two distinct modes: somal translocation and glia-guided locomotion. Cells that exhibit 'somal translocation' extend a leading process or a pia-attached process, which becomes progressively thicker and shorter as the soma advances towards the pial surface, with its terminal remaining attached to the pial surface (Morest, 1970; Nadarajah et al., 2001). These cells migrate in a smooth continuous fashion. In contrast, 'locomoting' neurons are freely migrating

cells along radial glia guides, which exhibit a relatively short leading process that maintains its length. These cells migrate by saltatory movements and at about half the speed of translocating cells (Rakic, 1978; Nadarajah et al., 2001). Interestingly, locomoting cells translocate in their final phase of migration. Recent real-time imaging studies have proposed that cortical projection neurons undergo distinct phases of locomotion (Noctor et al., 2004). In phase one, the postmitotic neuron migrates from the VZ to the SVZ; in phase two, it stops and displays multipolar morphology, and also detaches from the glial fibre (Tabata and Nakajima, 2003); in phase three, the decision phase, it goes back to the VZ or continues moving towards the pia; in phase four, final radial locomotion takes place.

Cortical layer formation

As mentioned earlier, the mature mammalian neocortex consists of six layers of neurons that have distinct morphology and functions. The formation of these layers requires the correct migration of postmitotic neurons from the cortical proliferative zones to their final destinations in both radial and tangential directions. Radial migration in the neocortex accounts for the major neuron positioning and is commonly disrupted in cortical layering defects. Radial neocortical layering in mouse occurs between E11.5 and E18.5. In early corticogenesis, dividing progenitor cells occupy the VZ, and this first wave of neurons then moves radially to the pial surface, forming a thin mantle layer of cortical primordium called the PPL. Somal translocation has been proposed to be the major mode of migration during the formation of this layer (Nadarajah et al., 2001; Nadarajah and Parnavelas, 2002; Nadarajah et al., 2003a). At E13.5, the second wave of neurons splits the PPL into a superficial layer I and a deeper SP, establishing the CP in between. Starting from E14.5, the CP expands in an "inside-out" manner, with waves of postmitotic neurons coming from the VZ/SVZ at different times and migrating past their predecessors to form the more superficial layers (Angevine and Sidman, 1961; Rakic, 1974; Caviness, Jr., 1982). Cortical plate neurons (layers II-VI) utilize glia-guided locomotion, and their laminar fate is determined early in the cell cycle (McConnell and Kaznowski, 1991).

Several signalling pathways have been identified to crucially regulate neocortical layering: Reelin/VLDLR/ApoER2/Dab1 (see below), Cdk5/p35/p39 (see below), Lis1 (Reiner et al., 1995), Dcx (Gleeson et al., 1998; Francis et al., 1999; Gleeson et al.,

1999; Bai et al., 2003), filamin-1 and FILIP (Fox et al., 1998; Nagano et al., 2002), transcription factors (Pax6; Schmahl et al., 1993; Emx2; Mallamaci et al., 2000a; Tbr1; Hevner et al., 2001; Brn1/2; McEvilly et al., 2002; Sugitani et al., 2002; p73; Meyer et al., 2004).

Origin and migration of cortical interneurons

Cortical GABAergic interneurons in rodents originate from the ventral forebrain (for reviews see (Parnavelas, 2000; Corbin et al., 2001; Marin and Rubenstein, 2003). The majority of cortical interneurons emanate from the medial ganglionic eminence (GE), and eventually colonize the entire cortex, including neocortex, hippocampus and piriform cortex (Pleasure et al., 2000). The caudal GE (Nery et al., 2002), and to a small degree, the lateral GE (de Carlos et al., 1996; Anderson et al., 1997; Tamamaki et al., 1997; Anderson et al., 2001), also contribute to the cortical interneuron population.

Tangential migration of cells within the developing cortex was first identified during clonal analysis studies (O'Rourke et al., 1992; Luskin et al., 1993; Tan and Breen, 1993; Tan et al., 1995; Mione et al., 1997; Tan et al., 1998); however, these investigations failed to reveal the identity of the tangentially migrating cells. In separate studies of the morphology and orientation of cells at the corticostriatal junction, it appeared that GABAergic neurons had migrated from the ventral forebrain towards cortex (Van Eden et al., 1989; DeDiego et al., 1994).

Direct evidence that these cells are derived from the MGE comes from (i) tracing of cells labelled with fluorescent dyes in organotypic brain slices (Wichterle et al., 1999; Lavdas et al., 1999; Anderson et al., 2001; Jimenez et al., 2002; Nadarajah et al., 2002; Polleux et al., 2002) (ii) focal injection, in vivo, of [3H] thymidine into the GE (Anderson et al., 2002), (iii) transplantation studies (Wichterle et al., 1999; Anderson et al., 2001; Wichterle et al., 2001; Polleux et al., 2002; Valcanis and Tan, 2003; Wichterle et al., 2003; Xu et al., 2004), and (iv) studies of mutant mice with defective MGE development (Anderson et al., 1997; Anderson et al., 1999; Casarosa et al., 1999; Sussel et al., 1999).

The journey of cortical interneurons is long and tortuous. Once born in the proliferative zones of the GE, they acquire a tangential (parallel to the pia) route of migration.

Tangential migration of interneurons

Tangentially migrating interneurons first populate the PPL of the cortical anlage, as early as E12.5 in mouse (del Rio et al., 1992). Shortly thereafter, a second migratory stream of interneurons appears within the SVZ/IZ (E13.5 in mouse (del Rio et al., 1992). The stream of migrating interneurons within the PPL is then split by the emerging wave of early-born CP neurons (E14.5 in mouse). A consequence of this splitting is the appearance of three parallel streams of migrating interneurons: in layer I, the SP, and the SVZ/lower IZ. It is still not clear to what extent each of the early streams, contributes to the cortical interneuron population. At the same stage, spare interneurons also appear in the CP, and their number, orientation, maturation, and position within the CP change during the prenatal and early postnatal period (E14.5-P12). From the third postnatal week, interneurons adopt their adult position and polymorphic appearance. The same is the case in the rat (Van Eden et al., 1989).

There are many factors, intrinsic and environmental, that affect tangential migration of cortical interneurons: (i) transcription factors: *Dlx genes* (Anderson et al., 1997); *Nkx2.1* (Sussel et al., 1999); *Mash1* (Casarosa et al., 1999); *Arx* (Kitamura et al., 2002); *Pax6* (Jimenez et al., 2002); *Emx1/2* (Shinozaki et al., 2002); *Lhx6* (Alifragis et al., 2004); *Vax1* (Taglialatela et al., 2004); (ii) motogenic factors: HGF-SF/MET (Powell et al., 2001; Levitt et al., 2004); BDNF,NT-4/TrkB/PI3K (Polleux et al., 2002); GDNF/GFRα1 (Pozas and Ibanez, 2005); (iii) chemotropic factors (diffusible gradients): attractive (SDF1/CXCR4; Nadarajah et al., 2003b; Stumm et al., 2003; neuregulin1/ErbB4; Flames et al., 2004) and repulsive (semaphorin 3A and 3F/neuropilin1 and 2; Marin et al., 2001; Tamamaki et al., 2003; while in studies of Zhu et al. (1999) and Wichterle et al. (2003) Slit1,2 were described as repulsive cues, study of Marin et al. (2003) showed no effect of Slit1,2 and netrin1/UNC5H,DCC on interneuron migration); (iv) adhesive (contact) factors: permissive (TAG1; Denaxa et al., 2001; Tanaka et al., 2003); (v) other: $GABA_BR1$ (prenatal; Lopez-Bendito et al., 2003); neurosteroids/$GABA_AR$ (perinatal; Grobin et al., 2003); COUP-TF nuclear receptors (Tripodi et al., 2004).

Radial migration of interneurons

Little is known about how tangentially migrating interneurons integrate into specific cortical layers. It is believed that interneurons, similar to projection neurons, migrate radially in the final stage of their journey to the cortex. However, it is still not known whether interneurons and projection neurons use the same mechanisms of radial migration.

'Inside-out' mode of migration

It is widely thought that cortical interneurons are born in an 'inside-out' manner, and that their final location within the cortical layers depends on their date of birth. Furthermore, it is believed that contemporaneously born interneurons and pyramidal cells will reside within the same cortical layer (Miller, 1985; Fairen et al., 1986; Peduzzi, 1988; Anderson et al., 2002; Ang, Jr. et al., 2003; Valcanis and Tan, 2003; Hevner et al., 2004). However, this view is not shared by all (Yozu et al., 2004).

Interneuron-specific radial modes of migration

Recent time-lapse studies described several intracortical modes of interneuron migration: *multidirectional* within the MZ (Ang, Jr. et al., 2003; Tanaka et al., 2003), *outward* towards the CP/MZ from the IZ/SVZ (Polleux et al., 2002; Tanaka et al., 2003), *inward* towards the CP from the MZ (Polleux et al., 2002; Ang, Jr. et al., 2003; Tanaka et al., 2003) and towards the VZ (Nadarajah et al., 2002). It is still not known whether intracortical interneuron migration is neurophilic (e.g. communication with the projection neurons of the same age or Cajal-Retzius cells) and/or gliophilic (e.g. communication with radial glia).

(i) Multidirectional migration within the MZ

Using flat-mount cortical preparations and real-time microscopy, two groups independently observed that a substantial proportion of prenatal GABAergic neurons migrate in all directions within the MZ (Ang, Jr. et al., 2003; Tanaka et al., 2003). This could explain the spread of GABAergic neurons over the entire cortex (Tanaka et al., 2003). Interestingly, CR cells also displayed multidirectional orientation similar to the direction of leading processes of interneurons located below them, emphasising the

possibility that CR cells could provide positional cues for the migrating interneurons (Ang, Jr. et al., 2003).

(ii) Outward migration from the IZ/SVZ

Polleux et al. (2002) described the invasion of the CP by GE-derived neurons both from the IZ (outward) and the MZ (inward) using *in vitro* transplantation experiments. Tanaka et al. (2003) went further in investigating migration of cortical interneurons to the CP by using *GAD67-GFP* knock-in mice. These authors studied the initial migration of these cells from the IZ/SVZ towards the MZ at E13.5. They described that this outward migration was more prominent at E15.5, and was accompanied with inward migration of cells from the MZ to the CP. Hevner and colleagues confirmed the existence of outward interneuron migration, and specified that this mode of movement was characteristic of late (after E15.5) born interneurons (Hevner et al., 2004).

(iii) Inward migration from the MZ (or layer I)

Apart from Polleux et al. (2002) and Tanaka et al. (2003), other authors also described the inward mode of interneuron migration. Ang and colleagues (Ang, Jr. et al., 2003) anticipated that GABAergic interneurons, migrating within the cortical MZ, descend ('dive') into the underlying cortex to assume positions with isochronically-generated, radially-derived neurons. Similarly, a Reelin-independent postnatal inward radial migration of middle- and late-born interneurons from the MZ to the CP has been proposed (Hevner et al., 2004).

(iv)Ventricle-directed migration

There is evidence that cortical interneurons may migrate inwardly towards the VZ, in what has been termed 'ventricle-directed migration, perhaps to receive signals that may ultimately assist them in correctly integrating into cortex (Nadarajah et al., 2002; Nadarajah and Parnavelas, 2002).

(v) Branched migration

Nadarajah and colleagues also described multipolar cortical interneurons that are highly motile in the formation and retraction of their processes, and referred to them as 'branching cells' (Nadarajah et al., 2003a).

Communication with pyramidal neurons and radial glia

The mechanisms on how interneurons could communicate with pyramidal neurons and/or radial glia are elusive. There are a few possible ways e.g. (i) via gap-junctions, or (ii) through the formation of transmembrane-ligand/receptor bonds. Hevner et al. (2004) suggested that the laminar position of interneurons within the cortex may be determined by interactions with projection neurons born on the same day. It has been shown that the layering deficit in *p35* mutants is linked to improper neuronal-glial interactions in radial migration (Gupta et al., 2003).

CORTICAL CONNECTIONS WITH THE THALAMUS

For the nervous system to develop functionally, it must undergo a highly complex process of forming a precise network of spatial connections. For this to occur, projecting axons must find or form the correct pathways to the 'areal' targets (inter-areal pathfinding). Within these areas, the invading axons undergo a finer process of pathfinding and synapse formation (intra-areal pathfinding), e.g. in the development of topographic maps in which the spatial arrangement of the projecting axons is reflected in the order of their intra-areal synaptic connections. This framework provides the background for studying the mechanisms that coordinate the assembly of the highly ordered connections of the mammalian neocortex during development, including connection with the thalamus.

Connections between cortex and thalamus in the adult

The thalamus is a large, dual lobed structure that is mainly made of nuclear groups that relate to specific functions in the cerebrum. Importantly, the thalamus (i) plays a role in motor control; (ii) receives somatosensory, auditory, and visual signals, and relays sensory signals to the cerebral cortex; and (iii) is involved in consciousness. The main sensory input to the neocortex comes from the dorsal thalamic nuclei, which in turn receive a reciprocal set of connections. The thalamic axons project mainly to cortical neurons in layer IV and, to a lesser degree, to neurons in layers I, III and VI. Neurons in layer VI project back to the thalamus.

Connections between cortex and thalamus during development

The first thalamic fibres to reach the cortex leave their place of origin early in development, before the thalamus even receives any sensory information from the periphery. Thalamocortical axons (TCAs) arise from the dorsal thalamus and turn towards the ventral thalamus, before traversing the diencephalic-telencephalic boundary. TCAs enter the ventral telencephalon by E13.5 in mouse, running through the internal capsule and medial GE, and finally cross the cortico-striatal boundary at E14.5 in mouse (see review Lopez-Bendito and Molnar, 2003). During their journey through the subcortical areas, TCAs encounter cells in the thalamic reticular nucleus (Mitrofanis and Guillery, 1993) and primitive internal capsule (Metin and Godement, 1996), as well as early corticofugal fibres (see reviews Molnar and Blakemore, 1995 and Lopez-Bendito and Molnar, 2003). TCAs arrive at the appropriate cortical regions by E15.5, and accumulate for some time within the SP, forming side branches and synaptic connections (from E16.5 to E19.5). The final target for TCAs is mainly cortical layer IV.

Although thalamocortical fibres take a complicated route on their way to the cortex, there is a spatial order of thalamic nuclei and their projections towards the corresponding areas in the cortex. This spatial topography has two levels, inter-areal and intra-areal topography. The former occurs first, and is activity-independent e.g. in rodents, thalamic nuclei are roughly arranged following a caudolateral to rostromedial gradient within the dorsal thalamus, whereas their corresponding targets are found in caudorostral progression in the cortex. In contrast, intra-areal topography develops postnatally, after thalamic axons associate with the SP neurons, and is activity-dependent (Marin, 2003; Lopez-Bendito and Molnar, 2003).

Thalamocortical axon pathfinding

In order to find a proper and ordered way to specific cortical regions, TCAs could receive instructions from different sources:

(i) Guidance cues, their receptors, and signalling pathways

Thalamic axons navigate to their subcortical (thalamic reticular nucleus, primitive internal capsule cells) and cortical (SP, layer IV) targets under the guidance of both

attractive and repulsive guidance cues, and these molecules can either be diffusible or associated with cell surfaces or the extracellular matrix. The nature of the response depends on the receptor and the cell signalling pathway. For example, the hypothalamus releases a repulsive signal for TCAs, possibly slit (Braisted et al., 1999), while the MGE secretes netrin1 that can act as an attractive signal for both CFAs and TCAs (Metin et al., 1997; Braisted et al., 2000); the cortex contains cell-bound and secreted molecules that can guide TCAs, eg. LAMP, COUP-TFI, cadherins, ephrins/ephrinR, neutrophins/p75, semaphorins (reviewed by Lopez-Bendito and Molnar, 2003).

(ii) Transcription factors

Transcription factors might have dual role in the pathfinding of cortical connections; they can regulate directly the expression of guidance molecules and their receptors or they can play a role in defining territories through which axons travel. Abnormalities of TCA development have been described in several mutants lacking transcription factors that are expressed along their route to the cortex. For example, in Gbx2 (expressed in the dorsal thalamus; Miyashita-Lin et al., 1999; Hevner et al., 2002), Mash1 (expressed in the ventral telencephalon; Tuttle et al., 1999), and Pax6 (expressed in the pallium and thalamus; Stoykova et al., 1996; Hevner et al., 2002) mutants, TCAs fail to innervate the cortex; in Tbr1 (expressed in the pallium and diencephalon-telencephalon boundary; Hevner et al., 2001; Hevner et al., 2002), Emx2 (expressed in the pallium and most ventral part of the ventral telencephalon; Lopez-Bendito et al., 2002a), Pax6 and Gbx2 mutants (Hevner et al., 2002) CTAs are misrouted.

(iii) Corticofugal axons and guidepost cells in the thalamic reticular nucleus and internal capsule

It has been suggested that a direct contact between TCAs and early corticofugal fibres in the ventral telencephalon could contribute to the generation of an orderly map of the thalamus in cortex, as these fibres meet, associate and possibly exchange positional information about final target areas ('handshake hypothesis'; Molnar and Blakemore, 1995). In favour of this model of mutual influence: (i) it has been shown that both fibre systems develop aberrantly and do not arrive at their final targets in Gbx2, Pax6, Tbr1 mutants (Hevner et al., 2002); (ii) in COUP-TFI mutant (Zhou et al., 1999), SP cells and

their projections are missing (after E16.5) and, consequently, just a few TCAs pass through the IC and arrive in the cortex. However, arguments against this attractive model are: (i) TCAs and CTAs do not fasciculate and take different routes, as revealed in studies of their distribution using carbocyanine dyes (Bicknese et al., 1994); (ii) CFAs collapse when they contact thalamic axons (from Price and Willshaw, 2000), and (iii) there is evidence that TCAs can arrive in the SP even before CTAs enter the thalamus (de Carlos and O'Leary, 1992).

This model has recently been supplanted by another model in which it has been proposed that thalamic fibres, destined for cortex, could be 'primed' about their final position in the cortex even before they meet their cortical counterparts. It has been suggested that such events may take place in the subcortical intermediate targets, e.g. in the thalamic reticular nucleus and ventral part of the GE where putative guidepost cells may issue precise pathfinding directions. This idea is supported by studies with knock-out mice for transcription factors normally expressed in the ventral telencephalon, such as Dlx1/2, Ebf1 (Garel et al., 2002; Garel and Rubenstein, 2004), and Mash1 (Tuttle et al., 1999). Furthermore, it has been found that ephrin-A/EphA signalling mediates the establishment of proper thalamocortical topology in the ventral telencephalon (Dufour et al., 2003), and this particular pathway is under the control of the Neurogenin 2 gene, expressed in a discrete region of the thalamus (Seibt et al., 2003). In carnivores and primates, the corticothalamic fibres are directed by a transient neuronal population in the internal capsule (Letinic and Kostovic, 1996; Adams et al., 1997).

It appears, therefore, that the proper development of TC projections depends on the correct expression of axon guidance genes and transcription factors along their entire route to the cortex, and there is a possibility that their subcortical intermediate targets possess a spatial map of the cortex that is a milestone for the developing fibres. Interestingly, the subcortical guidepost cells are misplaced in Pax6 and Emx2 mutants, indicating that the position of these cells is in fact directly influenced by signals from the developing cortex.

Role of the subplate layer

Once the TCAs cross the cortico-striatal boundary, they encounter the SP. The SP derives from the PPL (Marin-Padilla, 1971), and during prenatal development contains a

heterogeneous population of neurons. The majority of neurons are pyramidal in shape with an apical dendrite reaching layer I, and express calretinin (del Rio et al., 2000), Golli (Landry et al., 1998; Hevner et al., 2001), and Tbr1 (Hevner et al., 2001). These neurons are spiny (Valverde et al., 1989) and form synaptic connections with thalamic axons as early as E15 in mice (del Rio et al., 2000). Approximately 17% of SP neurons are GABAergic, and horizontally oriented, with the majority expressing calbindin, calretinin and NPY (del Rio et al., 2000). This indicates that they are migrating cortical interneurons. The SP is more prominent in primates (Kostovic and Rakic, 1990) than in rodents. Subplate neurons are a transient population of cells that disappears after birth (Price et al., 1997), although there is evidence to suggest that sublayer VIb in adult rodents represents the remnants of the SP (Valverde et al., 1989). Subplate neurons control multiple steps of cortical development. They first emit descending projections towards the thalamus (Molnar and Blakemore, 1995; del Rio et al., 2000), although the first corticofugal fibres, most likely transitory, might originate from either early PPL neurons (Meyer et al., 1998) or even layer V neurons (Clasca et al., 1995). The corticothalamic fibres grow concomitantly with the thalamic axons in mice (Molnar et al., 1998b), rats (de Carlos and O'Leary, 1992; Molnar et al., 1998a) and hamsters (Metin and Godement, 1996), but advances first in kittens (McConnell et al., 1989; Allendoerfer and Shatz, 1994). A few studies favour the role of corticothalamic fibres in guiding thalamocorical fibres (Molnar and Blakemore, 1995; Lopez-Bendito and Molnar, 2003; see above). There is no other direct evidence on how SP neurons would lead TCAs to the proper cortical areas. Nevertheless, thalamocortical fibres do contact the SP neurons and participate in the assembly of the first microcircuits within the developing cortex (Allendoerfer and Shatz, 1994). Subplate neurons receive synaptic input from TCAs before these invade the cortex following a waiting period - the duration of which is species dependent - during which the cortical layers are being generated. The waiting period is longer in primates and carnivores. In rodents, thalamic axons usually invade the CP slowly after waiting for a day (Molnar and Blakemore, 1995; del Rio et al., 2000), or even soon after arriving in the SP (Catalano et al., 1991; de Carlos and O'Leary, 1992). However, a massive penetration of TCAs into more mature CP occurs postnatally. Subplate neurons also establish early projections into the CP where they arborize extensively in layer IV. It is likely that thalamic axon ingrowth towards the final target, layer IV neurons, appears to be regulated by the maturational

state of the cortex. At the time of arrival of TCAs into the SP, the immature CP is non-permissive for axonal ingrowth (Gotz et al., 1992; Molnar and Blakemore, 1995; Tuttle et al., 1995; Henke-Fahle et al., 1996). Eventually, the CP becomes more permissive for thalamic axons through the differential expression of several molecules, including extracellular matrix proteins, LAMP (limbic system-associated membrane protein; Mann et al., 1998; ephrins; Gao et al., 1998; cadherins 6 and 8; Rubenstein et al., 1999).

What is the role of thalamocortical fibres and the SP in cortical development?

According to the 'protomap' model of cortical development, thalamocortical fibres are not involved in the initial, rough arealization of the cortex. This has been clearly shown in studies on mutant mice deficient in genes that define dorsal thalamus (e.g. Gbx2; Wassarman et al., 1997) or ventral telencephalon (Mash1; Guillemot et al., 1993). In both mutants, while thalamacortical axons fail to reach the cortex, formation of the functional cortical areas is not affected (Miyashita-Lin et al., 1999; Nakagawa et al., 1999).

However, TCAs are held in activity-dependent interactions with the SP cells, and this might lead to their realignment to exact functional areas before they enter the cortex. Therefore, the SP neurons play a role in the growth of TCAs into the cortex and then, via an activity-dependent mechanism, affect the precise segregation of thalamocortical afferents, which in turn could influence fine morphological differentiation of cortical neurons. The roles of the SP have been shown in studies where SP neurons were chemically ablated (Ghosh et al., 1990; Ghosh and Shatz, 1992; Ghosh and Shatz, 1994; Xie et al., 2002), not developed (in Tbr1 mutant; Hevner et al., 2001), or prematurely eliminated (in COUP-TFI mutant; Zhou et al., 1999).

REELIN

Reelin is an extracellular matrix protein important for proper formation of the brain. Reelin deficiency results in the *reeler* phenotype. *Reeler* is a natural animal mutant, first described in 1950's (Falconer, 1951), with malformations in the cerebral cortex, hippocampus and cerebellum. The major neurological symptoms in *reeler* mouse are

ataxia and an intentional tremor. In humans, mutation of the *reelin* gene is the cause of the Norman-Roberts type of lissencephaly ("smooth brain") characterized by severe delay in neurological and cognitive development, hypotonia and epilepsy (Hong et al., 2000). There is a possible role for the *reelin* gene in conditions such as schizophrenia and autism (Fatemi, 2005).

The *reelin* gene is approximately 450 kb long and maps to mouse chromosome 5 and human 7q22. The *reelin* mRNA is about 12kb and consists of 65 exons. The *reelin* gene encodes a large protein (3461 aa long and 387 kDa predicted molecular mass) that is produced and secreted by CR cells in the MZ (preplate layer/layer I) and cerebellar granular cells (D'Arcangelo et al., 1995; Ogawa et al., 1995; Tissir and Goffinet, 2003). Reelin protein then acts through the extracellular milieu on the migrating CP neurons and Purkinje cells by binding to the very low density lipoprotein receptor (VLDLR), the apolipoprotein E receptor 2 (ApoER2), $\alpha 3\beta 1$ integrin (Dulabon et al., 2000) and protocadherins (Senzaki et al., 1999). The signal is then transduced by tyrosine phosphorylation of the intracellular adaptor Dab1 (Howell et al., 1999; Keshvara et al., 2001). The major kinase responsible for Dab1 phosphorylation in the Reelin pathway is Fyn, although Src and Yes kinases also play a minor role (Arnaud et al., 2003). In mice, mutations of Dab1 (*scrambler* and *yotary*; the latter being spontaneous; Howell et al., 1997; Sheldon et al., 1997; Ware et al., 1997) and double mutations of two lipoprotein receptors (VLDLR and ApoER2; Hiesberger et al., 1999; Trommsdorff et al., 1999), generate similar phenotypes to the reeler mutation, and will be referred to as *reeler*-like mutations.

Reeler and reeler-like phenotype

In the cerebral cortex of the *reeler* mouse, cortical layering occurs in an 'outside-in' pattern since the later born neurons fail to migrate past those born earlier (Caviness, Jr., 1982). In addition, early born neurons fail to split the PPL; this layer is consequently called superplate layer (Caviness, Jr., 1982). Thalamocortical axons stream towards the SP cells within the superplate layer, crossing over the CP cells stuck below (Molnar et al., 1998b).

CYCLIN-DEPENDENT KINASE 5

Cyclin-dependent kinase 5 (Cdk5) is a proline-directed serine/threonine cyclin-dependent kinase that is not involved in regulation of the cell cycle. Instead, it plays an important role in postmitotic neurons, and is implicated in the formation and maintenance of the nervous system. Deregulation of Cdk5 might contribute to the pathology of neurodegenerative diseases, such as Alzheimer's disease, Parkinson's disease and amyotrophic lateral sclerosis. Cdk5 has two known activators, p35 and p39.

Cdk5 is a distinctive member of the Cdk family

Cdk5 was identified on the basis of its close primary sequence homology and identical substrate specificity to Cdc2 (also named Cdk1). Cdc2 is a prototype member of the Cdc2-like kinase family. This family of kinases, and their regulatory subunits known as cyclins, regulate important transitions in the eukaryotic cell cycle. For example, Cdc2-cyclin-B is essential for the progression from G2 to M phase, while Cdk2-cyclin-A plays role in the progression from G1 to S phase. In the process of regulating the cell cycle, both Cdc2 and Cdk2 phosphorylate protein substrates predominantly at sites displaying the consensus phosphorylation site motif (S/P)PX(K/H/R) (Moreno and Nurse, 1990).

A large number of Cdc2-like protein kinases have been isolated from mammalian cells in recent years. While most of the Cdc2-like protein kinases are cell cycle regulators, Cdk5 has major functions unrelated to the cell cycle. Cdk5 was identified from (i) different human cell lines, based on cdc2 sequence-homology screening (named PSSALRE kinase; Meyerson et al., 1991; Meyerson et al., 1992); (ii) bovine brain, based on ability to phosphorylate short peptide containing the consensus motif recognized by Cdc2; Lew et al., 1992a; Lew et al., 1992b); (iii) adult rat brain cDNA library, using a mouse Cdc2 as a probe (named nclk – neuronal cdc2-like kinase; Hellmich et al., 1992); (iv) bovine brain (named TPKII – tau protein kinase II; Ishiguro et al., 1992); and (v) normal human fibroblast cell line WI38 (named Cdk5; Xiong et al., 1992). This novel kinase has been referred to as a cyclin-dependent kinase based on its ability to associate with cyclins D1 (Xiong et al., 1992) and E (Miyajima et al., 1995). Homologues of Cdk5 from human (Meyerson et al., 1992), bovine (Lew et al., 1992a),

rat (Hellmich et al., 1992), and mouse (Tsai et al., 1993) share 99% identity with each other at the protein level, suggesting that this protein is highly conserved within vertebrate species. Despite having 58% and 62% sequence identity with Cdc2 and Cdk2, respectively, it is believed that Cdk5 does not play a role in cell-cycle regulation.

Pattern of Cdk5 expression and its kinase activity

Cdk5 is present in all tissues, throughout the life, although its highest expression and associated kinase activity are detected in the nervous system (Meyerson et al., 1992; Tsai et al., 1993; Ino et al., 1994; Zheng et al., 1998). Cdk5 activity correlates with the expression of Cdk5-specific activators, p35 and p39, which is highest in postmitotic neurons (Zheng et al., 1998). Cdk5 is present in the cytoplasm/plasma membrane, particularly in axons (Tsai et al., 1993), as well as within the nucleus (Ino and Chiba, 1996). It has been reported that astrocytes can express Cdk5 (Tanaka et al., 2001).

Regulation of Cdk5 activity

Binding to the regulatory subunits, p35 and p39, and post-translational phosphorylation/dephosphorylation of the Cdk5 are key regulatory steps in its activation. In addition, association of Cdk5 with inhibitors plays a role in the regulation of Cdk5 activity. Regulation of Cdk5 activity makes this protein kinase distinct from other Cdks.

p35 and p39 regulatory subunits

p35, and its homologue p39, are regulatory subunits of Cdk5 (Ishiguro et al., 1994; Lew et al., 1994; Tsai et al., 1994; Tang et al., 1995). p39 shares 57% amino acid sequence identity with p35. p35 and p39 are mostly expressed in neurons, and are often referred to as neuron-specific activators of Cdk5. p35, along with Cdk5, is also expressed in myocytes, where they participate in muscle differentiation and patterning (Lazaro et al., 1997; Philpott et al., 1997; Fu et al., 2001). p35 and p39 display minimal sequence homology to known cyclins. However, p35 may adopt a tertiary structure similar to that of cyclin A, and this may to some extent explain how p35, a non-cyclin, activates a cyclin-dependent kinase (Tang et al., 1997). Nevertheless, p35 and p39 represent a new

type of regulatory subunit for cyclin-dependent kinase activity specialized in postmitotic tissues.

p35 and p39 are widely expressed in the nervous system, especially in postmitotic neurons (Zheng et al., 1998).The spatial and temporal expression of p35 and p39 in the CNS seems to be complementary. The expression of p35 is rather broad and at its highest during prenatal and early postnatal period (Tomizawa et al., 1996; Delalle et al., 1997; Zheng et al., 1998). In contrast, p39 expression is more restricted being most prominent in the hippocampus and cerebellum; p39 is hardly expressed in prenatal CNS (Tang et al., 1995; Cai et al., 1997; Zheng et al., 1998).

p35 and p39 are enriched in plasma membrane (Humbert et al., 2000; Niethammer et al., 2000; Fu et al., 2001) owing to an N-terminal myristoylation signal motif (Patrick et al., 1999). p35 is particularly expressed at the cell periphery, including the lamellipodia and filopodia structures (Nikolic et al., 1996; Nikolic et al., 1998). Cdk5 is present in both the cytoplasm and cell membrane, and its subcellular distribution is dictated by p35 and p39. Therefore, the physiological substrates of Cdk5 are likely to be transmembrane or membrane-associated. Recent studies have also revealed the expression of Cdk5 and p35 in the nucleus (Ino and Chiba, 1996; Gong et al., 2003; Fu et al., 2004).

p35 is an unstable, short-lived protein, with a half-life of 20-30 minutes (Patrick et al., 1998). It is either phoshorylated by Cdk5 and then multi-ubiquitylated and degraded through the ubiquitin-proteasome pathway (Patrick et al., 1998; Saito et al., 1998), or cleaved to p25 by calpain, a calcium-dependent cystein protease (Patrick et al., 1999; Kusakawa et al., 2000; Lee et al., 2000). These two ways of p35 elimination are age-dependent. While fast phoshorylation of p35 and its proteosomal degradation is more of a feature of the embryonic brain and has a neuroprotective role, cleavage of p35 to p25 by calpain is found mainly in the adult brain and could lead to Cdk5 neurotoxicity (Hisanaga and Saito, 2003; Saito et al., 2003). The Cdk5 kinase activity is deregulated by the cleavage of p35 to p25. p25/Cdk5 complex is soluble, long-lasting, and shows higher phosphorylation activity to tau protein. This complex formation could lead to neuronal cell death seen in neurodegenerative diseases, such as Alzheimer's disease and amyotrophic lateral sclerosis (Patrick et al., 1999). Patzke and Tsai (2002) have shown that conversion of p39 to p29 is also mediated by calpain, and that p29 could contribute to deregulation of Cdk5 induced by neurotoxic insult.

Post-translational phosphorylation/dephosphorylation of Cdk5

The cyclin/Cdk activity is regulated by other proteins as well. For a Cdk (e.g. Cdk2) to be activated, it must be phosphorylated at a particular threonine residue, T160, by CAK (Cdk-activated kinase) and at the same time to be dephosphorylated on residues T14 and Y15. T14 and Y15 are initially phosphorylated by the dual-specificity kinases Wee1 and Myt1, and this inhibits activity of conventional Cdks (Gu et al., 1992). Interestingly, whereas the conventional Cdks require T160 phosphorylation by CAK for maximal activation, this site is dispensable for Cdk5 full activation, though Cdk5 contains the equivalent S159 residue (Qi et al., 1995; Poon et al., 1997). The structural analysis of p25/Cdk5 predicts that upon phosphorylation on S159, the activation of Cdk5 would probably be inhibited (Tarricone et al., 2001). Furthermore, although T14 and Y15 are conserved in Cdk5, Cdk5 is neither phosphorylated nor inhibited by the Wee1 kinase *in vitro* (Poon et al., 1997). Cables, a novel adaptor protein, associates Cdk5 to the non-receptor tyrosine kinase, c-Abl, which phosphorylates Y15 of Cdk5, and consequently enhances its activity (Zukerberg et al., 2000).

Cdk5 inhibitors

Cdk inhibitors (CKIs) are small proteins that act to inhibit Cdk activity by binding to them and blocking their catalytic activity. CKIs of Cip/Kip family efficiently inhibit conventional Cdks, but cannot inhibit Cdk5 (Lee et al., 1996); $p27^{Kip1}$, and related broad CKIs ($p21^{Cip1}$, $p27^{Kip2}$), do not bind to p35 and, therefore, the p35/Cdk5 complex remains active in postmitotic neurons. There is an increasing number of Cdk5-specific endogenous inhibitors (C42; Ching et al., 2002; DbpA; Moorthamer et al., 1999; and ribosomal protein L34; Moorthamer and Chaudhuri, 1999). The synthetic inhibitors, such as roscovitine, oleumicin, purvalanol, paullones, butyrolactone (Sausville, 2002) are not specific in blocking Cdk5 activity; they are also known to antagonise Cdc2 and Cdk1. However, more needs to be learned about the effects of these inhibitors, both endogenous and synthetic, since they have implications for our understanding of important cellular biological processes and may potentially lead to the development of therapeutic applications in the fullness of time.

Cdk5 phosphorylation activity: substrates

Cdk5 is a proline-directed kinase that phosphorylates serine and threonine immediately upstream of a proline residue. Cdk5 consensus phosphorylation site motif is (S/T)PX(K/H/R), where S or T are the phosphorylatable serine and threonine, P is the proline residue in the +1 position, and basic residues, such as lysine, histidine, and arginine, in the +3 position. Cdc2 and Cdk2 have identical substrate specificity to Cdk5 (Moreno and Nurse, 1990). Cdk5 associates with and phosphorylates numerous proteins involved in neuron migration. Deregulation of Cdk5 activity often leads to neuron cell death.

Role of Cdk5

The most prominent roles of Cdk5 are related to cortical layer formation during the development and neurodegeneration in adulthood.

In CNS development

Cdk5 regulates cytoarchitecture in the CNS as revealed in studies of *p35* and *Cdk5* knock-out (KO) mice. These studies reveal critical functions of Cdk5 in neuronal migration and axon patterning.

The *Cdk5* KO mouse dies perinatally (Ohshima et al., 1996), and shows disruption in neuronal layering of many brain structures, such as cerebral cortex, hippocampus, olfactory bulb, and cerebellum, although other regions are also affected (Ohshima et al., 1996; Gilmore et al., 1998; Ohshima et al., 1999). The lethality of the *Cdk5* KO can be completely rescued by expressing the Cdk5 transgene under the p35 promoter, indicating a role of neuronal Cdk5 in survival (Tanaka et al., 2001). The cerebral cortex of the *p35* KO mouse displays a similar inverted layering of cortical neurons to that reported in the *Cdk5* KO mouse. However, these animals display mild disruptions in the hippocampus and cerebellum, possibly due to the compensation of p39 (Chae et al., 1997; Kwon and Tsai, 1998). Unlike the *Cdk5* KO mouse, the *p35* KO is viable and fertile, but has increased susceptibility to seizures (Chae et al., 1997) due to structural abnormalities in hippocampus (Wenzel et al., 2001). Whereas the *p39* KO mouse displays a normal phenotype, the *p35/p39* double KO mouse exhibits

indistinguishable characters reminiscent of the *Cdk5* KO mouse, suggesting that p35 and p39 are necessary and sufficient for Cdk5 activation (Ko et al., 2001).

It has been reported that the PPL in *p35* or *Cdk5* mutant mice splits properly, but subsequent waves of migrating neurons fail to pass this layer and accumulate below the SP, resulting in inverted cortical layering (Gilmore et al., 1998; Kwon and Tsai, 1998; reviewed by Gupta and Tsai, 2003). Preplate splitting in *p35/Cdk5* mutants will be examined in this thesis (chapter 5). While Cdk5 plays an important role in radial migration of projection neurons, its role in cortical interneuron migration is still unsolved. A few groups have suggested Cdk5-independent migration of these cells (Gilmore and Herrup, 2001; Patzke et al., 2003; Hammond et al., 2004). This will be discussed in greater detail in chapter 4a.

Both *p35* and *Cdk5* KO mice have a defect in fasciculation of several axonal tracts, including the thalamocortical fibres. It has been described that the TCAs stream towards the ectopic SP and then run parallel to the pia without touching it (Gilmore et al., 1998; Kwon et al., 1999). This is in contrast to reeler mice, where axons run over the CP and dip into the pial surface (Molnar et al., 1998b). Abnormal axon patterning could be a secondary consequence of aberrant neuronal positioning. This will also be examined in this thesis (chapter 5).

How can the phenotypic consequences of the loss of p35 and Cdk5 be explained in molecular terms?

(i) Control of cytoskeletal dynamics and organization

Cdk5 associates with all three major components of neuroskeleton: actin, microtubules, and neurofilaments, and, thus, is directly responsible for neuron morphology, movement, and secretion. Several *in vitro* studies have shown that p35/Cdk5 is essential for neurite outgrowth during neuronal differentiation in the cerebral cortex (Nikolic et al., 1996b) and cerebellum (Pigino et al., 1997; Paglini et al., 1998). p35/Cdk5 associates with Rac GTPase and its effector Pak1 kinase in actin-rich neuronal growth cones, and inhibits Pak1 activity (Nikolic et al., 1998). Moreover, p35/Cdk5-mediated phosphorylation of Pak1 on threonine 212 residue plays a direct role in neurite morphogenesis (Rashid et al., 2001).

Cdk5 is also associated with the microtubule cytoskeleton (Ishiguro et al., 1992; Sobue et al., 2000). It has been suggested that it might influence microtubule dynamics by phosphorylating microtubule-associated proteins, including MAP1B (Kawauchi et al., 2005), Dcx (Tanaka et al., 2004), and tau (Paudel et al., 1993) which in turn might affect microtubule stability, or by phosphorylating Ndel1 (formerly known as NUDEL) and FAK to regulate the dynein motor complex. Cdk5 is involved in microtubule-dependent neurokinesis during neuronal migration. First, in *p35* KO both nucleokinesis-mediated somal translocation (E13.5) and glia-guided locomotion (E16.5) are disrupted. Neurons in *p35* KO migrate mainly through a glia-independent mechanism, and display a 'branched mode of migration' characterized by dynamic branching of leading processes and branch-to-branch movements. Authors concluded that this abnormal migration is responsible for defects in inside-out layering of the cortex, but not for splitting of the PPL which they described as normal (Gupta et al., 2003). Second, Cdk5 phosphorylates focal adhesion kinase (FAK) at serine 732, and this phoshorylation is important for proper integrity of perinuclear microtubules, and pull of the nucleus towards the advanced centrosome (Xie et al., 2003; Xie and Tsai, 2004). Third, doublecortin, a protein mutated in X-linked lissencephaly, is a Cdk5 substrate (Tanaka et al., 2004b). Phosphorylation of Dcx at serine 297 decreases the ability of Dcx to bind and stabilize microtubules, and therefore induce migration. Fourth, another target for a role of Cdk5 in the organization of microtubules constitutes the protein NudE-like (Ndel1), expressed in migrating cortical neurons (Niethammer et al., 2000; Sasaki et al., 2000). Ndel1, substrate of Cdk5 (Niethammer et al., 2000), interacts with Lis1 to maintain the function of dynein (Shu et al., 2004), which in turn influences neuronal migration.

Neurofilaments, members of the intermediate-filament family, reside in axons, and during axonal transport become heavily phosphorylated. Abnormality in neurofilament phosphorylation has been correlated with amyotrophic lateral sclerosis (Manetto et al., 1988). Cdk5 phosphorylates heavy and medium molecular weight neurofilaments (Lew et al., 1992b).

(ii) Role in adhesion

Cell-cell adhesion in the cortex comes in two different forms. Migrating neurons can either use other neurons to attach to or interact with radial glia fibres. p35/Cdk5 might regulate neuron-neuron adhesion by binding to β-catenin. Overexpression of p35/Cdk5 reduces the interaction between β-catenin and N-cadherin, which results in a decrease of N-cadherin levels at the surface (Kwon et al., 2000). Lack of p35 or Cdk5 could lead to increased adhesion between the early and late born neurons, and prevent their proper positioning in inside-out fashion.

In synaptic transmission

A number of proteins are involved in Cdk5-dependent synaptic transmission. Since this process is not a primary focus of this thesis, commentary on this is limited to a list of relevant molecules, grouped by function in synaptic transmission, that are known substrates of Cdk5:

(i) neurotransmitter release: Munc-18, synapsin 1 (Cheng and Ip, 2003)

(ii) synaptic vesicle endocytosis: amphiphysin 1 (Floyd et al., 2001), dynamin 1 (Tan et al., 2003; Tomizawa et al., 2003).

(iii) receptor signalling: NMDA (NR2A; Wang et al., 2003); dopamine (DARPP-32; Bibb et al., 1999; Bibb et al., 2001 and cocaine; reviewed by Gupta and Tsai, 2001); GFRα1, GDNF receptor (Ledda et al., 2002); cadherine-mediated (Kwon et al., 2000; Kesavapany et al., 2001); AChR receptor (Fu et al., 2001); ErbBs, neuregulin receptors (Fu et al., 2001; Li et al., 2003).

(iv) learning and memory: (Ohshima et al., 2005).

In transcriptional control

The p35/Cdk5 complex associates with signal transducer and activator of transcription 3 (STAT3) and phosphorylates STAT3 on the serine 727 residue. Furthermore, neuregulin enhances the serine phosphorylation of STAT3 and transcription of STAT3-specific target genes, such as c-fos and junB, in a Cdk5-dependent manner (Fu et al., 2004). This reveals a role of Cdk5 in control of transcription.

In cell death

Cdk5 is associated with apoptotic cell death during development and tissue remodelling (Zhang et al., 1997). For instance, Cdk5 activation induces cell death in hippocampus by phosphorylating NMDA receptors (Wang et al., 2003). Inhibition of Cdk5 prevents neuronal cell death and mitochondrial dysfunction (Weishaupt et al., 2003).

In neurodegeneration

Cdk5 deregulation is implicated in various neurodegenerative diseases such as Alzheimer's (Paudel et al., 1993; Patrick et al., 1999), Parkinson's (Smith et al., 2003), and Niemann-Pick type C diseases (Bu et al., 2002), amyotrophic lateral sclerosis (ALS; Manetto et al., 1988; Nguyen et al., 2001) and ischemia (Green et al., 1997).

Alzheimer's disease is a neurological disease that belongs to the group of dementia. It is characterized by two pathological hallmarks, senile plaques and neurofibrilar tangles. The latter consists of mainly filaments of hyperphosphorylated tau. Patrick et al. (1999) showed that p25, a truncated form of p35, accumulates in neurons in the brains of patients with Alzheimer's disease. This accumulation is correlated with an increase in Cdk5 kinase activity. The p25/Cdk5 complex hyperphosphorylated tau, which reduced tau's ability to associate with microtubules.

Parkinson's disease is a motor disorder characterized by loss of dopamine. In mice, Smith et al. (2003) showed that administration of MPTP, a toxin that damages the nigrostriatal dopaminergic pathway, resulted in an increase of Cdk5 expression and activity. Inhibition of Cdk5 attenuated the loss of dopaminergic neurons caused by MPTP. Therefore, it has been suggested that Cdk5 may be a regulator of dopaminergic neuron degeneration in Parkinson's disease.

ALS is a neurological disorder that selectively affects motor neurons of brain and spinal cord. Nguyen et al. (2001) found that Cdk5 activity and the p23/p35 ratio were abnormally elevated in the spinal cord of superoxiddismutase1 (SOD1) transgenic mice, a mouse model of ALS.

Relation with Reelin

Reelin and Cdk5 are either distinct or overlapping pathways involved in neuron migration. Mice that are deficient for both *p35* and *Dab1* (or *p35* and *reelin*) have

neocortical-layering phenotype that differs from that of mice that are deficient for either gene alone (Ohshima et al., 2001). Therefore, it is most likely that p35/Cdk5 and Reelin/Dab1 act together in a parallel manner to coordinate neuronal migration (Beffert et al., 2004).

Tyrosine phosphorylation of Dab1, on tyrosine (Y198 and Y220) residues, by Src-family kinases, is crucial for active Reelin-signalling (Arnaud et al., 2003; Bock and Herz, 2003). Interestingly, Dab1 is a p35/Cdk5 substrate (serine 491), independent of the Reelin-signalling cascade (Keshvara et al., 2002). Thus, although Dab1 provides a point of convergence for the Reelin and p35/Cdk5 pathways to maybe operate through common signalling components for their respective effects, this convergence point can be regulated differently. Non-receptor tyrosine kinase abl, associates directly with Dab1, and indirectly with p35/Cdk5 complex via Cables (Zukerberg et al., 2000), can also promote overlapping or distinct signalling functions of the Reelin and Cdk5 pathways.

Cdk5, p35 and p39 gene/protein ID

The *Cdk5* gene is about 5 kb long and maps to mouse chromosome 5 (Ohshima et al., 1995) and human 7q36 (Demetrick et al., 1994). The mouse and human *Cdk5* mRNAs each comprise 12 exons, and have an open reading frame of 879 bases. There are no known splice variants of *Cdk5*. Indeed, the *Cdk5* gene encodes a protein of 292 aa in both mouse and human, which is detectable as a 31 kDa molecule by SDS-PAGE.

The *p35* gene (a.k.a. CDK5R1) spans ~4kb of genomic DNA, and maps to mouse chromosome 11 and human chromosome 17. In both mouse and human, the *p35* mRNA comprises a single exon which contains an open reading frame of 924 bases. This encodes a protein of 307 aa which is detectable as a 35 Da molecule by SDS-PAGE.

The *p39* gene (a.k.a. CDK5R2) spans ~2.5 kb of genomic DNA and maps to mouse chromosome 1 and human chromosome 2. The mRNA comprises a single exon, with an open reading frame of 1110 bases in mouse and 1104 bases in human. These give rise to proteins of 369 and 367 aa, respectively, and are detectable as molecules of 39 kDa by SDS-PAGE.

AIMS OF THE THESIS

This thesis is mainly focused on the role of Cdk5 in neuronal migration and formation of axonal projections in the developing cerebral cortex. There are three main aims:

(i) Revision of the role of Cdk5 in forming the cerebral cortical cytoarhitecture

(ii) Investigation of the role of p35/Cdk5 pathway in interneuron migration; role of neuregulin/ErbB4 pathway in interneuron migration; and search for the link between these two pathways

(iii) Study of the role of Cdk5 in proper PPL splitting and, consequently or independent, TCA positioning

Figure 1-1. Neocortical layers

(A) Developing cortical layers (PPL stage).

(B) Developing cortical layers (CP stage): migrated cells (layers I, IV, V, VI) and migrating cells (layers II and III).

(C) Mature cortical layers (I-VI).

PPL – preplate layer; IZ – intermediate zone; VZ – ventricular zone; SVZ – subventricular zone; SP – subplate layer; GM – grey matter; WM – white matter.

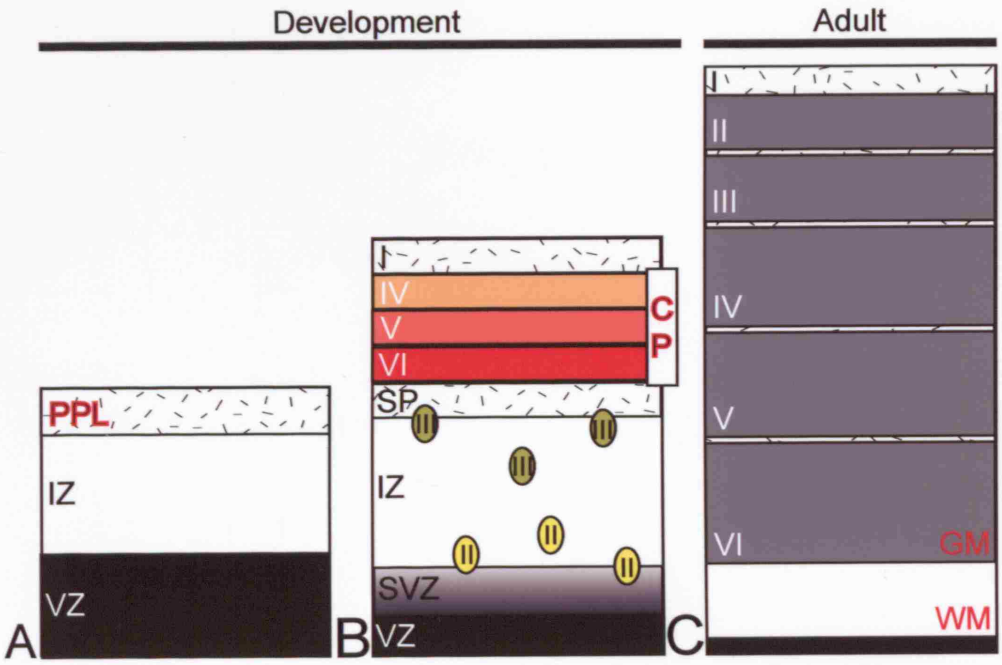
Development
Adult
PPL
IZ
VZ
A
IV
V
VI
CP
SP
IZ
SVZ
VZ
B
I
II
III
IV
V
VI
GM
WM
C

Figure 1-2. Cortical projection neurons and interneurons

Cortical projection neurons originate from the dorsal telencephalon, whilst cortical interneurons come from the ventral telencephalon (GE).

Cx – cortex; GE – ganglionic eminence.

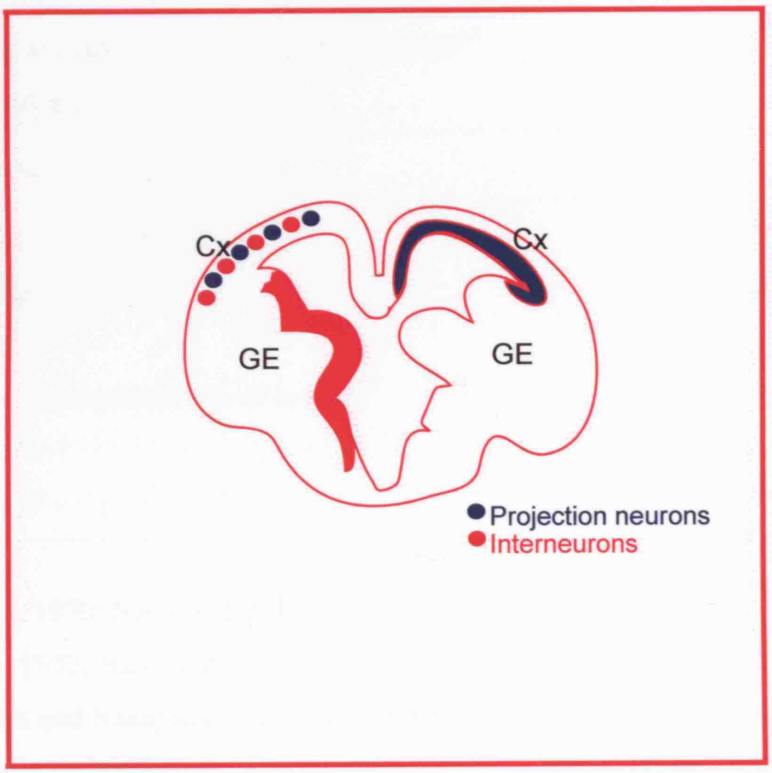
Cx
Cx
GE
GE
Projection neurons
Interneurons

Table 1-1. Currently known modes of cortical neuron migration

PROJECTION NEURONS
Radial migration
Somal (nuclear, perikaryal) translocation[a]
Locomotion (glia-guided)[b]
Multipolar migration (phase in locomotion)[c,d]
Branched in *p35* mutants[e]
INTERNEURONS
Tangential migration[f]
Radial migration
Inward[g]
Ventral-directed (version of inward)[h]
Outward[i]
Branched[j]

[a]Morest, 1970; Nadarajah et al., 2001

[b]Rakic, 1972; Nadarajah et al., 2001

[c,d]Tabata and Nakajima, 2003; Noctor et al., 2004

[e]Gupta et al., 2003

[f] see reviews: Parnavelas, 2000; Marin and Rubenstein, 2001

[g]Tanaka et al., 2003; Ang, Jr. et al., 2003; Hevner et al., 2004

[h]Nadarajah et al., 2002

[i]Tanaka et al., 2003; Hevner et al., 2004

[j]Nadarajah et al., 2003

CHAPTER 2

Materials and Methods

ANIMALS

Animals were maintained by UCL Biological Services. All procedures were performed under licence and in accordance to the regulations of the UK Home Office and the UCL Animal Ethics Committee.

Rats

Rats (Spraque-Dawley) were supplied by UCL Biological Services.
For staging of rat embryos, the day of vaginal plug formation was considered as embryonic day 1 (E1) and day of birth was calculated as postnatal day 1 (P1). Pregnant dams were culled by cervical dislocation. Embryos were anaesthetized by hypothermia prior decapitation.

Mice

p35 knockout mice (C57/Black6 background) and brains from *Cdk5* litters were kindly provided by Margareta Nikolic (Imperial College, London, UK).
For staging of mouse embryos, midday of the day of vaginal plug formation was considered as E0.5 and day of birth was calculated as P0. Pregnant dams were culled by cervical dislocation. Embryos were anaesthetized by hypothermia prior decapitation. Postnatal mice were anaesthetized by either hypothermia (P0-P5) or using halothane (older then P5).

Genotyping

Genotypes were determined by polymerase chain reaction (PCR) on genomic tail DNA. Tails were treated with 500 μg/ml of Proteinase K in lysis buffer (200mM NaCL, 100mM Tris-HCL pH 8.5, 5mM EDTA, 0.2% SDS) at 55°C overnight. Genomic DNA was extracted by phenol-chloroform method and eluted in water.

Three-primer PCR reaction was used for the determination of genotype. The following primers were used:
Forward (p35up): ACGCAGATCCGCAGGACTAAAC
Reverse1 (p35down): CAGAGCATGTAGAGGAAGACCACA
Reverse2 (Neo): GGAGAGGCTATTCGGCTATGAC

The following PCR conditions were used: 94°C, 2 min; (denaturation - d) 94°C, 1 min; (annealing - a) 60°C, 1 min; (extension - e) 72°C, 2 min; 35 cycles; final extension 72°C, 7 min.

PCR products were identified by 1% agarose gel electrophoresis. p35up and p35down primers amplify the region 750bp present only in nonrecombinant genomic DNA at the p35 gene locus (wild-type mice), whilst primers p35up and Neo amplify the region of 1.3kb specific to the genomic deletion (p35 mutant mice).

For further analysis, *p35* littermates were used whenever possible. *p35* heterozygous mice did not show any abnormal phenotype and were used as controls.

Dissection

The embryos were dissected in cold artificial cerebral spinal fluid (ACSF). ACSF consists of 25mM KCl, 2mM KH_2PO_4, 25mM HEPES, 37mM D-glucose, 10mM $MgSO_4$, 175mM sucrose, 0.5mM $CaCl_2$ in 1L of distilled water (all reagents were from Sigma). The pH of ACSF was set to 7.4 with NaOH. Penicillin/Streptomycin solution

(5000units penicillin/5000μg streptomycin; GibcoBRL) was added before ACSF solution was filtered through 0.2μm membrane and kept at 4°C.

Brains were carefully removed and either fixed in 4% paraformaldehyde (PFA) or used for obtaining tissue cultures (organotypic, explants, dissociated), proteins and RNA/DNAs. In some instances, brains were further dissected and cortices, ganglionic eminence (GE), medial GE, lateral GE, and thalami were isolated.

TISSUE CULTURES

Organotypic forebrain (slice) cultures

The mouse/rat brains were carefully removed, embedded in 3.5% low-melting point agarose (Sigma), and 300 μm thick coronal slices of forebrain were cut on a vibratome (Camden Instruments) in ice cold oxygenated ACSF, pH 7.4. The slices were then mounted onto porous nitrocellulose filters (13μm diameter, 0.45 μm pores size; Millipore) and transferred into 24-well sterile culture dishes containing ice-cold ACSF. Forebrains slices were used for the CMFDA experiments (chapter 4A), for electroporation (EP; chapter 4B), and for obtaining thalamic explants used in a collagen assay (chapter 5). After experimental procedures, the slices or explants were incubated in 'slice' medium at 37°C in a 5% CO_2 humidified incubator. The medium was changed every day. The 'slice' medium (50 ml) comprises Dulbecco's modified Eagle medium (DMEM-F12; Sigma; contains HEPES, $NaHCO_3$, and phenol-red), 5% heat-inactivated foetal bovine serum (FBS; GibcoBRL), 1x N2 supplement (GibcoBRL), 100 μM L-glutamine (GibcoBRL), 2.4g/L D-glucose (Sigma), 250units penicillin/250μg streptomycin. The slices and explants (in collagen) were fixed in prewarmed 4% PFA overnight at 4°C.

Primary cultures of mammalian cells

Dissociated cultures of mouse/rat embryonic neurons

The brains of mouse/rat pups were carefully dissected and the cerebral cortices and the medial GE were transferred in ACSF. The cortices and medial GE were incubated in

0.05% trypsin with 100μg/ml DNaseI in Neurobasal medium (GibcoBRL) for 15 min at 37°C. Trypsinisation was quenched by addition of Neurobasal medium containing 10% FCS for 5min at 37°C. The excised cortical and GE tissues were then triturated with a fire-polished Pasteur pipette until no cellular aggregates were visible. The homogenous cellular suspension was subsequently pelleted by centrifugation at 1,000 x g for 3min. The supernatant was discarded and the pellet was resuspended in dissociated cell culture (DCC; 50ml) growth media (Neurobasal medium, 2mM L-glutamine, 2500units penicillin/2500μg streptomycin, with 1:50 dilution of B27, GibcoBRL). 100μl of cells were plated out on 13mm poly-L-lysine:laminin coverslips at a density of 1-2million cells per millilitre and left for 30min at 37°C to attach. Following attachment, the cells were overlaid with DCC media, and incubated at 37°C with 5% CO_2. The media was changed daily. After 1, 3, or 4 days *in vitro* (DIV), the cells were fixed in prewarmed 4% PFA for 20min, and rinsed in PBS prior to immunocytochemistry. The primary neuronal cultures were used in chapters 4A and 4B.

Preparation of Poly-L-Lysine:Laminin coated coverslips

13mm glass coverslips were immersed in concentrated chromic sulphuric acid overnight, rinsed in tap water for several hours, and stored in 70% EtOH. As required, these were place in 24-wells under sterile conditions, and left to dry in a tissue culture hood. 100μl aliquots of poly-L-lysine:laminin solution (10μg/ml:10μg/ml), made up in sterile double-distilled (dd) H_2O, were added per coverslip. Having been left to dry out overnight in a tissue culture hood, the coverlslips were rinsed three times with sterile ddH_2O prior to use.

Mammalian cell lines

COS7 cells

COS7 cells were obtained from the monkey African green kidney, and transformed with SV40. These cells were cultured in DMEM-F12 with 10% FBS and 2mM glutamine, and incubated at 37°C in 5% CO_2. COS7 were passaged by trypsination (0.25% trypsin in DMEM-F12 at 37°C, 5% CO_2, for 5 min) after a single wash with sterile PBS at room temperature. The activity of the trypsin solution was quenched by the addition of an

appropriate volume of growth medium, and the resultant cell suspension was used in seeding as desired. COS7 cells were used in transient transfection assays in chapter 4C.

GN11 cell line

The GN11 cell line has been obtained by genetically targeted tumorigenesis of gonadotropin-releasing hormone neurons in mice (Radovick et al., 1991c), and was a kind gift of Roberto Maggi (University of Milano, Italy). The cell line has characteristics of neurons. GN11 neurons show a strong chemomigratory response *in vitro* (Maggi et al., 2000), and are good model to study molecular mechanisms of neuron migration.

GN11 neurons were cultured as a monolayer at 37°C in a humified CO_2 incubator in 'GN11 medium' containing DMEM-F12 with 10% foetal bovine serum, 2mM L-glutamine and antibiotics (2500 units penicillin/2500 μg streptomycin). The cells were propagated as it was described for COS7 cells. Reduced GN11 medium was used during *in vitro* migratory assay (chapters 4B and 4C); it consists of DMEM-F12 and 2mM L-glutamine. GN11 cells were also plated on poly-L-lysine coated coverslips and used in transient transfection experiments and immunocytochemical analysis (chapter 4B).

***In vitro* migratory assay (Boyden chamber)**

Chemotaxis, a migratory response of cells, including neurons, to chemotropic gradient, was studied using a modified Boyden chamber (Boyden, 1962; Neuroprobe). The Boyden chamber contains two compartments, upper (cell chamber) and lower (chemotropic chamber), separated by a PVP-free polycarbonate filter through which cells migrate. Filters were available in different average pore sizes. The porous filters were pretreated with 0.5M acetic acid, rinsed in PBS twice, and coated, from both sides, with gelatine/PBS (for GN11 neurons) or with poly-L-lysine:laminin (10μg/ml:10μg/ml; for MGE-derived cells).

Chemomigration assay of GN11 neurons

GN11 neurons were trypsinized (in 0.25% trypsin in DMEM-F12 for 5min at 37oC), transfered into GN11 medium, and span down at 1,000 x g for 3min. Cells were resuspened in reduced GN11 medium containing 0.1% BSA/PBS, span down again at

1,000 x g for 3min, and resuspended again in reduced GN11 medium supplemented with 0.1% BSA/PBS, and cell numbers were estimated using a haemocytometer. For a 48-well microchemotaxis (Boyden) chamber, at least $4x10^6$ cells in 2ml were needed. 27µl of negative control (reduced GN11 medium) or positive control (reduced GN11 medium with 1% FBS) or chemotropic factor were put in the lower compartments, and 49µl of $2x10^6$ cells/ml suspension was added in the upper compartment of each well. A gelatine/PBS pre-coated PVP-free polycarbonate filter, pore size 8µm, was placed between two the compartments. GN11 neurons were incubated for 3 hours at 37°C in a 5% CO_2 humidified incubator and fixed in pre-chilled methanol (for 2min). The cells attached to the upper surface of the filter, which failed to migrate through the pore, were washed in PBS and scraped off. The cells that had migrated through the pore to the lower compartment and adhered to the lower surface of the filter were stained using Tiazin (for 1min) and Eosin (for 1min), rinsed in water and mounted onto a glass slide. The images of three fields from each well were collected using digital camera and the number of migrated cells was counted in each filed. Results were expressed as mean number of migrated cells per well ± standard error of the mean (SE) and the significance was calculated by the Student's *t*-test (Microsoft Excel)

Chemomigration assay of interneurons

MGE was removed from the embryos at E13.5 and mechanically dissociated as described in dissociated cell culture method. The cells were pelleted by centrifugation at 1,000 x g for 3min and resuspened in DCC medium without antibiotics. Migration of MGE-derived cells was studied using Boyden chamber; poly-l-lysin/laminin (10µg/ml:10µg/ml) pre-coated filters containing 10 µm pores were used. For chemotaxis, 27 µl of Neurobasal medium with 10% FBS was added in the lower compartment, and 49 µl of a $2x10^6$ cells/ml suspension was added to the upper compartment of each well. Neurobasal medium, without any supplements, put in the lower compartment, was used as a negative control. After overnight incubation (up to 16 hours) at 37°C in a 5% CO_2 humidified incubator, the chamber was disassembled, and the cells that had migrated through the filter pores were fixed in pre-warmed 4% PFA (for 5min), stained with Tiazin and Eosin (for 1min each) and counted as described for GN11 neurons.

HISTOLOGY

Solutions

Phosphate-buffered saline

1x Phosphate buffered saline (PBS) Dulbecco A, pH 7.4 (VWR) was made up according to the manufacturer's instructions.

4% paraformaldehyde (PFA)

-4% PFA (VWR), pH 7.4, was freshly made in 1xPBS.

Immunohistochemistry

Prior to immunohistochemistry procedure, the tissue was adequately fixed in 4% PFA. The embryonic brains were fixed by immersion for at least 1 day, whilst postnatal animals were first cadio-perfused and the brains were then postfixed for 2 hours or longer.

The coronal sections were obtained by cutting forebrains using a vibratome, cryostat or freezing microtome. For vibratome, brains were embedded in 4% agarose (ICN) prepared in 1xPBS; for crysostat, brains were cryoprotected in 30% sucrose in 1xPBS and frozen in OCT; for freezing microtome, brains were snap-frozen directly on dry ice dust. The thickness of the sections was dependent on the cutting technique used: 50μm and 100μm (vibratome), 20μm (crysostat), and 40μm (freezing microtome). The sections were either free-floating or mounted onto Superfrost Plus glass slides (VWR) during the immunohistochemical experiments.

Two methods of immunohistochemistry were used: (i) immunoperoxidase and (ii) immnoflurescence.

(i) In the immunoperoxidase method, sections were first treated with 0.3% H_2O_2 in 1xPBS (or methanol), to block endogenous peroxidase activity, for 20min at room temperature, followed by three washes in 1xPBS. The sections were then bathed in

blocking solution containing 5% normal goat serum (NGS, Sigma) and 0.5% Triton X-100 (Sigma) in 1xPBS, for an hour at room temperature, and subsequently incubated with primary antibodies (Table 2-1), diluted appropriately in blocking solution, overnight at RT. The following day, the sections were washed in 1xPBS and incubated with biotinylated secondary antibodies (Table 2-2) for 30min at room temperature. The sections were then processed using the avidin-biotin-peroxidase complex (ABC-HRP kit, 1/100 dilution; Vector) for 2 hours at room temperature. Peroxidase enzyme activity was revealed and sections visualized using 0.005% 3,3'-diaminobenzidine tetrachloride (DAB in 1xPBS; Sigma) as chromogen and 0.005% H_2O_2 as substrate. Sections were rinsed, dehydrated, and mounted in DPX (VWR).

(ii) In the immunoflorescence method, sections were incubated in blocking solution containing 5% normal goat serum and 0.5% Triton X-100 in 1xPBS, for an hour at room temperature. The sections were then treated with primary antibodies (Table 2-1), diluted appropriately in blocking solution, overnight at RT. For double-labelling, two antibodies, raised in different hosts, were used. After several washes in 1xPBS, sections were incubated with fluorescence–conjugated secondary antibodies (Table 2-2) for 2 hours at room temperature. Again, several washes with 1x PBS were performed, and the sections were stained with bisbenzimide (2.5μg/ml, Sigma) for 7min. Immunolabelled sections were mounted in CytoFluor solution containing 50% glycerol in 1xPBS.

Immunocytochemistry

Fixation of cells, obtained form primary neuronal cultures or cultures of GN11 cell, was performed by removing tissue culture media and adding an appropriate volume of 4% PFA in 1xPBS, prewarmed to 37°C. Cells were incubated with fixative for 20min, and then washed three times with an appropriate volume of 1x PBS. Coverslips were stored, immersed in 1x PBS, at 4°C. Immunoreaction was performed broadly in the same manner as described for slide-mounted tissue sections, except that coverslips were placed culture side up on strips of Parafilm mounted on glass slides.

Nissl staining

To study cortical cytoarchitecture, sections were stained with 0.025% thionin solution (Sigma). Alternatively, semi-thin (1μm) sections, from glutaraldehyde-osmium fixed, Epon embedded tissues, were visualized by alkaline Toluidine blue. In immunofluorescence experiments, tissue architecture or cell nuclei were detected with 2.5μg/ml bisbenzimide.

Digital image capture and analysis

Standard light microscopy for the DAB- and Nissl-stained samples was undertaken with the Leica DMR microscope and digital images captured with the Leica DC 500 digital camera. All images were finally processed in Adobe Photoshop 5.5.
Immunofluorescence reacted samples were excited, viewed and photographed under a conventional fluorescence microscope (Leica, DMR), and also a Leica TCS SP2 confocal laser scanning microscope where appropriate. Prior to image-capture with the confocal microscope, the power of the laser, pinhole, offset and gain were optimized to eliminate cross-talk. A sequential series of images was captured, with those from a single optical plane being compared directly for the assessment of antigen co-localisation. The confocal images were reconstructed using the MetaMorph software and plates were assembled using Photoshop 5.5 (Adobe).

BrdU injections and staining

Bromodeoxyuridine (BrdU) is a synthetic thymidine analogue that incorporates into dividing cells during the S (synthesis) phase of the cell cycle. BrdU (Sigma; 50 μg/g of body weight) was administered intraperitoneally (i.p.) into timed-pregnant mice at E11.5 (chapter 5), E13.5, E15.5, and E17.5 (chapter 4A). BrdU was completely dissolved in sterile 1x PBS prior to injection by vortexing the solution and placing it at 37°C for 1-2 hours. Pregnant dams (E15.5 and E18.5; chapter 5) were culled by cervical dislocation. Alternatively, postnatal animals were killed and transcardially perfused at P12 (chapter 4A). Embryonic and postnatal brains were isolated and fixed in 4% PFA for at least 3

days. Embryonic brains were embedded in 4% agarose and cut into 50μm (E15.5) or 100μm (E18.5) thick Vibratome sections. Postnatal brains were snap-frozen on dry ice and cut into 40μm thick Freezing Microtome sections. BrdU staining, using a mouse anti-BrdU-antibody was performed by the standard immunohistochemistry method (as described above). Prior to that, and in order to access incorporated BrdU, sections were treated with 2M HCl for 45min, followed by 30min treatment with 0.1 M boric acid, and rinsed three times in 1x PBS. Only heavily labelled $BrdU^+$ cells, those labelled during the cumulative BrdU labelling period, were used for analysis.

PROTEINS

Protein isolation

Protein isolation from forebrain tissue and cell lines (GN11 and COS7)

Mouse/rat GE and cortices were lysed in pre-chilled lysis buffer containing protease (PMSF, aprotinin, leupeptin, pepstatin) and tyrosine or serine/threonine phosphatase inhibitors (sodium orthovanadate or sodium fluoride, correspondingly) using a Dounce homogeniser. The quantity of lysis buffer used to homogenise the tissue varied with the quantity of tissue. Similarly, confluent plates of cell lines were placed on ice, growth medium from the plates was aspirated and replaced with an appropriate volume of lysis buffer, and left on ice for 20min. The cells were then scraped into pre-chilled Eppendorf tubes. Two different lysis buffers were used; one for detecting the ErbB receptors (ErbB4 lysis buffer: 50mM Tris-HCl, pH 8, 150mM NaCl, 1% Nonidet P-40 and protease/phosphatase inhibitors) and the other for Cdk5 immunoprecipitation (Cdk5 lysis buffer: 25mM Tris-HCl, pH 7.4, 150mM NaCl, 5mM EDTA, pH 8.0, 1% Triton X-100 and 10% glycerol and protease/phosphatase inhibitors).

The cell suspension obtained from forebrain tissue or cell lines was centrifuged at 13,000 rpm for 8min at 4°C and the supernatant (containing cytoplasmic and membrane fractions) was collected for kinase assay (chapter 4A) or Western blot analysis (chapters 4B and 4C). Protein concentration was determined using the Bio-Rad Protein Assay.

Bio-Rad protein assay

Protein concentrations of lysates were determined using Bio-Rad Protein Assay based on Bradford method. It utilizes the dye Coomassie blue G-250, which is red-brown at pH bellow 1 but turns blue when binding to protein, causes a shift in the pKa of the bound dye. One microlitre of each lysate was added to 800 ml of water and 200 ml of Bio-Rad reagent. The absorbance readings of these samples were recorded at a wavelength of 595 nm. These values were then compared to a curve drawn from a set of standards (standard curve). 20μg of sample protein was used for western blotting, unless stated otherwise.

SDS-PAGE

Sodium dodecyl sulphate polyacrylamide gel electrophoresis (SDS-PAGE)

SDS-PAGE was essentially performed as described by (Sambrook and Russel, 2001). Gels were prepared in a vertical gel electrophoresis separation system (Mini Protean III™ apparatus, Bio-Rad), with resolving gel layer containing acrylamide, Tris pH 8.8, SDS, ammonium persulphate, and TEMED. The percentage of acrylamide was dependent on the size of the protein of interest. The stacking gel contained 5% acrylamide in Tris pH 6.8, SDS, ammonium persulfate, and TEMED. Protein samples were mixed with sample buffer, denaturated at 95°C for 5min, and resolved at a constant voltage (100V) in 1x running buffer (25mM Tris, 250mM glycine, 0.1% w/v SDS, pH8.3). Electrophoresis was continued until the proteins of interest had migrated to the end of the resolving gel, as determined by reference to the Rainbow molecular weight markers (Amersham).

Staining of SDS-PAGE gels with Coomassie R250

Gels were carefully removed from the electrophoresis system. The stacking gel was cut off with a sharp scalpel and discarded, whilst the resolving gel was immersed in Coomassie blue solution containing 0.24 % w/v Coomassie Brilliant Blue R250, 50% v/v methanol, 10% v/v glacial acetic acid, and left under gentle agitation for at least an hour. Having been fixed and stained, the gel was then transferred to a de-staining solution (25% methanol, 7% glacial acetic acid) to remove the unbound dye. The gel was left under gentle agitation until bands of stained protein had become clearly visible against an unstained background, a process typically requiring at least four hours.

Western blot

Transfer of proteins to PVDF membranes (Western blot)

Resolved proteins were transferred from SDS-PAGE gels to PVDF membranes (Bio-Rad) using the wet transfer method, originally described by (Towbin et al., 1992). The SDS-PAGE gel, a PVDF membrane and six appropriately sized pieces of 3mm Whatman paper (Whatman International Ltd.) were pre-soaked in ErbB4 transfer buffer (48mM Tris-Base, 39mM glycine, 0.075% w/v SDS and 20% v/v methanol) and assembled in the Mini Protean III™ apparatus, as instructed by the manufacturer. The transfer was conducted overnight at 30V, 4°C.

Immunodetection of proteins on Western blots

PVDF membranes were incubated for 1hr with blocking solution containing 5% w/v Marvel in PBST (0.2% Triton X-100 made in 1xPBS). Primary antibody, raised against the protein of interest, was diluted in the blocking solution to suitable final concentration (Table 2-1), and was incubated with the membrane for an hour at room temperature or overnight at 4°C. Three 10min washes were performed with PBST, before the horse radish peroxidase conjugated secondary antibody (Table 2-2), diluted in blocking solution, was applied. After 1 hour of incubation, the PVDF membrane was again washed 3x10min with PBST. Enhanced Chemiluminescence reagent (ECL; Amersham) was used, as per the manufacturer's instructions. The membrane was quickly wrapped in Sarawrap and placed in a cassette under film (Kodak X-OMAT). Films were developed after varying exposure times (30s to 30min) to visualise immunodetected proteins.

RNA AND DNA

RNA extraction

Animal tissue

Tissues were immediately dissected, and removed to a sterile Petri Dish, containing ice-cold DEPC-treated 1xPBS, where they were first rinsed and then diced into small pieces with a sterile scalpel blade. Diced tissue was collected and immersed in an appropriate volume of ice-cold Trizol reagent (Gibco-BRL). The homogenisation of diced tissue was performed with a sonicating probe, set to full-power (3x20s, returning samples to ice for 1min between treatments). Samples were subsequently incubated for 5min at room temperature on a shaking platform, before being centrifuged at 10,000 x g, 4°C, for 10min to pellet unwanted cellular debris. The supernatant was collected and thoroughly mixed with 0.2 volumes of chloroform, before being centrifuged at 10 000 x g, 4°C, for 5min in Phase-Lock tubes (Eppendorf). The aqueous layer was removed, mixed with 2 volumes of ice-cold isopropanol, and stored at -80°C for at least 1 hour. RNA was pelleted by centrifugation at 10,000 x g, 4°C, 30min, then washed with ice-cold 70% ethanol made with DEPC-treated ddH_2O, and centrifuged at 10,000 x g, 4°C, for 5min. The supernatant was discarded, and the pellet left to dry under cover at room temperature for 5min. RNA was resuspended in a suitable volume of DEPC-treated ddH_2O, aliquoted and stored at -80°C.

GN11 cell line

Cells cultured in 10 cm Petri dish were washed in 1xPBS and subsequently lysed in an appropriate volume of TRIzol reagent. Total RNA was extracted as described previously, except that sonication was omitted.

DNaseI treatment of extracted RNA

Genomic DNA contamination was eliminated from extracted total RNA samples by treatment with DNaseI. A commercially available kit was used, as per the manufacturer's instructions (DNA-free; Ambion).

Assessment of RNA integrity

1μg of each total RNA sample was resolved on 1%-TAE agarose gel made with DEPC-treated ddH_2O, and inspected by UV transillumination for the integrity of the ribosomal bands.

Reverse transcription polymerase chain reaction (RT-PCR)

Reverse transcription (first-strand DNA synthesis)

First-strand DNA synthesis from total RNA was performed using avian myeloblastosis virus reverse transcriptase (AMV-RT). Briefly, 1μg of total RNA was mixed with 500ng of Random primers (hexamers), and made up to a total volume of 12μl with DEPC-treated ddH_2O (mix1). This sample was incubated at 65°C for 10min to permit the annealing of primers to RNA, and then cooled on ice for 5min. 500 μM dNTPs, 20-40U RNasin, 1xAMV-RT buffer, and 20 units of AMV-RT were added to mix1 to give a final volume of 20 μl, and incubated at 42°C for 45min. Samples were placed on ice, aliquoted and stored at -20°C for the longterm. All reagents were purchased from Promega.

Polymerase chain reaction (PCR)

Each PCR amplification of DNA was performed in a total reaction volume of 50μl in a 0.5ml thin-walled Eppendorf tube. Products were amplified with either the proof-reading DNA polymerase, *Pfu* (Promega; template DNA, 400nM Forward Primer, 400nM Reverse Primer, 200μM dNTPs, 1x *Pfu* buffer, 1.5units *Pfu* DNA polymerase) or the non-proof-reading DNA polymerase, *Taq* (Qiagen; template DNA, 1 μM Forward Primer, 1 μM Reverse Primer, 500μM dNTPs, 1x $MgCl_2$-free *Taq* buffer, 2mM $MgCl_2$, 2units *Taq* DNA polymerase). *Pfu* was always used for cloning and *Taq* for analytical PCR. Template DNA was (i) single-stranded DNA generated by reverse transcription from RNA (~50ng/reaction), (ii) plasmid DNA (1-10ng/reaction), or (iii) genomic DNA (~50ng/reaction). Polymerase chain reaction was performed in a Thermalcycler (Helena BioSciences). Programme settings, comprising denaturation (d), annealing (a), and extension (e), and a total number of cycles were adjusted accordingly.

A-tailing of Pfu-generated PCR products

Pfu DNA polymerase is proof-reading enzyme (i.e. it possesses 3′→5′ exonuclease activity), which generates blunt-ended DNA products. In order to adapt *Pfu*-generated PCR products for cloning into the pGem-T Easy PCR cloning vector (Promega), adenine-tails were added by *Taq* DNA polymerase. Briefly, PCR products were purified with GFX columns (Amersham), and then incubated with *Taq* DNA polymerase (1x $MgCl_2$-free buffer, 2.5mM $MgCl_2$, 200μM dATP, 5units Taq DNA polymerase) for 20min at 70°C.

Agarose gel electrophoresis

1% or 2% agarose-TAE gel was used in resolving DNA samples. 1% or 2% w/v agarose was made up with 1x TAE buffer (0.4M Tris, 0.2M sodium acetate, 20mM EDTA, pH8.3) in a Duran bottle, boiled, and left to cool to approximately 50°C before ethidium bromide was added to a final concentration of 0.2μg/ml. The solution was poured to an appropriate depth in a gel tray containing a comb with suitably sized teeth, and left for 45min to set. DNA samples were mixed with 10x loading buffer (ddH_2O; 50% v/v glycerol and 3% bromophenol blue) immediately prior to well-loading. For fragment size comparison, samples were run against 30μl of 1kb or 100bp DNA ladders (GibcoBRL).

Preparation of DNA fragments

DNA digestion by restriction endonuclease

DNA was incubated with the desired restriction endonuclease(s), diluted in a suitable buffer, for a minimum of 1 hour at the appropriate temperature. At least 2 units of (each) enzyme per microgram of DNA were used in these reactions. Care was taken to ensure that glycerol did not exceed 10% of the total reaction volume and, where appropriate, other measures were taken to prevent the 'star-activity' that is associated with some enzymes.

Generation of blunt-ended DNA

In the absence of compatible restriction sites for subcloning, 'sticky-ends' were blunted with the modifying enzyme T4 DNA polymerase (Promega). This enzyme possesses 5′ to 3′ polymerase activity for filling-in 5′ overhangs, and 3′ to 5′ exonuclease activity for trimming back 3′ overhangs. DNA ends were modified in the presence of a suitable restriction endonculease buffer and 100μM dNTPs. 15 units of enzyme were added per μg of DNA. The reaction was incubated at room temperature for 10min before purification of the DNA with GFX columns (Amersham) as per the manufacturer's instructions.

Isolation and purification of DNA fragments

Restriction endonuclease-digested, and/or end-modified, DNA samples were mixed with an appropriate volume of 10x loading buffer and resolved on a 1% agarose gel, containing 0.2μg/ml ethidium bromide. DNA fragments were visualized on a UV transilluminator, at a low power setting, and were quickly and carefully excised with a clean scalpel. The DNA fragment was subsequently extracted from the gel using the GFX columns as per the manufacturer's instructions. The purified DNA was ultimately eluted in an appropriate volume of autoclaved double-distilled water.

DNA ligations

Ligation reactions were performed in thin-walled 0.5ml Eppendorf tubes. Reactions consisted of an appropriate amount of linearized gel-purified vector (typically ~100ng), an appropriate molar ratio of gel-purified insert (between 1 to 3 copies of insert per copy of backbone), 1x T4 DNA ligase buffer and 3 units of T4 DNA ligase (Promega) made up to a final volume of 20μl with autoclaved double distilled water. Ligation reactions were either left at room temperature for several hours ('sticky-end' ligations), incubated at 4°C overnight (for optimal efficiency with the pGem T Easy PCR cloning vector system), or incubated in a thermal cycler ('blunt-end' ligations). The latter were performed in a Thermocycler, in which the samples were incubated at 16°C for 1min followed by 37°C for 1min, for 30 cycles. The final step comprised 30mins incubation

at 22°C. 10µl of the reaction product were used in the transformation of 200µl of competent *Escherichia coli*.

Bacterial propagation of plasmid DNA

Bacterial strains

DH5α (Invitrogen) and XL10gold (Stratagene) chemically competent strains of *Escherichia coli* bacteria were used for the standard propagation of plasmid DNA.

BL21 (DE3) (Stratagene) strain of *Escherichia coli* bacteria was used for the expression of GST-fusion proteins. It lacks the bacterial OmpT and Lon proteases, which can significantly impair the recovery of intact recombinant protein. Furthermore, it is a lysogen (i.e. has phage viral DNA integrated in its genome) of a modified λDE3 phage carrying a hybrid transgene encoding bacterial T7 RNA polymerase under the control of the IPTG-sensitive *lacUV5* promoter.

Transformation of competent bacteria

200µl of competent bacteria were transformed through the addition of an appropriate volume of extracted plasmid DNA or ligation reaction product. Bacteria were incubated with DNA on ice for 30min and subsequently heat-shocked at 42°C for 45 seconds. These cells were then incubated on ice for a further 5min. 800µl of autoclaved Luria Broth (LB; Invitrogen), pre-warmed to 37°C, was added to each transformation. These were then transferred to an orbital shaker set to 37°C and 300rpm for an hour. The transformed cells were plated onto LB Agar plates containing the 100µg/ml of ampicillin. Where detection of β-galactoside activity was desirable, e.g. in using the pGem T Easy PCR cloning vector, LB Agar additionally contained a final concentration of 100µg/ml 4-chloro, 5-bromo, 3-indolyl-β-galactosidase (X-Gal, Insight Biotechnology, Ltd.), derived from a stock of 20mg/ml in dimethyl formamide.

Bacterial growth on LB agar plates

Bacterial LB Agar plates were incubated at 37°C overnight, to support colony formation, and were then stored at 4°C until required.

Extraction of plasmid DNA

Small scale (mini-prep)

The "mini-prep" DNA extraction method is derived from the alkaline lysis method originally described by (Birnboim and Doly, 1979). Individual colonies of transformed bacteria were picked from antibiotic LB Agar plates and were each used to inoculate a single 5ml starter preparation of LB media, containing the appropriate antibiotic selective agent (i.e. 100μg/ml ampicillin). Inoculates were incubated overnight at 37°C in an orbital shaker, set to 300rpm. Cells were collected from 3ml of culture media by centrifugation at 600xg for 10min, and Wizard® *Plus* Minipreps DNA Purification System (Promega) was used to isolate plasmid DNA, according to the manufacturer's instructions. DNA pellet was resuspended in 60μl of autoclaved double-distilled water and stored at -20°C. DNA yields varied, dependent on the nature of the plasmid (i.e. whether it was a 'high copy number' vector), but typically ranged from 100-300ng/μl following resuspension in water. The purified plasmids were used for DNA sequencing and for obtaining large scale (maxi prep) of plasmid DNA.

Identification of positive bacterial colonies

Analytical digestion of mini-prep DNA by restriction endonucleases

Clonal analysis was usually performed by restriction endonuclease digestion of plasmid DNA obtained by mini-prep extraction. Typically, 1μl of Mini-Prep DNA were digested in a total volume of 20μl. 10 units of enzyme were included in the reaction with a suitable buffer, as indicated by the manufacturer; where two or more enzymes were used, care was taken to ensure that (i) a suitable buffer was used to achieve the highest enzymatic activity, and (ii) glycerol levels did not exceed 10%. Restriction endonuclease digestions were incubated at a suitable temperature for 1-2 hours. Samples were resolved on a 1% agarose gel containing 0.2mg/ml ethidium bromide, and visualized on a UV transilluminator.

Screening by PCR

Occasionally, large numbers of colonies were screened by PCR. This was advantageous when insertional efficiency was low, and mini-prep DNA extraction on such scale as was necessary to identify a positive clone would have been labour-intensive. In these instances, colonies were randomly picked from the desired LB Agar plate, and each mixed by pipetting in 20µl LB containing the appropriate selective agent. 1µl of each of these diluted clonal samples was used for PCR, each in a total reaction volume of 50µl.

DNA sequencing

All plasmid DNA samples for sequencing were submitted at sufficient purity (A_{260}/A_{280} greater than 1.8) and at the correct concentration (~100ng/ml). Samples were analysed using an ABI automated fluorescent dye sequencing facility (DNA Sequencing Facility, Department of Biochemistry, University of Cambridge, UK). SP6, T7 and T3 sequencing primers were provided by the DNA Sequencing Facility. All other sequencing primers were submitted at a concentration of 10pmol/µl, along with the relevant plasmid DNA samples.

Table 2-1. The primary antibodies used in this thesis, as they appeared

Antigen	Abbr.	Host	Clone type	Dilution	Supplier
Bromodeoxyuridine	BrdU	mouse	Monoclonal, clone BU5.1	$1/100^{H}$	Progen
Microtubule-associated protein 2	MAP2	mouse	Monoclonal, clone A-20	$1/500^{H}$	Sigma
Neurofilament proteins	NFm,h*	mouse	Monoclonal	1/100	Zymed
Glial fibrillary acidic protein	GFAP	rabbit	Polyclonal	1/400	Dako
p35		rabbit	Polyclonal	$1/100^{H}$, $1/1000^{WB,IP}$	Santa Cruz
Cdk5		mouse	Monoclonal, clone DC27	$1/5^{H,WB,IP}$	A gift from MN**
γ-aminobutyric acid	GABA	rabbit	Polyclonal	$1/1000^{H}$	Sigma
Calbindin	CB	rabbit	Polyclonal	$1/5000^{H}$	SWant
TAG1		mouse	Monoclonal	1/100	DSHB
Calretinin	CalR	rabbit	Polyclonal	$1/2000^{H}$	SWant
ErbB2		rabbit	Polyclonal	$1/100^{H}$, $1/1000^{WB}$	Santa Cruz
ErbB3		rabbit	Polyclonal	$1/100^{H}$, $1/1000^{WB}$	Santa Cruz
ErbB4		rabbit	Polyclonal	$1/100^{H}$, $1/1000^{WB,IP}$	Santa Cruz
c-myc		mouse	Monoclonal, clone 9E10	$1/100^{H}$	Sigma
α-tubulin		mouse	Monoclonal, clone DM1A	$1/1000^{H}$	Sigma
Phospho-threonine-proline	pTP	mouse	Monoclonal, clone 42H2	$1/4000^{WB}$	Cell Signalling
Nogo-A		mouse	Monoclonal, Clone 6DP	$1/20^{H}$	A gift from GSK***
β-III-tubulin		mouse	Monoclonal, clone SDL.3D10	$1/500^{H}$	Sigma
FLAG		mouse	Monoclonal, clone M2	$1/100^{H}$	Sigma

H - immunohisto- or immunocytochemistry; WB – western blot; IP - immunoprecipitation

*m,h – medium and heavy; ** MN - Margareta Nikolic; ***GlaxoSmithKline plc.

Table 2-2. The secondary antibodies used in this thesis

Antibody	Host	Conjugated with	Working dilution	Supplier
Anti-rabbit IgG	Goat	Biotin	1/200	Vector
Anti-mouse IgG	Goat	Biotin	1/200	Vector
Anti-rabbit IgG	Goat	FITC*	1/400	Molecular probes
Anti-mouse IgG	Goat	FITC	1/400	Molecular probes
Anti-rabbit IgG	Goat	TRITC**	1/400	Molecular probes
Anti-mouse IgG	Goat	TRITC	1/400	Molecular probes
Anti-rabbit IgG	Goat	HRP***	1/5000	Amersham
Anti-mouse IgG	Goat	HRP	1/5000	Amersham

*FITC – fluorescein-5-isothiocyanate; Alexa Fluor 488. **TRITC – tetramethylrhodamine-5-(and-6)-isothiocyanate; Alexa Fluor 568. ***HRP – horse radish peroxidase.

CHAPTER 3

Cdk5 and cortical cytoarchitecture

INTRODUCTION

The neocortex is a layered structure, both in development and adulthood, which is established through the pattern of neuronal cell migration. The first neocortical neurons, born in the proliferative zone (VZ), migrate towards the pia to form the PPL. The PPL is then divided into two layers, LI and SP, by the emerging CP projection neurons. These neurons migrate and settle in an 'inside-out' order, such that earlier born neurons reside in deeper layers (e.g. VI and V) whilst neurons born later occupy more superficial layers (e.g IV, II-III) of the mature cortex. Interneurons and non-neuronal cells, such as astrocytes, oligodendrocytes, and microglia, also contribute to the volume of the cortical layers. The idea that cortical histogenesis proceeds in an 'inside-out' pattern came from (Ramon y Cajal, 1911) who had stated that the deep projection neurons go ahead with differentiation compared to the superficial ones. This was confirmed by neuronal birthdating techniques, based on incorporation of radioactive (tritiated thymidine; Angevine and Sidman, 1961) or non-radioactive (5-Bromo-2-DeoxyUridine, BrdU; Miller and Nowakowski, 1988) DNA precursors at different time points during corticogenesis.

The *reeler* mouse (Falconer, 1951), carrying a mutation in the *reelin* gene (D'Arcangelo et al., 1995; Ogawa et al., 1995), is the first mutant described to have an abnormal laminar pattern of the cerebral cortex (Caviness, Jr. and Sidman, 1973; Caviness, Jr., 1982). In this mutant, the orderly 'inside-out' deposition of neocortical neurons is disturbed and the layering pattern is inverted. Reelin, an extracellular matrix protein secreted by CR cells, binds to VLDLR and ApoER2 receptors that are expressed on migrating projection neurons to regulate Dab1 tyrosine phosphorylation (reviewed by Tissir and Goffinet, 2003). The VLDLR/ApoER2 (Trommsdorff et al., 1999) and Dab1 (Howell et al., 1997) mutant phenotypes are almost identical to that of the *reeler* mouse.

p35, a regulatory subunit of Cdk5, activates Cdk5 in postmitotic cortical neurons (Tsai et al., 1994; Zheng et al., 1998). Cdk5 regulates by phosphorylation the dynamics of molecules important in neuronal migration and adhesion. Mice with a mutation in either the *Cdk5* or *p35* gene display a cortical lamination defect similar to *reeler* (Ohshima et al., 1996; Chae et al., 1997; Gilmore et al., 1998; Kwon and Tsai, 1998; Dhavan and Tsai, 2001; Lambert de and Goffinet, 1998; Lambert de and Goffinet, 2001; Gupta et al., 2002; Cruz and Tsai, 2004). *Cdk5* mutants die perinatally and have a more serious defect in cortical development than *p35* knockouts. Mice deficient in both *p35* and its homologue *p39* have a similar severe phenotype to that seen in the *Cdk5* mutants. The principal difference between the *reeler* and *p35/Cdk5* phenotype concerns the PPL, which only splits in the latter.

The aim of this chapter is to refine known facts as well as to present novel findings regarding cortical histogenesis in *p35* mutant mice. This results chapter serves also as an introduction to the following results chapters.

SUMMARY OF MATERIALS AND METHODS

Animals

p35 and *Cdk5* litters were used in this study. Animal brains were fixed in 4% PFA by immersion (embryonic) or perfusion/immersion (postnatal), and cut coronally using the Vibratome (embryonic; 50 μm and 100 μm) or Freezing Microtome (postnatal; 40 μm).

Nissl staining

Thionin and Toluidine blue solutions were used to label cortical cytoarchitecure.

BrdU injections

BrdU was injected i.p. into timed-pregnant mice at E13.5, E15.5, and E17.5 and distribution of BrdU-labelled cells was studied at P12. BrdU-labelled cells were revealed by immunohistochemistry.

Immunohistochemistry

Coronal forebrain sections were immuno-labelled using the peroxidase method. The following primary antibodies were used: mouse anti-BrdU, mouse anti-NF (m and h), mouse anti-MAP2, and rabbit anti-GFAP (see Table 2-1).

Quantification of cortical thickness

The absolute thickness of the Nissl-stained lateral cortex in embryos and motor, somatosensory, and olfactory cortex in postnatal animals was measured. The measurements of the latter were taken at two levels, rostral (anterior commissural) and caudal (rostral hippocampus). The relative layer thickness was calculated as a percentage of the entire telencephalic wall thickness. Both, absolute and relative thicknesses were expressed as mean ± standard error of the mean (SEM). At least 3 brains from each genotype were used for analysis.

RESULTS

Neocortical layers in development: a Nissl study

In order to study developmental changes in prenatal neocortical layers in *p35* +/- and *p35* -/- mice, Nissl staining was used.

Pre-cortical plate period (until E13.5)

During the pre-CP developmental stage (E13.5 and earlier), no difference in the morphology of cortical layers of *p35* +/- and *p35* -/- mice was observed (data not shown). The developing cortex consisted of the VZ, IZ, and a thin PPL.

Cortical plate period (from E14.5)

In the early CP stage (E14.5), splitting of the PPL by arriving CP neurons occurred, and two new layers appeared (LI and SP). The absolute thickness of LI (22.5±3.7 μm

vs.22.5±4.7 μm), CP (35.5±2.8.3 μm vs. 38.5±1.3 μm) and telencephalic wall (TW; 309.5±5.6 μm vs. 307.5±5.6 μm) as well as the relative contribution of LI (~ 7%) and CP (~12 %) to the total thickness of the TW did not differ between *p35* mutant and control cortices (Fig.3-1A,B; Fig.3-2).

A clear difference in the neocortical layer phenotype between the two genotypes appeared at E16.5. The compact CP, located between LI and the SP, was significantly thinner in *p35* -/- mice (67.5±7.8 μm vs. 124.2±1.5 μm) accounting for 13% of the total TW thickness, as opposed to 23% in control brains (Fig.3-1C,D; Fig.3-2). There was a visible accumulation of cells below the compact CP in the *p35* mutant mice (Fig.3-1D). These cells, situated within the IZ, represented ectopic CP cells and, thus, this cellular part of the IZ was often referred to as 'ectopic' CP. There was no obvious difference in LI (38.8±5.5 μm vs. 33.3±3.8 μm) and TW (521.3±6.6 μm vs. 538.3±7.9 μm) thickness between *p35* mutants and control mice, and in fact the contribution of LI to total TW thickness was 7%, as it was at E14.5 (Fig.3-1C,D; Fig.3-2).

By E19.5, and just before birth, the difference between *p35* hetero- and homozygous cortices became more striking. In *p35* mutant brains, LI was significantly thicker (96.7±4.2 μm vs. 63.3±7.2 μm), whilst the compact CP was significantly thinner (81.7±3.1 μm vs. 283.3±6.7 μm) compared to the control brains (Fig.3-1E,F; Fig.3-2A,C). To compare *p35* -/- vs. *p35* +/-, LI accounted for 11% vs. 8%, whilst the compact CP accounted for 9% vs. 37% of total TW thickness (Fig.3-2B,D). Interestingly, the accumulation of cells at three sites, LI, compact CP, and ectopic CP, in *p35* mutant mice gave an impression of a 'triple' cortex (Fig.3-1F). Surprisingly, the whole TW was thicker in the *p35* mutants compared to control mice (898.3±7.5 vs. 758.3±23.9; Fig.3-2E).

Toluidine blue-stained semi-thin (1 μm) sections showed, in a more elaborate way, clear differences between *p35* +/- and *p35* -/- cortices (Fig.3-3). In *p35* -/- mice, the TW was thicker and the compact CP was thinner (Fig.3-3B) compared to control mice (Fig.3-3A). Also, in *p35* mutant mice, cortical axons were intermingled among ectopic CP neurons located in the IZ, giving an impression of a fan (Fig.3-3B). These axons seemed to even penetrate the compact CP. LI in *p35* -/- brains appeared thicker, more cellular and without a clear border with the compact CP (Fig.3-3C) compared to LI in control brains (Fig.3-3D).

In addition, *Cdk5* littermates (E18.5) were also compared, and changes regarding the cortical layers were similar to those found in the *p35* littermates. In *Cdk5* +/+ mice, the morphology of the cortical layers was similar to that observed in *p35* control mice (Fig.3-1G). However, in *Cdk5* +/- mice, the compact CP was slightly thinner and mild accumulation of cells was observed in the IZ (Fig.3-1H). Interestingly, in *Cdk5* -/- mice, the existence of a 'triple' cortex, seen in *p35* mutant mice, was confirmed (Fig.3-1I).

Mature cortical layers: Nissl and BrdU studies

In order to study the position of mature cortical layers, Nissl and BrdU birthdating techniques were applied.

First, I used the Nissl method to study the cytoarchitecture of control and *p35* mutant mouse forebrain at P12. Two coronal planes of forebrain were examined: (i) rostral – cut at the level of the anterior commissure (ac) and (ii) caudal – cut at the level of the rostral hippocampus. On both planes, motor (M), somatosensory (SS) and olfactory (O) cortical zones were visible to variable extents. In both genotypes, all forebrain structures were present. In control mice at both levels, the cerebral neocortex had visible layers I-VI and underlying white matter (Fig.3-4A,C,E,G). In *p35* mutant mice, no distinguishable layers or white matter were seen (Fig.3-4B,D,F,H). In addition, in the hippocampus of control mice, the pyramidal layer was sharply bordered with other hippocampal layers (Fig.3-4G). In contrast, in the *p35* mutants, pyramidal cells were found within and beyond the pyramidal layer, in the stratum oriens (Fig.3-4H). Presence of barrels, the functional representation of the whiskers in layer IV of the somatosensory cortex, was evident in the *p35* +/- mice (Fig.3-4G). However, the barrels were not visible in the *p35* mutant mice (Fig.3-4H). Finally, the thickness of the TW, that included the cortex and underlying white matter, was measured in three cortical areas (M, SS, O) at rostral (ac; Fig.3-4I) and caudal (rostral hippocampus; Fig.3-4J) levels. In *p35* mutant mice, M and SS areas of the cortex were significantly thicker compared to the same areas in control mice, and this result was found at rostral and caudal planes (rostral plane, M: 2±0.04 mm vs. 1.7± 0.02 mm; S:1.6±0.02 mm vs. 1.5±0.04 mm; caudal level, M:1.4±0.04 mm vs. 1.2±0.02 mm; S:1.5±0.04 mm vs. 1.3±0.008 mm; Fig.3-4K,L). In contrast, the

thickness of the O cortex did not differ between the two genotypes (rostral, caudal; 0.9±0.02 mm vs. 0.9±0.04 mm; Fig.3-4K,L).

The position of layers (II-VI) in mature neocortex depends on the time of their origin. Therefore, the BrdU birthdating technique was used to determine the position of mature neocotical layers in *p35* +/- and *p35* -/- mice. A single injection of BrdU, which is incorporated into cells during S phase, was administrated at E13.5, E15.5, and E17.5 to label layers VI/V, IV/III/II, and II, respectively. The positions of BrdU-labelled cells in the neocortex were analyzed by immunohistochemistry at P12. The progenitors labelled with BrdU at E13.5 were spread in the whole forebrain. In the neocortex, $BrdU^+$ cells were found mainly in layers VI/V in control mice. However, in the *p35* mutant mice, $BrdU^+$ cells resided in the whole depth of the neocortex, but primarily in the upper half (Fig.3-5; Table 3-1). In control mice, the cells that incorporated BrdU at E15.5 were observed mainly in layers II and III, with a few $BrdU^+$ cells found in layer IV. In contrast, in *p35* mutant mice, $BrdU^+$ cells were found at two sites; most of them were captured in the lower part of the neocortex, and there was a clear layer of $BrdU^+$ cells aligned next to pia (Fig.3-6; Table 3-1). When E17.5 dividing cells were labelled with BrdU, they were confined to layer II in control neocortices. In the *p35* mutant neocortex, however, $BrdU^+$ cells occupied a large deep area, primarily in the dorsal regions (Fig.3-7; Table 3-1). Also, it appeared that there were more $BrdU^+$ cells in the *p35* mutant compared to control neocortex. A summary of the position of $BrdU^+$ cells in the neocortex in *p35* control and mutant mice is presented in Table 3-1 and Fig.3-8.

Mature neocortical layers and cells: an immohistochemical study

Next, the position and morphology of cortical cells, such as neurons and astrocytes, were examined. Neuronal markers, such as antibody to neurofilament (NF, medium and heavy) and antibody to the microtubule-associated protein 2 (MAP2), were used. Anti-NF antibody marks neurons in layers II, III, and V, as well as axons, whilst anti-MAP2 antibody shows preference to neuronal soma and dendrites. To label astrocytes, an antibody to the intermediate filament glial fibrillary acidic protein (GFAP) was used.

In control mice, NF^+ cells were large neurons of layer V and small neurons of layers II-III; NF^+ fibres were located below the cortex (Fig.3-9A,C). In contrast, in p35 mutant mice, large NF^+ neurons were found mostly positioned below the pial surface,

whilst small NF^+ neurons were found in the lower parts of the cortex, intermingled among NF^+ fibres that ran through the cortex (Fig.3-9B,D). In p35 +/- cortices, MAP2 immunoreactivity was mainly found in neuronal somata and radially-oriented apical dendrites (Fig.3-10A,C,E). However, in p35 mutant cortices, there was a loss of radial orientation of the dendrites marked with antibody to MAP2 (Fig.3-10-B,D,F).

In p35 +/- mice, $GFAP^+$ astrocytes were found mainly clustered in the white matter and in cortical layers I and VI at P12 (Fig.3-11A,C). However, in p35 mutant mice, $GFAP^+$ astrocytes were fewer compared to control littermates, and scattered through the depth of the cortex (Fig.3-11B,D). In control mice, the hippocampal pyramidal layer was devoid of $GFAP^+$ astrocytes (Fig.3-11E), whilst in p35 mutant mice this layer was widely invaded by such cells (Fig.3-11F).

DISCUSSION

Developing neocortical layers

Layer I

In *p35* mutant mice, LI became thicker than in control mice as early as E17.5, but this phenotype was clearly visible from E18.5. More cells were found in *p35* -/- LI and, in addition, the border of LI with compact CP, which was relatively sharp in control mice, was uneven and hardly visible in *p35* mutants. These findings about the morphology of perinatal LI in *p35* mutant mice are original, and will be discussed in further detail in chapters 4a and 5, when the position of cortical interneurons and PPL splitting in these mutants are examined.

Cortical plate

To reiterate, in *p35* mutant mice there was a compact CP, located between LI and SP, and loose, ectopic CP located within the IZ. The compact CP was visibly thinner in *p35* mutant mice compared to control mice from E15.5 onwards. However, the compact CP in *p35* mutants significantly increased in size with time. Whilst the precise cause of this phenomenon is not known, there are several potential factors which – singly or in

conjunction – could explain this: (i) a new wave of projection neurons, (ii) inward/outward migration of interneurons, or (iii) invasion of fibres.

The Doublecortin (Dcx) mutation gives rise to a neuronal migration disorder in females known as subcortical band heterotopia (Gleeson and Walsh, 2000). Interestingly, Tanaka et al. (2004a) described a similar phenotype, also termed 'double cortex', in *Cdk5* mutants. In this chapter, the cortical phenotype in either *p35* or *Cdk5* mutants was described as 'triple cortex'. It was obvious that apart from accumulation of cells in the compact CP (layer 2 according to Tanaka et al., 2004a), and ectopic CP located within the IZ (layer 4 according to Tanaka et al., 2004a), there was an additional thick layer of cells within LI.

Mature neocortical layers

Neocortical layers are indistinct in p35 mutants

In control mice all neocortical layers as well as the barrels were clearly noticeable. In *p35* mutant mice, however, neocortical layers were indistinct and the barrels invisible. The phenotype seen in *p35* mutant mice could be explained by BrdU birthdating studies. In *p35* -/- neocortex, there was an overlap in the position of progenitors labelled with BrdU at different time points (Fig.3-8H) and, thus, the neocortical layers could not be distinguished as they were in the control neocortex (Fig.3-8G).

Neocortical layers are inverted in p35 mutants

BrdU birthdating studies also revealed that while in control mice neocortical layers were produced in undoubtedly 'inside-out' order, in *p35* mutant mice neocortical layer settlement occurred mostly in an outside-in fashion. The distribution of NF^+ neurons confirmed that the position of neocortical layers in *p35* mutant mice was inverted compared to control mice. BrdU incorporates in any progenitor cell type during cell division. The next logical question is which cell type is following this inverted pattern within the neocortex: pyramidal neurons, interneurons, or both? This issue will be discussed in chapter 4A.

Telencephalic wall is thicker in p35 mutants

In *p35* mutant mice, the TW was significantly thicker compared to control mice, and this was first observed at E17.5. Also, the dorsal and lateral parts of the postnatal (P12) cortex, corresponding to motor and somatosensory cortical areas, were wider in the *p35* mutant mice. Interestingly, the thicker cortex in *p35* mutants, at P12, especially in the dorsal parts, coincided with an increased number or accumulation of $BrdU^+$ cells (labelled at E17.5). The increased number or accumulation of $BrdU^+$ cells could be explained through four possible mechanisms: (i) increased proliferation of E17.5 progenitors, (ii) decreased cell death of E17.5 progenitors, (iii) misposition of E17.5 progenitors, or (iv) anomalous position of the cortical fibres.

It is unlikely that altered proliferation could explain thickening of the cortex in *p35* mutant mice, as p35 is found exclusively in postmitotic neurons (Tomizawa et al., 1996; Delalle et al., 1997; Zheng et al., 1998) and Cdk5 is thus considered a postmitotic kinase. Controversially, Cdk5 has been reported to control both cell death and survival (Zhang et al., 1997; Cheung and Ip, 2004). I have performed TUNEL, a method for detection of apoptotic cells, and could not observe any difference in the number and distribution of $TUNEL^+$ cells between *p35* heterozygous and homozygous mice (data not shown). It is possible that accumulation of E17.5-born $BrdU^+$ cells was due to their defective migration; these cells could not reach the outer cortex, which had a larger circumference, and remained confined to a small region of the inner cortex. Finally, a proposed defasciculation (Kwon et al., 1999) as well as abnormal spreading of cortical fibres could be the cause of increased volume of the cortex. Volumetric studies would be a useful tool to solve this problem.

Cortical axons are misplaced in p35 mutants

The white matter was not noticeable in Nissl preparations of *p35* mutant mice. The cortical axons, afferent and efferent, labelled with antibody to NF, were found loosely running through the cortex at P12, instead of being positioned in a tight band beneath the cortex. This has already been observed in studies of (Kwon et al., 1999) and (Gilmore et al., 1998). However, the unique finding in this chapter was that prenatal cortical axons seemed to invade the compact CP prematurely. This will be discussed further in chapter 5.

Other neocortical cells: glia

The cortical layers and neurons are mispositioned in *p35* mutant mice. There is a question whether other cortical cells, such as macroglia, are affected by the lack of Cdk5 activity. Interestingly, astrocytes can express Cdk5 (Tanaka et al., 2001). In this study, it has been described that cortical and hippocampal astrocytes were misplaced in *p35* mutants. It would be interesting to investigate whether the migration of astrocytes is a Cdk5-dependent mechanism and to ascertain whether the distribution of astrocytes depends on the position of neurons and their axons. Astrocytes originate from two different sites, either arising from radial glia or the SVZ of the developing cortex (Jacobsen and Miller, 2003; Goldman, 2004). It has been proposed that their pattern of migration is largely a reflection of the organization of the neural environment (Jacobsen and Miller, 2003).

Nonetheless, more research will have to be undertaken before the precise mechanism of Cdk5 involvement in corticogenesis becomes clear.

Figure 3-1. Loss of Cdk5 activity alters the morphology of the developing neocortex

Coronal sections of the developing cortex stained with Nissl (thionin).

(A-B) E14.5; (A) *p35* +/- mice; (B) *p35* -/- mice. No difference in cortical morphology was observed between the two genotypes.

(C-D) E16.5; (C) *p35* +/- mice; (D) *p35* -/- mice. The compact CP was thinner in the *p35* mutants. Vertical line is showing the location of ectopic CP neurons.

(E-F) E19.5; (E) *p35* +/- mice; (F) *p35* -/- mice. The compact CP was thinner, whilst LI and the IZ were thicker in the *p35* mutants.

(G-I) E18.5; (G) *Cdk5* +/+ mice; (H) *Cdk5* +/- mice; (I) *Cdk5* -/- mice. The *Cdk5* mutants exhibited phenotypes identical to those of the *p35* mutant mice.

(F,I) The position of the 'triple cortex' indicated by three (*).

LI – layer I; CP – cortical plate; cCP – compact cortical plate; eCP – ectopic cortical plate; SP – subplate; IZ intermediate zone; SVZ – subventricular zone; VZ – ventricular zone. Scale bars, 200 μm (A-D, G-I); 500 μm (E-F).

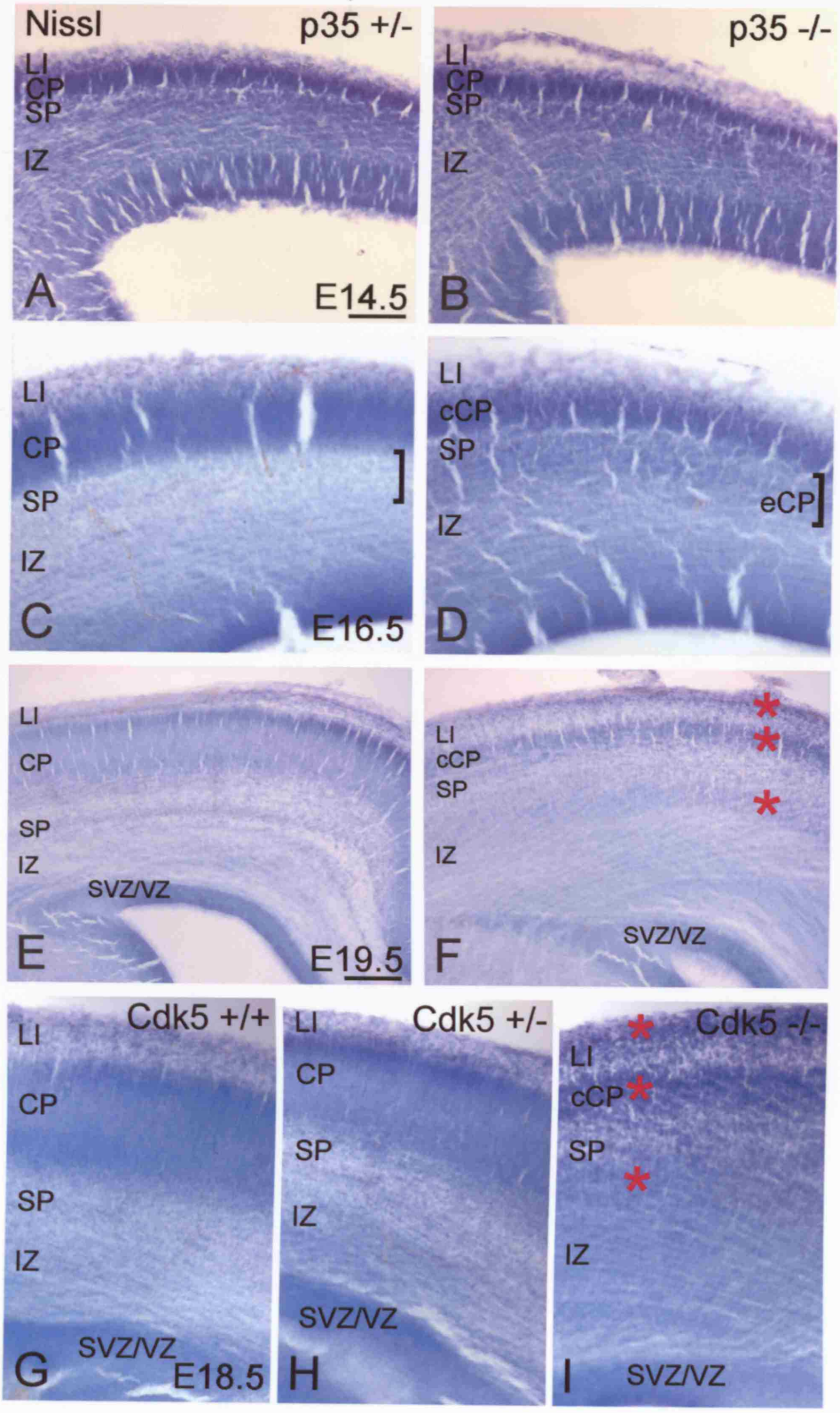
Nissl
p35 +/-
LI
CP
SP
IZ
A
E14.5
p35 -/-
LI
CP
SP
IZ
B
LI
CP
SP
IZ
C
E16.5
LI
cCP
SP
IZ
eCP
D
LI
CP
SP
IZ
SVZ/VZ
E
E19.5
LI
cCP
SP
IZ
SVZ/VZ
F
Cdk5 +/+
LI
CP
SP
IZ
SVZ/VZ
G
E18.5
Cdk5 +/-
LI
CP
SP
IZ
SVZ/VZ
H
Cdk5 -/-
LI
cCP
SP
IZ
SVZ/VZ
I

Figure 3-2. Loss of Cdk5 activity alters the thickness of the developing neocortical layers and telencephalic wall

(A-B) Absolute (A) and relative (B) thickness of LI was increased in *p35* mutants compared to controls at E19.5.

(C-D) Absolute (C) and relative (D) thickness of the compact CP was decreased in *p35* mutants compare to controls from E16.5.

(E) Absolute thickness of the TW was increased in *p35* mutants compared to controls at E19.5.

Developing neocortical layers were stained with Nissl (thionin). Absolute thickness of the layers or TW was measured in lateral neocortex. Relative layer thickness was calculated as a percentage of the entire TW thickness. The results were expressed as mean±SEM (standard error of the mean). Error bars represent SEM. Number of brains used for each genotype (*p35* +/- and *p35* -/-) and age (E14.5, E16.5, E19.5) was n=3; * $p<0.05$, *** $p<0.005$; Student's *t*-test.

LI – layer I; CP- cortical plate; TW – telencephalic wall.

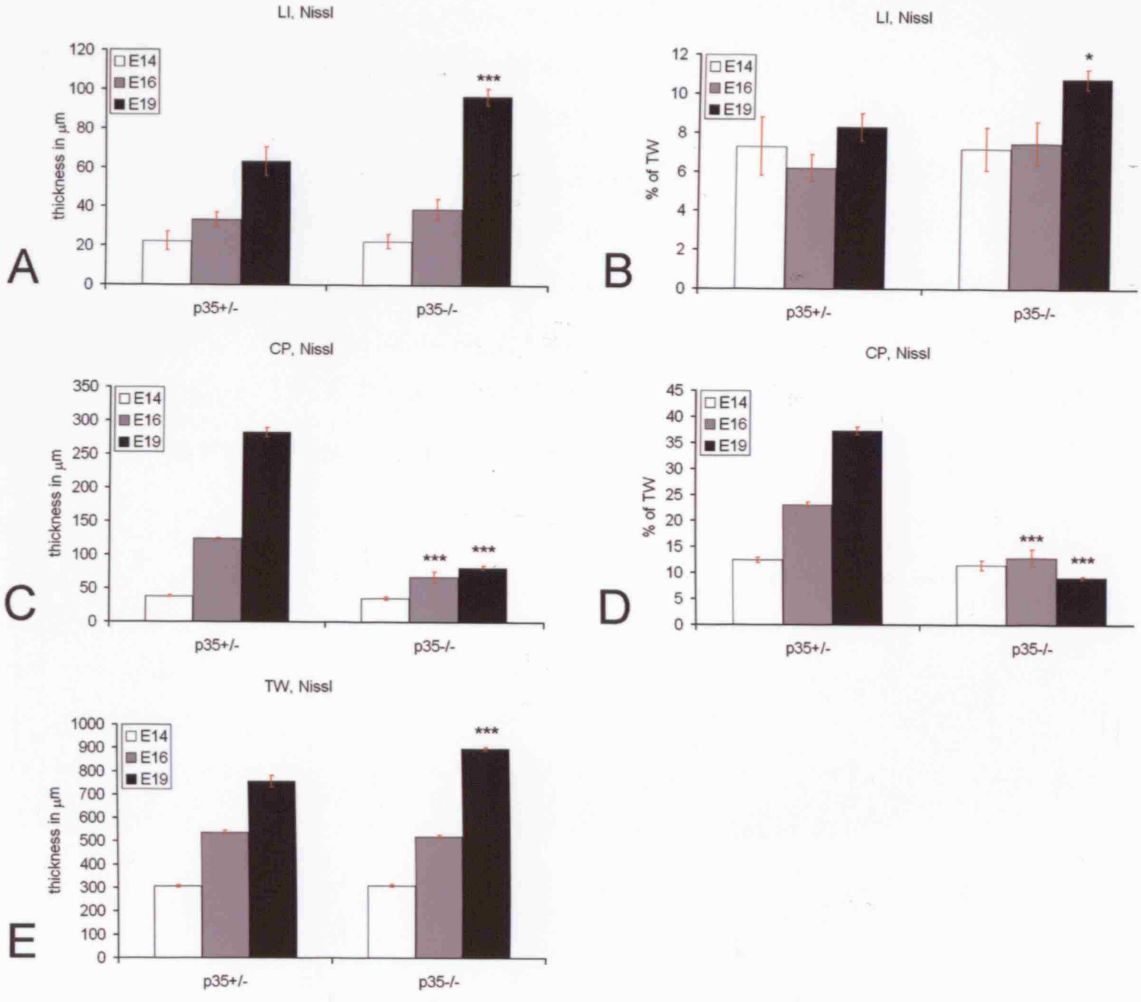
A
LI, Nissl
thickness in µm
E14
E16
E19
p35+/-
p35-/-
***
B
LI, Nissl
% of TW
*
C
CP, Nissl
D
CP, Nissl
E
TW, Nissl

Figure 3-3. Loss of Cdk5 activity markedly alters the morphology of the perinatal developing neocortex

Semi-thin (1 μm) sections of the cerebral cortex were stained with Nissl (toluidine blue) at E19.5.

(A) The morphology of cortical layers in *p35* +/- mice.

(B) The compact CP was thin in *p35* -/- mice; arrows point to empty spaces, between compact CP cells, where fibres run. Also, the IZ was atypically thick and cellular, containing ectopic CP cells.

(C) LI sparse cell population clearly separated from underlying CP in *p35* +/- mice.

(D) In *p35* -/- mice, LI was unusually thick and cellular, and with no clear border with the compact CP.

LI – layer I; CP – cortical plate; cCP – compact cortical plate; SP – subplate; IZ/eCP intermediate zone/ectopic cortical plate; SVZ – subventricular zone; VZ – ventricular zone. Scale bars, 50 μm (A-B); 25 μm (C-D).

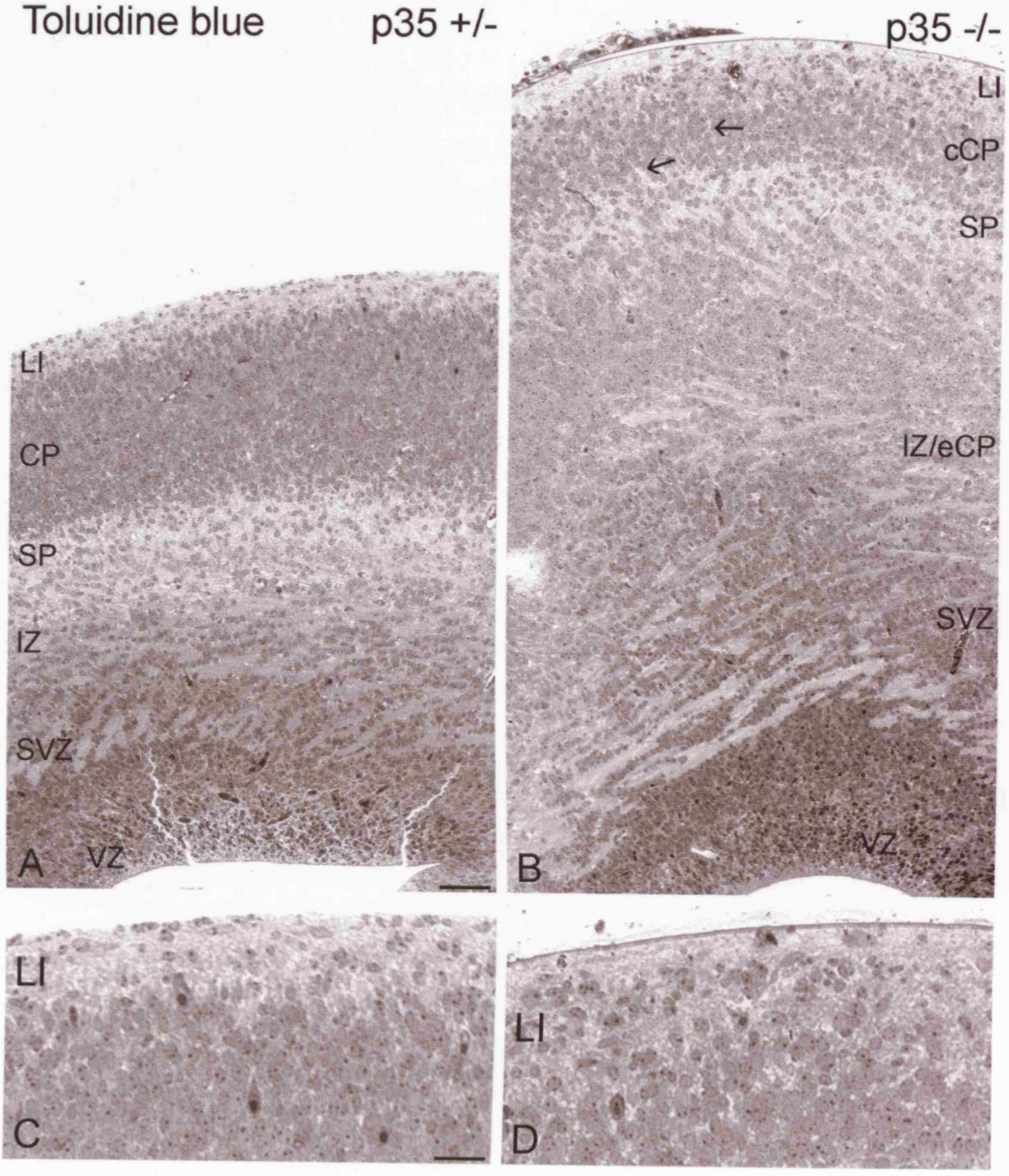
Toluidine blue
p35 +/-
p35 -/-
LI
CP
SP
IZ
SVZ
VZ
A
LI
cCP
SP
IZ/eCP
SVZ
VZ
B
LI
C
LI
D

Figure 3-4. Loss of Cdk5 activator p35 alters postnatal forebrain cytoarchitecture

P12 mouse forebrain cut coronally, at anterior commissure (ac) level (A-B,E-F, I,K) and rostral hippocampal (hipp) level (C-D, G-H, J,L), and stained with Nissl (thionin). (A-D) Low magnification; (E-H) High magnification.

(A,E) Rostral forebrain; *p35* +/- mice. Note presence of distinguishable layers and white matter.

(B,F) Rostral forebrain; *p35* -/- mice. Cortical layers were indistinct and white matter absent.

(C,G) Caudal forebrain; *p35* +/- mice. Note presence of the barrels (*).

(D,H) Caudal forebrain; *p35* -/- mice. Barrels were invisible. Hippocampal pyramidal neurons were spread within and outside the pyramidal layer (arrow; H).

(I-L) Absolute thickness of the telencephalic wall, including grey and white matter, was measured at rostral (I,K) and caudal (J,L) levels. (I,J) Black lines on drawings, taken from (Paxinos and Watson, 1982), depict cortical areas (M,SS,O) where measured. (K-L) The TW was significantly thicker in M and SS areas of the *p35* +/- compared to the control mice. The results were expressed as mean thickness ± SEM (standard error of the mean). Error bars represent SEM. Number of brains used for quantification for each genotype was n=3; * $p<0.05$, *** $p<0.005$; Student's *t*-test.

Cx – cortex; BG – basal ganglia; m – motor; ss – somatosensory; o – olfactory; Th – thalamus; cc – corpus callosum; wm – white matter. Roman numerals designate mature neocortical layers. Scale bars, 500 μm (A-D); 200 μm (E-H).

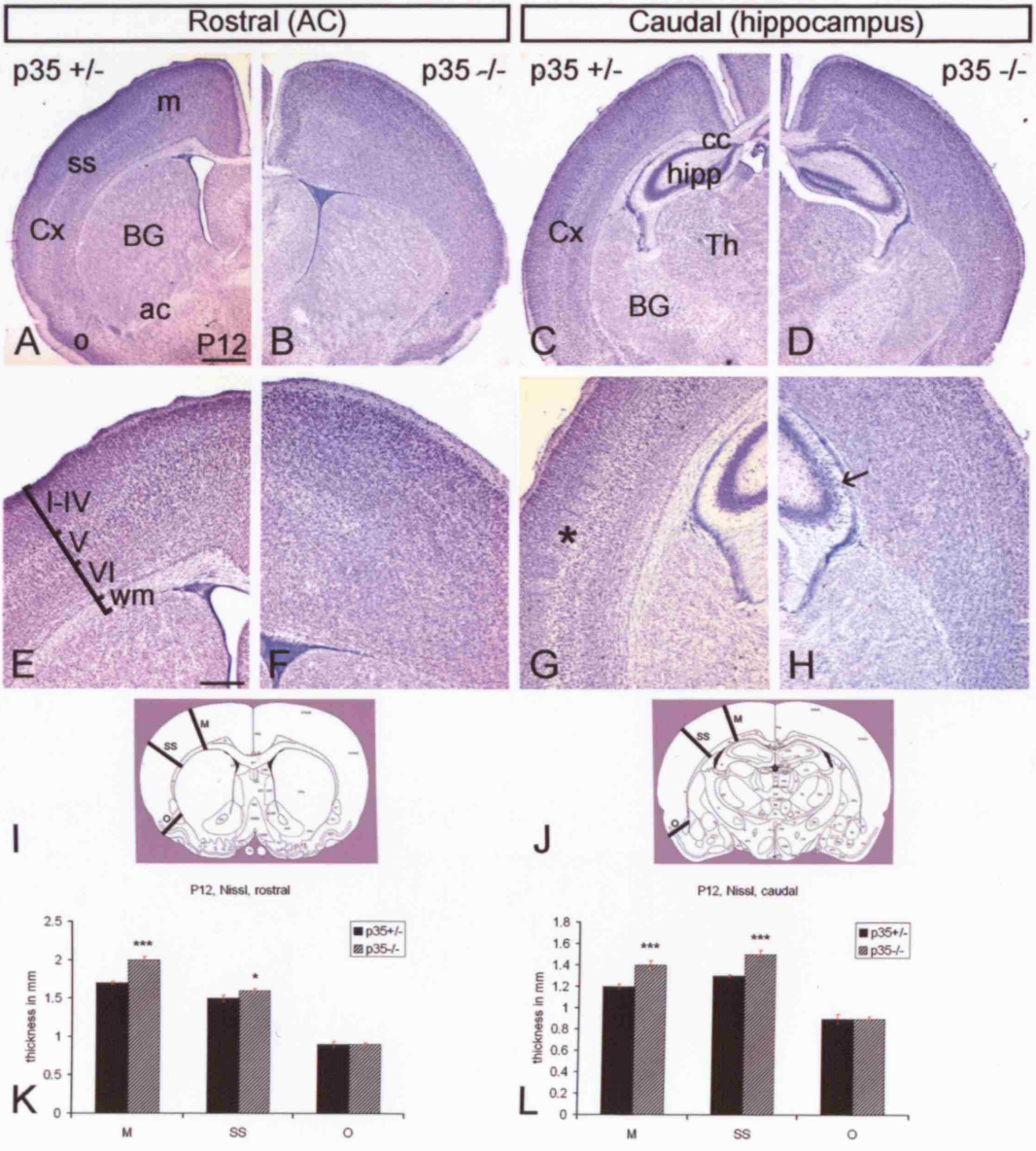
Rostral (AC)
Caudal (hippocampus)
p35 +/-
p35 -/-
m
ss
Cx
BG
ac
o
P12
A
B
cc
hipp
Th
C
D
I-IV
V
VI
wm
E
F
*
G
H
I
J
P12, Nissl, rostral
P12, Nissl, caudal
p35+/-
p35-/-
thickness in mm
K
L
M
SS
O

Figure 3-5. Inverted position of E13.5-born cortical cells in *p35* mutants

Coronal sections of P12 forebrain labelled with antibody to bromodeoxyuridine (BrdU). Injection of BrdU was given at E13.5.

(A-B) Forebrain; (A) *p35* +/-; (B) *p35* -/-.

(C-D) Cortex and hippocampus. (C) *p35* +/-; (D) *p35* -/-.

(E-F) Neocortex. In *p35* +/- (E), $BrdU^+$ cells were mainly present in the inner half of the neocortex, whilst in the *p35* -/- (D), $BrdU^+$ cells were found throughout the depth of the neocortex, although the majority of labelled cells populated the outer half of the cortex.

Cx – cortex; BG – basal ganglia; hipp – hippocampus; Th – thalamus. Roman numerals designate mature neocortical layers. Scale bars, 500 μm (A-B); 200 μm (C-D); 100 μm (E-F).

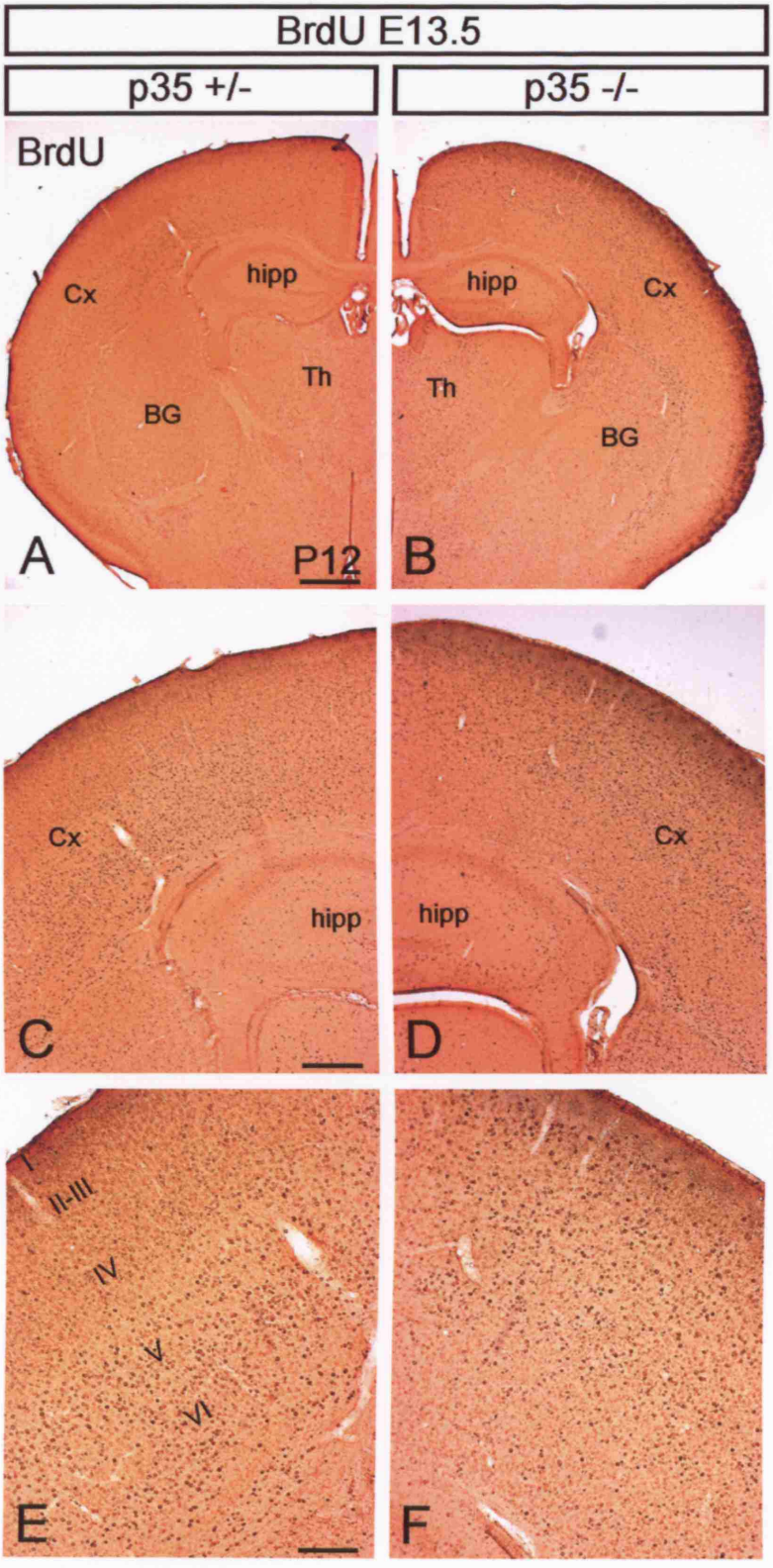
BrdU E13.5
p35 +/-
p35 -/-
BrdU
Cx
hipp
Th
BG
A
P12
B
C
D
I
II-III
IV
V
VI
E
F

Figure 3-6. Misplaced E15.5-born cortical cells in *p35* mutants

Coronal sections of P12 forebrain labelled with antibody to bromodeoxyuridine (BrdU). Injection of BrdU was given at E15.5.

(A-B) Forebrain. (A) *p35* +/-; (B) *p35* -/-.

(C-D) Cortex and hippocampus. (C) *p35* +/-; (D) *p35* -/-.

(E-F) Neocortex. In *p35* +/- (E), $BrdU^+$ cells were present in the superficial layers of the neocortex (layers II-IV), whilst in the *p35* -/- (D), $BrdU^+$ cells populated two areas; with most of the labelled cells present in the deeper half of the neocortex and a thin layer of $BrdU^+$ cells located below the pia.

Cx – cortex; BG – basal ganglia; hipp – hippocampus; Th – thalamus. Roman numerals designate mature neocortical layers. Scale bars, 500 μm (A-B); 200 μm (C-D); 100 μm (E-F).

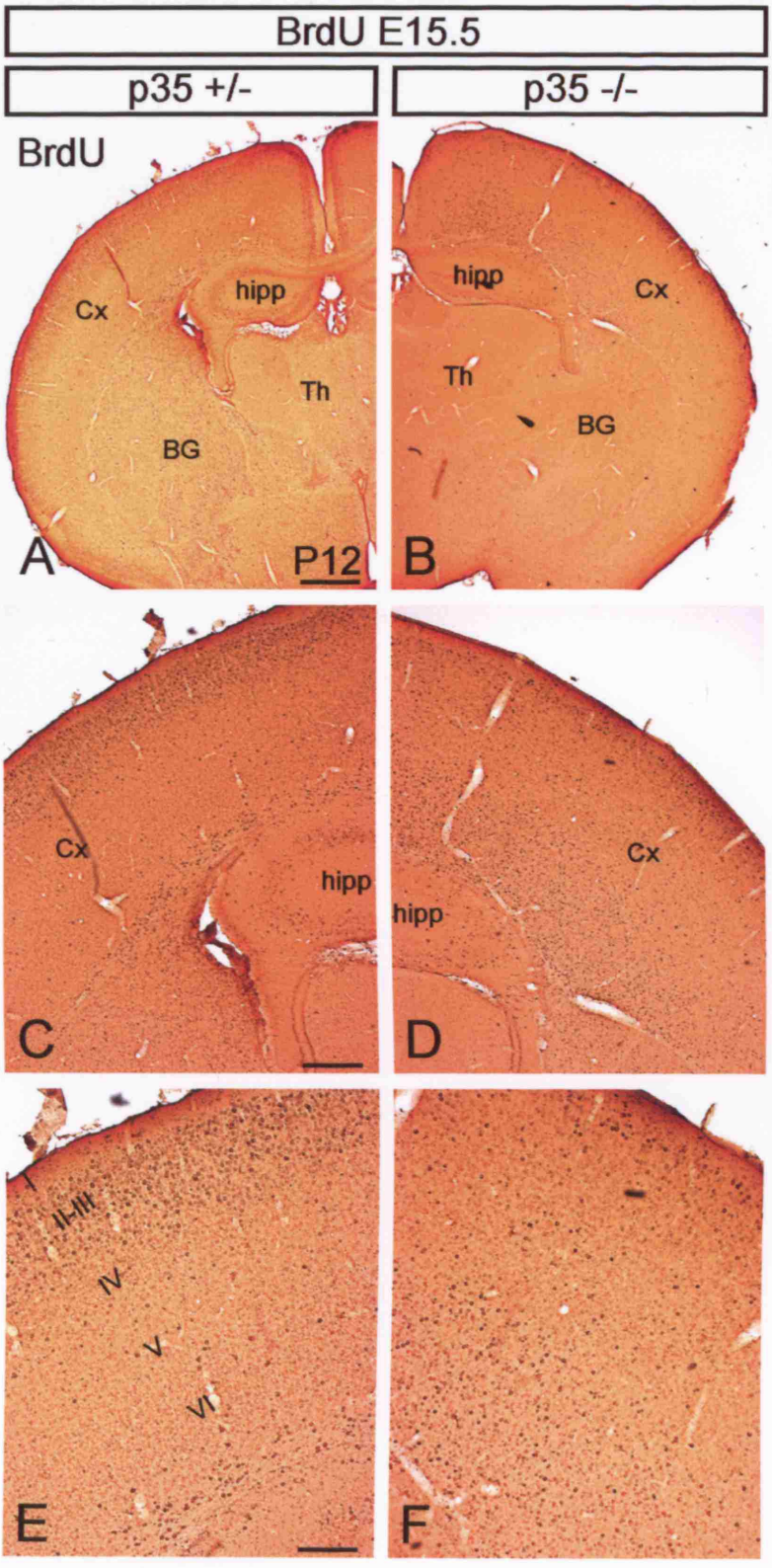
BrdU E15.5
p35 +/-
p35 -/-
BrdU
Cx
hipp
Th
BG
A
P12
B
C
D
E
F
I
II-III
IV
V
VI

Figure 3-7. Inverted position of E17.5-born cortical cells in *p35* mutants

Coronal sections of P12 forebrain labelled with antibody to bromodeoxyuridine (BrdU). Injection of BrdU was given at E17.5.

(A-B) Forebrain. (A) *p35* +/-; (B) *p35* -/-.

(C-D) Cortex and hippocampus. (C) *p35* +/-; (D) *p35* -/-.

(E-F) Neocortex. In *p35* +/- (E), $BrdU^+$ cells were present in the outmost part of the cortex (layer II), whilst in the *p35* -/- (D), $BrdU^+$ cells were found in the inner part of the cortex.

Cx – cortex; BG – basal ganglia; hipp – hippocampus; Th – thalamus. Roman numerals designate mature neocortical layers. Scale bars, 500 μm (A-B); 200 μm (C-D); 100 μm (E-F).

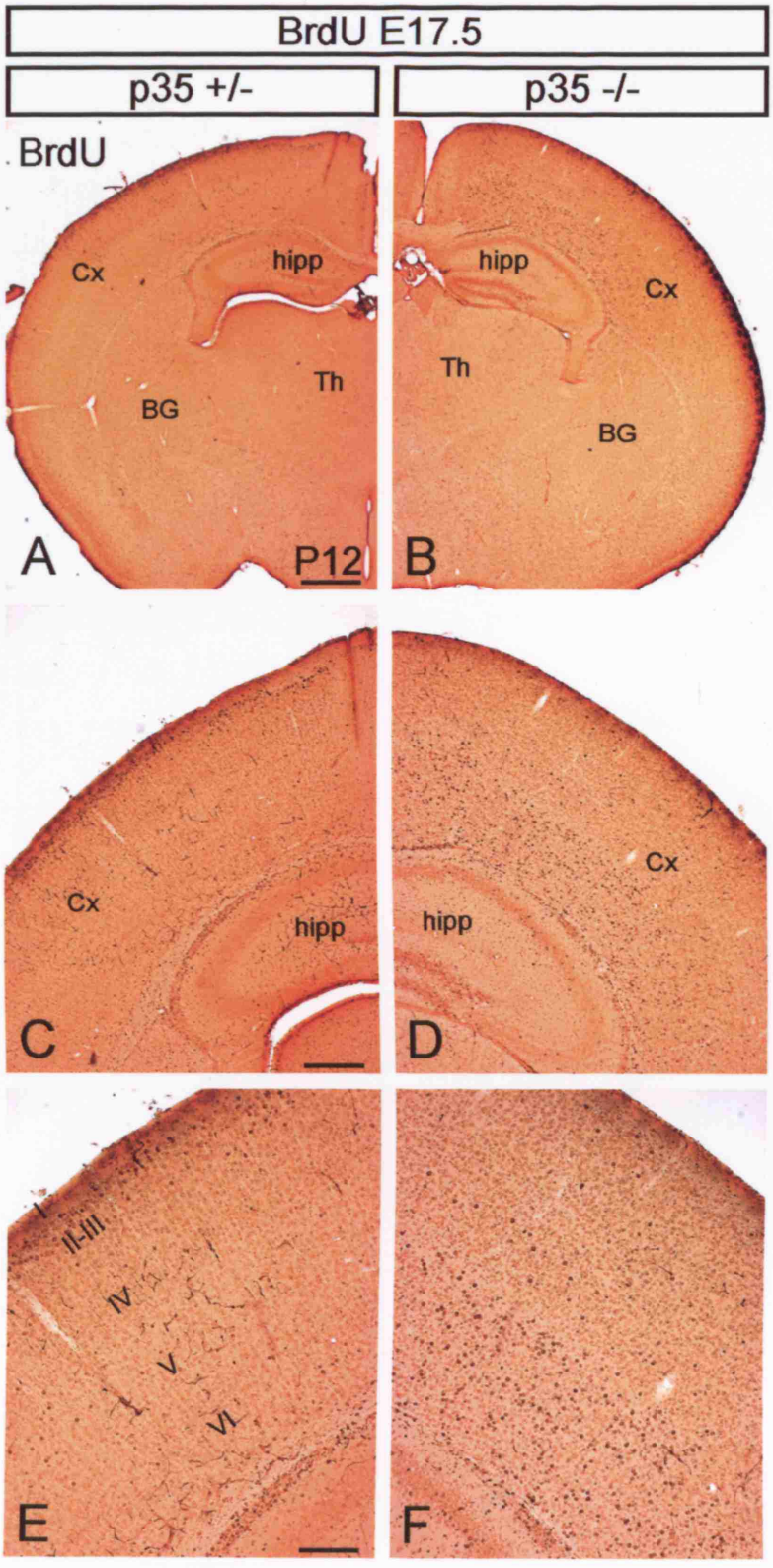
BrdU E17.5
p35 +/-
p35 -/-
BrdU
Cx
hipp
Th
BG
A
P12
B
C
D
E
F
I
II-III
IV
V
VI

Figure 3-8. Indistinct and inverse mature cortical layers in *p35* mutants

A schematic illustration of neuronal birthdating experiments, depicting a defect in neuronal migration in *p35* mutant mice. Neuronal progenitors were labelled with bromodeoxyuridine (BrdU) at E13.5 (A-B), E15.5 (C-D), and E17.5 (E-F). Position of $BrdU^+$ cells in the neocortex were analyzed at P12. Each dot corresponds to a single $BrdU^+$ cell. Dotted panels represent the overall distribution but not the real number of $BrdU^+$ cells in the neocortex. Roman numerals designate mature neocortical layers.

(G-H) Dotted panels, representing cells born at E13.5 (red), E15.5 (yellow), and E17.5 (green), were superimposed in order to illustrate relation between the layers born at different times. In *p35* +/- (G), the neocortical layers were well separated and made in an 'inside-out' fashion, whilst in *p35* -/- (H), these layers were mixed and generated mostly in an inverted, 'outside-in' manner.

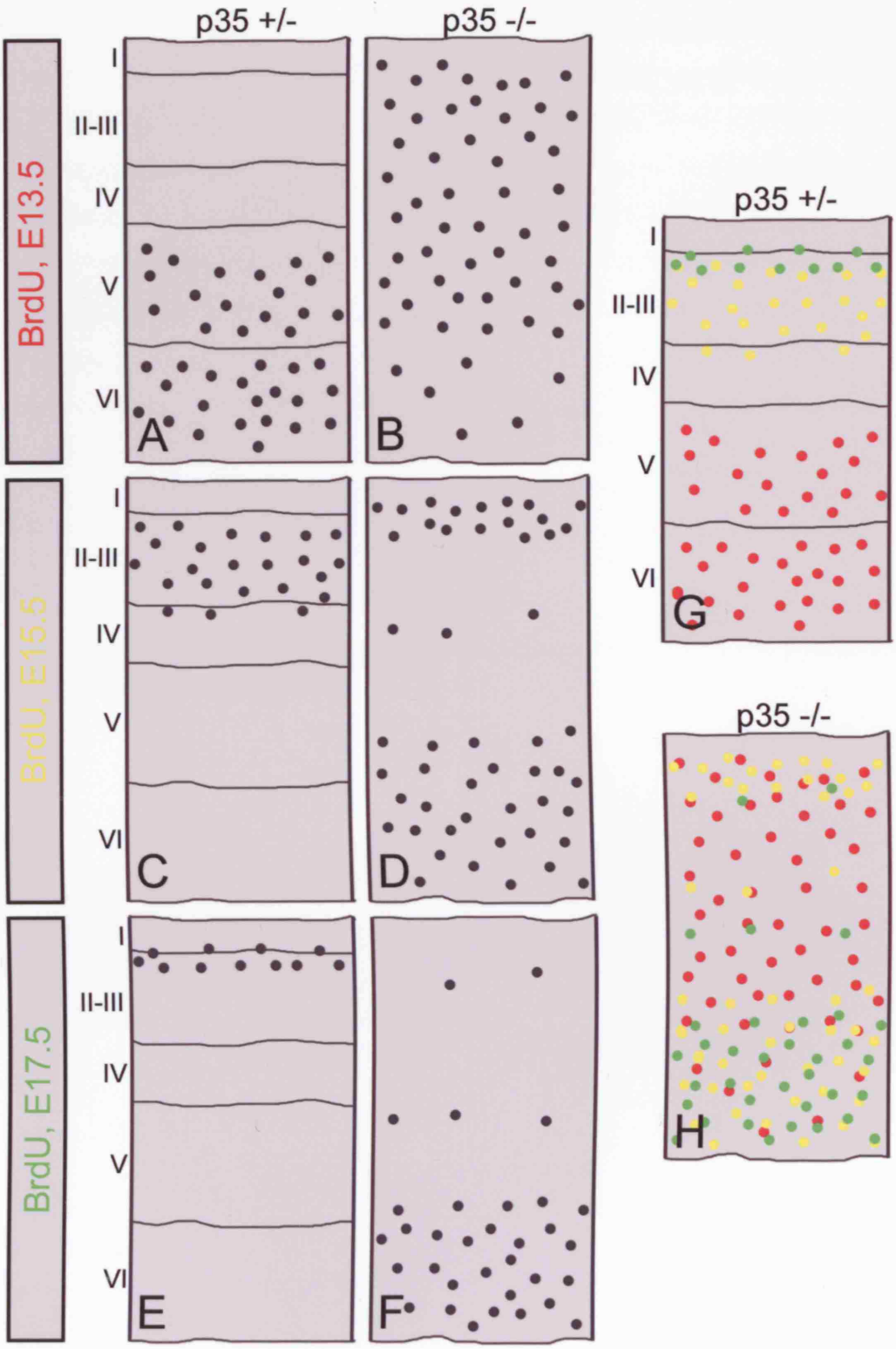
p35 +/-
p35 -/-
BrdU, E13.5
BrdU, E15.5
BrdU, E17.5
I
II-III
IV
V
VI
A
B
C
D
E
F
p35 +/-
p35 -/-
G
H

Figure 3-9. Cortical projection neurons and axons are misplaced in *p35* mutants
Coronal sections of P12 forebrain labelled with antibody to neurofilament (NF) proteins at rostral (A,B) and caudal (C-D) levels.
In control mice (A,C), NF^+ neurons were found in layer V (large neurons; large arrows) and layers II-III (small neurons; small arrows); NF^+ fibres were located below the cortex (open arrow). In *p35* mutant mice (B,D), large NF^+ neurons (large arrows) were mostly present in the superficial part of the cortex, whilst small NF^+ neurons (small arrows) were found in the lower half of the cortex, intermingled among NF^+ fibres that ran through the cortex (open arrow). Roman numerals designate mature neocortical layers. Scale bars, 200 μm.

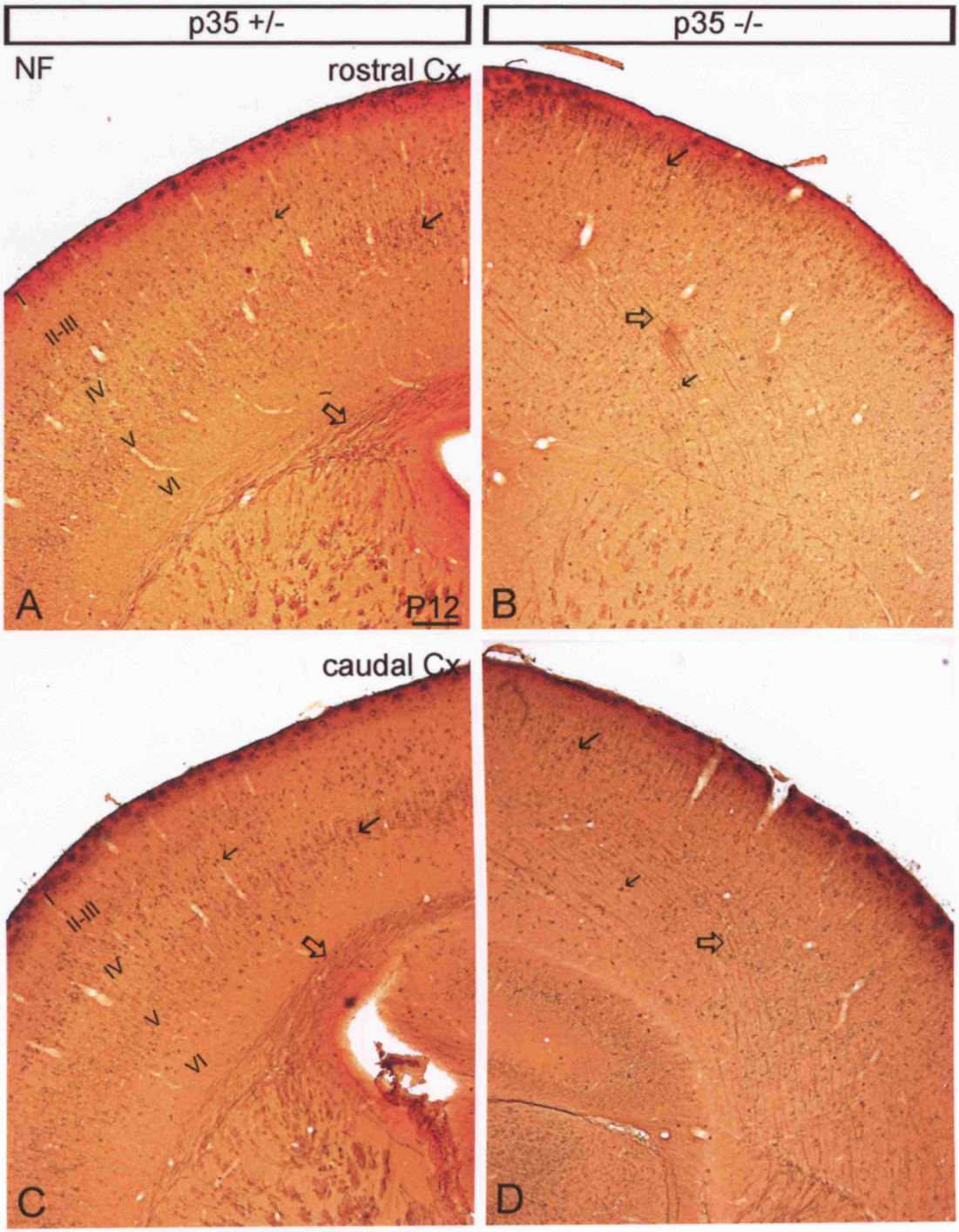
p35 +/-
p35 -/-
NF
rostral Cx
caudal Cx
I
II-III
IV
V
VI
A
B
C
D
P12

Figure 3-10. Loss of radial orientation of the apical dendrites in *p35* mutants

Coronal sections of P12 forebrain labelled with antibody to microtubule-associated protein 2 (MAP2).

(A-B) Forebrain. (A) *p35* +/-; (B) *p35* -/-.

(C-D) Cortex and hippocampus. (C) *p35* +/-; (D) *p35* -/-.

(E-F) Neocortex. In *p35* +/- (E), $MAP2^+$ apical dendrites of projection neurons were radially arranged. The radial alignment of apical dendrites was not observed in the *p35* -/- (D).

Cx – cortex; BG – basal ganglia; hipp – hippocampus; Th – thalamus. Scale bars, 500 μm (A-B); 200 μm (C-D); 100 μm (E-F).

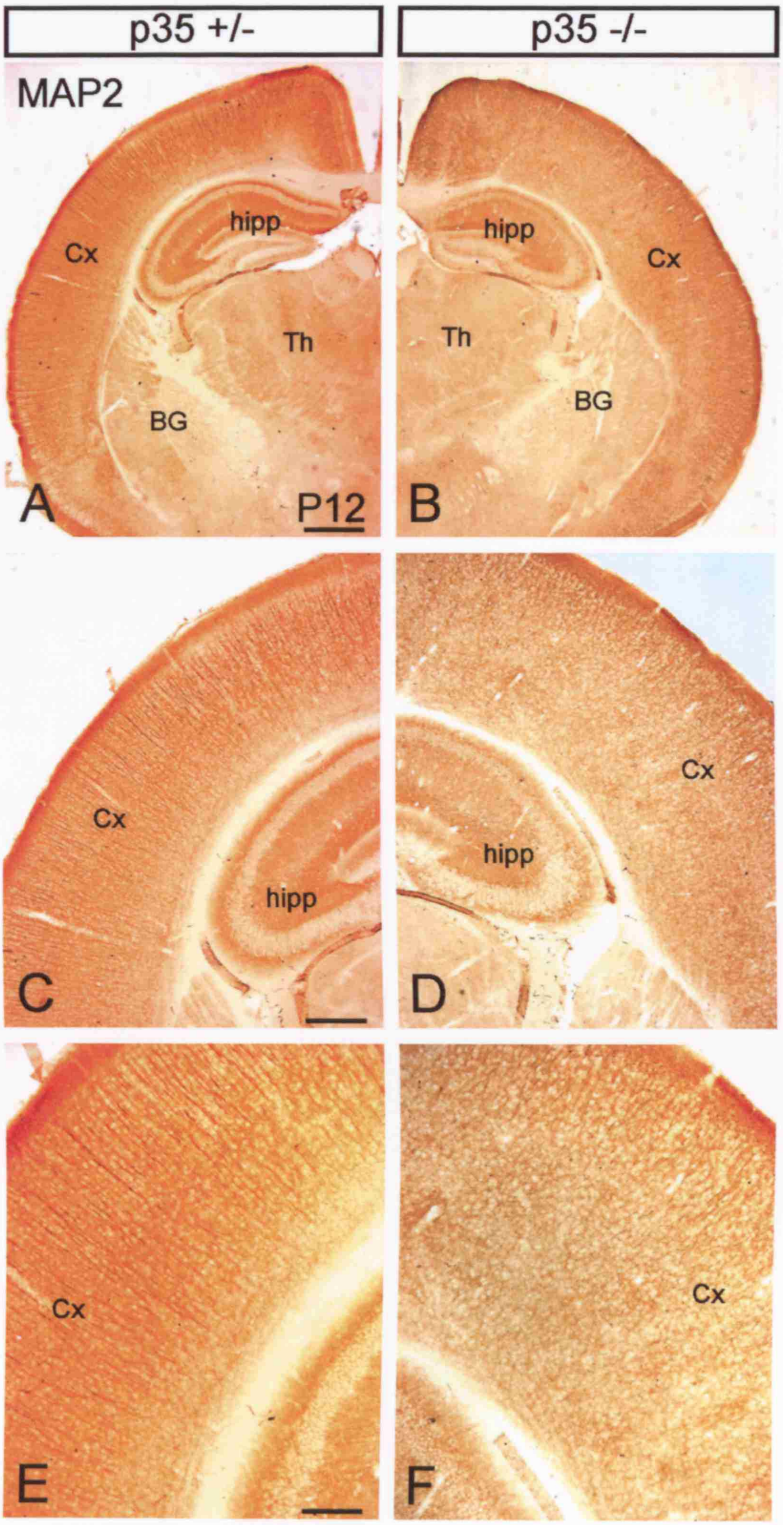
p35 +/-
p35 -/-
MAP2
hipp
Cx
Th
BG
A
P12
B
C
D
E
F

Figure 3-11. Astrocytes are misplaced in *p35* mutants

Coronal sections of P12 forebrain labelled with antibody to glial fibrillary acidic protein (GFAP).

(A-B) Cortex and hippocampus. (A) *p35* +/-; (B) *p35* -/-.

(C-D) Neocortex. In *p35* +/- mice (C), $GFAP^+$ astrocytes were found in white matter (wm) and in most inner (layer VI) and most outer (layer I) parts of the cortex. In *p35* -/- mice (D), $GFAP^+$ astrocytes were rarely scattered in the cortex.

(E-F) Hippocampus. In *p35* +/- (E), $GFAP^+$ astrocytes were sparsely populated in the pyramidal layer (p) of the hippocampus, whilst in the *p35* -/- (F), $GFAP^+$ astrocytes invaded this layer.

Cx – cortex. Roman numerals designate mature neocortical layers. Scale bars, 200 μm (A-B); 100 μm (C-F).

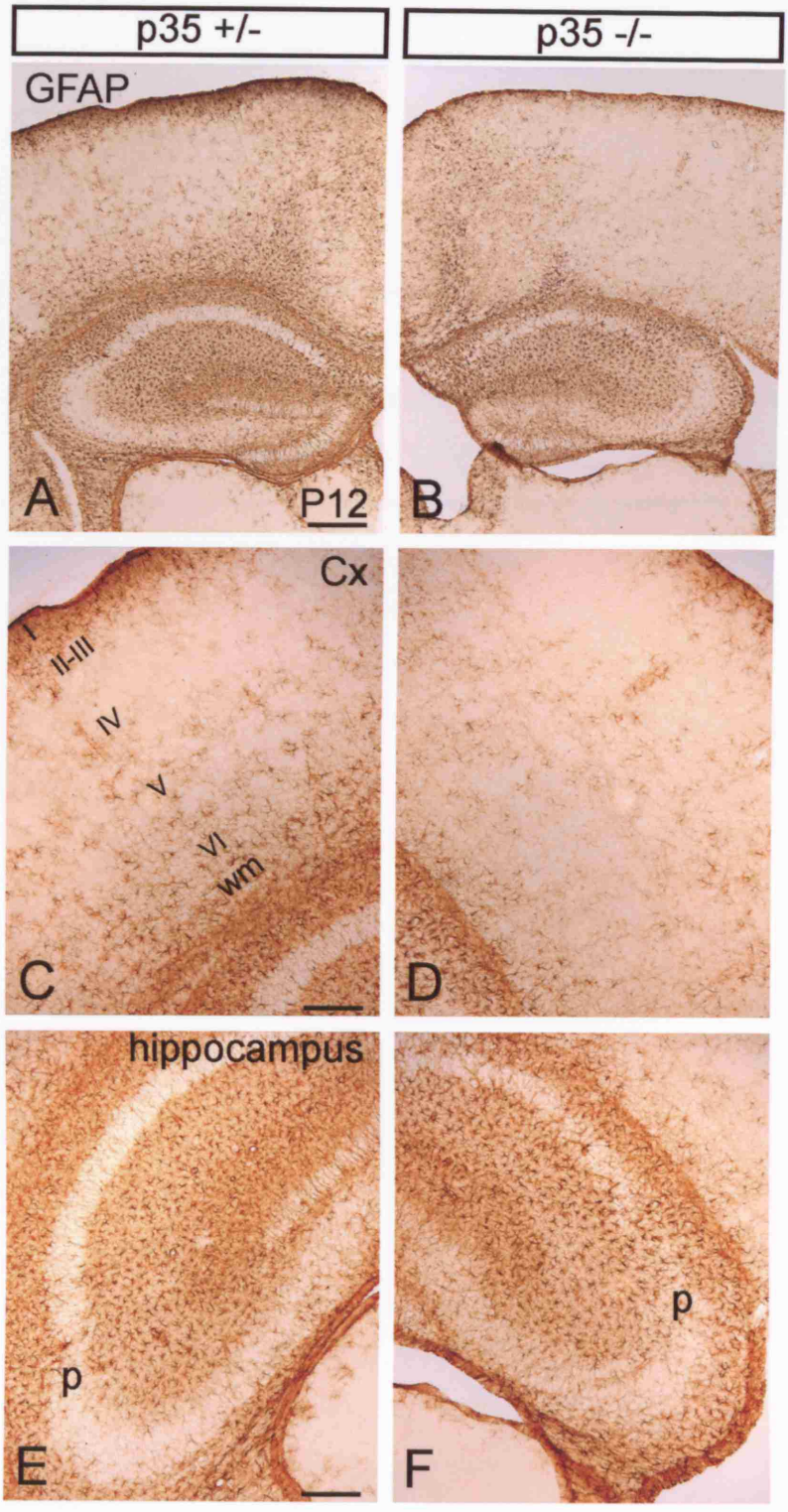
p35 +/-
p35 -/-
GFAP
A
P12
B
Cx
I
II-III
IV
V
VI
wm
C
D
hippocampus
p
E
p
F

Table 3-1. Position of $BrdU^+$ cells in the neocortex

	$BrdU^+$ cells in the neocortex at P12	
	p35 +/-	*p35 -/-*
E13.5	Layers V,VI	Depth of cortex
E15.5	Layers II,III,IV	Lower (thick band) and upper (thin band) cortex
E17.5	Layer II	Lower cortex (1/3 of total)

CHAPTER 4A

An inward migration defect of cortical interneurons in *p35* mutants

INTRODUCTION

Cortical interneurons originate from the ventral telencephalon and populate the cortex in a layer-specific manner (for reviews see Parnavelas, 2000; Corbin et al., 2001; Marin and Rubenstein, 2001; Marin and Rubenstein, 2003). Initially, cortical interneurons travel tangentially in the developing cortex in defined streams through the PPL and SVZ/lowerIZ and, after PPL splitting, through LI, SP and SVZ/lowerIZ. The tangential routes and some of the molecular mechanisms that govern cortical interneuron migration have been the subject of intensive investigation recently (reviewed by Marin and Rubenstein, 2003).

Little is known about how interneurons become incorporated into the CP. It has been suggested that they first spread tangentially throughout the cortex, travelling in all directions within LI (Ang, Jr. et al., 2003; Tanaka et al., 2003) or from lateral to medial cortex, in the SVZ (Tanaka et al., 2003), seeking appropriate areas in which to reside (termed areal distribution by Ang, Jr. et al., 2003). Once cortical interneurons find their areal identity, they migrate radially towards the CP in search of the correct layer. It has been reported recently that these cells enter the CP by inward migration from LI (Polleux et al., 2002; Ang, Jr. et al., 2003; Tanaka et al., 2003; Hevner et al., 2004), and by outward migration, from the SVZ/IZ (Polleux et al., 2002; Tanaka et al., 2003; Hevner et al., 2004). However, these two radial movements do not explain how cortical interneurons find the right layer.

It has been proposed that cortical interneurons, just like projection cells, settle in an 'inside-out' order, and that isochronically-born cortical interneurons and projection neurons exist in the same cortical layer (Miller, 1985; Fairen et al., 1986; Peduzzi, 1988; Anderson et al., 2002; Ang, Jr. et al., 2003; Valcanis and Tan, 2003; Hevner et al.,

2004). However, it is still unknown whether cortical interneurons follow the 'inside-out' law of positioning by communicating with projection neurons/radial glia or whether they travel independently. Also, there is a question as to where these cells receive laminar information, either during their tangential route or later on, along the cortical radial axis. It has been suggested that the laminar cues for migrating cortical interneurons may be present in the cortical VZ (Nadarajah et al., 2002). Finally, the laminar signals that lead cortical interneurons to the correct position remain unknown. Mice that have cortical laminar defects could serve as a tool to study mechanisms of radial migration and lamina-specific settlement of cortical interneurons.

Recent studies proposed a Reelin-independent (Hevner et al., 2004) and p35/Cdk5-independent (Gilmore and Herrup, 2001; Patzke et al., 2003; Hammond et al., 2004) mechanism of cortical interneuron migration. However, data on expression of the p35/Cdk5 complex in cortical interneurons and related Cdk5 activity are not available. Moreover, there is lack of a detailed study of the morphology and distribution of cortical interneurons in *p35* and *Cdk5* mutants that might give insight into how these cells correctly become incorporated into the cortex.

MATERIALS AND METHODS

Animals

The embryonic and postnatal brains from *p35* and *Cdk5* litters were fixed and used for immunohistochemistry procedures. Alternatively, embryonic cortices and GE from the *p35* litters were used for preparing cell lysates for *in vitro* kinase assay or primary neuronal cultures for immunocytochemical expression studies. Also, embryonic slice cultures were used for CMFDA experiments, and MGE cells for *in vitro* migratory assay.

Dissociated cell cultures

Primary neuronal cultures of cerebral cortex and MGE were obtained according to the protocol described in general Materials and Methods. The cortical and MGE cells were

grown on poly-L-lysine/laminin coated coverslips and incubated in DCC medium at 37°C in a 5% CO_2 humidified incubator for 1 or 3 days *in vitro* (DIV). The medium was changed daily. The cells were then fixed in prewarmed 4% PFA for 20 min at room temperature and subjected to immunocytochemical staining.

Immunocytochemistry and immunohistochemistry

The immuno-labelling of the mouse tissue was performed as described in general Materials and Methods. In brief, the cells or vibratome sections were incubated overnight at room temperature with the following primary antibodies: rabbit anti-p35, mouse anti-Cdk5, rabbit anti-GABA, rabbit anti-CB, mouse anti-TAG1, and rabbit anti-CalR. The reaction was visualized by either immunofluorescence or immunoperoxidase method. The cell nuclei and overall cytoarchitecture were revealed using bisbenzimide- or thionin-staining.

Quantification of interneurons in the cortex

(i) Embryonic

For quantification of CB^+ cells in the embryonic cortex of control and *p35* mutant mice, a radial column, 100 μm wide, of the lateral developing cortex, was divided in three 'stripes' containing LI/SP/CP, IZ, and SVZ/VZ, and CB^+ cells were counted in each 'stripe'. The relative number of CB^+ cells in each stripe was calculated as a percentage of total number of CB^+ cells in all three stripes. The absolute and relative numbers of CB^+ cells were expressed as mean ± standard error of the mean (SEM). At least 3 brains from each genotype were used for analysis. In addition, the absolute and relative thicknesses of the 'stripes' were calculated in the same way.

(ii) Postnatal

For quantification of CB^+ or $CalR^+$ cells in the postnatal cortex of control and *p35* mutant mice, a radial column, 100 μm wide, of the somatosensory or motor cortex, was divided in twenty equal bins, and CB^+ or $CalR^+$ cells were counted in each bin. The relative number of CB^+ or $CalR^+$ cells in each bin was calculated as a percentage of total

number of CB^+ or $CalR^+$ cells in all bins, and was expressed as mean percentage ± SEM. At least 3 brains from each genotype were used for analysis.

In vitro kinase assay

The Cx and GE, obtained from *p35* +/- and *p35* -/- mice, were homogenized in the Cdk5 lysis buffer. Cdk5 was isolated from the cell lysates by immunoprecipitation. In brief, 40 µl of mouse anti-Cdk5 antibody was incubated with 200 µl of lysates at 4°C for an hour. 100 µl of Protein G sepharose beads, prepared as 10% solution in Cdk5 lysis buffer, were then added, and the suspension was incubated for another hour at 4°C on a shaking platform. Immunoprecipitates were washed three time with lysis buffer and three times with kinase buffer (30mM HEPES, pH 7.2, 10mM $MgCl_2$, 5 mM $MnCl_2$, 1mM DTT). The washed beads were then incubated with kinase buffer containing 2 µg of histone H1 and 1 µCi(^{32}P)γATP in a final volume of 50 µl for 30min at room temperature. After incubation, 50 µl of 2x sample buffer was added and the samples were processed for SDS-PAGE and autoradiography.

In vitro migratory assay (Boyden chamber)

The chemotactic assay, using E13.5 MGE-derived cells, obtained from *p35* +/- or *p35* -/- mice, and 10% FBS as a chemoattractant, was performed exactly as described in general Materials and Methods.

Organotypic slice cultures and CMFDA tracing experiments

Organotypic slice cultures of embryonic (E13.5 and E14.5) mouse forebrain were prepared as described in general Materials and Methods. Brains slices 300 µm thick were mounted onto porous nitrocellulose filters and transferred into 24-well sterile culture dishes containing 500 µl of medium. They were subsequently incubated for an hour in a sterile incubator (37°C, 5% CO_2) prior to application of the tracer dye. CMFDA (5-chloromethylfluorescein diacetate; Molecular probes) is a dye that freely diffuses through the membranes of live cells. To label live migrating interneurons in the

organotypic forebrain slices CMFDA-coated tungsten particles were pushed into the MGE (Alifragis et al., 2002). After applying the dye, the slices were incubated in the 'slice' medium for 36-48 hours to follow the migration of neurons.

Coating of tungsten particles with CMFDA

CMFDA (1mg) was dissolved in DMSO to yield a stock solution of 10mM, and subsequently diluted in ethylene dichloride (ED) to yield a concentration of 1mM. Fifty micrograms of tungsten particles (0.8μm; Bio-Rad) were spread evenly as a thin layer on a glass microscope slide to which 100μl of CMFDA in ED was added. As the solvent evaporated, the precipitated dye was mixed well with the particles (using a blade) to ensure complete coating. The coated particles were stored at 4°C and applied with aids of glass micropipettes.

Quantification of CMFDA-positive cells

For quantification of $CMFDA^+$ cells that migrated into the cortex of control and *p35* mutant mice, a radial column, 500 μm wide, of the lateral developing cortex, was divided in three equal zones, and $CMFDA^+$ cells were counted in each zone. The relative number of $CMFDA^+$ cells in each zone was calculated as a percentage of total number of $CMFDA^+$ cells in all three zones, and was expressed as mean percentage ± (SEM). 20 brains from each genotype were used for analysis.

RESULTS

Co-expression of p35 and Cdk5 in cortical interneurons and the Cdk5 activity in the developing forebrain

I first investigated whether Cdk5 and its regulatory subunit p35 were expressed in cortical interneurons, at the site of their origin (MGE) as well as in the cortex, during corticogenesis (E13.5-E18.5). Expression studies of 1- and 3-day old dissociated cell cultures of MGE and cortex were undertaken using immunofluorescence with anti-p35, -Cdk5, and -GABA antibodies. Bisbenzimide was used to label the nuclei of the cells.

MGE in *wild-type* mice contained mostly $GABA^+$ neurons (Fig.4A-1A), at E14.5, and these cells also expressed p35 protein (Fig.4A-1B). There was no p35 expression detected in the *p35* mutants (data not shown). In comparison, Cdk5 expression was found in prenatal GABAergic cortical interneurons in both *p35* +/- and *p35* -/- mice (Fig.4A-1C-H). *p35* heterozygous mice served as control in this and further experiments.

Next, the spatio-temporal profile of Cdk5 activity in control and *p35* mutant mice was studied. Cdk5 was isolated from prenatal GE and cortex (E13.5, 14.5, 18.5) and its activity was assessed by *in vitro* kinase assay. Cdk5 obtained from control GE and cortex showed activity that was developmentally regulated and increased with time. However, GE and cortex from the *p35* mutant mice showed no Cdk5 activity (Fig.4A-2). In conclusion, Cdk5 was present, but not active, in prenatal cortical interneurons in *p35* mutant mice.

Interneurons migrate from the GE towards the cortex in *p35* mutants *in vivo*

In order to label early migrating interneurons, an antibody to calbindin (CB), a calcium-binding protein, was used. The CB antibody has been found to mark a large subpopulation of interneurons in the developing mouse forebrain (Anderson et al., 1997; Ang, Jr. et al., 2003). CB^+ interneurons were found to enter the telencephalic wall in two sequential streams, earlier through the PPL (at E12.5) and later at the border between the SVZ and IZ (at E13.5). There was no apparent difference in cortical interneuron distribution, morphology and time of entering the cortex from the GE between control and *p35* mutant mice (Fig.4A-3).

Migratory properties of *p35*-deficient interneurons are altered *in vitro*

Next, a difference in migratory properties of *p35*-deficient cortical interneurons compared to the control was studied *in vitro*. To determine whether Cdk5 mediates migration of interneurons towards directional guidance cues, such as foetal bovine serum (FBS), an *in vitro* migratory assay (Boyden chamber) was performed using dissociated E13.5 MGE from *wild-type* and *p35* mutant mice. The migration of MGE-derived cells towards negative control (Neurobasal medium) did not differ between

genotypes. However, the chemotactic response to 10% FBS was robust in control and significantly reduced in *p35*-deficient MGE-derived cells (Fig.4A-4A).

In order to study the pattern of cortical interneuron migration from MGE towards the cortex *in vitro*, CMFDA experiments were carried out in organotypic forebrain slice cultures obtained from the control and *p35* mutant mice. The CMFDA crystal was placed in the MGE, at either E13.5 or E14.5, and the position of migrating $CMFDA^+$ cells in the telencephalic wall was analyzed 36-48 hours later. Results from 5 experiments for each age indicated that $CMFDA^+$ cells coming from the MGE certainly migrated into the cortical anlage in both genotypes. However, a significant difference in distribution of $CMFDA^+$ cells in the *p35* mutant mice was found; they tended to populate proliferative zones significantly more than in the control slices (Fig.4A-4B-E).

Prenatal distribution and number of cortical interneurons in control mice, *p35* and *Cdk5* mutants

To further investigate the position and number of cortical interneurons in control mice and in *p35* or *Cdk5* mutants, immunoperoxidase (DAB) or immunofluorescence techniques were carried out using anti-CB antibody, in conjunction with Nissl staining which was used to determine the position of cortical layers. CB^+ cells were examined in three telencephalic wall 'stripes' containing: 1) LI/CP/SP, 2) IZ, and 3) SVZ/VZ.

The number, but not pattern of distribution, of CB^+ cells is different in p35 mutants

CB^+ cells in control or *p35* mutant mice at E16.5 exhibited the morphology of migrating neurons, and were found in defined regions in the upper (LI/CP/SP) and lower (SVZ) cortical wall, and rarely scattered in the IZ (Fig.4A-5A,B). CB^+ cells in control mice were mainly tangentially oriented (Fig.4A-5C), whilst their orientation in *p35* mutants was multidirectional, especially within the LI/CP/SP stream (Fig.4A-5D). The distribution of CB^+ cells in the cortex of control and *p35* mutant mice at E19.5 was similar to that of E16.5 (Fig.4A-6A,B). In both ages, regardless of the genotype, CB^+ cells seemed to be mainly located in the LI/CP/SP 'stripe', and only rarely in the IZ and SVZ/VZ.

To precisely determine the absolute and relative contribution of CB^+ cells in each 'stripe' for the two genotypes, CB^+ cells were counted and 'stripe' thickness was measured at E19.5. The number of CB^+ cells in both genotypes was highest in the LI/CP/SP 'stripe' compared to the IZ or SVZ/VZ (*p35* -/-, 155.9±7.6 vs. 26.2±2.1 or 27±1.4 cells per radial column; *p35* +/-, 118±4.8 vs. 15.8±0.7 or 17.2±0.8 cells per radial column; Fig.4A-8A). However, the number of CB^+ cells in each 'stripe' as well as the total number of CB^+ cells was higher in *p35* mutants compared to controls (LI/CP/SP, 155.9±7.6 vs. 118.2±4.8 cells per radial column; IZ, 26.2±2.1 vs. 15.8±0.7 cells per radial column; SVZ/VZ, 27±1.4 vs. 17.2±0.8 cells per radial column; TW, 209.1±10.3 vs.151.2±5 cells per radial column; Fig.4A-8A). Notably, the LI/CP/SP 'stripe' was thinner (278.3±4.4 vs. 479.8±11.4 μm) and IZ 'stripe' was thicker (530±16.5 vs. 217.5±9.1 μm) in *p35* mutant compared to control mice (Fig.4A-8B). The relative contribution of CB^+ cells in each 'stripe' was almost identical in the two genotypes (~75% in LI/CP/SP, ~10% in IZ, ~12% in SVZ/VZ; Fig.4A-8C). However, the contribution of LI/CP/SP and IZ to the total thickness of the TW was different in the two genotypes (LI/CP/SP ~ 30% in *p35* -/-, and ~ 60 % in control; IZ ~ 60 % in *p35* -/-, and 30% in control; Fig.4A-8D). In conclusion, CB^+ cells in control and *p35* mutant mice were found mostly in LI/CP/SP regardless of its thickness. Rarely, CB^+ cells were observed in IZ and SVZ/VZ.

Accumulation of CB^+ cells in LI in p35 and Cdk5 mutants

In control mice, at E19.5, CB^+ cells in LI/CP/SP were distributed evenly (Fig.4A-6A,C). However, in *p35* mutant mice there was an increase of CB^+ cells close to the pia (Fig.4A-6B,D). To more accurately determine the position of CB^+ cells, immunofluorescence histochemistry was performed on coronal cortical sections using an antibody to CB to label interneurons, and bisbenzimide to mark developing layers. These experiments clearly showed an accumulation of CB^+ cells in LI of *p35* mutants (Fig.4A-7B,D,F), whereas these cells were sparsely observed in LI of control mice (Fig.4A-7A,C,E).

An atypical distribution of cortical CB^+ cells, observed in *p35* mutants, was also seen in *Cdk5* mutants at E15.5 and E18.5. In *Cdk5* +/+, *Cdk5* +/-, and *Cdk5* -/-, at E15.5, CB^+ cells were mainly confined to LI/CP/SP and SVZ regardless of the compact CP

thickness (Fig.4A-9A,B,C) as found in the *p35* litters. Also, there was an obvious accumulation of CB^+ cells in LI of *Cdk5* mutants at E18.5 (Fig.4A-9F) compared to either wild type (Fig.4A-9D) or heterozygous mice (Fig.4A-9E).

Final position and number of cortical interneurons are affected in *p35* mutants

Cortical interneurons originate from the ventral forebrain and subsequently populate the cortex. This long journey finishes during the early postnatal period, determined as P7 in mice by some authors (Ang, Jr. et al., 2003). In order to study the postnatal position and number of cortical interneurons in control and *p35* mutant mice, immunohistochemical experiments were carried out at P5 and P12 on forebrain coronal sections using antibodies to CB and calretinin (CalR).

At P5, a few days before cortical neurons reach their final positions, CB^+ cells, mostly interneurons, were located in the prospective layers V and VI, and some in layer II of control animals (Fig.4A-10A,C). Interestingly, layer IV was devoid of interneurons, an observation previously reported by del Rio et al. (1992). In contrast, a significant difference in location and number of cells was observed in *p35* mutant mice compared to controls. CB^+ cells were found to be spread throughout the entire depth of the cortex in *p35* mutant mice without a gap layer, as was noted in *p35* +/- mice (Fig.4A-10B,D). There was a significant accumulation of CB^+ cells in the upper part of the cortex, just below the pial surface. The number of CB^+ cells, without accurate quantification, appeared higher in *p35* mutant compared to control cortices.

Next, P12 forebrain was cut and analyzed at two levels: anterior commissure (ac) and rostral hippocampus, as well as in the dorsomedial (motor – M – cortex) and ventrolateral (somatosensory – SS – cortex) regions of each coronal plane. CB- and CalR- immunostained forebrain sections, obtained from *p35* +/- and *p35* -/- genotypes, were then subjected to qualitative and statistical analyses.

CB^+ cells were found to predominantly populate the lower parts of the control cortex, particularly layer V (Fig.4A-11A), while the same cells resided in the upper cortex of the *p35* null mice (Fig.4A-11B). $CalR^+$ cells were present mostly in the upper parts of the control cortex (layers II-IV), and $CalR^+$ fibres ran within the white matter, below the cortex (Fig.4A-11C). In contrast, in *p35*-deficient mice, $CalR^+$ cells were

spread evenly in the cortex, above and below CalR$^+$ fibres running within the cortex (Fig.4A-11D).

To accurately determine the distribution of the interneurons in the cortex, CB$^+$ and CalR$^+$ were counted in 20 bins of either SS or M cortex (bin 1 closest to the white matter), and the relative percentage of cells per bin were plotted in horizontal bar graphs (Fig.4A-12). In control P12 somatosensory and motor cortex, CB$^+$ cells were mainly found in layer V (bins 6-10; Fig.4A-12A,B). In *p35* mutant mice, these cells were mainly located in the central part of the somatosensory (bins 9-14; Fig.4A-12A) and upper part of the motor cortex (bins 15-19; Fig.4A-12B). In control mice, CalR$^+$ cells were most abundant in layers II-IV of both somatosensory and motor cortex (bins 12-18; Fig4A-12C,D). The density of CalR$^+$ cells in *p35* mutant somatosensory and motor cortex had two peaks, in the lower and upper cortices (bins 5-10 and bins 16-20; Fig4A-12C,D), and this was more distinct in the motor cortex. In conclusion, the inverted distribution of CB$^+$ and CalR$^+$ cells in *p35* mutant mice was more pronounced in the dorsomedial cortex.

The number of CB$^+$ and CalR$^+$ cells was also altered in *p35* mutants compared to their control littermates. There was a significant increase in the number of CB$^+$ cells in both somatosensory and motor areas of the *p35*-deficient cortex (SS: 107.3±5.9 vs. 81.1±3.7; M: 165.3±6 vs. 110.7±5.9 cells per radial column; Fig.4A-13A). CalR$^+$ cells were more numerous in the somatosensory cortex in the *p35* null mice compared to control (111.6±9.3 vs. 83±6.7 cells per radial column; Fig.4A-13B). No difference in the number of CalR$^+$ cells in the motor cortex was observed between the two genotypes (102.86±7.9 vs. 100.7±9.4 cells per radial column; Fig.4A-13B).

DISCUSSION

In this study, I described for the first time that cortical interneurons expressed p35 and Cdk5. I also observed that, in *p35* mutant mice, Cdk5 was not active in the prenatal telencephalon. Whether cortical interneuron migration is Cdk5-dependent or -independent is still an open question.

Some studies, using chimeras, suggested a Cdk5-independent mechanism of cortical interneuron migration. In these chimeric models, wild-type cells were mixed

with either *p35* (Hammond et al., 2004) or *Cdk5* (Gilmore and Herrup, 2001) mutant cells. The main finding that came from these chimeric studies is that interneurons from both genotypes, wild-type and mutant, appear capable of migrating into the cortex consisting of either mutant or wild-type cells. However, these studies did not consider the laminar fate of cortical interneurons in the mutants.

Cdk5-independent migration of cortical interneurons from the ventral telencephalon

Cortical interneurons, in both *p35* and *Cdk5* mutants, have no problem entering the cortex from the ventral telencephalon and at the same time as control mice. This suggests that the initial migration of cortical interneurons to the cortex does not depend on Cdk5 and is in accord with findings using chimeric models. However, abnormal kinetics and morphology of *p35*-deficient interneurons were found in this study. In the migratory assay, the chemotactic response to multiple guidance cues present in FBS was impaired in the *p35* mutant compared to *wild-type* MGE-derived cells. Gilmore and Herrup (2001) suggested that the general locomotive abilities of *Cdk5*-deficient cerebellar neurons were intact. There is a possibility that cortical interneurons and cerebellar neurons do not share the same migratory properties, at least the one mediated by Cdk5. The Cdk5 pathway might also be selectively involved in different phases of interneuron migration; turned off when interneurons travel into the cortex and turned on when they are in the cortex. In accord with this hypothesis, the leading processes of *p35*-deficient interneurons in the cortex were disorganized, perhaps indicating a directional defect at the time when they are about to radially migrate into the CP.

Radial migration of cortical interneurons might be a Cdk5-dependent process

This study demonstrated that CB^+ and $CalR^+$ cells that label different subopulations of cortical interneurons were misplaced in postnatal *p35* mutant mice, after their migratory period had ceased. Also, it seems that interneurons, like $BrdU^+$ cells, followed an inverted, outside-in migration order in *p35* mutant cortex, indicating coordination in laminar positioning between cortical cells in the mutant. It has already been proposed that interneuron laminar positions may be determined through interactions with

projection neurons born on the same day (Miller, 1985; Fairen et al., 1986; Peduzzi, 1988; Anderson et al., 2002; Ang, Jr. et al., 2003; Valcanis and Tan, 2003; Hevner et al., 2004). However, if this is correct, one should expect accumulation of interneurons in the IZ of mutant mice where the ectopic CP and most of the projection neurons are found (Fig.3-1), and this is not the case. This study clearly demonstrated that most of the cortical interneurons were located in LI/CP/SP, and not in the IZ, indicating that these cells do not communicate directly with projection neurons, at least perinatally. It was also shown here that there was a remarkable accumulation of cortical CB^+ interneurons in LI, in both *p35* and *Cdk5* mutant mice. This could suggest a defect in inward radial migration that is reflected in the position of mature CB^+ interneurons; these were found mostly in the upper part of the cortex. In conclusion, it is reasonable to propose that: (i) tangential migration of cortical interneurons from GE does not depend on Cdk5 activity, (ii) prenatal migrating interneurons do not communicate with projection neurons directly, (iii) the defect in interneuron laminar positioning in *p35* mutants could occur before they reach the CP, and (iv) the radial inward migration of cortical interneurons is a Cdk5-dependent event. In light of the last hypothesis, it would be interesting to follow the inward migration of cortical interneurons, from LI into the CP, in control and *p35* mutant mice by real-time microscopy.

Figure 4A-1. Cdk5 is expressed in *p35*-deficient GABAergic interneurons

(A-B) Cultured neurons from E14.5 *wild-type* MGE immunoreacted for (A) GABA or (B) p35, and stained with bisbenzimide (BB) to show nuclei. Note that a majority of MGE cultured cells expressed GABA and p35.

(C-F) Cultured neurons from E14.5 *p35* +/- (C,E) and *p35* -/- (D,F) MGE (C-D) and cortices (E,F) immunoreacted for GABA and Cdk5, and stained with bisbenzimide, clearly showing expression of Cdk5 in GABAergic neurons (arrows).

(G-H) Cultured neurons from E17.5 *p35* +/- (G) and *p35* -/- (H) cortices immunoreacted for GABA and Cdk5 and stained with bisbenzimide. Arrows point to GABAergic cells that expressed Cdk5.

MGE – medial ganglionic eminence; Cx – cortex; DIV – days in vitro. Scale bar, 25 μm.

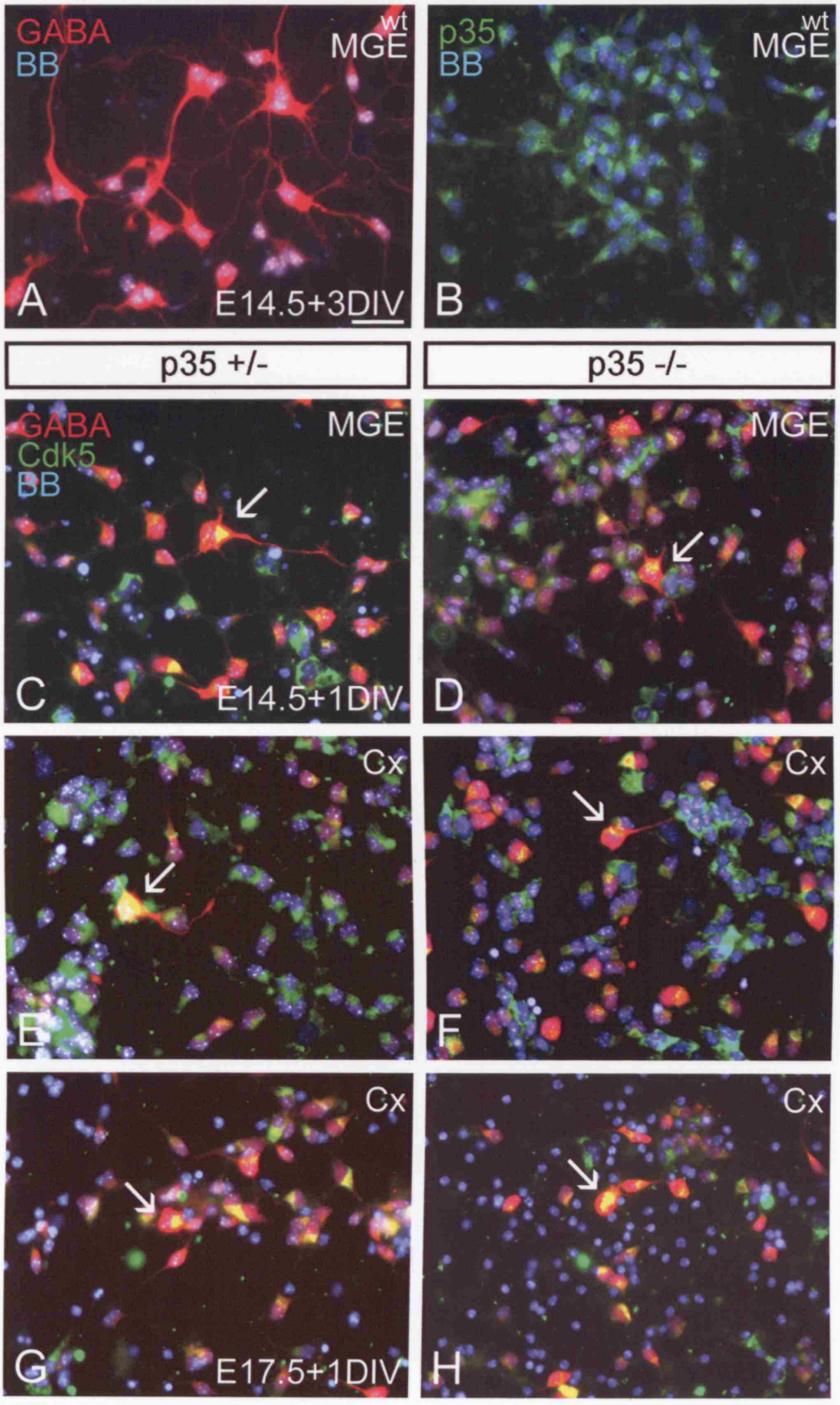
GABA
BB
wt
MGE
A
E14.5+3DIV
p35
BB
wt
MGE
B
p35 +/-
p35 -/-
GABA
Cdk5
BB
MGE
C
E14.5+1DIV
MGE
D
Cx
E
Cx
F
Cx
G
E17.5+1DIV
Cx
H

Figure 4A-2. Loss of Cdk5 activity in *p35*-deficient prenatal GE and Cx

Cdk5 was isolated from the cell lysates of GE and Cx by immunoprecipitation. Cdk5 activity was measured by an *in vitro* radioactive kinase assay in presence of histone H1, as described in Materials and Methods. This assay showed abolished Cdk5 activity in the prenatal GE and Cx of *p35* -/- compared to *p35* +/- mice. GE – ganglionic eminence; Cx – cortex.

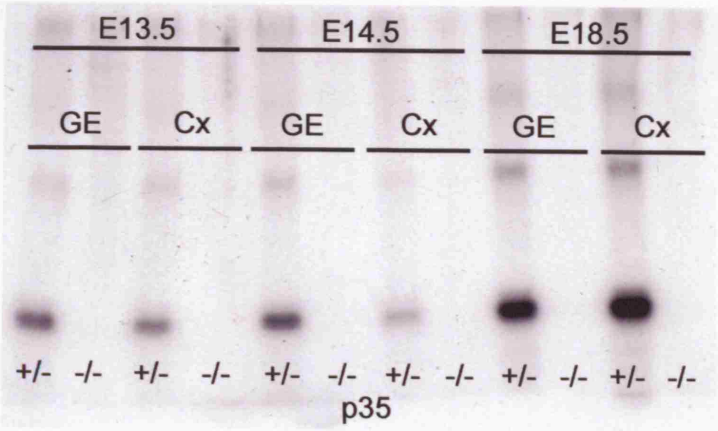

Cdk5 activity

Figure 4A-3. Cortical interneurons migrate out from the GE in *p35* mutants

Coronal sections of E13.5 forebrain labelled with antibody to calbindin (CB;A-D) and adhesion protein TAG1 (C-D).

(A-B) CB^+ interneurons migrated in clearly defined streams from the GE towards cortex in both (A) *p35* +/- and (B) *p35* -/- mice.

(C-D) The distribution of CB^+ cells and $TAG1^+$ cells/fibres within the cortex did not differ between the two genotypes.

PPL – preplate layer; IZ – intermediate zone; SVZ – subventricular zone. Scale bars, 250 μm (A-B); 100 μm (C-D).

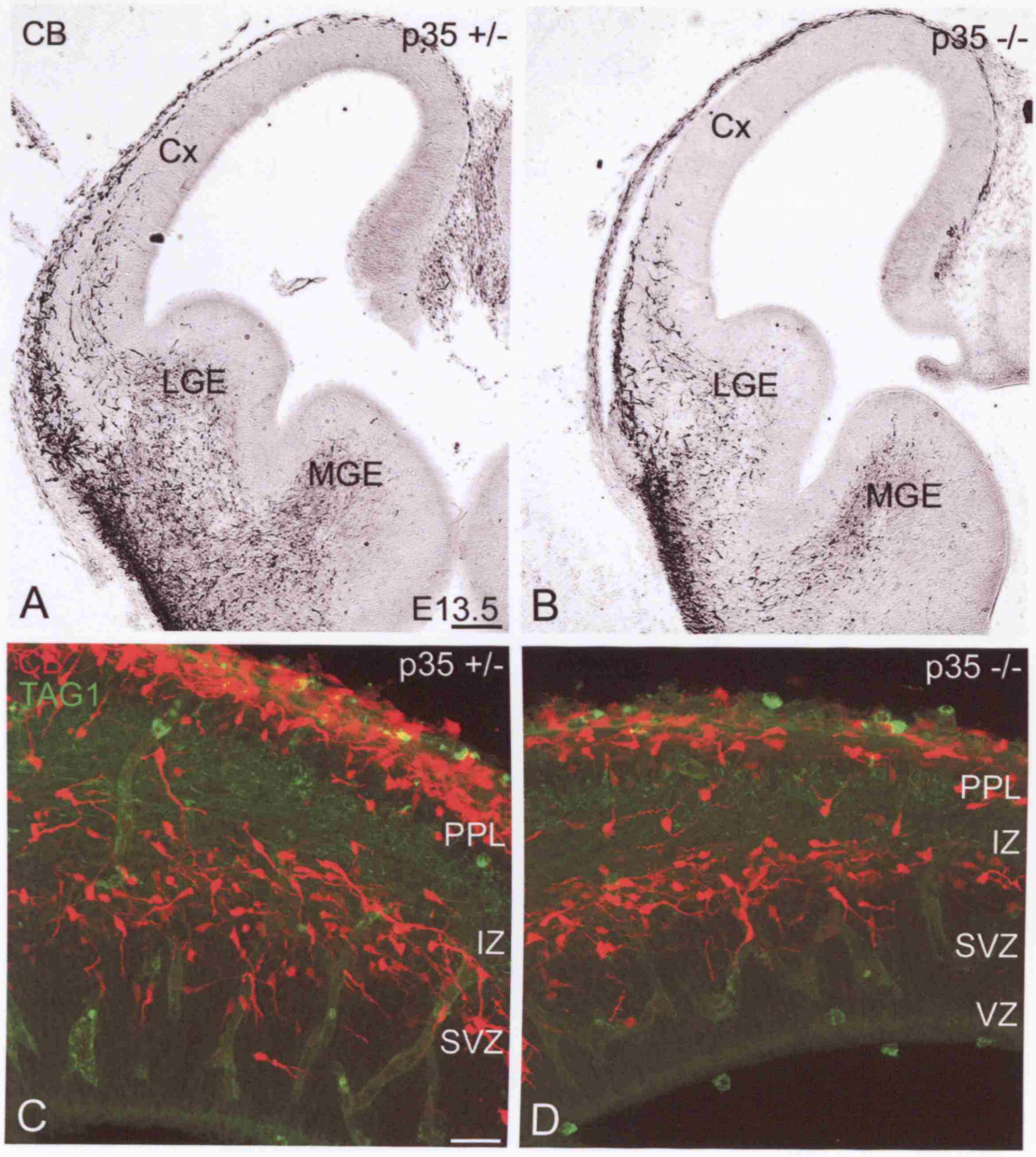
CB
p35 +/-
Cx
LGE
MGE
A
E13.5
p35 -/-
Cx
LGE
MGE
B
CB
TAG1
p35 +/-
PPL
IZ
SVZ
C
p35 -/-
PPL
IZ
SVZ
VZ
D

Figure 4A-4. Migration of *p35*-deficient MGE-derived cells is altered *in vitro*

(A) Chemotactic response of MGE-derived cells (E13.5), from *wild-type* (wt) and *p35* mutant mice, to negative control (Neurobasal medium) and 10% FBS, after 16 hours in Boyden chamber. The results were expressed as mean number of migrated cells ± standard error of the mean (SEM) from 3 experiments. Error bars represent SEM. *$p<0.05$; Student's *t* test.

(B,C) MGE cells were labelled by fluorescent dye (CMFDA) in forebrain slices and their migration into the cortex analyzed after 36 hours.

(D) The telencephalic wall was divided into 3 equal zones, from the LV to the pia, and the percentage of $CMFDA^+$ cells in each zone compared between *p35* hetero- and homozygous littermates. The results were expressed as mean percentage ± SEM from 5 experiments. Error bars represent SEM.

(E) This analysis showed a significantly higher aggregation of CMFDA-labelled cells present in the zone closest to the ventricle in *p35* -/- cortex. *$p<0.05$; Student's *t* test.

FBS – foetal bovine serum; MGE – medial ganglionic eminence; Cx – cortex; CMFDA - 5-chloromethylfluorescein diacetate; LV – lateral ventricle. Scale bar, 250 μm (B,C).

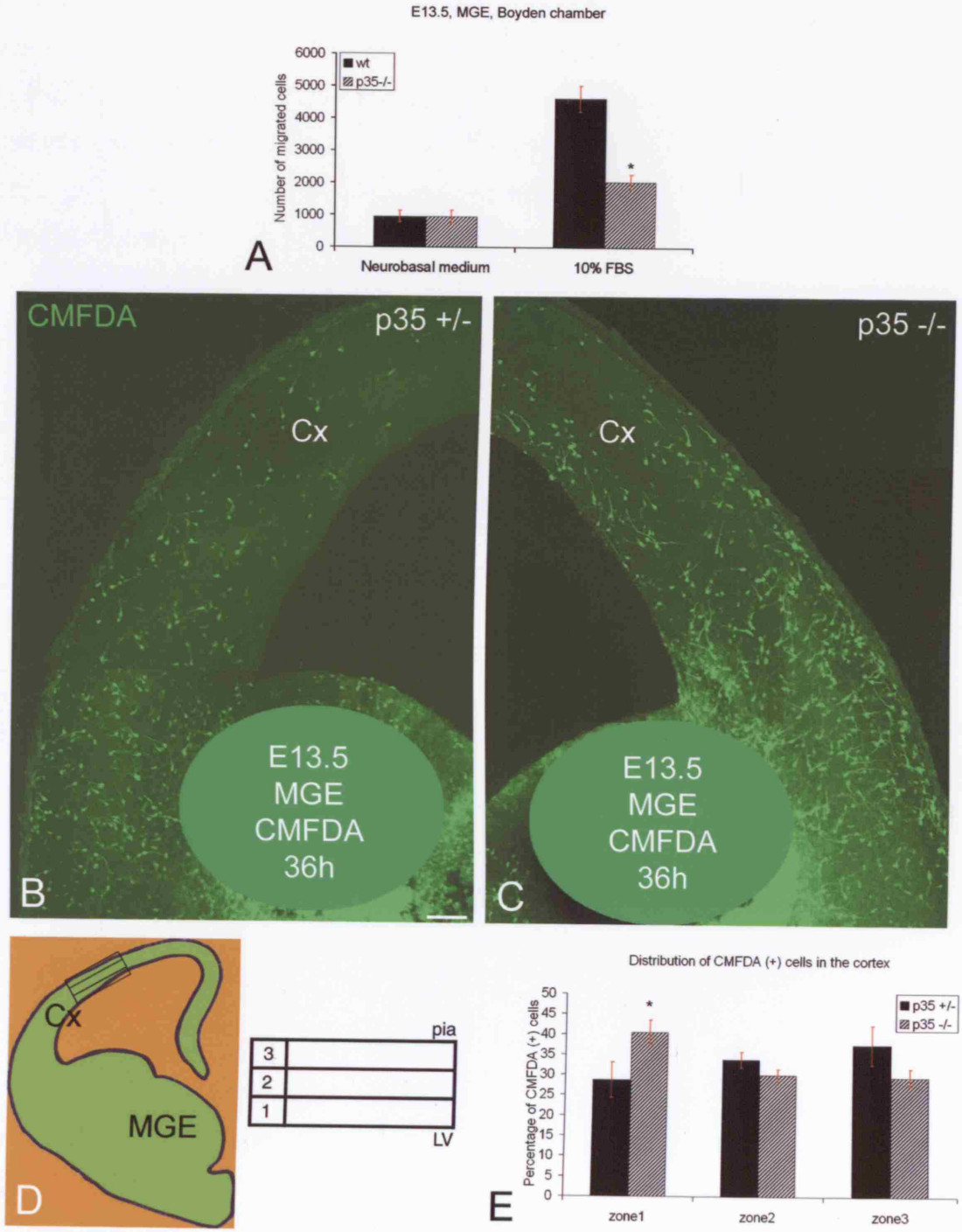
E13.5, MGE, Boyden chamber
Number of migrated cells
6000
5000
4000
3000
2000
1000
0
wt
p35-/-
*
A
Neurobasal medium
10% FBS
CMFDA
p35 +/-
Cx
E13.5
MGE
CMFDA
36h
B
p35 -/-
Cx
E13.5
MGE
CMFDA
36h
C
Cx
MGE
D
pia
3
2
1
LV
Distribution of CMFDA (+) cells in the cortex
Percentage of CMFDA (+) cells
50
45
40
35
30
25
20
15
10
5
0
*
p35 +/-
p35 -/-
zone1
zone2
zone3
E

Figure 4A-5. Tangential migratory routes of cortical interneurons are altered in *p35* mutants

Coronal sections of E16.5 forebrain labelled with antibody to calbindin (CB), and visualized with peroxidase-DAB (A-B) or fluorescence (C-D) method.

(A-B) CB^+ interneurons migrated along three (LI, SP, SVZ) distinct streams in both (A) *p35* +/- and (B) *p35* -/- mice. In *p35* -/- cortex, the position of the SP stream was more superficial (due to the thinner CP). CB^+ cells were also present in the CP and IZ in both genotypes.

(C-D) Tangentially oriented leading processes of CB^+ cells, observed in *p35* +/- (C), were not clearly apparent in *p35* -/- mice.

DAB – diaminobenzidine; LI – layer I; CP – cortical plate; SP – subplate; IZ – intermediate zone; SVZ – subventricular zone; VZ – ventricular zone. Scale bars, 250 μm (A-B); 100 μm (C-D).

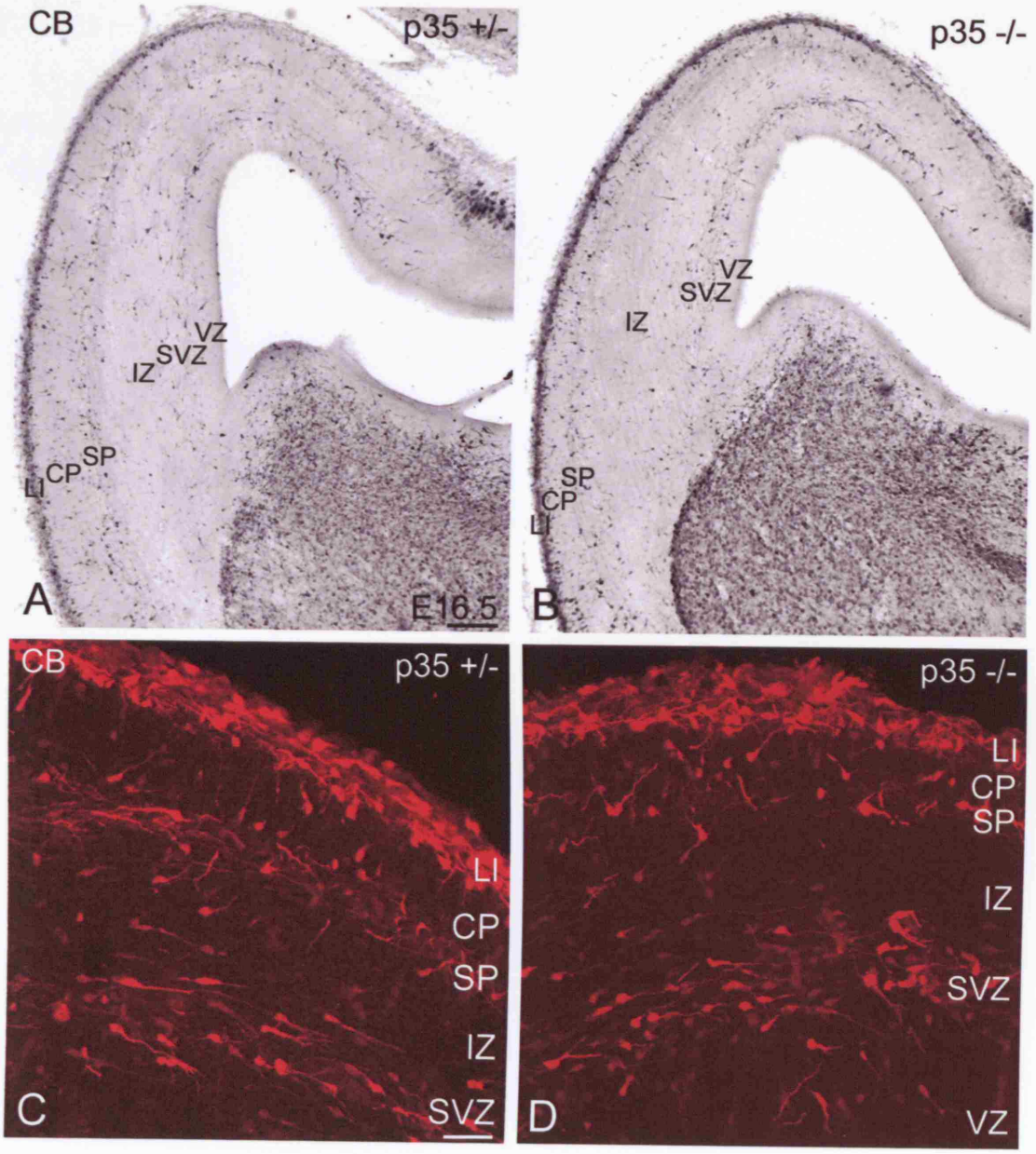
CB
p35 +/-
VZ
SVZ
IZ
SP
CP
LI
A
E16.5
p35 -/-
VZ
SVZ
IZ
SP
CP
LI
B
CB
p35 +/-
LI
CP
SP
IZ
SVZ
C
p35 -/-
LI
CP
SP
IZ
SVZ
VZ
D

Figure 4A-6. Cortical interneurons accumulate in the upper part of the developing cortex in *p35* mutants

Coronal sections of E19.5 forebrain labelled with antibody to calbindin (CB).

(A-B) CB^+ cells were mainly located in the upper part of the cortex, in zones LI/CP/SP, and only rarely in the IZ and SVZ/VZ, in both *p35* +/- (A) and *p35* -/- (B) mice. Note a significant accumulation of CB^+ cells in LI of *p35* -/- mice (C) that was not observed in *p35* +/- mice (D).

LI – layer I; CP – cortical plate; SP – subplate; IZ – intermediate zone; SVZ – subventricular zone; VZ – ventricular zone. Scale bars, 500 μm (A-B); 200 μm (C-D).

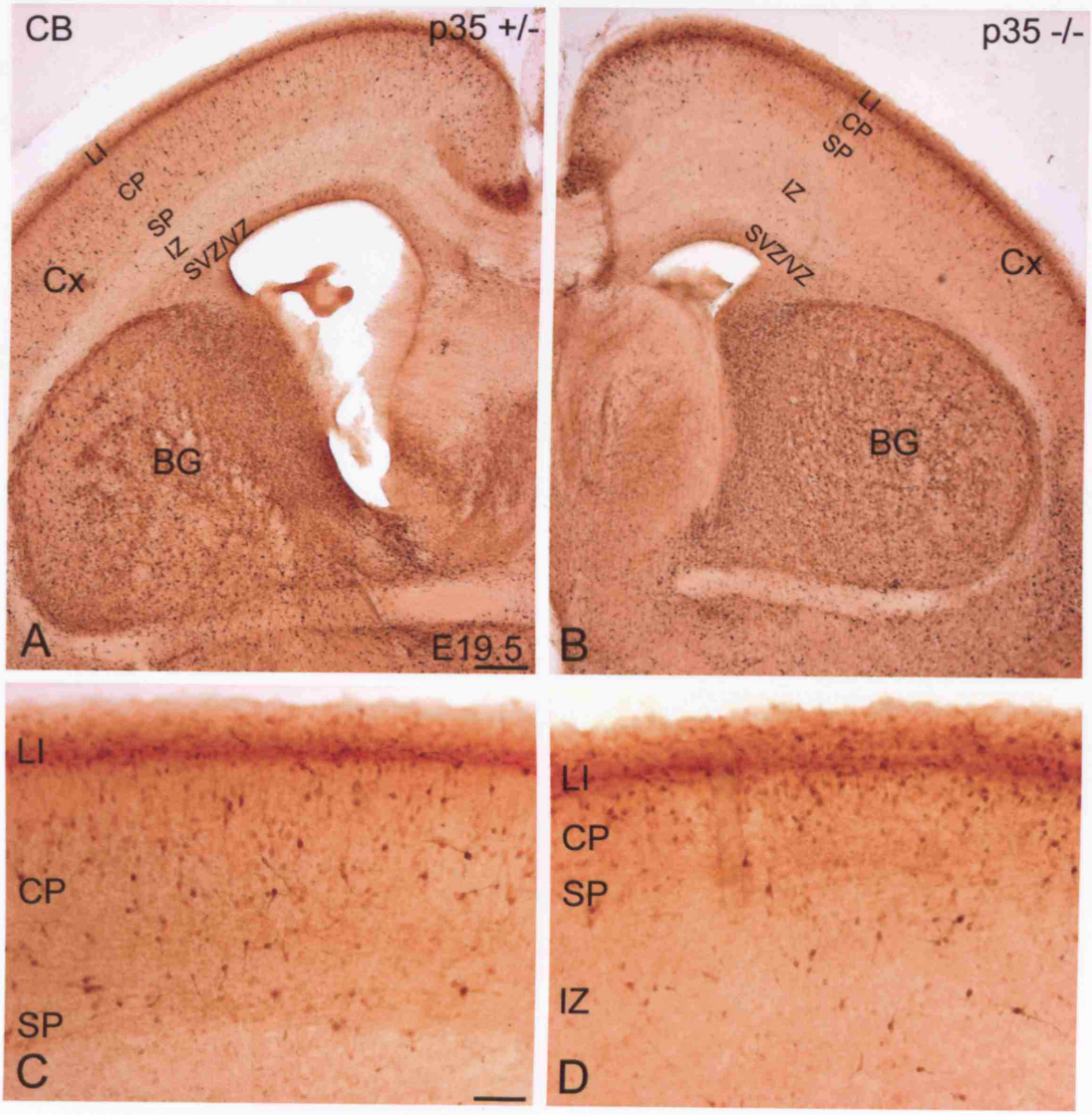
CB
p35 +/-
LI
CP
SP
IZ
SVZ/NZ
Cx
BG
A
E19.5
p35 -/-
LI
CP
SP
IZ
SVZ/NZ
Cx
BG
B
LI
CP
SP
C
LI
CP
SP
IZ
D

Figure 4A-7. Cortical interneurons accumulate in layer I of the developing cortex in *p35* mutants

Coronal sections of E19.5 cortex stained with bisbenzimide (BB), a nuclear marker, to label cortical layers, and immunoreacted for calbindin (CB), to label cortical interneurons. Images were taken using confocal microscope.

(A-B) Bisbenzimide; LI was thicker and more cellular in *p35* mutants (A) compared to the controls (B).

(C-D) In *p35* +/- mice (C), CB^+ cells were spread throughout the LI/CPSP, whilst in the *p35* -/- mice, these cells were mostly aggregated in LI, although CB-immunoreactivity was found in the compact CP and SP.

(E-F) An overlay of (C-D).

Oblique white lines depict border between the layers.

LI – layer I, CP – cortical plate; SP – subplate. Scale bar, 200 μm.

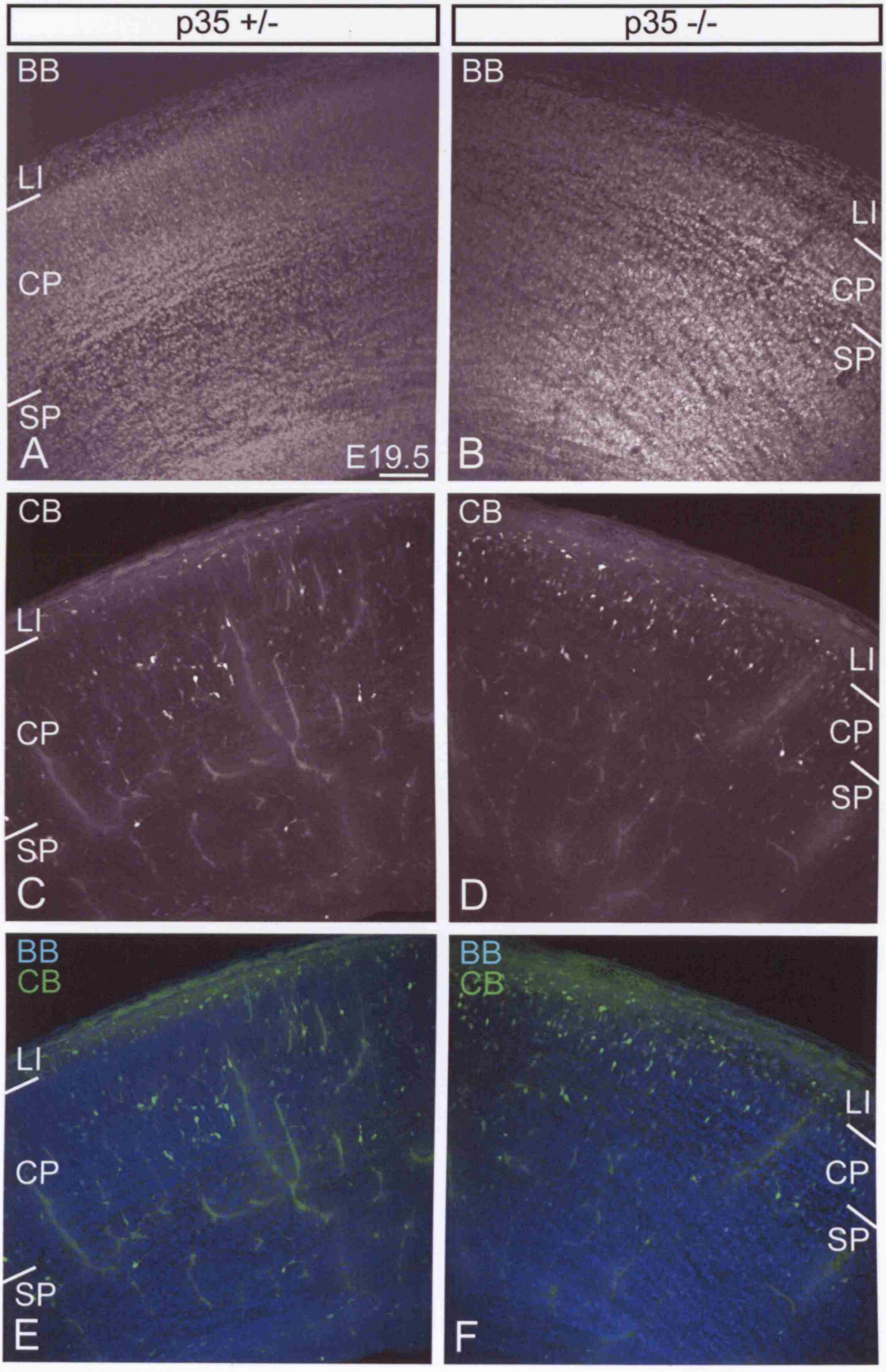
p35 +/-
p35 -/-
BB
LI
CP
SP
A
E19.5
B
CB
C
D
E
F

Figure 4A-8. Loss of Cdk5 signalling increases the number of prenatal cortical interneurons and their accumulation in the compact CP region

Coronal sections of E19.5 cortex were immunoreacted for calbindin (CB), to label cortical interneurons, and stained with thionin (Nissl stain), to mark developing cortical layers. For quantification, the telencephalic wall was divided into three arbitrary 'stripes', LI/CP/SP, IZ, and SVZ/VZ. The number of CB^+ cells and thickness of each 'stripe' was measured in lateral neocortex. The relative 'stripe' number of CB^+ cells was calculated as a percentage of total number of CB^+ cells. Similarly, relative 'stripe' thickness was calculated as a percentage of the entire TW thickness. The results were expressed as mean ±SEM (standard error of the mean). Error bars represent SEM.

(A) In both genotypes, the number of CB^+ cells was highest in the LI/CP/SP 'stripe' compared to the IZ or SVZ/VZ. Although, the number of CB^+ cells in each 'stripe' and the total number of CB^+ cells was higher in *p35* -/- than in *p35* +/- mice.

(B) The LI/CP/SP 'stripe' was thinner and IZ 'stripe' was thicker in *p35* -/- compared to *p35* +/- mice.

(C) This graph shows the relative contribution of CB^+ cells in each 'stripe' being almost identical in the two genotypes

(D) The contribution of LI/CP/SP and IZ to the total thickness of the TW was inverted in the two genotypes.

3 brains were used for each genotype; *** $p<0.005$; Student's *t*-test;

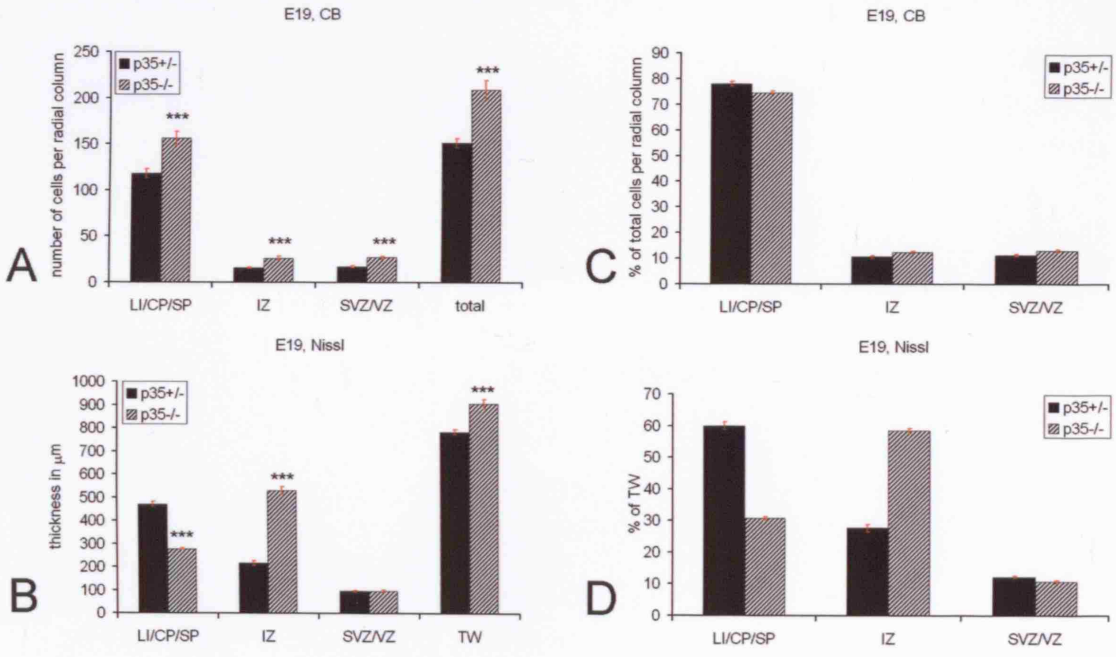
A
E19, CB
number of cells per radial column
p35+/-
p35-/-
***
LI/CP/SP
IZ
SVZ/VZ
total
C
E19, CB
% of total cells per radial column
LI/CP/SP
IZ
SVZ/VZ
B
E19, Nissl
thickness in µm
TW
D
E19, Nissl
% of TW

Figure 4A-9. Cortical interneurons accumulate in layer I of the developing cortex in *Cdk5* mutants

Coronal sections of E15.5 (A-C) and E18.5 (D-F) cortex labelled with antibody to calbindin (CB). *Cdk5* +/+ (A,D); *Cdk5* +/- (B,E); *Cdk5* -/- (C,F).

(A-C) CB^+ cells were mainly found in LI, SP and SVZ in all genotypes, regardless of the layer position, e.g. the SP layer was located closer to the pial surface in *Cdk5* mutants.

(D-F) A majority of CB^+ cells were located in LI/CP/SP in all genotypes. Note a substantial accumulation of CB^+ cells in LI of the *Cdk5* mutant.

LI – layer I; CP – cortical plate; c – compact; SP – subplate; IZ – intermediate zone; SVZ – subventricular zone; VZ – ventricular zone. Scale bar, 200 μm.

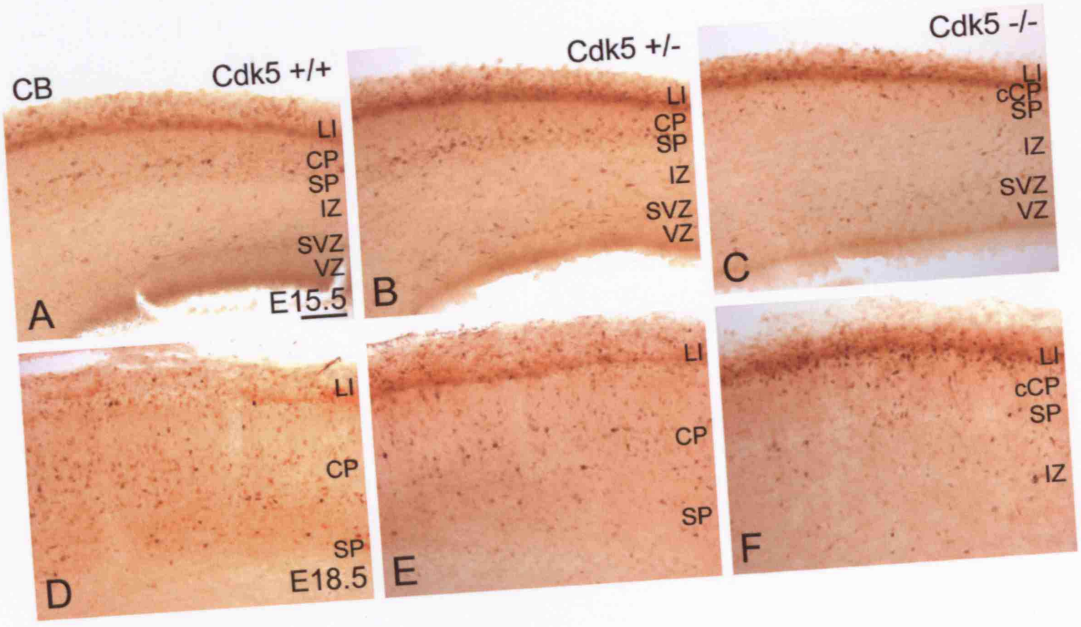
CB
Cdk5 +/+
LI
CP
SP
IZ
SVZ
VZ
A
E15.5
Cdk5 +/-
B
Cdk5 -/-
cCP
C
D
E18.5
E
F

Figure 4A-10. Cortical interneurons are misplaced in the postnatal (P5) *p35* mutants

Coronal sections of P5 cortex labelled with antibody to calbindin (CB).

(A,C) In *p35* +/- mice, CB+ cells were mainly found in all neocortical layers except layer IV. In contrast, in *p35* -/- mice (B,D), CB^+ cells heavily populated the whole depth of the neocortex, and aggregated notably in its uppermost and lowermost parts. Roman numerals designate mature neocortical layers. Scale bars, 500 μm (A-B); 250 μm (C-D).

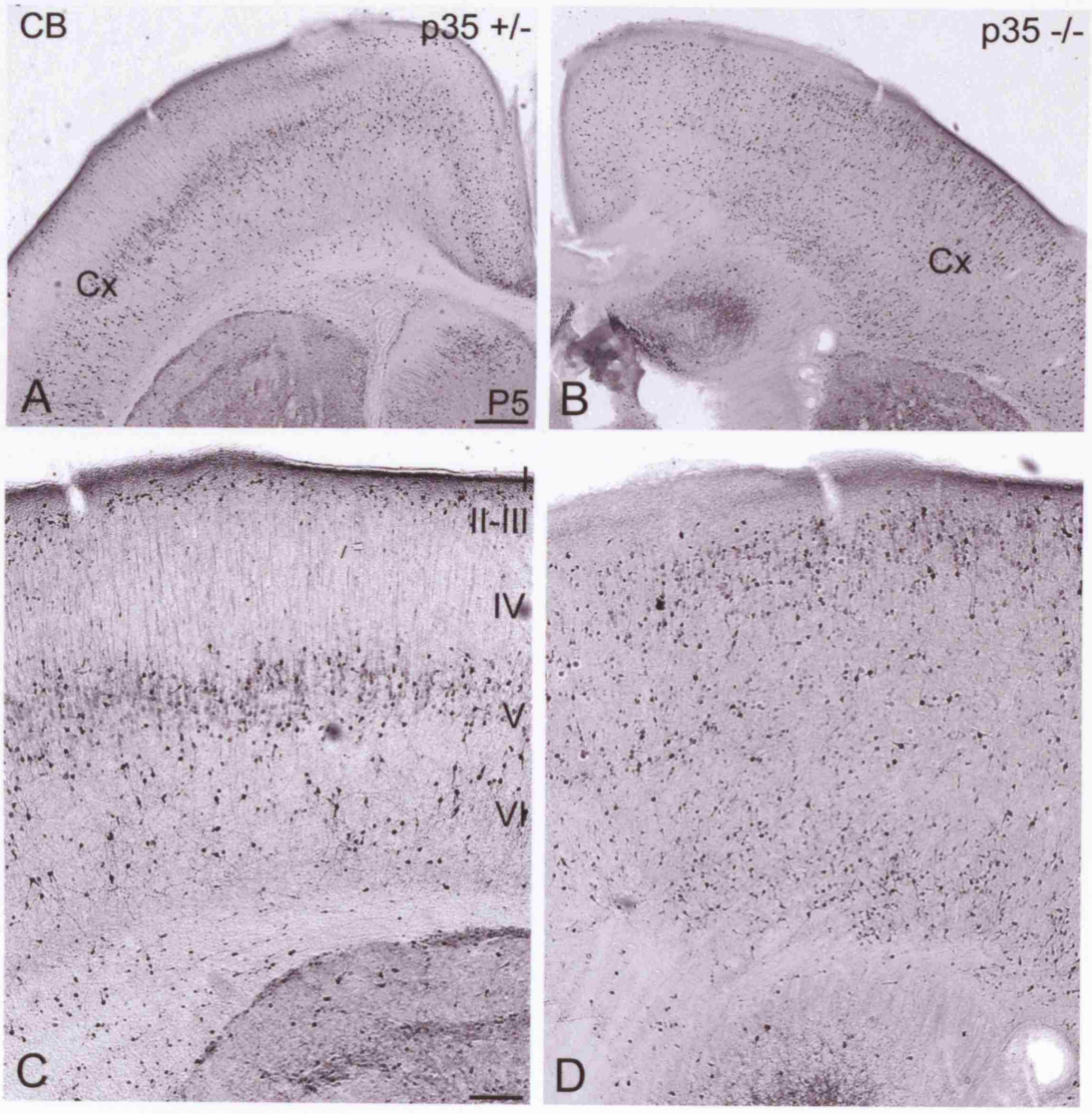
CB
p35 +/-
Cx
A
P5
p35 -/-
Cx
B
I
II-III
IV
V
VI
C
D

Figure 4A-11. Cortical interneurons are misplaced in the postnatal (P12) *p35* mutants

Coronal sections of P12 neocortex labelled with antibodies, to calbindin (CB) and calretinin (CalR).

(A-B) In the *p35* +/- mice (A), CB^+ cells mostly populated lower layers (V and VI), whilst in the *p35* -/- mice (B), these cells tended to reside in the superficial part of the cortex.

(C-D) In the *p35* +/- mice (C), $CalR^+$ cells were observed predominately in the upper half of the cortex, whilst in the *p35* -/- mice (D), $CalR^+$ populated the whole depth of the cortex. Note that $CalR^+$ thalamocortical fibres were located below the cortex in *p35* heterozygous (C) and within the cortex in *p35* homozygous (D) cortices.

Roman numerals designate mature neocortical layers. Scale bar, 250 μm.

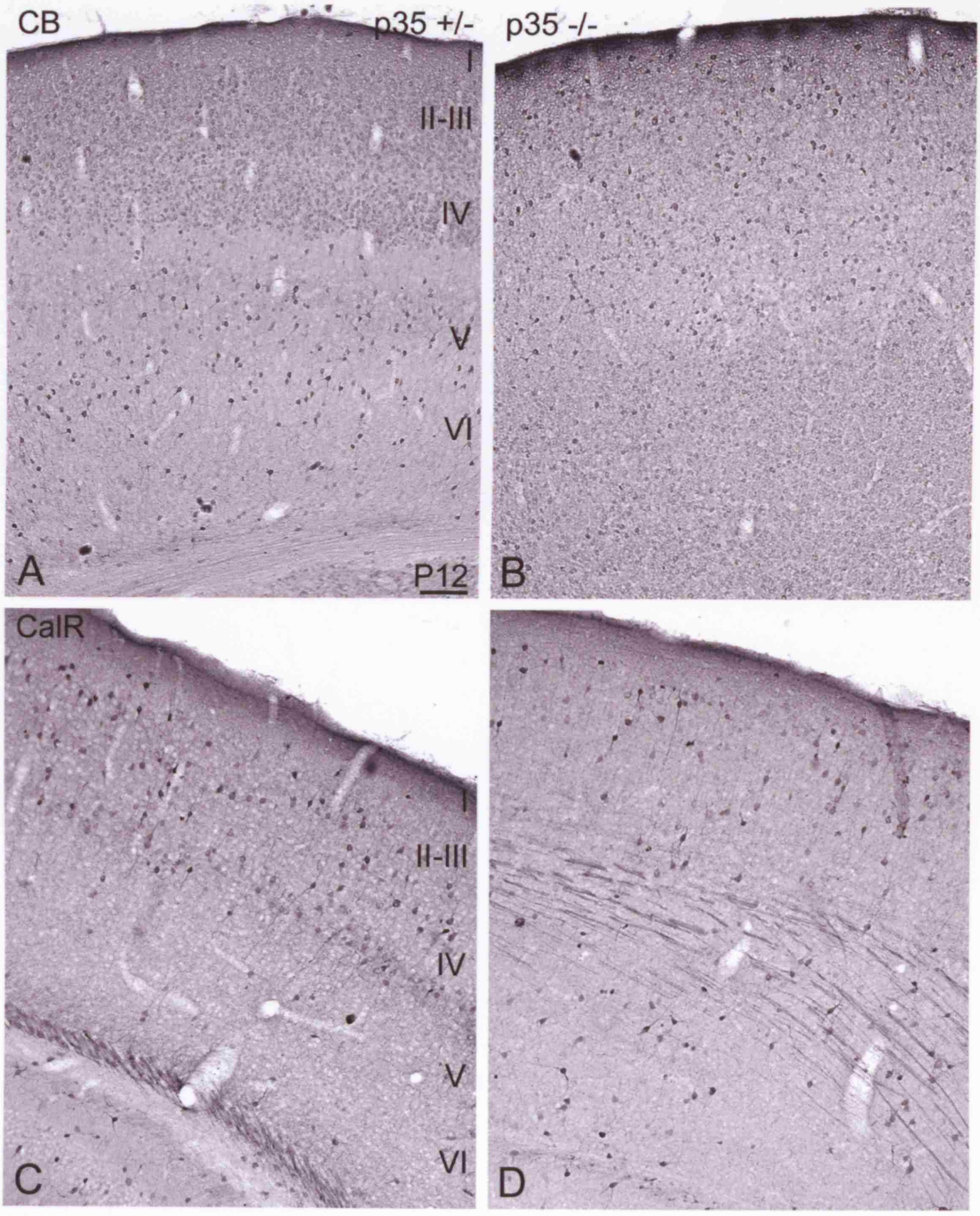
CB
p35 +/-
I
II-III
IV
V
VI
A
P12
p35 -/-
B
CaIR
I
II-III
IV
V
VI
C
D

Figure 4A-12. Mostly inverted position of postnatal cortical interneurons in *p35* mutants

P12 neocortex was labelled with antibodies, to calbindin (CB) and calretinin (CR), and divided into equal horizontal stripes (bins). Bin1 is closest to the lateral ventricle. The immuno-positive cells were counted in each bin. Results represent the percentage of CB^+ or CR^+ in each bin relative to the total number of labelled cells, and were presented as mean percentage ± SEM (standard error of the mean). Error bars represent SEM. Three sections from at least three brains for each genotype were used for analysis.

(A,B) Graphs show the distribution of CB^+ cells in somatosensory and motor cortex; Note a complete inversion in position of CB^+ cells in motor cortex of the *p35* mutant (B).

(C,D) Graphs show the distribution of CR^+ cells in somatosensory and motor cortex; CR^+ cells were misplaced in *p35* mutants, and that was more pronounced in the motor cortex (D).

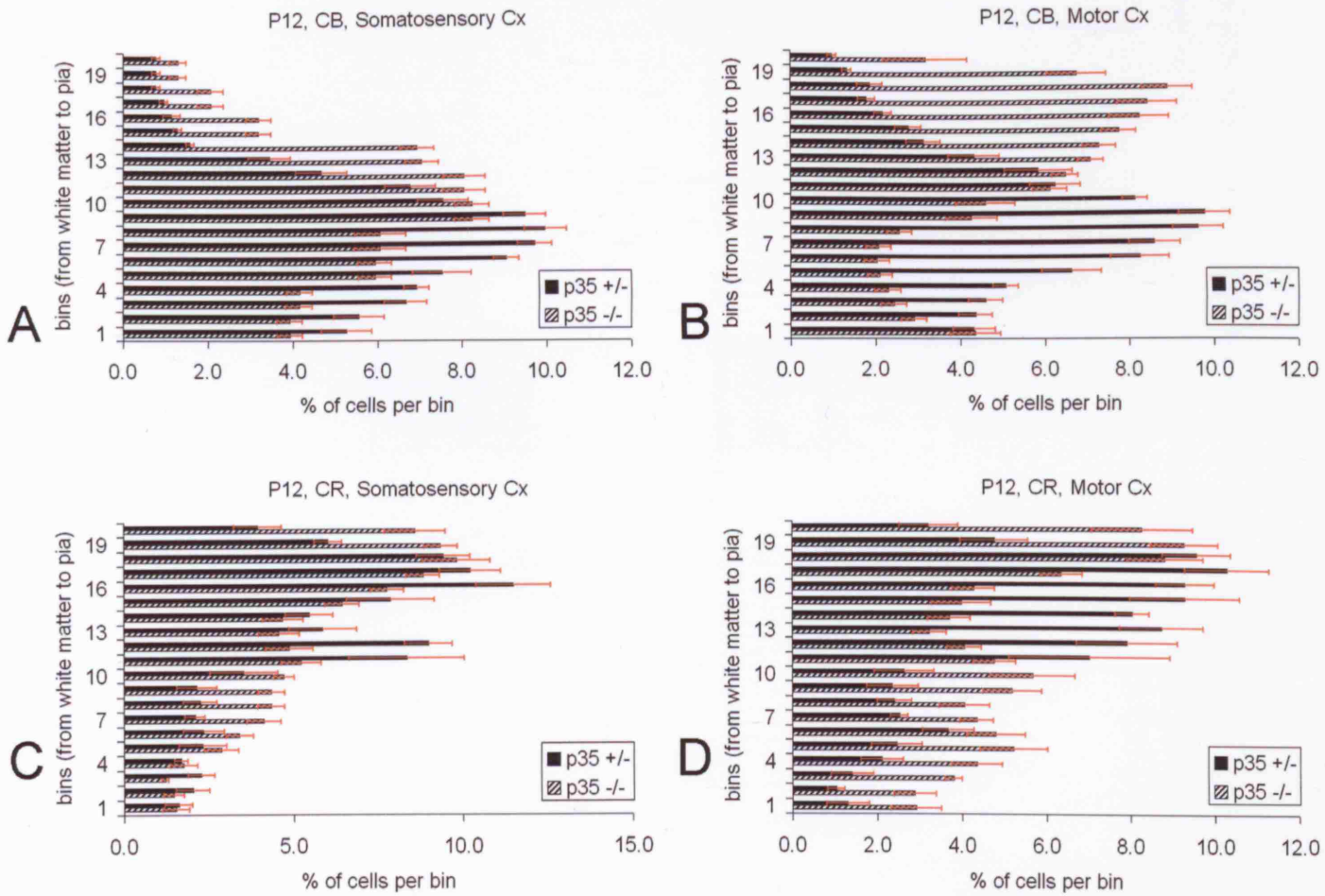
A
P12, CB, Somatosensory Cx
bins (from white matter to pia)
19
16
13
10
7
4
1
0.0
2.0
4.0
6.0
8.0
10.0
12.0
% of cells per bin
p35 +/-
p35 -/-
B
P12, CB, Motor Cx
bins (from white matter to pia)
19
16
13
10
7
4
1
0.0
2.0
4.0
6.0
8.0
10.0
12.0
% of cells per bin
p35 +/-
p35 -/-
C
P12, CR, Somatosensory Cx
bins (from white matter to pia)
19
16
13
10
7
4
1
0.0
5.0
10.0
15.0
% of cells per bin
p35 +/-
p35 -/-
D
P12, CR, Motor Cx
bins (from white matter to pia)
19
16
13
10
7
4
1
0.0
2.0
4.0
6.0
8.0
10.0
12.0
% of cells per bin
p35 +/-
p35 -/-

Figure 4A-13. Loss of p35 increases the number of cortical interneurons in the postnatal cortex

P12 neocortex was labelled with antibodies, to calbindin (CB) and calretinin (CR). Quantification of the number of CB^+ (A) and CR^+ (B) cells in somatosensory and motor cortex in control (black bar) and *p35* mutant (striped bar) mice.

The results were presented as mean number of immuno-positive cells ± SEM (standard error of the mean). Error bars represent SEM. 3 brains were used for each genotype (*p35* +/- and *p35* -/-); * $p< 0.05$; *** $p<0.005$; Student's *t*-test.

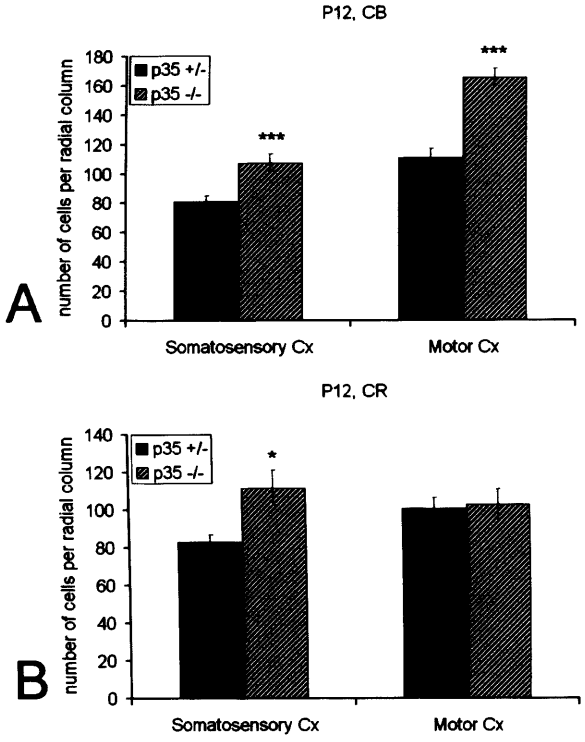
P12, CB
A
number of cells per radial column
p35 +/-
p35 -/-
***
***
180
160
140
120
100
80
60
40
20
0
Somatosensory Cx
Motor Cx
P12, CR
B
number of cells per radial column
p35 +/-
p35 -/-
*
140
120
100
80
60
40
20
0
Somatosensory Cx
Motor Cx

CHAPTER 4B

ErbB4 receptor mediates PI3K-independent tangential cortical interneuron migration

INTRODUCTION

Cortical interneurons originate from the ventral forebrain and populate the cortex by following tangential routes of migration (see reviews Parnavelas, 2000; Marin and Rubenstein, 2001; Marin and Rubenstein, 2003) through the PPL and IZ/SVZ. There are many factors, intrinsic and environmental, that regulate their tangential migration: transcription factors (Nkx2.1; Sussel et al., 1999; Lhx6; Alifragis et al., 2004; Dlx1/2; Anderson et al., 1997; Mash1; Casarosa et al., 1999), chemotropic factors (semaphorins class III; Marin et al., 2001; SDF1; Stumm et al., 2003), adhesive molecules (TAG1; Denaxa et al., 2001) and growth factors (BDNF; Polleux et al., 2002; GDNF; Pozas and Ibanez, 2005).

Neuregulins (NRGs), a family of growth factors, exert their function through the ErbB family of receptors, and are important for cell proliferation, survival, differentiation, and migration (Lemke, 1996; Burden and Yarden, 1997; Gassmann and Lemke, 1997). NRG1,2,3,4, encoded by at least four genes, *Nrg1,2,3,4*, have numerous alternative spliced isoforms, and all bind to and activate ErbB receptors via epidermal growth factor (EGF)-like domain, which is important for their bioactivity (Buonanno and Fischbach, 2001). NRG1, also known as neu differentiation factor – NDF (Peles et al., 1992), heregulin (Holmes et al., 1992), acetylcholine receptor-inducing activity – ARIA (Falls et al., 1993), and glial growth factor (Marchionni et al., 1993), is widely expressed in the nervous system. NRG1 proteins, soluble or transmembrane, are grouped as type I, II, (both soluble; referred to as NRG-Ig) and III (transmembrane; referred to as NRG-(cysteine-rich domain)CRD) (Buonanno and Fischbach, 2001; Falls, 2003). NRG1 is important for the development of various glial and neuronal populations in the peripheral and central nervous systems (Falls, 2003). NRG1 can also play a role in

oncogenesis (Burden and Yarden, 1997). Recently, the gene that encodes NRG1 has been identified as a potential susceptibility gene for schizophrenia (Stefansson et al., 2002; Corfas et al., 2004).

The ErbB family, ErbB1 (also known as the epidermal growth factor receptor – EGFR or HER1), ErbB2 (HER2 or c-neu), ErbB3 (HER3), and ErbB4 (HER4), comprise a group of receptor tyrosine kinases that interact with ligands from the EGF superfamily, including NRGs, subsequently dimerize, catalytically activate each other by cross-phosphorylation, and then stimulate various signalling pathways (Burden and Yarden, 1997; Olayioye et al., 2000). NRGs only bind to ErbB3 and ErbB4 which leads to formation of homodimers or heterodimers, often including ErbB2. ErbB2 has no known ligand, and NRGs interact with ErbB2 only after binding ErbB3 or ErbB4 and, thus, ErbB2 serves as a co-receptor (Olayioye et al., 2000). ErbB3 is not active as a homodimer.

ErbB4 (v-erb-a erythroblastic leukemia viral oncogene homolog 4, avian) is a 180-kDa glycoprotein that mediates the effects of the NRG family of growth factors (Plowman et al., 1993; Junttila et al., 2000; Olayioye et al., 2000; Gullick, 2001; Fig.4B-1). Likewise, ErbB4 may also function as a receptor for betacellulin, heparin-binding epidermal growth factor-like growth factor, epiregulin, and epidermal growth factor (Burden and Yarden, 1997; Elenius et al., 1997b; Fischbach and Rosen, 1997; Riese and Stern, 1998; Olayioye et al., 2000). Activation of ErbB4 with its ligands leads to diverse cellular responses, such as proliferation, survival, chemotaxis, and differentiation (Junttila et al., 2000). During development, ErbB4 is expressed mainly in neural tissues and myocardium *in vivo*. *ErbB4* null mice die around E10-11 with defects in hindbrain and heart trabeculae (Gassmann et al., 1995). Similar phenotype has been observed in *NRG1* and *ErbB2* single mutants (Lee et al., 1995; Meyer and Birchmeier, 1995; Kramer et al., 1996). ErbB4 can also regulate differentiation of the mammary gland (Jones et al., 1999) and may play a role in oncogenic transformation in human tumours (Srinivasan et al., 1998). Recently, it was demonstrated that two pairs of naturally occurring ErbB4 isoforms exist in human and mouse tissues (Junttila et al., 2000; Fig.4B-1). These isoform pairs are differentially expressed in tissues such as heart and brain, suggesting that they may have specific functions. One pair of ErbB4 isoforms differs within the extracellular juxtamembrane domain (isoforms JMa and JMb that have 23 or 13 alternative amino acids, respectively) and in susceptibility to being cleaved by matrix

metalloproteinases (MMP) in response to phorbol ester treatment (Elenius et al., 1997a). JMa isoform is prone to MMP processing which results in the generation of a 120 kDa soluble receptor extracellular domain and a membrane-bound 80 kDa fragment (Vecchi et al., 1996). The other pair of ErbB4 isoforms differs in the cytoplasmic tail domain by the presence (Cyt1 isoform) or absence (Cyt2 isoform) of a 16-amino acid sequence including a tyrosine residue in the context of a consensus-binding site for phosphatidylinositol-3-OH kinase (PI3K; Peles et al., 1992; Elenius et al., 1999). Both, Cyt1 and Cyt2, can activate the mitogen-activated protein kinase (MAPK) signalling pathway (Kainulainen et al., 2000). Therefore, there are at least two signalling pathways that have been shown to be involved in NRG signalling via the ErbB4 receptor: PI3K/Akt and mitogen-activated protein kinase (MAPK)/extracellular signal-regulated protein kinase (ERK) pathways.

PI3K is a signal transduction molecule that mediates several responses important for both normal development and malignant transformation. PI3K contains a tightly associated p110 catalytic subunit and regulatory subunit p85. Upon ligand binding and the subsequent stimulation of intrinsic tyrosine kinase activity, many receptor tyrosine kinases, such as ErbB4 receptor, can recruit PI3K regulatory domain, via SH2 domains. Consequently, PI3K activates the serine/threonine kinase Akt/protein kinase B and plays an essential role in cell survival and chemotaxis (reviewed by Rodgers and Theibert, 2002).

NRGs and their receptors have been implicated in neuron morphogenesis and migration. NRG1 regulates neurite outgrowth in cultured retina (Bermingham-McDonogh et al., 1996), cerebellar granular cells (Rieff et al., 1999), and hippocampal neurons (Gerecke et al., 2004). NRG1 plays a role in radial glia formation, thus affecting radial migration of granular neurons in cerebellum and projection neurons in cortex (Anton et al., 1997; Rio et al., 1997). Radially migrating neurons express NRG1 which activates ErbBs receptors on radial glia and promotes radial glia identity in combination with Notch signalling (Patten et al., 2003; Schmid et al., 2003). In the developing forebrain, NRG1 is expressed in the proliferative zones of the cortex and striatum from around E12.5 in mouse (Assimacopoulos et al., 2003), and may assist in the migration of cortical interneurons from the ventral forebrain. It has been shown recently that the ErbB4 receptor is expressed on the surface of tangentially migrating cortical interneurons (Yau et al., 2003). ErbB4 receptor has also been reported to be involved in

NRG-mediated chemotaxis of fibroblasts (Kainulainen et al., 2000), and the PI3K signalling pathway has been implicated in this process (Kainulainen et al., 2000).

Here, I cloned the rat ErbB4 receptor to investigate its role, and that of the PI3K pathway, in the tangential migration of cortical interneurons from the ventral telencephalon. I found that although the ErbB4 receptor plays a role in the tangential migration of interneurons, this process could occur through an ErbB4-PI3K-independent mechanism.

Over the course of my thesis two papers appeared, addressing the same issue (Flames et al., 2004; Gambarotta et al., 2004).

MATERIALS AND METHODS

Animals

Rat E16-17 brains were used for obtaining total RNA (RT-PCR, cloning), proteins (Western blotting), primary neuronal cultures, and forebrain slices.

GN11 neurons

GN11 neurons are immortalized mouse neuroendocrine cells (Radovick et al., 1991b) that possess a high capacity for migration (Maggi et al., 2000). These cells were used for RT-PCR and Western blot analysis, DNA transfection experiments followed by analytic immunocytochemistry, and in a chemotactic assay.

RNA isolation and PCR

The rat E16 forebrain and GN11 neurons were processed for RNA isolation and cDNA amplification as described in general Materials and Methods.

(i) RT-PCR for detecting ErbB2,3,4 receptors

Sequences of PCR primers are shown in the Table 4B-1. Primers were chosen to be common for both mouse and rat sequences, with an exception for ErbB2.

Table 4B-1. RT-PCR primers for detecting ErbB2,3,4 receptors

Name	Primers	Amplicon size
Rat ErbB2	F: CCGCAATGATCATCATGGA	511 bp
	R: TCCTGGTAGCAGAGCTGAG	
Mouse ErbB2	F: CCGCAGTGATCATCATGGA	511 bp
	R: TCCTGGTAGCAGAGCTGAG	
Rat, mouse ErbB3	F: AGATGGGCAACTCTCAGG	277 bp
	R: CCATCGTAGACCTGGGTT	
Rat, mouse ErbB4	F: CAGAGAACAAACTGAGCT	432 bp
	R: TCATGTTGGAAGGCCATGG	

1 µl (50 ng) of ssDNA was used for the PCR reaction. The following PCR conditions were used: *Taq* polymerase (Qiagen); (d) 94°C, 2min; (a) 60°C, 1min; (e) 72°C, 2min; 35 cycles; final extension 72°C, 7min; the rat E16 or GN11 ssDNA was used as a template.

(ii) Three-primer PCR for discrimination between Cyt1 and Cyt2 isoforms

The following primers were used:

Forward Cyt1/Cyt2 (P1): GAGACCCTCAAAGATACCT

Reverse Cyt1-specific (P2): GAGGGCTGTGTCCAATTT

Reverse Cyt1/Cyt2 (P3): TGAGTGCTACTGTCCTCT

Cyt1 and Cyt detection from the rat E16 forebrain and GN11 ssDNA libraries (method 1)

1 µl (50 ng) of ssDNA was used for the PCR reaction. The following PCR conditions were used: *Pfu* polymerase (Promega); (d) 94°C, 2min; (a) 60°C, 1min; (e) 72°C, 2min; 35 cycles; final extension 72°C, 7min. Whilst primer pair P1/P2 would amplify a single band of 222 bp, when Cyt1 was present, primer pair P1/P3 would detect bands of 442 bp or 394 bp, when Cyt1 or Cyt2 were present, respectively. If both isoforms were present, both bands would be amplified.

Cyt1 and Cyt 2 detection from bacterial colonies carrying myc-tagged clones (method 2)

A single colony was picked up with a toothpick, put in an eppendorf tube containing 20 µl of LB/antibiotic, and incubated at 37°C for an hour, with shaking. 1 µl of the suspension was used for the PCR reaction. The following PCR conditions were used: *Taq* polymerase (Qiagen); (d) 94°C, 2min; (a) 60°C, 1min; (e) 72°C, 2min; 35 cycles; final extension 72°C, 7min. The primer triplet P1/P2/P3 would amplify either of the two bands of 442 bp and 222 bp, when Cyt1 was present, or a single band of 394 bp, when Cyt2 was present.

Western blotting

Protein isolation, SDS-PAGE, and protein transfer onto immunoblot membranes have been described in the general Materials and Methods. The ErbB protein expression, in developing rat E17 forebrain and GN11 neurons, was analyzed by immunoblotting and enhanced chemiluminescence. Primary antibodies used were to detect ErbB2, ErbB3 and ErbB4 receptors (see Table 2-1). A peroxidase-conjugated goat anti-rabbit antibody was used as a secondary antibody. The blot was developed using Amersham ECL reagents and exposed to X-ray. The X-ray films were scanned and analyzed using PhotoShop 5.5 (Adobe).

Dissociated cell cultures

Primary cultures of E16 MGE cells were obtained according to the protocol described in general Material and Methods. The MGE-derived cells were incubated in DCC medium at 37°C in a 5% CO_2 humidified incubator for 4 days *in vitro* (DIV). The medium was changed daily. The cells were then fixed in prewarmed 4% PFA for 20min at room temperature and subjected to immunocytochemical staining.

GN11 transfection

GN11 cells were plated onto poly-L-lysine coated coverslips ($5x10^4$ cells/per coverslip) or onto 10 cm Petri dish ($2.5x10^6$ cells/per dish) for next day transfection. The following day, the GN11 medium was replaced with GN11 medium without antibiotics. Three hours later, GN11 neurons were transfected with different DNA plasmids using Lipofectamine reagent (Invitrogen) according to manufacturer's protocol. Twenty four to forty eight hours after transfection, GN11 cells were either fixed in prewarmed 4% PFA and analysed by immunocytochemistry or used for FACS sorting.

Immunocytochemistry

The immunofluoresence cytochemistry was performed as described in general Materials and Methods. To detect receptors, rabbit anti-ErbB2,3,4 antibodies were used. To detect intracellular localization of each receptor, mouse anti-MAP2 antibody was used. MAP2 is a neuron-specific microtubule-associated protein that localizes to the cell body and dendrites. In post-transfection experiments, presence of c-myc-tagged constructs was detected by using a mouse anti-c-myc antibody. All antibodies were incubated overnight at room temperature. Secondary antibodies (FITC, TRITC) were incubated for 2 hours at room temperature. After rinsing coverslips with 1xPBS, cell nuclei were labelled with Bisbenzimide (BB).

Organotypic slice cultures

Organotypic slice cultures of embryonic rat telencephalon were prepared as described in general Materials and Methods. In brief, rat E16 300 μm-thick coronal forebrain slices were cut in ACSF using a vibratome. Only slices containing both cortex and GE were collected and placed onto nitrocellulose porous membranes. The sections were used for electroporation experiments.

***In vitro* electroporation**

DNA (50 nl of 2 μg/μl plasmid) was injected focally into the MGE of coronal slice cultures by microinjector (Picospritzer^{r} II, IntraCel) through a glass micropipettes. Square pulses were generated using an electroporator (Electrosquare porator; ECM 830 BTX). The following electroporation conditions were used: voltage pulse of 70 V, 3 pulses with duration of 5 ms, and 100 ms interval between pulses. Sections were incubated in 'slice' medium at 37°C in a 5% CO_2 humidified incubator for at least 48 hours, changing medium every 24 hours. Slices were fixed in prewarmed 4% PFA, overnight at 4°C. Images of migrating GFP^+ cells were taken at the confocal microscope, and analysis of migratory properties of electroporated cells was performed using MetaMorph software.

Quantification of eGFP-positive cells

For quantification of $eGFP^+$ cells that migrated into the cortex, a radial column, 500 μm wide, of the lateral developing cortex, was divided in three equal zones, and $eGFP^+$ cells were counted in each zone. The relative number of $eGFP^+$ cells in each zone was calculated as a percentage of total number of $eGFP^+$ cells in all three zones, and was expressed as mean percentage ± standard error of the mean (SEM). The data obtained were result of 6 experiments.

GN11 transfection and FACS sorting

GN11 cells were transfected with different DNA plasmids (pCAG-eGFP, pCAG-Cyt1-eGFP, pCAG-Cyt2-eGFP) prior to FACS sorting. The transfection of GN11 cells was carried out as described above. Twenty four to forty eight hours after transfection, GN11 neurons were trypsinized, pelleted by centrufugation at 1,000 x g for 3min, resuspended in 2ml of GN11 medium, and cell numbers were estimated using a haemocytometer. The cells were span down again at 1,000 x g for 3min and 10-12x10^6 cells were resuspended in 1 ml of GN11 medium, and transfferd in 5 ml Falcon tubes to the FACS sorting machine (MoFlo cell sorter, DakoCytomation). GFP^+ cells were collected into tubes, and prepared for chemotaxis experiments (see below).

In vitro migratory assay (Boyden chamber)

Chemotactic response of GN11 neurons to NRG1β was studied using the Boyden chamber as described in general Materials and Methods. Recombinant human NRG-$1\beta_{176-246}$, containing the EGF-like and juxtamembrane domains of the major NRG-1 isoform found in the central nervous system (Meyer and Birchmeier, 1994), was obtained from R&D. NRG1β powder was reconstituted in sterile 1% BSA/PBS to make up a stock solution (10 μg/ml). For chemotaxis, different concentrations of NRG1β, diluted in reduced GN11 medium, were used (10, 20, 100, and 200 ng/ml).

For chemotaxis after transfection and FACS sorting, a million of GFP^+ GN11 cells, overexpressing different plasmids (pCAG-eGFP, pCAG-Cyt1-eGFP and pCAG-Cyt2-eGFP), were resuspended in reduced GN11 medium containing 0.1% BSA/PBS and subjected to *in vitro* migratory assay (Boyden chamber) as described in general Materials and Methods. Chemoattractant NRG1β was used here in concentrations of 100 and 200 ng/ml.

RESULTS

ErbB2 and ErbB4 receptors are expressed in the developing forebrain and GN11 neurons

NRGs exert their function through the ErbB tyrosine kinase receptors: ErbB2,3, and 4. Thus, I first examined the expression of NRG-specific receptors in the developing rat forebrain and GN11 neurons at the level of mRNA and protein using RT-PCR, Western blot, and immunohistochemistry. I found that both developing rat forebrain (E16) and GN11 neurons express *ErbB2* and *ErbB4* receptor mRNA that was detectable by RT-PCR (Fig.4B-2A). Only rat forebrain exhibited *ErbB3* mRNA expression. However, by Western blot analysis, ErbB3 receptor signal was not detected in either forebrain or GN11 neurons (Fig.4B-2B). The strongest ErbB2 and ErbB4 signals were detected in GN11 cells and in the GE, respectively. Low ErbB4 signal was observed as two faint bands in GN11 neurons compared to a single, strong band in rat E17 forebrain. Immunohistochemistry experiments on primary neuronal cultures of rat MGE and cortex (data not shown) confirmed the Western blot data regarding the expression of ErbB receptors (Fig.4B-3). ErbB2 and ErbB4 immunoreactivity (Fig.4B-3A,E) was detected in neurons, confirmed by co-localization with the neuronal marker MAP2 (Fig.4B-3B,F), both in the cytoplasm and at the cell membrane. ErbB2 was localized to perikarya, dendrites and axons (Fig.4B-3A,B), whereas ErbB4 was confined to the somatodendritic axis (Fig.4B-3E,F). In contrast, ErbB3 immunoreactivity was faint and at the level of background (Fig.4B-3C,D).

In conclusion, ErbB2 and ErbB4 receptors are expressed in developing forebrain and GN11 neurons. Only traces of *ErbB3* receptor mRNA, but not the protein, are found in the developing forebrain. GN11 neurons do not express ErbB3 receptor. Both, developing forebrain and GN11 neurons are excellent models to study NRG-induced neuronal migration exclusively via ErbB2/ErbB4 receptors.

Cyt1 and Cyt2 expression in the developing rat forebrain and GN11 neurons

Rat ErbB4 receptor has two intracellular isoforms, Cyt 1 and Cyt2. The former has a unique tyrosine (Y^{1056}) residue that binds to PI3K and, via this pathway, mediates NRG-dependent cell chemotaxis. To assess if both intracellular ErbB4 isoforms were expressed in developing rat forebrain (E16) and GN11 neurons, RT-PCR was performed using single-stranded DNA libraries from these samples in conjunction with Cyt1 and Cyt2 discriminating primers (Fig.4B-4; see material and methods).

Unfortunately, despite repeated attempts, the RT-PCR produced only partially explicable results. At first sight, it appeared that Cyt1 was expressed in both rE16 forebrain and GN11 neurons when using the Cyt1-specific primers. However, this was confounded by the absence of a corresponding Cyt1 band using the non-specific Cyt1,Cyt2 primers. Indeed, these non-specific primers were found to give rise to only one product, which appeared to correspond to Cyt2 when compared with the positive control; furthermore, this product was only detected in the rat developing forebrain and not in GN11 cells. In summary, I believe that Cyt1 is expressed by rE16 forebrain and GN11 cells, and that Cyt2 is only expressed by rE16 cells. However, owing to the problems outlined above, the RT-PCR will need to be repeated to obtain a definitive answer.

Cloning the rat ErbB4 receptor

In order to study the function of the ErbB4 receptor and its isoforms (Cyt1 and Cyt2) in the migration of neurons (interneurons and GN11), the rat ErbB4 receptor was cloned.
The cloning of this receptor was performed through two steps: a dominant negative form of the rat ErbB4 receptor (dnErbB4), truncated for most of the intracellular part including the tyrosine kinase domain, was cloned first (Fig.4B-1). Then, the Cyt1 and Cyt2 intracellular forms of the receptor (Fig.4B-1) were cloned and ligated into dnErbB4 using a unique restriction site.

Cloning the rat DnErbB4

Rat DnErbB4 was cloned by PCR from a rat adult forebrain single-stranded DNA library using the proofreading DNA polymerase *Pfu*.

Rat DnErb4 cloning primers (I)
Forward primer: CACGAATTCTGAGACTTGC
Reverse primer: GTAAAAGTCCTTGGCTCGG
PCR conditions
95°C, 2min, pause; add Pfu enzyme; (d) 95°C, 1min 30 s; (a) 55°C, 1min 45 s; (e) 72°C, 5min; 27 cycles; final extension 72°C, 10min

Pfu polymerase generates blunt-end PCR fragments. Therefore, the PCR product was first A-tailed using Taq DNA polymerase prior to ligation into the pGEM-T Easy vector (Promega). The identities of the clones were confirmed by sequencing. However, sequencing showed that only the rat DnErbB4-JMa form was successfully cloned, and this plasmid was termed DnErbB4-JMa-TE.

In order to add the myc epitope, the rat DnErbB4 was cloned again by PCR using the *Pfu* polymerase and the DnErbB4-JMa-TE vector as a template. The primers, forward and reverse, incorporating an *Apa* I and a *Xba* I restriction endonuclease site, respectively, were designed to introduce the myc epitope in frame.

Rat DnErb4 cloning primers (II) with *Apa* I and *Xba* I sites
Forward primer: CAGT ***GGGCCC*** CACGAATTCTGAGACTTGC (with ***Apa*** **I** site)
Reverse primer: CAGT ***TCTAGA*** CCCGAGCCAAGGACTTTTAC (with ***Xba*** **I** site)
PCR conditions
95°C, 2min, pause; add Pfu enzyme; (d) 95°C, 1min 30 s; (a) 55°C, 1min 45 s; (e) 72°C, 5min; 30 cycles; final extension 72°C, 10min

The PCR product was ligated into pcDNA3.1mychis B(-) (Invitrogen; Fig.4B-5A) between the *Apa* I and *Xba* I sites of the multiple cloning site (Fig.4B-5B). The plasmid was named pcDNA3.1-DnErbB4-JMa-mychis.

Cloning the rat Cyt1 and Cyt2 ErbB4 isoforms

The intracellular part of rat ErbB4 receptor was cloned by PCR from a rat adult forebrain single-stranded DNA library using *Pfu* polymerase. The primers, forward and reverse, incorporating a *BsrG* I and a *Xba* I restriction endonuclease site, respectively, were designed to introduce the myc epitope in frame. Reverse primer contained the stop codon that was mutated (TGA→AGA) in order to permit the expression of the contiguous myc sequence.

Rat Cyt1, Cyt2 isoform cloning primers with integral *BsrG* I and *Xba* I sites F: GGACCTGACAAC***TGTACA***AAGTGT (with ***BsrG* I** site) R: CAGT ***TCTAGA*** GCTCTCACCACAGTATTCC (with ***Xba* I** site, **stop codon** mutated) PCR conditions 95°C, 2min, pause; add Pfu enzyme; (d) 95°C, 1min 30 s; (a) 55°C, 1min 45 s; (e) 72°C, 5min; 33 cycles; final extension 72°C, 10min

Cyt1 and Cyt2 isoforms were selected by PCR screening of bacterial clones using specific sets of primers that could distinguish between the two isoforms (same as Fig.4B-4; Fig.4B-6A,B,C). After several attempts only the Cyt2 isoform had been isolated, hence the Cyt2 PCR product was ligated into the pcDNA3.1-DnErbB4-JMa-mychis plasmid (Fig.4B-6D) using the *BsrG* I and *Xba* I restriction sites (Fig.4B-6D). The plasmid was called pcDNA3.1-DnErbB4-JMA-Cyt2-mychis. After PCR detection of Cyt1, a short sequence of Cyt1 containing the PI3K-binding site was ligated into pcDNA3.1-DnErbB4-JMA-Cyt2-mychis using the *Cla* I and *Xho* I restriction sites (Fig.4B-6E). In both Cyt1 and Cyt2 clones, the *Cla* I restriction site was protected from cleavage as it was methylated by *Dam* methylase. To prevent *Dam* methylase activity, the plasmids were propagated in a *Dam*$^-$ bacteria strain before *Cla* I digestion.

All myc-tagged constructs were sequenced to confirm their correct identity. The expression of myc-tagged proteins was verified by anti-c-myc immunohistochemistry after transfection of the relevant plasmids into GN11 neurons (Fig.4B-7). C-myc immunoreactivity was neither detected in non-transfected GN11 neurons (Fig.4B-7A) nor in GN11 neurons transfected with the control, pcDNA3.1mychis vector (Fig.4B-7B,C). GN11 neurons transfected with pcDNA3.1-DnErbB4-JMa-mychis plasmid

(Fig.4B-7D-F), pcDNA3.1-Cyt1-JMa-mychis plasmid (Fig.4B-7G-I), pcDNA3.1-Cyt2-JMa-mychis plasmid (Fig.4B-7J-L), were c-myc^{+}, and immunorectivity was confined to the plasma membrane. This suggested that cloned ErbB4 receptors, truncated or full-length, were indeed targeted to the membrane.

The myc-tagged constructs were then subcloned into the multiple cloning site of the pCAG-IRES2-eGFP vector (a gift from Mikio Hoshino, Kyoto University, Japan; Fig.4B-8A) using *Afl* II (*Bst98* I) and *Cla* I blunt-ended sites, respectively, and the Nhe I site (Fig.4B-8B,C). The expression of EGFP (pCAG-IRES2-eGFP vector; Fig.4B-9A-C) and c-myc/EGFP (pCAG-DnErbB4-JMa-IRES2-eGFP, Fig.4B-9D-H; pCAG-Cyt1-JMa-IRES2-eGFP, Fig.4B-9I-M; pCAG-Cyt2-JMa-IRES2-eGFP, Fig.4B-9N-R) in GN11 neurons was confirmed by fluorescence microscopy and immunohistochemsitry after the transfection. While EGFP was detected in the cytoplasm of the GN11 neurons, the cloned ErbB4 receptors, revealed with anti-c-myc antibody, were found on the membrane. The rat ErbB4 isoforms, JMa-Cyt1 (accession number AY375306.1) and JMa-Cyt2 (accession number AY375307.1), were submitted to the GenBank by Gambarotta et al. in September 2003, whilst this work was under way. However, I can confirm that the sequences obtained in this study are in agreement with those deposited in GenBank.

The plasmids used in following *in vitro* migratory assays were renamed for easy reference: pCAG-IRES2-eGFP, pCAG-DnErbB4-JMa-IRES2-eGFP, pCAG-Cyt1-JMa-IRES2-eGFP, pCAG-Cyt2-JMa-IRES2-eGFP to pGAG-eGFP, pCAG-dnErbB4-eGFP, pCAG-Cyt1-eGFP, pCAG-Cyt2-eGFP.

ErbB4 receptor plays a role in tangential migration of cortical interneurons

The ErbB4 receptor is expressed on the surface of migrating cortical interneurons from the ventral forebrain (Yau et al., 2003b). In order to study the importance of this receptor in tangential migration of cortical interneurons, I introduced pCAG-eGFP (to serve as a control) and pCAG-dnErbB4-eGFP into the MGE of rat forebrain slices by *in vitro* electroporation, and analysed their migration in the cortex after 48-72 hours (Fig.4B-10A,B). I found a significant reduction of interneurons migrating into the cortex when they were transfected with the pCAG-dnErbB4-eGFP construct compared to forebrain slices transfected with the control vector. A small number of the green cells expressing

dnErbB4 were often found in the cortex just bellow the pia, but rarely close to the proliferative zones.

PI3K is not necessary for ErbB4-mediated migration of cortical interneurons and GN11 neurons

It has been shown that the ErbB4 Cyt2 isoform, unlike the Cyt1 isoform, does not mediate NRG1β-induced chemotaxis in NIH3T3 fibroblasts due to lack of PI3K-binding site (Kainulainen et al., 2000). However, another study showed that both ErbB4 isoforms can activate, directly or indirectly (via ErbB3 receptor), the PI3K pathway and induce NRG1β-mediated migration in neuronal progenitor cells ST14A (Gambarotta et al., 2004). In any case, PI3K has been proposed to be an important signalling molecule in ErbB4-mediated chemotaxis. Here, I further investigated the motogenic abilities of the two ErbB4 isoforms, Cyt1 and Cyt2, in forebrain interneurons and GN11 neurons.

In order to test the role of the ErbB4 receptor, and related signal molecule PI3K, in tangential migration of cortical interneurons, I introduced Cyt1 and Cyt2 ErbB4 isoforms into developing brain. Different constructs, pCAG-eGFP (served as a control), pCAG-Cyt1-eGFP, pCAG-Cyt2-eGFP, were introduced into the MGE by electroporation, and the migration of cells in the cortex was assessed 48-72 hours later (Fig.4B-10C,D). I found that interneurons transfected with the control vector, as well as with the plasmids containing Cyt1 and Cyt2, migrated into the cortex normally (Fig.4B-10A,C,D,E). This prompted me to hypothesize about an ErbB4-PI3K-independent migration of cortical interneurons. Expression of ErbB3 mRNA, but not the protein, in rat R16 forebrain could potentially enable a migratory response via Cyt2-ErbB3 interaction as suggested by Gambarotta et al. (2004). This possibility led to my adoption of a system completely devoid of ErbB3 receptor in order that such mechanism could be definitely excluded.

I used GN11 neurons, expressing ErbB2 and ErbB4 receptors, but not ErbB3, to confirm the results obtained in assays with cortical interneurons. GN11 neurons were transfected with different constructs, pCAG-eGFP (serves as a positive control), pCAG-Cyt1-eGFP, pCAG-Cyt2-eGFP, using Lipofectamine 2000 reagent. Different constructs, expressing GFP, were isolated by FACS, and subjected to an *in vitro* migratory assay

(Boyden chamber) with NRG1β (100 and 200 ng/ml) as a chemoattractant. Results from this assay confirmed my hypothesis about an ErbB4-PI3K-independent neuron migration. GN11 neurons showed a) a dose-dependent response to NRG1β (Fig.4B-11A), b) there was no difference in migratory properties of Cyt 1 and Cyt2 ErbB4 isoforms (Fig.4B-11B), and c) GN11 neurons, expressing either Cyt1 or Cyt2, migrated more compared to cells expressing a control vector only (Fig.4B-11B).

DISCUSSION

In this study, to reveal the role of the ErbB4 receptor in migration of interneurons, a dominant negative form of the rat ErbB4 receptor and its Cyt1 and Cyt2 isoforms were cloned. Results of the study showed: (i) the involvement of the ErbB4 receptor in the tangential migration of cortical interneurons *in vitro*; (ii) that the two NRG receptors, ErbB2 and ErbB4, but not ErbB3, are localised in developing forebrain neurons and GN11 cells; and (iii) that the ErbB4-mediated migration of cortical interneurons, and of GN11 cells is a PI3K-independent event.

Role of ErbB4 in cortical interneuron migration

There are several lines of evidence to support the notion that NRGs regulate the tangential migration of cortical interneurons. First, early expression of *Nrg1* mRNA (mouse E12.5 or E13.5) partially overlaps with the expression of *Lhx6* mRNA, thus with the migratory route of interneurons from the GE towards the cortex (Assimacopoulos et al., 2003; Flames et al., 2004). During that early period, *Nrg1-Ig* mRNA encoding secreted forms of NRG1 is expressed in the cortical proliferative zones (Flames et al., 2004), indicating a role for secreted NRG1 in attracting the subventricular stream of tangentially migrating cortical interneurons. *Nrg1-CRD* mRNA, which gives rise to the membrane-bound form of NRG1, is found to be expressed in the GE, and probably facilitates migration of interneurons through the GE (Flames et al., 2004). Secondly, it has been shown *in vitro* that NRG1 is a chemoattractant for the MGE-derived cells (Flames et al., 2004). Thirdly, the NRG receptor ErbB4 is expressed on migrating

cortical interneurons and co-localizes with the interneuron marker DLX2 (Yau et al., 2003c).

My *in vitro* loss-of-function experiments, using a dominant negative form of ErbB4 (dnErbB4) receptor lacking the tyrosine kinase domain, demonstrated an ErbB4-dependent migration of cortical interneurons from the MGE. This finding is in agreement with a recent study that shows (i) a significant reduction in migration to the cortex of interneurons expressing a dnErbB4 receptor, and (ii) a reduced number of cortical GABAergic interneurons in the adult cortex in conditional ErbB4 mutants (Flames et al., 2004). In these mutants the heart defects are rescued by expressing ErbB4 under a cardiac-specific myosin promoter (Tidcombe et al., 2003). I also found, using an *in vitro* migratory assay, that MGE-derived cells from either E13.5 mouse or E16 rat, a time of intense interneuron migration to the cortex, were attracted by NRG1β (data not shown); a similar finding has been reported by (Flames et al., 2004). However, this is contrary to the data of Li et al. (2004) demonstrating a repellent effect of NRGs on neurons.

Role of PI3K in NRG/ErbB4-induced neuron migration

Binding of NRGs to ErbB3 and ErbB4 receptors elicit their dimerization (homo- or hetero- with the ErbB2 receptor), tyrosine phosphorylation, and activation of downstream signalling pathways. The Cyt1, but not the Cyt2, isoform of the ErbB4 receptor is able to activate the PI3K pathway. It has been suggested that the PI3K pathway, activated upon ligand binding to ErbB4-Cyt1 isoform, is involved in cellular chemotaxis (Kainulainen et al., 2000). However, my *in vitro* experiments demonstrated a PI3K-independent mechanism for ErbB4-mediated migration of cortical interneurons from the MGE.

The study of Kainulainen et al. (2000) showed that chemotaxis of NIH 3T3 fibroblasts towards a gradient of NRG1β is regulated by the ErbB4-PI3K signalling pathway. However, we have to take in account that fibroblasts are not neurons and, perhaps, different signalling mechanisms of migration apply for these two cell groups.

Another group used ST14A cells (a neural progenitor cell line derived from the striatum of E14 rats) that endogenously express ErbB1, ErbB2 and ErbB3 receptors, but

no ErbB4 (Gambarotta et al., 2004). They introduced different intracellular isoforms (Cyt1 and Cyt2) of the ErbB4 receptor into ST14A cells, and reported a neuronal migration regulated by the PI3K pathway. They suggested that this was due to the action of the Cyt1 isoform itself or by heterodimerization of the Cyt2 isoform of ErbB4 receptor with the ErbB3 receptor, which possesses many PI3K binding sites. Expression of the ErbB3 receptor in their system precluded any exclusive interpretation of the role of the PI3K-binding site of the Cyt2 isoform of ErbB4 receptor in neuron migration.

The expression profile of neuregulin receptors in the developing forebrain is controversial. *ErbB2* and *ErbB4* mRNAs, but no *ErbB3* mRNA, were found to be expressed in the developing cortex and GE as detected by *in situ* hybridization (Fox and Kornblum, 2005). Likewise, another study showed the presence of ErbB2 and ErbB4, but not ErbB3, as detected by RT-PCR and Western blotting in mouse E14 striatum (Calaora et al., 2001). In this study, I found levels of *ErbB3* mRNA in the developing forebrain that were detectable by PCR. However, I was not able to detect any ErbB3 receptor at protein level, using either Western blotting or immunohistochemistry. Interestingly, Li et al. (2004) claimed that other ErbBs, apart from ErbB4, were not expressed in the cortex. In contrast, Anton et al. (1997) detected all three neuregulin receptors in developing cortex; ErbB2 was mainly expressed in glia (radial), while ErbB3 and ErbB4 in neurons (neuroblasts and posmitotic cells). Presence of all three neuregulin receptors on the developing cortical neurons was reported by Li et al. (2003). At last, ST14A cells, derived from E14 striatum, expressed ErbB2 and ErbB3, but not ErbB4 receptor (Gambarotta et al., 2004).

In order to eliminate any possible influence of the ErbB3 receptor in neuronal migration, I used GN11 neurons. GN11 neurons are an immortilized cell line of GnRH neurons obtained from an olfactory bulb tumour that retained the ability to migrate (Radovick et al., 1991; Maggi et al., 2000). I showed that GN11 neurons express both ErbB2 and ErbB4 receptors, but not ErbB3 (at both mRNA and protein level), and respond to NRG1β by migration towards its gradient in an *in vitro* migratory assay. GN11 neurons transfected with either the Cyt1 or Cyt2 isoform of the ErbB4 receptor migrated with no difference towards NRG1β, confirming again that a PI3K-independent neuronal migration occurs via the ErbB4 receptor.

Interestingly, it has been proposed that activation of the ErbB2/ErbB4 complex by neuregulins on hypothalamic astrocytes indirectly stimulates secretion of GnRH and thus contribute to the neuroendocrine control of mammalian sexual development (Ma et al., 1999). It would be interesting to see if GnRH neurons, from which GN11 neurons are derived, also express the ErbB2/ErbB4 receptor complex, and if they could secrete GnRH by their direct stimulation by neuregulins.

We still do not know which signalling pathway mediates ErbB4-dependent migration of cortical interneurons and of GN11 cells. At least two signalling pathways have been shown to be involved in neuregulin signalling via ErbB4 receptor: the PI3K and the MAPK pathways. ErbB4 receptor can activate MAPK/ERK (Cyt1, Cyt2 isoforms) and PI3K pathways, and my data suggest PI3K-independent ErbB4-mediated neuron migration. To further confirm this, I am in process of mutating the PI3K-binding site on the ErbB4 receptor (1056 residue; tyrosine into phenylalanine 1056). Interestingly, Polleux et al. (2002) found that interneuron migration towards the cortex was abolished if the MGE was treated with PI3K inhibitors, but not MAPK inhibitors, indicating that MAPK pathway is not involved in this process.

There is also a possibility that NRG binding to ErbB4 receptor expressed on the migrating neurons could activate other motogenic pathways, such as the Cdk5 pathway. This will be discussed in the next chapter (4C).

Figure 4B-1. Rat ErbB4 receptor, JMa/Cyt1 isoform

Ectodomain of the receptor contains ligand binding sites (L1,L2) and cystein-rich domains (yellow rhomboids). There are two juxtamembrane isoforms, JMa and JMb (differ in either 23 or 13 alternative amino acids). JMa isoform is susceptible to matrix metalloproteinases (MMP) fragmentation. Endodomain contains tyrosine kinase (TK) domain; DnErbB4 form of the receptor lacks most of the intracellular part of the receptor, including the TK domain (a black, thin horizontal line above TK domain represents a border between dnErbB4 and intracellular part of the receptor); TK domain provides sites for association with adaptor proteins. There are two intracellular isoforms, Cyt1 and Cyt2 (differ in 16 amino acids present in Cyt1). Cyt1 contains a unique tyrosine site ($Y1056^{JMa}$) for binding of PI3K; Cyt1 and Cyt2 isoforms can also activate MAPK pathway.

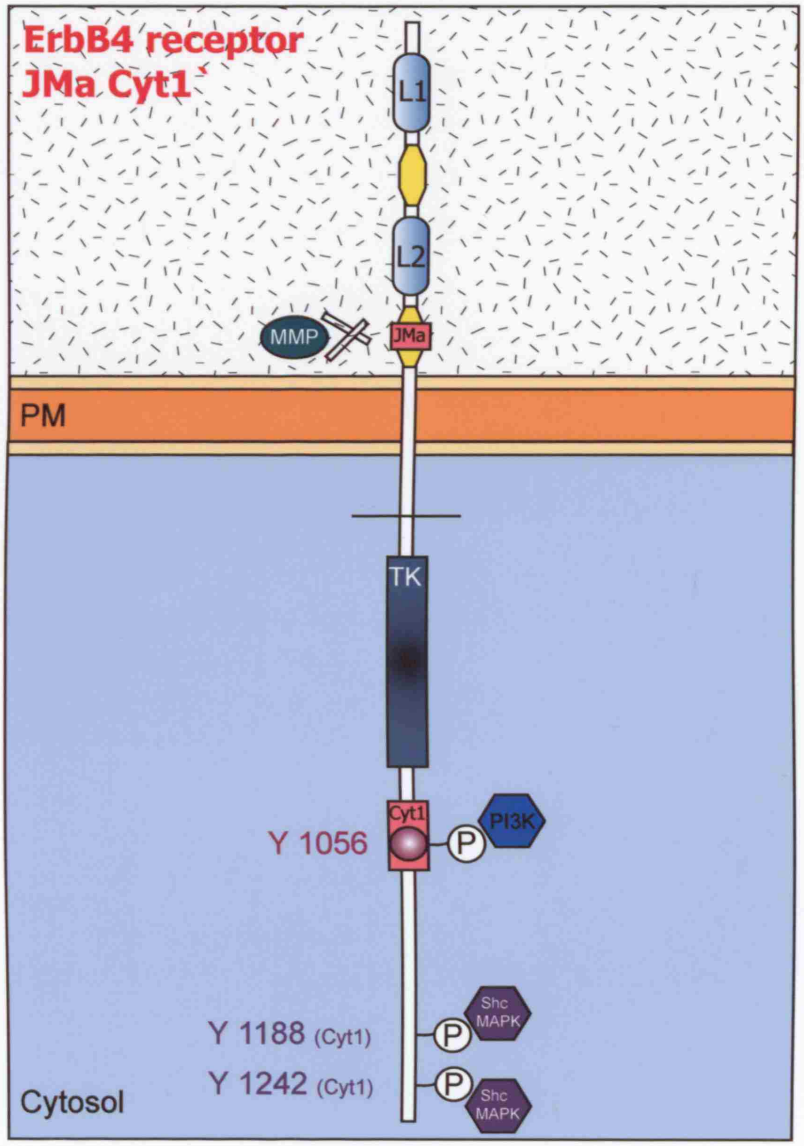
ErbB4 receptor
JMa Cyt1
L1
L2
MMP
JMa
PM
TK
Cyt1
PI3K
Y 1056
P
Shc
MAPK
Y 1188 (Cyt1)
Y 1242 (Cyt1)
Cytosol

Figure 4B-2. ErbB expression in the developing rat forebrain and GN11 neurons

(A) RT-PCR; developing forebrain (rE16) expressed *ErbB2,3,4* mRNAs, while GN11 neurons expressed *ErbB2,4*, but not *ErbB3* mRNAs. Water was used as a no-template control (NTC).

(B) Western blotting; ErbB3 protein was not present in either developing forebrain (rE17) or GN11 neurons. Different levels of ErbB2 and ErbB4 expression were found in the rE17 forebrain (GE, Cx) and GN11 neurons; ErbB2 was highly expressed in GN11 cells, whilst ErbB4 was abundant in rE17 GE.

r – rat; Cx – cortex; GE – ganglionic eminence.

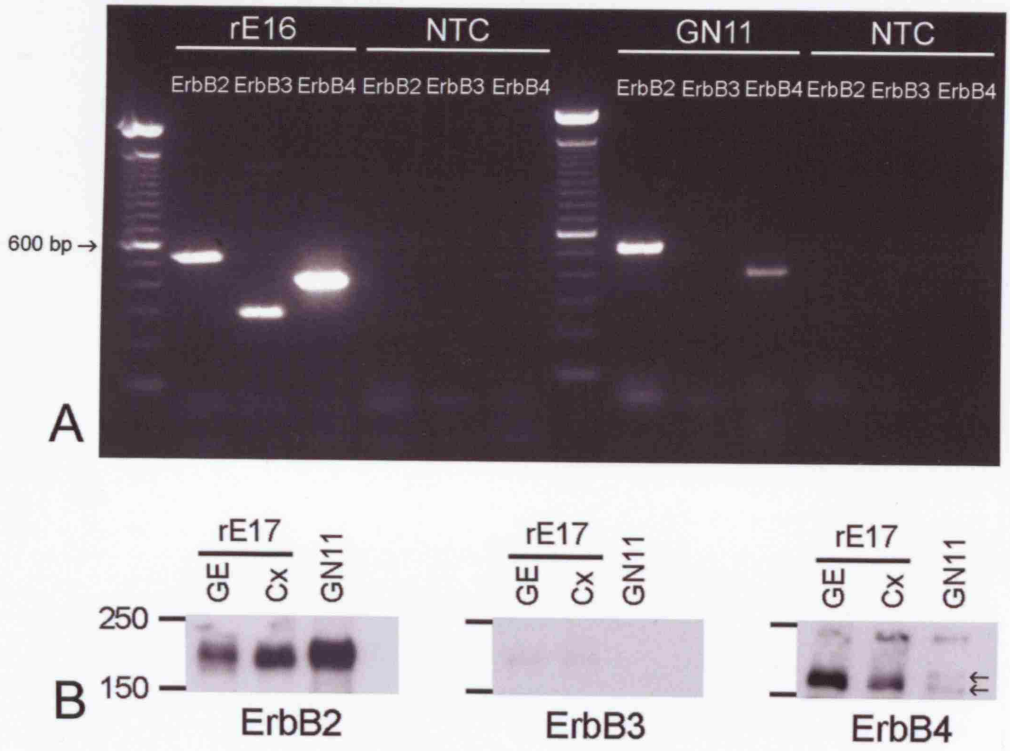
rE16
NTC
GN11
NTC
ErbB2 ErbB3 ErbB4 ErbB2 ErbB3 ErbB4
ErbB2 ErbB3 ErbB4 ErbB2 ErbB3 ErbB4
600 bp →
A
rE17
GE
Cx
GN11
250
150
B
ErbB2
ErbB3
ErbB4

Figure 4B-3. Expression of NRG-receptors in developing MGE

Confocal photomicrographs of dissociated cultures of rat E16 medial GE visualized by ErbB2 (A-B), ErbB3 (C-D), ErbB4 (E-F) and MAP2 (B,D,F) immunofluorescence. Antibody to MAP2 marks neuronal soma and dendrites.

(A-B) ErbB2 receptor was localized to perikarya, dendrites and axons. $ErbB2^{+}/MAP2^{-}$ process represents an axon (arrow).

(C-D) ErbB3 immunoreactivity was hardly detectable.

(E-F) ErbB2 receptor was clearly present in perikarya and dendrites.

GE – ganglionic eminence. Scale bar, 25 μm.

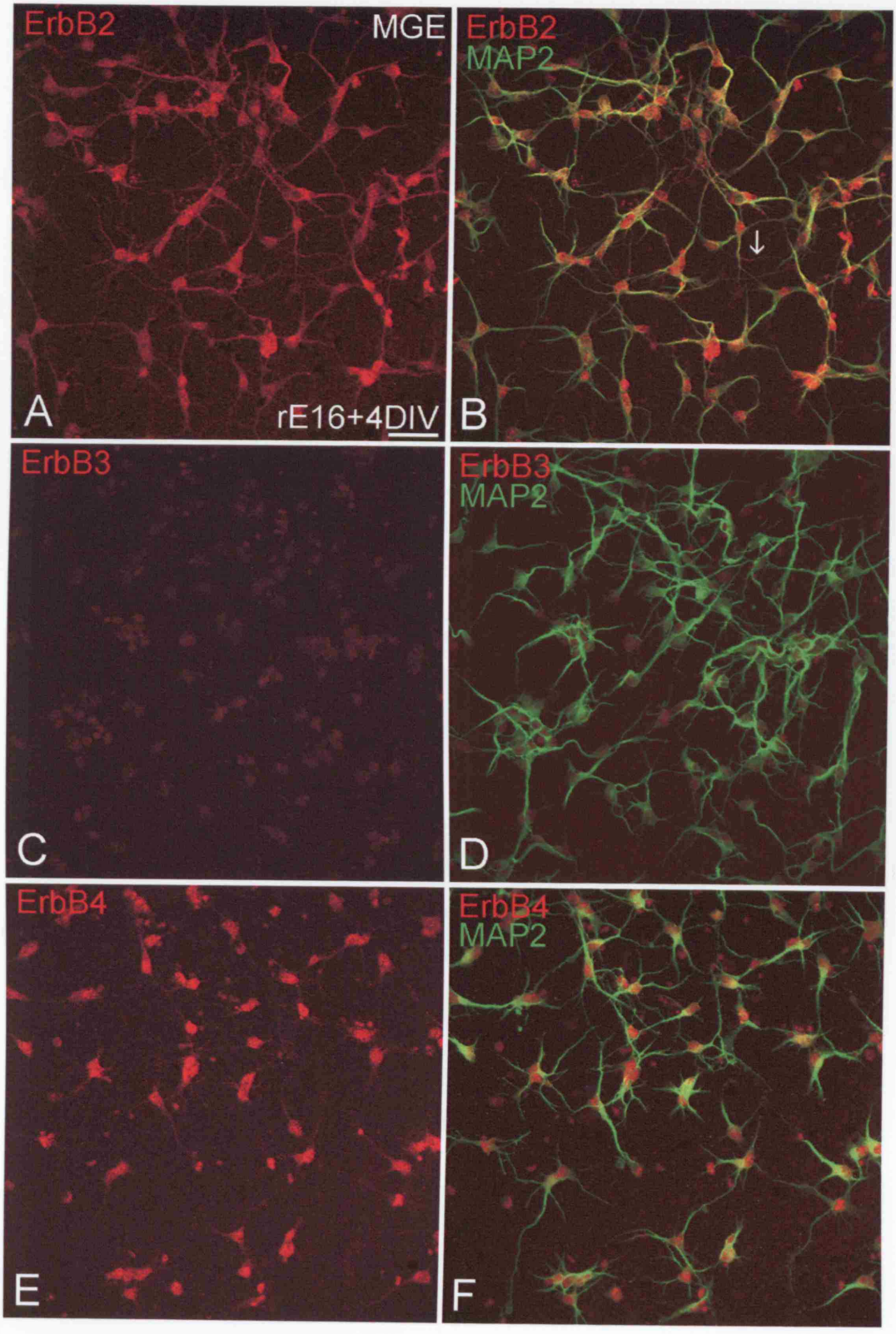
ErbB2
MGE
A
rE16+4DIV
ErbB2
MAP2
B
ErbB3
C
ErbB3
MAP2
D
ErbB4
E
ErbB4
MAP2
F

Figure 4B-4. Expression of Cyt1 and Cyt2 isoforms in developing forebrain and GN11 neurons

Cyt1 isofrom mRNA (222 bp) was present in the developing rat E16 forebrain and GN11 neurons. Cyt2 isoform mRNA (394 bp) was likely to be found in the developing rat E16 forebrain, but not in GN11 neurons. The positive controls for Cyt1 and Cyt2 isoforms were pCAG-Cyt1-eGFP (pCyt1; 222 bp) and pCAG-Cyt2-eGFP (pCyt2; 394 bp) plasmids, respectively.

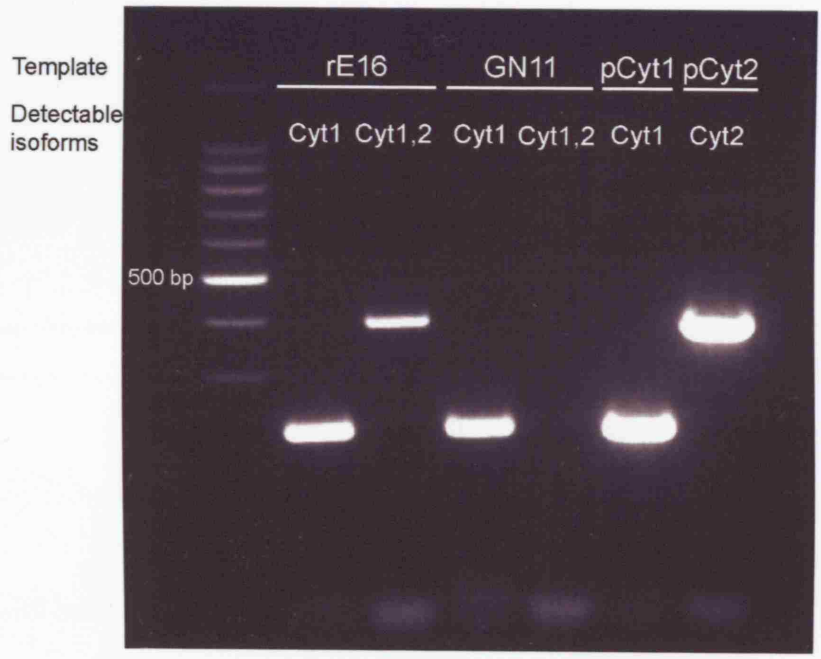
Template
Detectable isoforms
rE16
GN11
pCyt1
pCyt2
Cyt1
Cyt1,2
Cyt1
Cyt1,2
Cyt1
Cyt2
500 bp

Figure 4B-5. Myc-tagged DnErbB4-JMa

(A) Schematic representation of the multiple cloning sites of the pcDNA3.1mychis B (-) vector (Invitrogen).

(B) Schematic representation of pcDNA3.1-DnErbB4-JMa-mychis; rat DnErbB4-JMa cDNA insert was ligated into the pcDNA3.1mychis B (-) vector between *Apa* I and *Xba* I restriction sites.

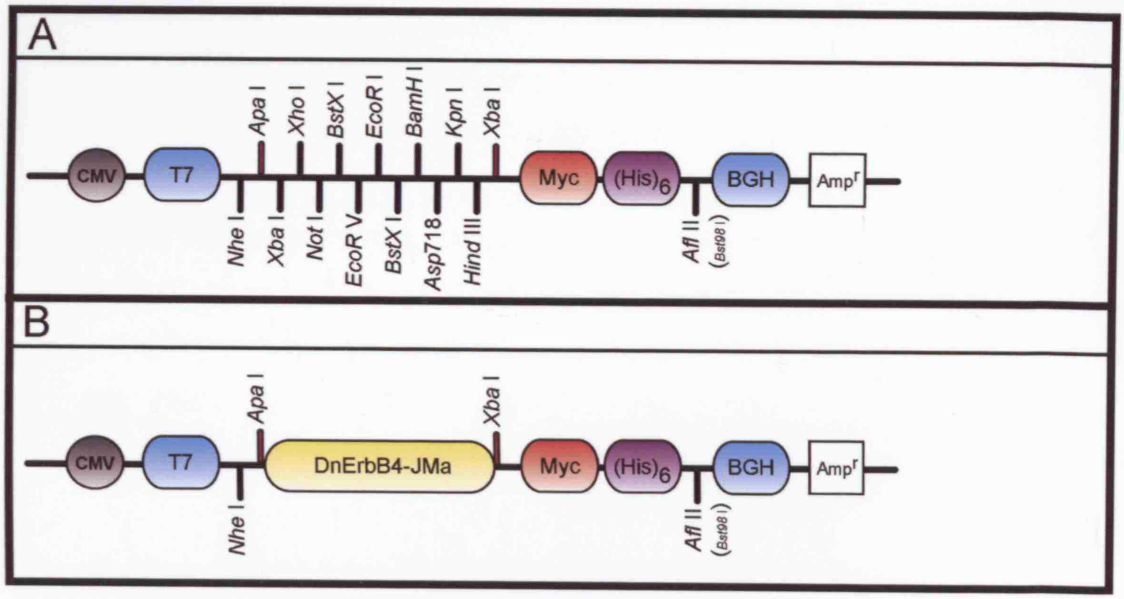
A
CMV
T7
Apa I
Xho I
BstX I
EcoR I
BamH I
Kpn I
Xba I
Nhe I
Xba I
Not I
EcoR V
BstX I
Asp718
Hind III
Myc
(His)6
BGH
Ampr
Afl II
(Bst98 I)
B
CMV
T7
Apa I
Nhe I
DnErbB4-JMa
Xba I
Myc
(His)6
BGH
Ampr
Afl II
(Bst98 I)

Figure 4B-6. Myc-tagged Cyt1 and Cyt2 isoforms

(A) Position of primers (red *) for detecting the Cyt1 and Cyt2 isoforms of the ErbB4 receptor.

(B) Sequence of primers (highlighted in red) for detecting the Cyt1 and Cyt2 isoforms of the ErbB4 receptor. Second primer for detecting the Cyt1 isoform is within the Cyt1-specific sequence (highlighted in pink).

(C) PCR screening of bacterial clones containing either Cyt1 or Cyt2 ErbB4 isoforms isolated from rat E16 forebrain single-stranded DNA library. Arrows indicate the position of bands corresponding to Cyt1 isoform (442 bp and 222 bp), and open arrow shows the position of band corresponding to Cyt2 isoform (394 bp). Cyt1 and Cyt2 clones were found in lanes 5,8 and 1,2,4,6,9,10,11,12, respectively. Lanes 13 and 14 contained positive controls, pCAG-Cyt1-eGFP (pCyt1) and pCAG-Cyt2-eGFP (pCyt2) plasmids.

(D) Cyt1 and Cyt2 cDNA inserts were intended to be ligated into the pcDNA3.1-DnErbB4-JMa-mychis plasmid between *BsrG* I and *Xba* I sites. The pcDNA3.1-Cyt2-JMa-mychis plasmid was successfully inserted (the bottom one).

(E) The short sequence of Cyt1 cDNA insert, cut between *Cla* I and *Xba* I sites, was introduced to pcDNA3.1-Cyt2-JMa-mychis plasmid using the same restriction enzymes.

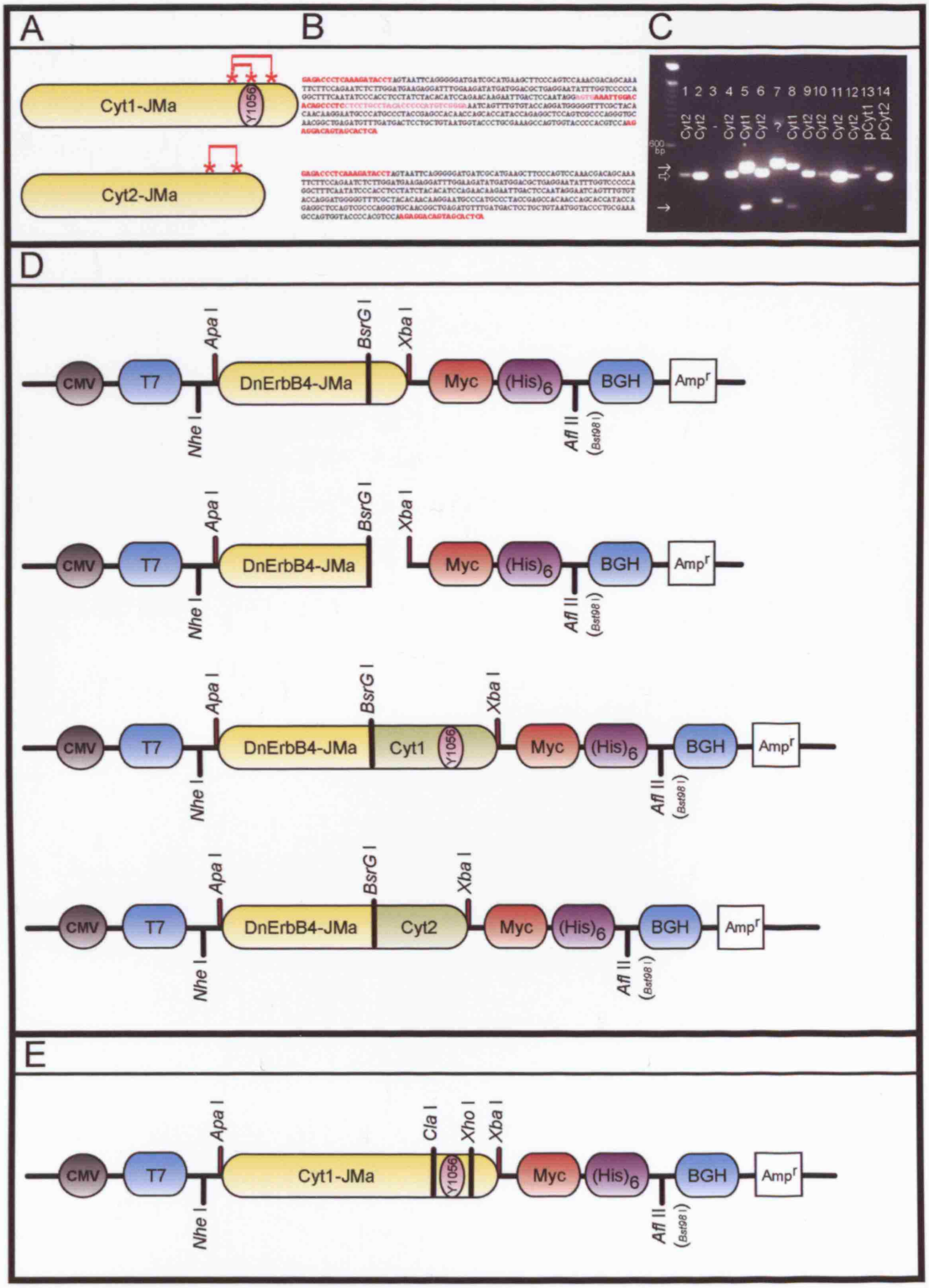
A
B
C
Cyt1-JMa
Y1056
Cyt2-JMa
1 2 3 4 5 6 7 8 9 10 11 12 13 14
Cyt2 Cyt2 - Cyt2 Cyt1 Cyt2 ? Cyt1 Cyt2 Cyt2 Cyt2 Cyt2 pCyt1 pCyt2
600 bp
D
CMV
T7
Apa I
Nhe I
DnErbB4-JMa
BsrG I
Xba I
Myc
(His)6
BGH
Ampr
Afl II
(Bst98 I)
Cyt1
Cyt2
E
Cla I
Xho I

Figure 4B-7. Transient expression of myc-tagged ErbB4 constructs in GN11 neurons

Cultured GN11 neurons were transfected with the myc-tagged ErbB4 constructs and visualized by c-myc immunofluorescence. Bisbenizimide (BB) was used to label nuclei. pcDNA3.1mychis vector and myc-tagged ErbB4 constructs were schematically illustrated (B,D,G,J). The engineered ErbB4 constructs correctly localized to the cell membrane, as expected given the knowledge that ErbB4 is a transmembrane receptor. This was confirmed by taking an additional, orthogonal view of confocal images and evaluating the labeled cells in three dimensions (F.I,L).

(A) Untransfected GN11 neurons.

(B-C) GN11 neurons transfected with pcDNA3.1mychis vector; No c-myc immunoreactivity was detected.

(D-F) GN11 neurons transfected with pcDNA3.1-DnErbB4-JMa-mychis plasmid.

(G-I) GN11 neurons transfected with pcDNA3.1-Cyt1-JMa-mychis plasmid.

(J-L) GN11 neurons transfected with pcDNA3.1-Cyt2-JMa-mychis plasmid.

Scale bar, 20 μm.

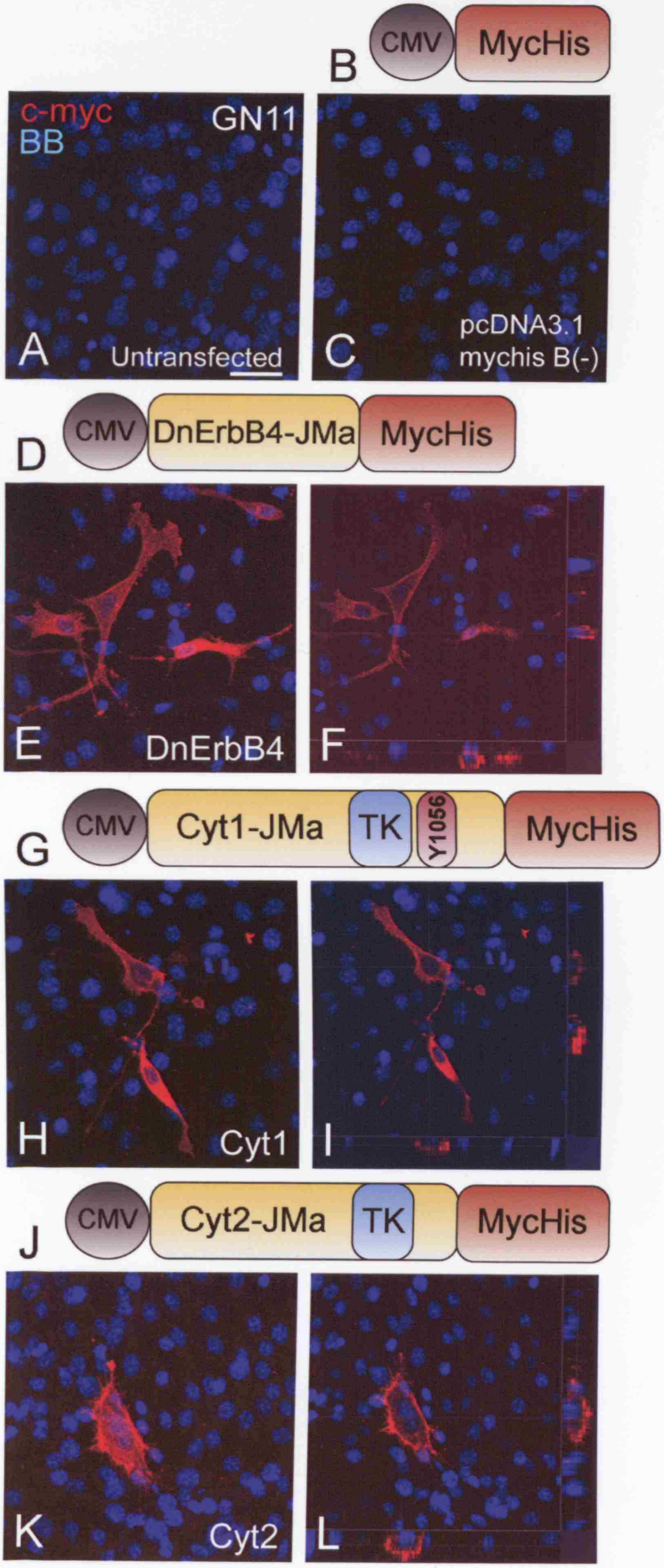
B
CMV
MycHis
c-myc
BB
GN11
A
Untransfected
C
pcDNA3.1
mychis B(-)
D
CMV
DnErbB4-JMa
MycHis
E
DnErbB4
F
G
CMV
Cyt1-JMa
TK
Y1056
MycHis
H
Cyt1
I
J
CMV
Cyt2-JMa
TK
MycHis
K
Cyt2
L

Figure 4B-8. Subcloning of myc-tagged ErbB4 constructs into pCAG-IRES2-eGFP vector

(A) Schematic representation of the multiple cloning sites of the pCAG-IRES2-eGFP vector (a gift from Mikio Hoshino, Japan); the vector was linearized with *Cla* I, blunted with T4 DNA polymerase and cut with *Nhe* I.

(B) Schematic representation of intermediate myc-tagged ErbB4 plasmids; the plasmids were linearized with *Afl* II (or its isomerase *Bst98* I), blunted with T4 DNA polymerase, cut with *Nhe* I, and ligated into the multiple cloning site of modified pCAG-IRES2-eGFP (A).

(C) Schematic representation of the pCAG-DnErbB4-JMa-IRES2-eGFP, pCAG-Cyt1-JMa-IRES2-eGFP, pCAG-Cyt2-JMa-IRES2-eGFP plasmids.

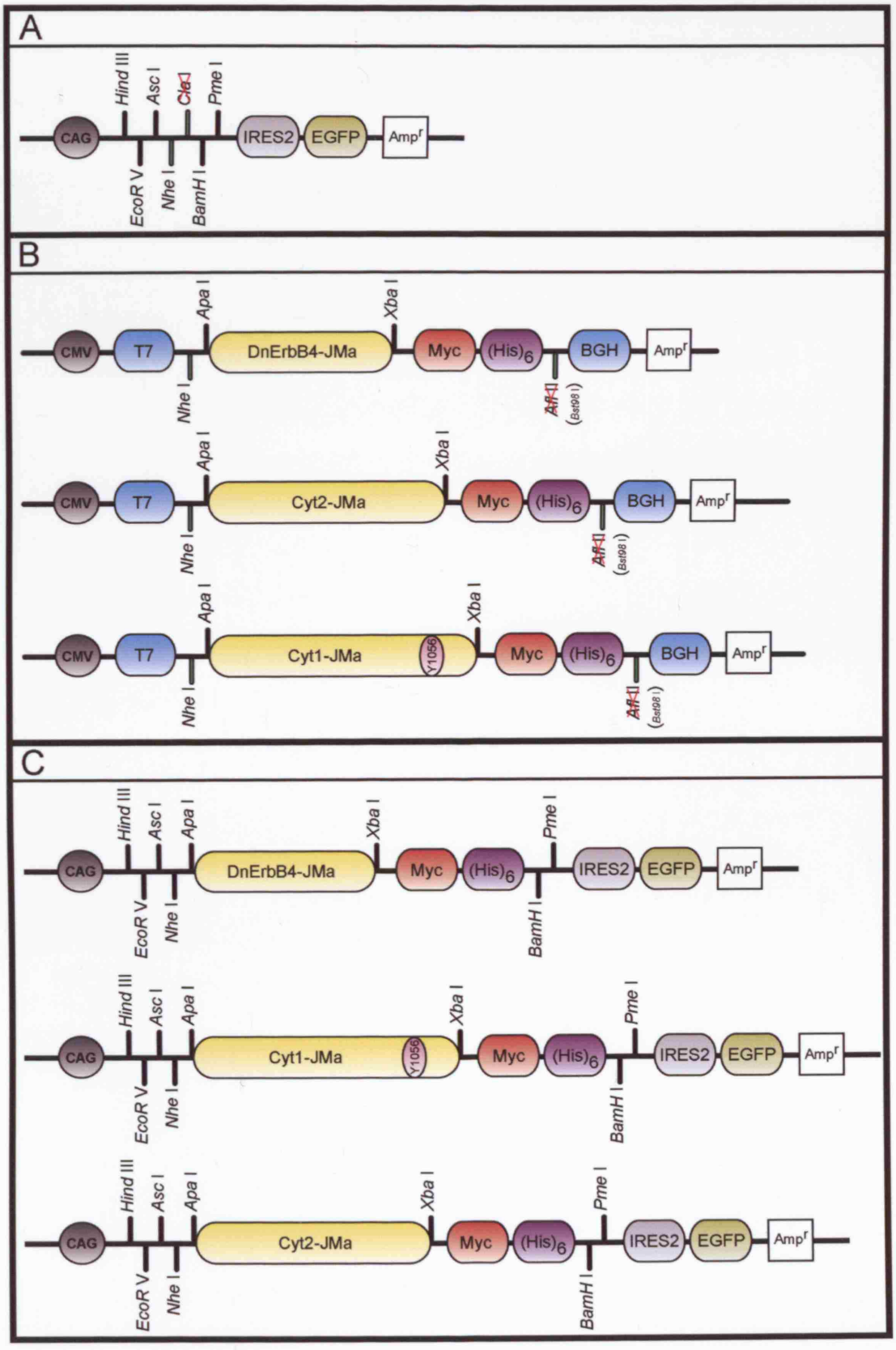
A
Hind III
Asc I
Cla I
Pme I
CAG
IRES2
EGFP
Amp^r
EcoR V
Nhe I
BamH I
B
Apa I
Xba I
CMV
T7
DnErbB4-JMa
Myc
(His)6
BGH
Amp^r
Nhe I
Aff II (Bst98 I)
Cyt2-JMa
Cyt1-JMa
Y1056
C

Figure 4B-9. Transient expression of EGFP-ErbB4myc constructs in GN11 neurons

Cultured GN11 neurons were transfected with EGFP-ErbB4myc constructs and visualized by c-myc and EGFP immunofluorescence. Bisbenizimide (BB) was used to label nuclei. pCAG-IRES2-eGFP and EGFP-ErbB4myc constructs were schematically illustrated (A,D,I,N). C-myc immunoreactivity was detected on the cell membrane (F,H, K,M,P,R), as expected localization of the ErbB4 receptor, whilst EGFP immunoreactivity was localized to the cell cytoplasm (B-C,G-H,L-M,Q-R).

(A-C) GN11 neurons transfected with pCAG-IRES2-eGFP.

(D-H) GN11 neurons transfected with pCAG-DnErbB4-JMa-IRES2-eGFP.

(I-M) GN11 neurons transfected with pCAG-Cyt1-JMa-IRES2-eGFP.

(N-R) GN11 neurons transfected with pCAG-Cyt2-JMa-IRES2-eGFP.

Scale bar, 25 μm.

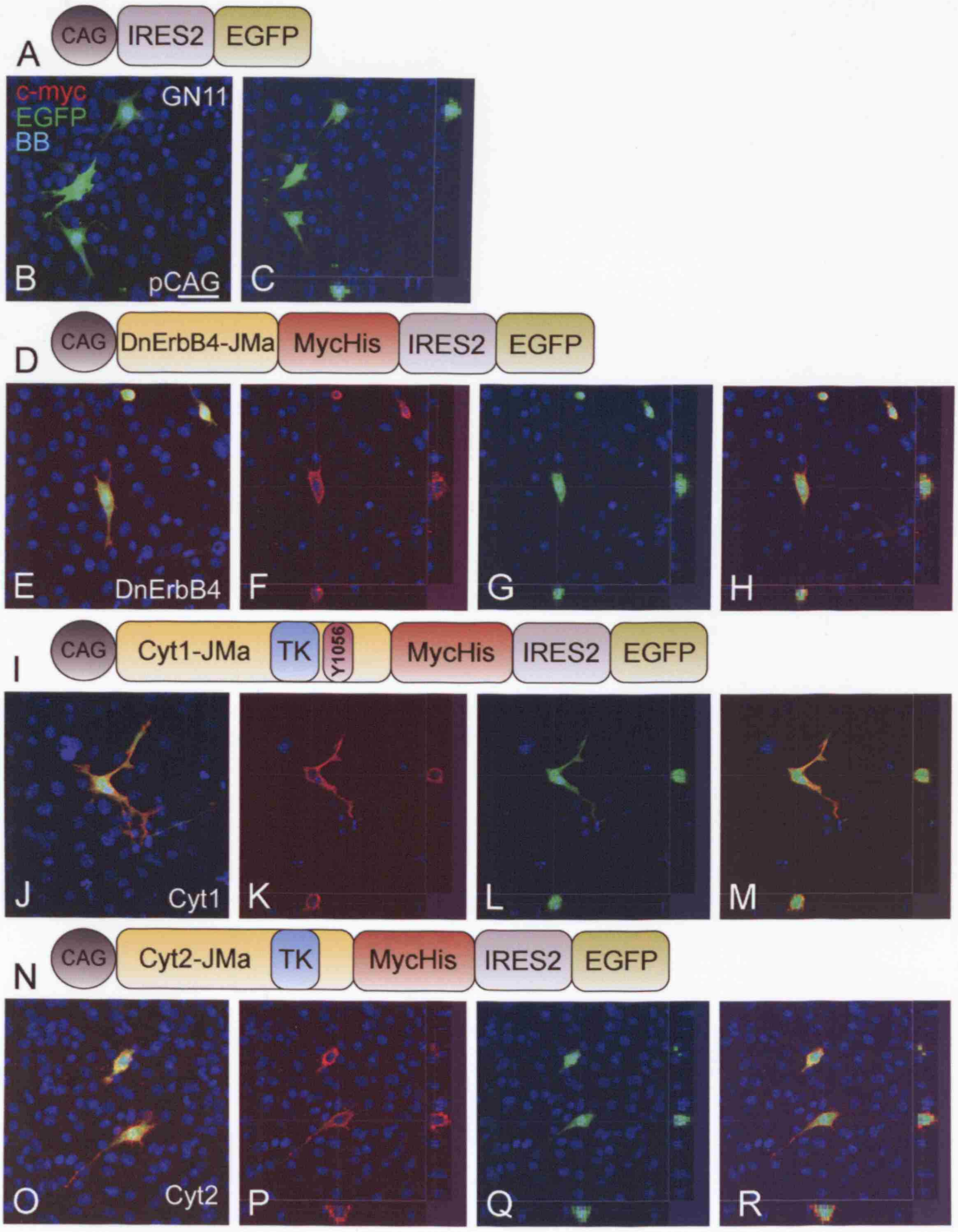
A
CAG
IRES2
EGFP
c-myc
EGFP
BB
GN11
B
pCAG
C
D
CAG
DnErbB4-JMa
MycHis
IRES2
EGFP
E
DnErbB4
F
G
H
I
CAG
Cyt1-JMa
TK
Y1056
MycHis
IRES2
EGFP
J
Cyt1
K
L
M
N
CAG
Cyt2-JMa
TK
MycHis
IRES2
EGFP
O
Cyt2
P
Q
R

Figure 4B-10. ErbB4 signalling mediates interneuron migration to the cortex in a PI3K-independent mechanism

Different eGFP-expressing plasmids (A,B,C,D) were electroporated (EP) into the MGE of rat E16 forebrain slices. Migration of $eGFP^+$ cells was analyzed after 48 hours using a confocal microscope. (A) pGAG-eGFP (pCAG, control); (B) pCAG-dnErbB4-eGFP (DnErbB4); (C) pCAG-Cyt1-eGFP (Cyt1); (D) pCAG-Cyt2-eGFP (Cyt2). Whilst interneurons, overexpressing dnErb4 could not make it to the cortex, no obvious difference in distribution of interneurons transfected with Cyt1 and Cyt2 compared to control (pCAG) was observed. (E) The telencephalic wall was divided into 3 equal zones, from the lateral ventricle (LV) to the pia (zone 1 being closest to the LV), and the percentage of $eGFP^+$ cells in each zone was then calculated. Data in the graph represent mean percentage of migrated cells ± SEM (standard error of the mean) from six independent experiments. Error bars represent SEM. No significant difference in migration of interenurons ovreexpressing control, Cyt1 or Cyt2 plasmid was observed. MGE – medial ganglionic eminence. Scale bar, 250 μm.

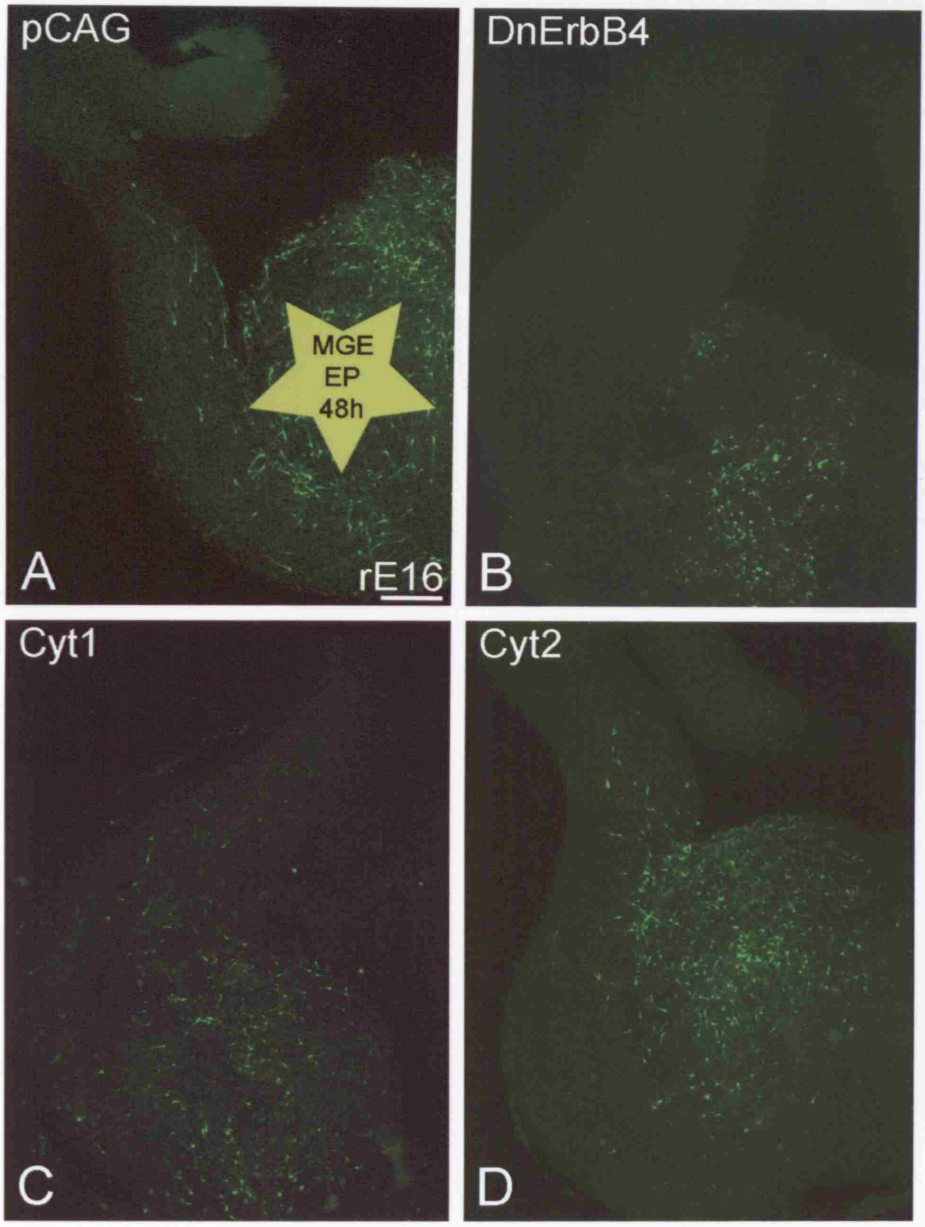
pCAG
MGE
EP
48h
A
rE16
DnErbB4
B
Cyt1
C
Cyt2
D

rE16, MGE EP

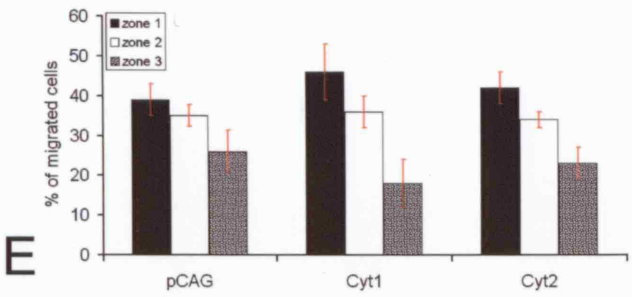
E
% of migrated cells
zone 1
zone 2
zone 3
60
50
40
30
20
10
0
pCAG
Cyt1
Cyt2

Figure 4B-11. ErbB4 signalling mediates directed neuron migration towards neuregulin 1β (NRG1β) in a PI3K-independent mechanism

(A) NRG1β induced a dose-dependent chemotaxis of GN11 neurons, performed in an *in vitro* migratory assay (Boyden chamber). DMEM and 1% FBS were used as negative and positive controls, respectively.

(B) Cultured GN11 neurons were transfected with pGAG-eGFP (pCAG, control), pCAG-Cyt1-eGFP (Cyt1), pCAG-Cyt2-eGFP (Cyt2). $eGFP^+$ cells were selected by FACS sorting and subjected to an *in vitro* migratory assay (Boyden chamber). Chemotactic response of Cyt1- or Cyt2-transfecetd GN11 cells, to either 100 ng/ml (grey bars) or 200 ng/ml (black bars) of NRG1β, was significantly increased (grey or black *) compared to control, pCAG-transfected GN11 cells. Notably, no difference in chemotactic response to NRG1β between Cyt1- and Cyt2-overexpressed GN11 neurons was observed.

Data in the histograms represent mean number of migrated cells per well ± SEM (standard error of the mean) from three independent experiments. Error bars represent SEM. Significance calculated by the Student's *t*-test; **p<0.01, ***<0.005.

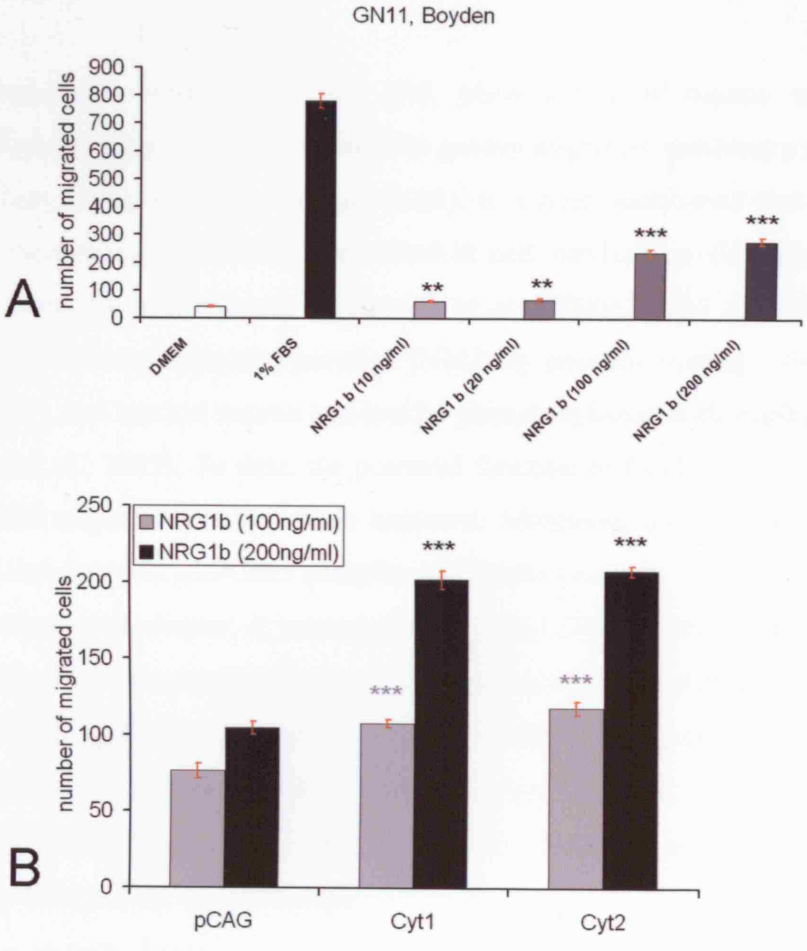
GN11, Boyden
A
number of migrated cells
900
800
700
600
500
400
300
200
100
0
**
**
***
***
DMEM
1% FBS
NRG1 b (10 ng/ml)
NRG1 b (20 ng/ml)
NRG1 b (100 ng/ml)
NRG1 b (200 ng/ml)
B
NRG1b (100ng/ml)
NRG1b (200ng/ml)
number of migrated cells
250
200
150
100
50
0
***
***
***
***
pCAG
Cyt1
Cyt2

CHAPTER 4C

Cdk5 plays a role in NRG1β-induced neuron migration and phosphorylates ErbB4 receptor

INTRODUCTION

Cdk5, in association with its activator p35, plays a role in neuron migration by controlled phosphorylation of components that govern migratory machinery (see reviews Gupta and Tsai, 2003; Tsai and Gleeson, 2005). It is now established that neuregulins (NRG) and their receptor ErbB4 are involved in cell survival, proliferation and most importantly chemotaxis (reviewed by Junttila et al., 2000). Cdk5 mediates synaptic transmission at the neuromuscular junction (NMJ) by phosphorylating ErbB3 receptor (Fu et al., 2001), and cortical neuron survival by phosphorylating both ErbB2 and ErbB3 receptors (Li et al., 2003). To date, the potential function of Cdk5 and its activators in NRG-mediated migration has not been explored. Moreover, there is no data on the biochemical link between p35/Cdk5 complex and ErbB4 receptor.

In the previous chapter, it was revealed that the GN11 neuronal cell line, which has potent migratory characteristics, expressed NRG-specific receptor ErbB4 and its co-receptor ErbB2 (Fig.4B-2). Also, GN11 neurons showed a strong chemotactic response to NRG1β in a dose-dependent fashion (Fig.4B-11A). Moreover, it was clearly shown that migration of GN11 neurons along a gradient of NRG1β, towards the source, is a PI3K-independent process (Fig.4B-11B).

In the present chapter, I report the findings of my research to date on (i) the potential role of Cdk5 in directed neuron migration towards NRG1β, and (ii) Cdk5-induced phosphorylation of ErbB4 *in vitro*.

MATERIALS AND METHODS

Animals

p35 litter was used in this study. GE and cortices were lysed in ErbB4 lysis buffer, and cell lysates run on a 7% denaturing polyacrylamide gel followed by immunoblotting with a rabbit anti-ErbB4 antibody.

GN11 neurons

GN11 neurons, a cell line of immortalized hypothalamic neurons, derived from olfactory bulb tumours, show a chemomigratory response *in vitro*. These cells were used an *in vitro* migratory assay and in immunocytochemical experiments.

In vitro migratory assay (Boyden chamber)

The assay was performed as described in general Materials and Methods. In this study, one half of GN11 cells were treated with 10 or 50 μM Roscovitine (Sigma) dissolved in DMSO. Untreated and Roscovitine-treated cells were then left for 30min at 37°C in a 5% CO_2 humidified incubator prior to migratory assay.

Roscovitine

Roscovitine is a potent, selective inhibitor of Cdc2, Cdk2, and Cdk5 (De Azevedo et al., 1997; Meijer et al., 1997) and acts by competing for the ATP binding domain of the kinases. Inhibitory concentration 50% (IC_{50}) of Roscovitine depends on the kinase: cdc2 (IC_{50} = 0.65 μM), cdk2 (IC_{50} = 0.7 μM), Cdk5 (IC_{50} = 0.2 μM). Roscovitine exhibits reduced sensitivity towards related kinases, such as Erk1 and Erk2 (IC_{50} = 34 μM and 14 μM, respectively).

Cytoskeleton

To study morphology of nuclei and organization of cytoskeleton, GN11 neurons, untreated and Roscovitine-treated, were plated in a concentration of $5x10^4$ cells/coverslip, fed with reduced GN11 medium, and left for 3 h (duration of Boyden chamber assay) or 24 h at 37°C in a 5% CO_2 humidified incubator. Cells were then fixed

in prewarmed 4% PFA for 20min, rinsed with PBS, and labelled for F-actin (phalloidin) and α-tubulin (microtubules). Cell nuclei were labelled with bisbenzimide (BB).

COS7 transfection

COS7 cells were cultured in 10 cm Petri dishes containing DMEM supplemented with 10% FBS, at 37°C and 5% CO_2. COS7 cells were transiently transfected using the calcium phosphate precipitation method. All reagents for the transfection were purchased from Clontech. Transfections were carried out on COS7 cells that were approximately 60% confluent. For each transfection, precipitates were made by mixing 15μg of plasmid DNA in 50 μl of 2.5 M $CaCl_2$ with 450 μl of sterile distilled water, and 500 μl of 2x HEPES-buffer saline (HBS; pH 7.1). The cells were then incubated with the precipitates overnight at 37oC in a 5% CO2 humidified incubator. The following morning, the cells were washed three times with sterile PBS, and after the final wash, the PBS was replaced with 10 ml DMEM containing 10% FBS. Following twenty-four hour incubation at 37oC in a 5% CO2 humidified incubator, the cells were lysed in ErbB4 lysis buffer and protein concentrations of the lysates were determined using the BioRad Protein Assay as described in general Materials and Methods.

Immunoprecipitation

In order to immunoprecipitate ErbB4 from transfected COS7 lysates, 1 μl of rabbit anti-ErbB4 antibody was incubated with 200 μl of lysates at 4°C for an hour. 100 μl of Protein A sepharose beads, prepared as 10% solution in ErbB4 lysis buffer, were then added, and the suspension was incubated for another hour at 4°C on a rocking platform. Immunoprecipitates were washed three times in ErbB4 lysis buffer, resuspended in 10 μl of 1x sample buffer, and run on a 10% denaturing polyacrylamide gel followed by immunoblotting with a mouse anti-phospho-threonine-proline antibody.

GST-fusion proteins

Cloning fragments of ErbB4 cDNA encoding serine- and threonine-containing peptides

Constructs expressing GST-S (853) and GST-T (1152) were created by inserting serine (853) and threonine (1152) fragments of ErbB4 receptor derived by PCR, using *Pfu* polymerase and pcDNA3.1-ratCyt1-JMa-mychis plasmid as a template, into the vector pGEX-4T2 (Amersham). The serine-containing fragment was cloned using the forward primer GTCAGGATCCGTGCGTTTACTGGGTGTGTGT and the reverse primer TGGAGGAAAGCCCTATGATGCTCGAGTGAC that incorporated *BamH* I and *Xho* I sites, respectively. The serine-containing insert was ligated into the pGEX-4T2 vector in frame, between *BamH* I and *Xho* I sites. The threonine-containing fragment was cloned using the forward primer GTCAGTCGACAGCAGAACTGGATGAAGA and the reverse primer ACTACCTGCAGGAATACGCGGCCGCTGAC that incorporated *Sal* I and *Not* I sites, respectively. The threonine-containing insert was ligated into the pGEX-4T2 vector in frame, between *Sal* I and *Not* I sites.

Preparation of GST-fusion proteins

Glycerol stocks of BL21 strain of *E. coli* colonies expressing the GST-S and GST-T proteins were picked and inoculated into fresh LB/ampicillin broth, followed by overnight growth at 37°C. The following morning, the overnight cultures were diluted into a 10-fold excess of LB/ampicillin broth and incubated at 37°C with shaking until the protein absorbance reading (A_{560}) reached 0.9-1. At this stage, 1M IPTG was added to give a final concentration of 0.5M, in order to induce expression of GST-fusion proteins and incubation was continued for a further 3 hours with shaking at 37°C. The cultures were centrifuged at 10,000 rpm for 10min to pellet the bacteria. The pellet was then resuspended in ErbB4 lysis buffer, containing protease and phosphatase inhibitors, and freeze-thawed in liquid nitrogen 3 times. The suspension was then sonicated on ice 2 x 2min. This was followed by centrifugation at 10,000 rpm for 20min. The protein supernatant was then incubated with gluthation-sepharose beads (10% stock in ErbB4 lysis buffer) for an hour at 4°C, after which the beads were washed three times with ErbB4 lysis buffer. In order to elute the protein, the beads were then incubated with 15mM gluthatione (Sigma) in ErbB4 lysis buffer, for 10min at room temperature. To isolate the GST-fusion proteins, the elute was dialysed against 3 litre of pre-chilled PBS

overnight at 4°C. In order to check for protein degradation and for comparison of protein fractions of uninduced and induced cells, 10µl of the protein supernatant was loaded on a 10% polyacrilamide gel and stained with Coomassie Blue. The protein concentration was determined using the BioRad protein assay. The GST-fusion proteins were stored at -80°C or used immediately for *in vitro* kinase assay.

***In vitro* kinase assay**

COS7 cells were transfected with p35 and Cdk5 and lysed in ErbB4 lysis buffer. The p35/Cdk5 complex was isolated from COS7 cell lysate by immunoprecipitation. 3 µl of rabbit anti-p35 antibody per kinase reaction were incubated with 500 µl of COS7 lysate for an hour at 4°C with shaking. This was followed by adding of 100 µl of protein A sepharose beads (10% stock in ErbB4 lysis buffer) per kinase reaction for an hour at 4°C with shaking. The beads were then washed 5 times in kinase buffer and briefly dried with vacuum.

2 µg of GST-S and GST-T proteins were incubated with p35/Cdk5-containing beads in kinase buffer (30mM HEPES, pH 7.2, 10mM $MgCl_2$, 5mM $MnCl_2$, 1mM DTT) supplemented with 1 µCi(^{32}P)γATP in a final volume of 50 µl for 30min at room temperature. Histone 1 (H1) and GST were used as positive and negative substrate controls, respectively. Non-transfected COS7 cell lysates served as a negative control for the Cdk5 kinase assay. The reaction was terminated by the addition of 50 µl of 2x sample buffer. Samples were separated by SDS-PAGE (12% gel) and (^{32}P)γATP incorporation was assessed by autoradiography. In addition, gels were stained with Coomassie Blue.

Site-directed mutagenesis

GST-T(A) was made by PCR mutagenesis that replaced T1152 with alanine. This was performed according to the QuikChange^{R} II XL Site-Directed Mutageneis Kit (Stratagene). The following primers were used for mutagenesis: GAAGAAGGCTACATGGCTCCCATGCATGACAAG (forward) and CTTGTCATGCATGGGAGCCATGTAGCCTTCTTC (reverse).

RESULTS

Roscovitine impairs NRG1β-induced chemotaxis of GN11 neurons

Cdk5 is a ubiquitously expressed kinase found in GN11 neurons (Fig.4C-1A). In order to investigate the role of Cdk5 in NRG1β-induced chemotaxis, GN11 neurons were treated with low (10 μM; Fig.4C-1B) and high (50 μM; Fig.4C-1C) concentrations of Roscovitine, to block Cdk5 activity prior to a 3-hour chemotactic assay *in vitro*. The response to negative (DMEM) and positive (1% FBS) chemotactic signals was the same in untreated and Roscovitine-treated (10 μM) GN11 neurons (Fig.4C-1B). However, treatment with Roscovitine (10 μM), significantly decreased the migration of GN11 neurons towards NRG1β, suggesting a role of Cdk5 in this process (Fig.4C-1B). High doses of Roscovitine (50 μM) caused a partial block in the migration of GN11 towards the positive chemotactic cue (1% FBS), probably via the Erk1/2 pathway alone or in conjunction with Cdk5, without affecting their basal migratory response (DMEM; Fig.4C-1C). Yet, the chemotactic response of GN11 neurons to low or high concentrations of Roscovitine (10 μM or 50 μM) did not differ significantly (Fig.4C-1C), confirming a specific role of Cdk5 in NRG1β-induced chemotaxis of GN11 cells.

In order to investigate whether Roscovitine treatment affected survival and overall cytoskeletal organization of GN11cells, the morphology of their nuclei and the distribution of their cytoskeletal proteins, microtubules and actin (data not shown), were monitored 3- and 24 hours after Roscovitine treatment. Neither condensation of nuclei, a marker of apoptotic cell death, or gross cytoskeletal organization were altered in Roscovitine-treated vs. Roscovitine-untreated GN11 neurons (Fig.4C-2). This implies that the observed impaired migration of Roscovitine-treated cells was not due to cell death or large, non-specific changes in their cytoskeleton, but rather to their specific response to inhibition of Cdk5 activity that probably directly affected the major mediator of NRG1β-induced GN11 neuron migration, the ErbB4 receptor.

Next, I explored whether the p35/Cdk5 complex (i) regulates ErbB4 expression, (ii) associates with ErbB4, and (iii) phosphorylates ErbB4, *in vivo* and *in vitro*. The ultimate goal of this research was to reveal whether NRG/ErbB4-induced neuron migration is indeed controlled by Cdk5.

p35/Cdk5 complex controls ErbB4 degradation *in vitro*

In order to study whether ErbB4 expression could be regulated by p35/Cdk5 *in vitro*, COS7 cells were co-transfected with ErbB4, p35, and either Cdk5 or its dominant negative (dn) form (Fig.4C-3A). Lysates of COS7 cells were then analysed by Western blot using anti-Cdk5, -p35, and –ErbB4 antibodies. Non-transfected COS7 cells expressed Cdk5, traces of p35 and no ErbB4. Co-transfection of p35 and ErbB4 increased their levels of expression in COS7 cells, although the expression of ErbB4 was higher when the receptor was transfected alone. In contrast, overexpression of Cdk5 in COS7 cells significantly decreased exogenous levels of both p35 and ErbB4, and this effect was less apparent when COS7 cells were co-transfected with dnCdk5 instead. This finding indicates a role for Cdk5 in ErbB4 turnover, at least *in vitro*.

ErbB4 expression in *p35*-deficient mutants

To assess whether the p35/Cdk5 complex could also regulate forebrain ErbB4 expression, prenatal GE and cortices of *p35* heterozygous and homozygous mice were analysed by Western blot. Overall, the expression of ErbB4 did not differ between the two genotypes, with the exception of E13.5 cortex (Fig.4C-3B). Similarly, ErbB4 expression was not altered in *Cdk5*-deficient compared to wild type mice (data not shown).

ErbB4 association with p35 *in vivo* and *in vitro*

In order to detect a biochemical interaction between ErbB4 and p35/Cdk5 *in vivo* and *in vitro*, either brains of wild-type and *p35*-deficient mice, or COS7 cells co-transfected with ErbB4 and p35, were lysed. Then, p35 or ErbB4 were immunoprecipitated and a Western blot analysis was used to detect the possible respective binding partners, ErbB4 or p35. After several attempts, I failed to determine whether ErbB4 associates with p35, *in vivo* and *in vitro*, owing to some technical problems (data not shown). These experiments will be repeated in due course.

Cdk5 phosphorylates ErbB4 threonine ($T1152^{JMa\text{-}Cyt1}$/ $T1136^{JMa\text{-}Cyt2}$) *in vitro*

Next, I studied whether Cdk5 could phosphorylate ErbB4 receptor. Normally, Cdk5 phosphorylates serine and threonine residues that lie upstream of a proline residue, but it preferentially phosphorylates sites that also contain a basic residue such as lysine, histidine or arginine in the +3 position. There are two optimal sites for Cdk5 phosphorylation in the rat ErbB4 receptor (Fig.4C-4): serine 853^{JMa} (amino acid sequence: SPNH) and threonine $1152^{JMa\text{-}Cyt1}$ or $1136^{JMa\text{-}Cyt2}$ (amino acid sequence: TPMH).

Evidence for ErbB4 phosphorylation by Cdk5 came from transfection studies, in which COS7 cells were first co-transfected with ErbB4, p35 and Cdk5, and ErbB4 was subsequently immunoprecipitated. Using anti-phospho-threonine-proline antibody, ErbB4 was found to be phosphorylated at a threonine-proline residue following transfection of ErbB4 alone, and this phoshorylation was significantly enhanced when the receptor was co-transfected with p35 and Cdk5 (Fig.4C-5A).

To further, and more specifically, investigate whether Cdk5 phosphoryates ErbB4, two fragments of the ErbB4 receptor, containing either $S853^{JMa}$ or $T1152^{JMa\text{-}Cyt1}$ ($T1136^{JMa\text{-}Cyt2}$), were fused to GST (Fig.4C-5B), expressed in bacteria (Fig.4C-5C) and purified. GST-fused $S853^{JMa}$ or $T1152^{JMa\text{-}Cyt1}$ ($T1136^{JMa\text{-}Cyt2}$) proteins are termed GST-S and GST-T throughout this chapter for ease of reference. After purification, the GST-S protein was intact but present in low yield compared to the cleaved and highly produced GST-T protein (Fig.4C-5C). Even so, both GST-fusion proteins were subjected to an *in vitro* Cdk5 kinase assay. GST-T protein was clearly present (Fig.4C-5D) and phosphorylated by Cdk5 (Fig.4C-5E). In contrast, GST-S protein was degraded and conclusions about Cdk5 phosphorylation could not be drawn. The residues composing the consensus site for Cdk5 phosphorylation at $S853^{JMa}$ or $T1152^{JMa\text{-}Cyt1}$ ($T1136^{JMa\text{-}Cyt2}$) are relatively well conserved among mammals and birds (Fig.4C-5F), supporting the notion that these sites may be of functional significance.

DISCUSSION

Neuregulins have been shown to play important roles in migration of neural and non-neural cells. The NRG receptor ErbB4 directly controls neuronal migration in the nervous system (Golding et al., 2000; Tidcombe et al., 2003; Anton et al., 2004; Gambarotta et al., 2004; Golding et al., 2004; Flames et al., 2004). The signalling events downstream of NRG/ErbB4 that underlie neuronal migration are still unclear. In this study, I reported that inhibition of Cdk5 activity impairs chemotactic response of neurons to NRG1β. Furthermore, I identified ErbB4 receptor as a substrate of Cdk5 *in vitro*. Surprisingly, I also discovered that Cdk5 might regulate ErbB4 degradation, at least *in vitro*.

Cdk5 in NRG1β-mediated migration

It is possible that NRG/ErbB signalling is required for cell movement *per se* as it is known to be necessary to maintain the *directed* migration of cells. In this (chapter 4B) and in previous studies (Gambarotta et al., 2004; Flames et al., 2004), it was proposed that NRG1β, acting through ErbB4 receptors, is able to attract neurons. Here, I showed that Cdk5 can mediate this process. It has been shown previously that Cdk5 plays a role in NRG signalling, but not in relation to cell migration (Fu et al., 2001; Li et al., 2003).

As was discussed in chapter 4B, at least two signalling pathways have been shown to be involved in NRG signalling: PI3K and MAPK (Kainulainen et al., 2000). The former, but not the latter pathway, has been proposed to be active in the tangential migration of cortical interneurons from the ventral telencephalon (Polleux et al., 2002). Similarly, and most specifically, it has been shown that ErbB4 signalling via PI3K activation plays an essential role in controlling NRG1β-induced neuron migration (Gambarotta et al., 2004). In contrast, I found that NRG1β-induced neuron migration is (i) a PI3K-independent event (chapter 4B) and (ii) blocked with high concentration of Roscovitine (50 μM) that potentially inhibits the Erk1/2 pathway. Therefore, my results suggest that activation of the MAPK pathway might be involved in NRG1β-stimulated chemotaxis. Nevertheless, low or high doses of Roscovitine, a potent Cdk5 inhibitor, impaired NRG1β-induced neuron migration (Fig.4C-1B,C). Roscovitine also inhibits

Cdc2 and Cdk2 kinases, which are both involved in regulation of the cell cycle. However, it must be emphasised that the inhibition of Cdc2 and Cdk2, and the subsequent arrest of proliferation, would not be expected to affect neuron migration in my short (3 hours) migratory assay employed here.

Interestingly, Cdk5 communicates with both PI3K and MAPK pathways. There is evidence that the PI3K pathway, via Akt-p70S6k, is the upstream regulator of Cdk5 activity (Sarker and Lee, 2004). In contrast, the study of Li et al. (2003) suggested that Cdk5 can act as an upstream effector of neuregulin-regulated cell survival via the PI3K pathway. Yet, it has been shown that nerve growth factor induces p35 expression in neurons through activation of the Erk pathway (Harada et al., 2001). Also, Cdk5 regulates the MAPK pathway in a negative manner via the phosphorylation of the MAPK component, meiosis-specific serine/threonine protein kinase (MEK1; Sharma et al., 2002).

ErbB4 phosphorylation by Cdk5

Cdk5 phosphorylates serine 1176 on ErbB2 receptor (Li et al., 2003) and ErbB3 (Fu et al., 2001) on threonine 871 and serine 1120 (Li et al., 2003). The present finding that Cdk5 phosphorylation of ErbB4, at threonine residue $1152^{JMa\text{-}Cyt1}$ ($T1136^{JMa\text{-}Cyt2}$), is a novel finding, and provides a new avenue of investigation. Naturally, further studies are needed to solve the enigma about the role of Cdk5 in the phosphorylation of ErbB receptors in cell proliferation, survival, migration or differentiation. Indeed, future studies should also help us to learn precisely where Cdk5 lies within the NRG signalling pathway.

Cdk5 in ErbB4 turnover

NRG1β induces Cdk5 activity, and it has been reported that Cdk5 activity is necessary for ErbB activation at the NMJ (Fu et al., 2001). Furthermore, NRG1β controls expression of p35 and Cdk5 in the same system (Fu et al., 2001). However, the role of Cdk5 in the regulation of ErbB4 expression has not been examined, although it can play a role in transcription (Fu et al., 2004). Here, I found that ErbB4 expression is not

altered in either *p35*- or *Cdk5*-deficient mice compared to control animals (Fig.4C-3B). However, in an *in vitro* COS7 co-transfection study, Cdk5 reproducibly induced degradation of ErbB4 receptor (Fig.4C-3A). This could be due to possible posttranslational modification of the receptor by Cdk5 that has already been reported in rapid turnover of the Cdk5 activator p35 as a protective, autoregulatory mechanism. In brief, it has been found that, shortly after Cdk5 activation, p35 is degraded by the ubiquitin-proteasome pathway (Patrick et al., 1998; Saito et al., 1998), and proteasomal degradation of p35 is promoted by phosphorylation (Patrick et al., 1998; Saito et al., 1998). Moreover, phosphorylation of p35 by Cdk5 stimulates the degradation of p35 by proteosomes (Hisanaga and Saito, 2003; Saito et al., 2003). This mechanism could explain the degradation of ErbB4 receptor in my study.

Future studies

In future, I will further investigate Cdk5 phosphorylation of the ErbB4 receptor and determine whether this process plays a role in neuron migration. Again, I will examine the $S853^{JMa}$ site for phosphorylation by Cdk5 *in vitro*. Then, the potential $S853^{JMa}$ and established $T1152^{JMa\text{-}Cyt1}$ ($T1136^{JMa\text{-}Cyt2}$) phosphorylation of the ErbB4 receptor by Cdk5 will be studied for specificity by mutating serine and threonine sites in the GST-S and GST-T proteins, respectively, and by performing a radioactive *in vitro* Cdk5 kinase assay. In fact, mutation of the threonine residue in the GST-T fragment has already been successfully completed by site directed mutagenesis of the respective expression vector (Fig.4C-5F). Also, the serine and threonine residues in the full length ErbB4 isoforms encoded by pCAG-Cyt1-JMa-eGFP and pCAG-Cyt2-JMa-eGFP will be mutated; these vectors will subsequently be used in studies on the role of Cdk5-phosphorylated ErbB4 receptor in neuron migration *in vitro*, and, more specifically, in cortical interneuron migration, both tangential and radial. I am also keen to raise antibodies against the Cdk5-phosphorylated epitopes of ErbB4 receptor and to study their forebrain expression and subcellular localization.

Figure 4C-1. Roscovitine partially impairs NRG1β-induced migration of GN11 neurons *in vitro*

(A) Expression of Cdk5 protein in GN11 neurons as seen in Western blot.

(B-C) Chemotactic response of GN11 neurons, untreated (grey bars) and Roscovitine-treated (red bars), to DMEM (negative control), 1% FBS (positive control), and NRG1β (100 ng/ml and 200 ng/ml) using a 3-hour long chemomigratory assay *in vitro* (Boyden chamber). GN11 neurons were treated with 10 μM (B) and 50 μM (C) concentrations of Roscovitine (in DMSO) 30min prior to the assay. Data in the histograms represent mean number of migrated cells per well ± SEM (standard error of the mean) from three independent experiments. Error bars represent SEM. Significance calculated by the Student's *t*-test; **$p<0.01$, ***<0.005.

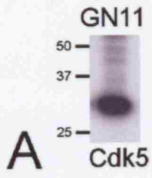
GN11
50
37
25
A
Cdk5

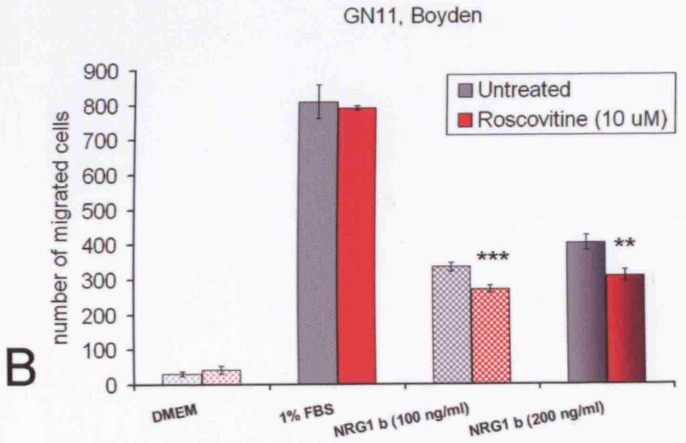
GN11, Boyden
number of migrated cells
900
800
700
600
500
400
300
200
100
0
Untreated
Roscovitine (10 uM)
***
**
B
DMEM
1% FBS
NRG1 b (100 ng/ml)
NRG1 b (200 ng/ml)

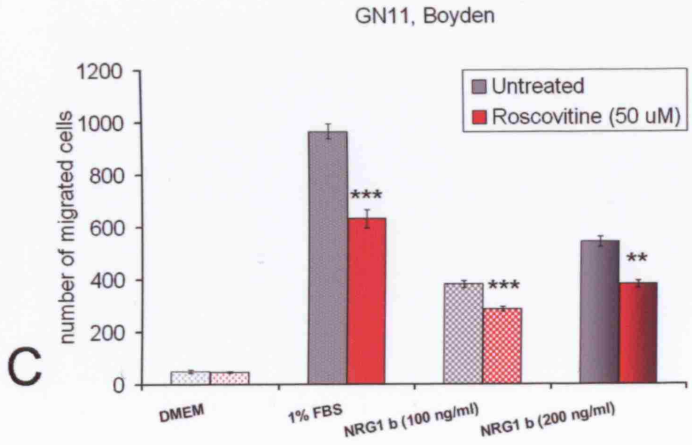
GN11, Boyden
number of migrated cells
1200
1000
800
600
400
200
0
Untreated
Roscovitine (50 uM)
***
***
**
C
DMEM
1% FBS
NRG1 b (100 ng/ml)
NRG1 b (200 ng/ml)

Figure 4C-2. Roscovitine treatment does not affect survival and gross cytoskeletal organization of GN11 neurons

Microtubules of cultured GN11 cells were visualized by α-tubulin immunofluorescence. Nuclei of the cells were stained with bisbenzimide (BB).

(A-B) Untreated GN11 neurons 3- and 24 hours after plating.

(C-F) Roscovitine-treated (10 μM) GN11 neurons 3- and 24 hours after plating.

(G-H) Roscovitine-treated (50 μM) GN11 neurons 3- and 24 hours after plating.

Scale bar, 25 μm.

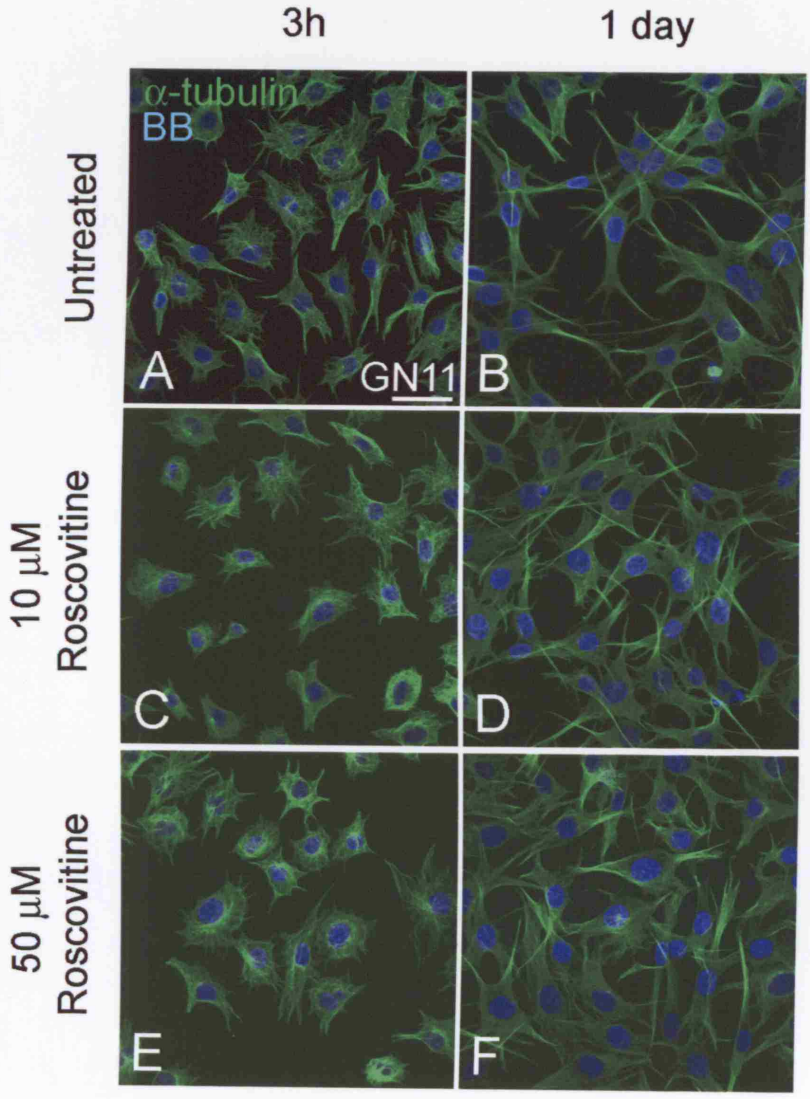
3h
1 day
α-tubulin
BB
Untreated
10 μM Roscovitine
50 μM Roscovitine
A
GN11
B
C
D
E
F

Figure 4C-3. Regulation of ErbB4 expression *in vitro and in vivo*

(A) Immunoblot of lysates from COS7 cells transfected with ErbB4, p35, Cdk5, and dn(dominatnt negative)Cdk5. Endogenous expression of Cdk5 (lane 1); Exogenous expression of ErbB4 (lane 2); Exogenous expression of p35 and ErbB4 (lane 3); Exogenous Cdk5 significantly reduced exogenous p35 and ErbB4 expression (lane 4); dn form of Cdk5 had less effect on exogenous p35 and ErbB4 expression than Cdk5 (lane 5).

(B) Western blot analysis of ErbB4 protein expression, in GE and cortices, of *p35* +/- and *p35* -/- mice, during mouse prenatal period (E13.5, 14.5, 18.5). * Full length; ** Truncated JMa isoform of ErbB4 receptor; ? A band recognized by anti-ErbB4 antibody, showing a protein that is developmentally regulated.

Cx – cortex; GE – ganglionic eminence.

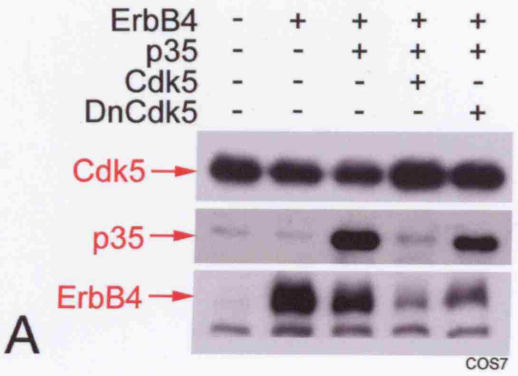
ErbB4 - + + + +
p35 - - + + +
Cdk5 - - - + -
DnCdk5 - - - - +
Cdk5
p35
ErbB4
COS7

A

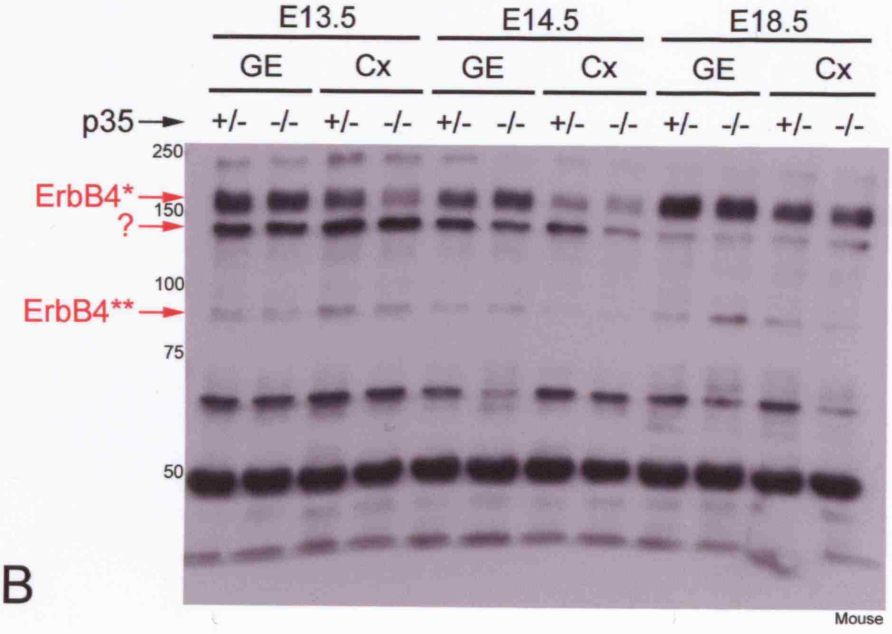
E13.5
E14.5
E18.5
GE
Cx
GE
Cx
GE
Cx
p35
+/- -/- +/- -/- +/- -/- +/- -/- +/- -/- +/- -/-
250
ErbB4*
150
?
100
ErbB4**
75
50
Mouse

B

Figure 4C-4. Rat ErbB4, JMa Cyt1 isoform

Optimal sites for Cdk5 phosphorylation of the rat ErbB4 receptor are shown as yellow-red lines (serine 853^{JMa} and threonine $1152^{JMa\text{-}Cyt1}$ or $1136^{JMa\text{-}Cyt2}$); p35/Cdk5 complex is presented as a red star; consensus sequences for Cdk5 phosphorylation are shown as yellow-orange circles.

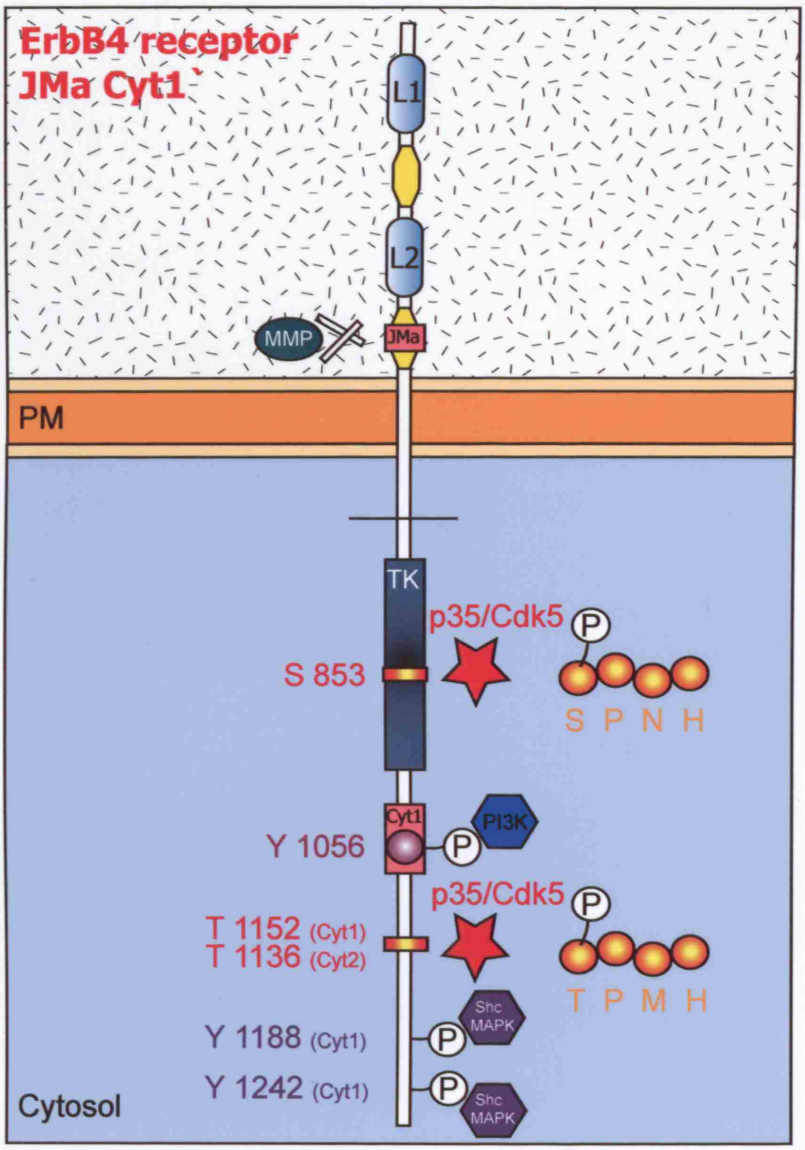
ErbB4 receptor
JMa Cyt1
L1
L2
MMP
JMa
PM
TK
p35/Cdk5
S 853
S P N H
Cyt1
PI3K
Y 1056
p35/Cdk5
T 1152 (Cyt1)
T 1136 (Cyt2)
T P M H
Shc
MAPK
Y 1188 (Cyt1)
Y 1242 (Cyt1)
Shc
MAPK
Cytosol

Figure 4C-5. Phosphorylation of ErbB4 by Cdk5 *in vitro*

(A) COS7 transfection with ErbB4, p35, Cdk5 followed by immunoprecipitation using anti-ErbB4 antibody and Western blotting using phospho-threonine-proline (pTP) antibody. Phosphorylation of threonine residues within ErbB4 receptor (lane 2) was enhanced in the presence of p35/Cdk5 (lane 3).

(B-C) Cloning of GST-S and GST-T proteins. (B) A schematic diagram of full length rat ErbB4-JMa-Cyt1 receptor and GST-fusion proteins; (C) Expression of GST-S and GST-T in BL21 bacteria before and after 0.5 M IPTG protein induction; GBP – glutathione-bead pulldown. The lysates of bacteria or GBP samples were loaded on a polyacrylamide gel and stained with Coomassie Blue.

(D-E) *In vitro* Cdk5 kinase assay, using p35/Cdk5 produced in COS7 cells. Histone 1 (H1) was used as positive control, and GST as a negative control. (D) Coomassie blue; (E) autoradigraph.

(F) Threonine 1152 in GST-T protein was mutated to alanine – GST-T(A) protein; sequence chromatogram.

(G) The Cdk5 consensus site for serine and threonine phosphorylation of ErbB4 receptor is conserved.

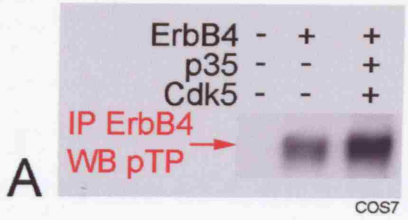

A

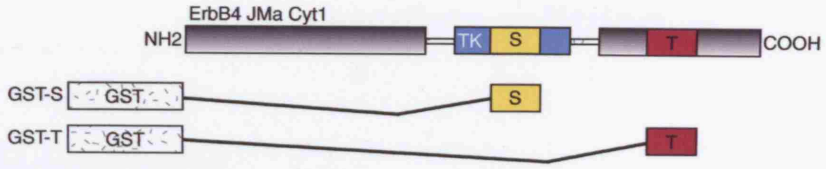

B

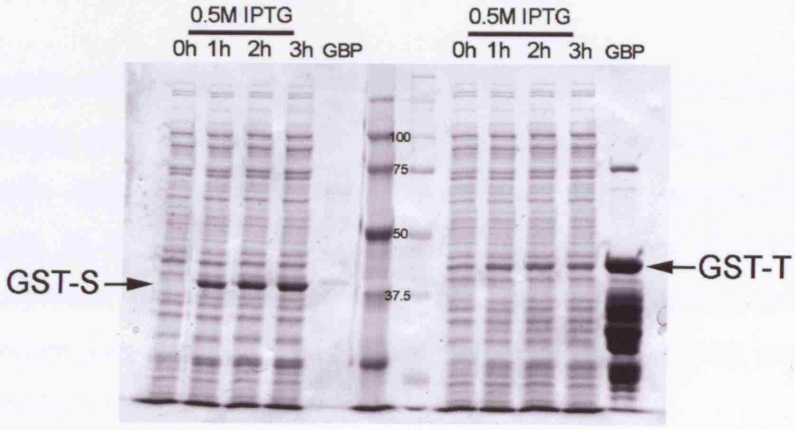

C

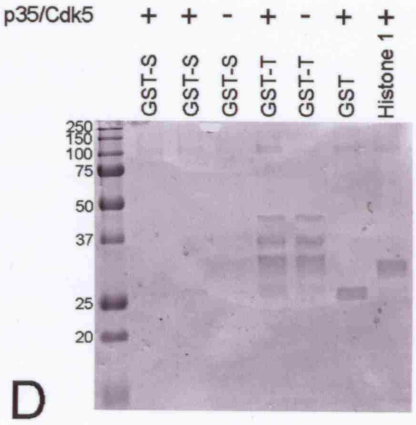

D

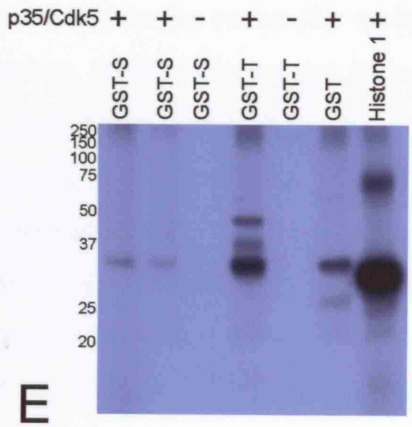

E

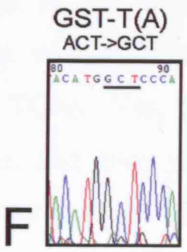

F

Serine

Rat	850	LVKSPNHVKITD	861
Mouse	916	LVKSPNHVKITD	927
Human	850	LVKSPNHVKITD	861
Chicken	1021	LVKSPNHVKITD	1032

Threonine

Rat	1149	GYMTPMHDKPKQ	1160
Mouse	1215	GYMTPMHDKPKQ	1226
Human	1149	GYMTPMRDKPKQ	1160
Chicken	1304	GYMTPMRDKPKT	1315

G

CHAPTER 5

Role of Cdk5 in thalamic axon pathfinding and preplate splitting

INTRODUCTION

The connections of the cerebral cortex with the thalamus are important mainly for the processing of motor and sensory information. These connections are established during the early stages of cortical development. Developing thalamocortical axons (TCAs) navigate in a highly ordered manner from the dorsal thalamus, via the ventral telencephalon, to specific areas of the cerebral cortex. Upon entering the cortex, they first accumulate within the SP, making synaptic contacts with neurons in that layer, before targeting layer IV.

Subplate layer neurons (Kostovic and Rakic, 1990) are transient cells that play a role in guiding thalamic axons towards and into the cortex (for review see Allendoerfer and Shatz, 1994; Molnar and Blakemore, 1995). It is not yet known how SP neurons guide thalamic axons to the correct areas of the cortex. It has been suggested that they send early projections to meet thalamic axons and then guide them to the cortex (reviewed by Lopez-Bendito and Molnar, 2003). It is still unknown whether these neurons act as an attractive, trophic, stop or permissive signal for TCAs. Yet, SP neurons receive functional synaptic input from the thalamus via TCAs, and relay this input to the CP well in advance of the invasion of thalamic axons into layer IV (for review see Allendoerfer and Shatz, 1994). This early circuitry plays a role in the maturation of the cortex. Thalamic axon ingrowth to layer IV is synchronized with the maturation of the CP; early in development, the CP is mostly non-permissive for axonal ingrowth (Gotz et al., 1992; Molnar and Blakemore, 1995; Tuttle et al., 1995), but eventually 'opens the door' for thalamic axons (Molnar and Blakemore, 1995).

The SP emerges from the PPL. The exact structure, origin, function, and fate of this layer (Marin-Padilla, 1971; Rickmann et al., 1977; Rickmann and Wolff, 1981)

remain unclear. The PPL contains a variety of neurons and fibres surrounded by a rich extracellular matrix (ECM). Preplate neurons are the earliest generated (E10.5-12.5 in mice), and precociously matured cortical neurons. Cajal-Retzius (CR) cells are the most distinct neuronal type in the PPL, located superficially, beneath the pial surface. They were first described by Cajal (Ramon y Cajal, 1891) and Retzius (Retzius, 1893). CR cells have a diverse morphology characterised by a large soma, and a thick and long horizontally-oriented process that gives rise to thin, radially ascending processes that contact the pia. These cells also possess a horizontal axon that does not leave the PPL. CR cells contact the apical dendrites of projection neurons, and coordinate early circuit activity in layer I that might control maturation of the cerebral cortex (Marin-Padilla, 1998). Meyer and colleagues described two types of CR cells: early, transient Retizus cells and late, persisting Cajal cells that correspond to the typical CR cells, at least in rodents (Meyer et al., 1999). CR cells secrete Reelin and play a role in controlling neuron migration and glia morphology (see review Soriano and del Rio, 2005). They also express calretinin (del Rio et al., 1995), glutamate (del Rio et al., 1995; Hevner et al., 2003b), glutamate receptors (Lopez-Bendito et al., 2002b; for review see Mienville, 1999), GABABR1 (Lopez-Bendito et al., 2002c), ErbB4 receptor (Li et al., 2004), Golli (Landry et al., 1998; Tosic et al., 2002), p53 homolog p73 (Meyer et al., 2002), and the pallial transcription factors Emx2 and Tbr1 (Hevner et al., 2001; Hevner et al., 2003b). The expression of GABA by CR cells is controversial (Meyer et al., 1999). Apart from CR cells, the PPL also comprises: (i) pyramidal-shaped neurons that express Golli, Tbr1 (Landry et al., 1998; Hevner et al., 2001; Hevner et al., 2003b) and calretinin (del Rio et al., 2000), and represent future SP neurons, and (ii) a range of small, migrating GABAergic interneurons, displaying various orientations, that express calbindin (del Rio et al., 2000) and Dlx (Rakic and Zecevic, 2003).

Traditionally, PPL neurons have been thought to originate from the cortical VZ (Marin-Padilla, 1998) and migrate by 'somal translocation' (Nadarajah and Parnavelas, 2002; Nadarajah et al., 2003a). However, these neurons have multiple sites of origin. For example, early CR cells, born E10.5-11.5, express the pallial transcription factors Tbr1 and Emx2, and are probably generated in the local VZ (Hevner et al., 2003b). However, a few studies have suggested that these early CR cells might come from the subpallium (MGE) in rats (Lavdas et al., 1999) and humans (Rakic and Zecevic, 2003). Later on, after the splitting of the PPL, CR cells can also populate layer I by tangential, subpial

migration from their origins in the peri-olfactory forebrain or cortical hem (reviewed by Soriano and del Rio, 2005). Future SP neurons are of pallial origin and are probably born within a day, around E11.5 or E12. GABAergic interneurons arrive in the PPL from the ventral telencephalon as early as E12.5 (Marin and Rubenstein, 2001).

Apart from glutamate and GABA, and their corresponding receptors, the PPL hosts other classical neurotransmitters, such as monoamines (serotonin, noradrenaline, dopamine; Marin-Padilla, 1998) which have been suggested to play a role in corticogenesis. Preplate cells also send early corticofugal (CF) projections to subcortical structures (Marin-Padilla, 1971; Molnar and Blakemore, 1995). These neurons associate with fibronectin (Pearlman and Sheppard, 1996) and chondroitin sulphate proteoglycans (CSPGs; Sheppard and Pearlman, 1997), both constituents of the ECM, and this association is maintained in layer I and SP after the PPL partition. These and a number of other ECM proteins might have roles in PPL splitting and cortical layer formation.

The PPL is split into the superficial layer I and deep SP by rising CP neurons (Marin-Padilla, 1998), at which point most of the PPL neurons occupy the SP (de Carlos and O'Leary, 1992). Layer I contains predominantly CR cells and the SP includes neurons that form synaptic contacts with TCAs. Both layers hold a variety of migrating GABA-containing interneurons. The splitting of the PPL is a very precise phenomenon and the underlying mechanisms are yet to be elucidated. Neurons of the PPL are essential for cortical development; they regulate the neuronal migration, and form the first cortical axonal connections. Interestingly, Hamasaki et al. (2001) have shown that a subset of early-generated neurons of the piriform PPL migrate inward and disperse within the striatum, and thus play a role in the development of subcortical structures. Most PPL cells disappear after birth, by means of cell death, migration into the cortex, or possible cell transformation.

Reelin is an extracellular matrix protein, secreted by CR cells (D'Arcangelo et al., 1995; Ogawa et al., 1995). It is important for the proper formation and splitting of the PPL, and for the 'inside-out' layering of the cortex (for review, see Tissir and Goffinet, 2003). In Reelin-deficient mice, *reeler* (Falconer, 1951), the partition of the PPL does not occur; hence layer I and SP neurons stay together in a layer called the superplate (Caviness, Jr., 1982). The layers below the superplate are indistinct and are generated in an 'outside-in' fashion (Caviness, Jr. and Sidman, 1973; Caviness, Jr., 1982). The Reelin pathway may or may not converge with the Cdk5 pathway, which is

also involved in cortical lamination (Chae et al., 1997; Gupta and Tsai, 2003). In mice deficient in Cdk5 or its major activator p35, the PPL seems to be split by the arrival of the early-born projection neurons (Gilmore et al., 1998; Kwon and Tsai, 1998). However, the late-born projection neurons fail to pass the ectopic SP and accumulate in predominantly 'outside-in' manner below it (Kwon and Tsai, 1998). This has suggested the hypothesis that the Reelin and Cdk5 pathways might be activated at different times during cortical development. Specifically, the Reelin pathway could be activated earlier and affect the formation and splitting of the PPL, while both pathways could play a role in positioning of the remaining layers (II-VI). As for the development of the TCAs, there are overlapping points between the Reelin and Cdk5 pathways. In normal mice, TCAs are guided towards the SP neurons, and in *reeler* mice they run in the direction of the SP neuron-containing superplate layer (Molnar et al., 1998b). However, in *Cdk5* or *p35* mutants, the same fibres apparently head for the ectopic SP and do not enter the CP prematurely or run towards the pia (Gilmore et al., 1998). It has been proposed that the arrangement of TCAs in both mutants is secondary to a positional defect in neurons. In *reeler*, postnatal TCAs correct their location and descend, branch and arborize in the layer that corresponds to layer IV (Molnar et al., 1998b). Both Reelin and Cdk5 pathways play a role in postnatal formation of the barrels that represent a topological replica of the array of facial vibrissae in the rodent somatosensory cortex (Woolsey and Van der, 1970). Barrels in *reeler* and *p35* KO mice are smaller, as detected by cytochrome oxidase, and are not clearly defined on Nissl preparations (Polleux et al., 1998a; Kwon et al., 1999).

In this chapter, the development of the thalamocortical connections is studied in greater detail than in previous studies. The focus will be on the positioning of TCAs and splitting of the PPL.

MATERIALS AND METHODS

Animals

Fixed brains from *p35* heterozygous and homozygous mice, at different stages of development (E14.5, E15.5, E16.5, E17.5, E18.5, P8), were uses for axon tracing studies and immunohistochemical experiments. In addition, rat E17 brains were used for explant/collagen preparations.

Axonal tracing

Carbocyanine dyes are widely used as anterograde and retrograde neuronal lipophilic tracers in living and fixed tissues. In our study, carbocyanine dyes were used to label axons (Godement et al., 1987) in fixed brains of littermate mice. The dorsal thalamus was exposed by transecting the brain with a fine knife at the caudal edge of the thalamus, in line with the occipital pole; to approach the internal capsule, a coronal cut was made more rostrally, at the level of mid-thalamus. Single crystals of the fluorescent carbocyanide dyes DiI (1,1'-dioctadecyl-3,3,3',3'-tetramethylindocarbocyanine perchlorate; Molecular probes) or DiA (4-[4-(dihexadecylamino)styryl]-*N*-methylpyridinium iodide; Molecular Probes) were placed in single or multiple locations in the neocortex, internal capsule or dorsal thalamus under a dissecting microscope. The crystals were selected, transferred, placed, and inserted in the brain tissue using a fine tungsten needle. After insertion of dye crystals, the brains were stored at room temperature or at 37°C in 4% PFA to allow dye diffusion. The incubation period and temperature were dependent on the embryonic stage and dye used; and ranged from 1- to 4 weeks (Table 5-1). After the incubation period, the brains were embedded in 4% agarose and cut into 50 μm (E14.5) or 100 μm (E16.5, 18.5, P3, P8) thick coronal sections on a vibratome. The cytoarchitecture of the brain was revealed by using bisbenzimide (BB) for 7min. The sections were mounted in 50% glycerol/1xPBS solution and coverslips sealed with nail varnish.

Table 5-1. Conditions used in axon tracing studies

Age	DiI	DiI/DiA
E14.5	-	3 d at 37°C; 4 d at RT
E16.5	2 weeks at 37°C	1 week at 37°C; 1 week RT
E18.5	2 weeks at 37°C	1 week at 37°C; 2 weeks RT
P3	3 weeks at 37°C	-
P8	4 weeks at 37°C	-

Immunohistochemistry

Immunohistochemistry was performed on 50 μm (E15.5) or 100 μm (E17.5) thick vibratome sections. Alternatively, fixed brains were cryoproteced in 30% sucrose in PBS at 4°C, embedded in OCT, frozen in dry ice, and sectioned at 15 μm using a cryostat. Calretinin (CalR) and Nogo-A antigens were visualized using immunoprexidase/DAB and immunoflurescence methods, respectively. Mouse anti-Nogo-A antibody was kindly supplied by GlaxoSmithKline plc. and all experiments using the antibody were performed with David Hunt, UCL. CalR is a calcium-binding protein, expressed in neurons in the PPL and in the emerging SP and layer I (particularly in CR cells). It is also found in prenatal corticopetal fibre systems, including thalamic axons (Fonseca and Soriano, 1995). Anti-Nogo-A antibody is a marker of developing axons (Tozaki et al., 2002; Hunt et al., 2003).

BrdU injection and staining

BrdU was injected i.p. into timed-pregnant mice at E11.5 and distribution of BrdU-labelled cells was studied at P12. BrdU-labelled cells were revealed by immunohistochemistry. BrdU staining, single or double (with antibody to CalR), was performed using the standard immunofluorescence method. Mouse anti-BrdU antibody

and rabbit anti-CalR antibody were used in this study. Sections were counterstained with bisbenizmide (BB) for 7 min.

Quantative measurements

Coronal sections of *p35* +/- and *p35* -/- forebrains, 100 μm thick, were immunolabelled using antibodies to BrdU and CalR, and counterstained with BB to label layers. Immunolabelled sections were analyzed using a confocal microscope. Multiple z-plane images (z stacks) were acquired throughout a section and analyzed using Metamorph software. $BrdU^+$ cells were counted in layer I, CP and SP on each z-plane confocal image that had clearly visible BrdU/CalR/BB staining. The percentage of the total number of $BrdU^+$ cells found within the layer I, CP and SP was calculated, and statistical analysis was performed using Microsoft Excel software (Student *t*-test).

Collagen gel co-cultures

Rat E17 forebrain slice cultures, described in general Materials and Methods, were further dissected, and explants of thalamus and lateral GE, 100–300 μm in diameter, were removed and used for collagen gel co-culture experiments.
Collagen gels were generated by adding 10% (v/v) of 10x concentrated DMEM (without phenol red) and 0.8 M sodium bicarbonate to an aliquot of collagen stock solution. Thalamus/LGE paired explants, 500 μm apart, were plated on 4-well dishes coated with poly-L-lysine and overlaid with 80 μl of collagen solution. Following polymerization (30min), the preparation was covered with 500 μl of 'slice' medium and cultured in a humidified, 5 % CO_2, 37°C incubator. After 48 hr *in vitro*, thalamus/LGE paired explants were fixed in 4% paraformaldehyde and immunostained with a monoclonal anti-beta-III-tubulin antibody.

Mouse semaphorin3F-FLAG plasmid

FLAG-tagged mouse semaphorin3F was created by inserting mouse semaphorin3F derived by PCR, using *Pfu* polymerase and pcDNA-mouse-sema3F plasmid as a template (a gift from Hannes Schmidt, Germany), into the vector p3xFLAG-CMV-8

(Sigma). The mouse semaphorin3F was obtained using the forward primer CTGA*GCGGCCGC*GAACTGGAGCCTGCTT and the reverse primer CTGA*TCTAGA*TAGGCTGGTCCTATGCAG that incorporated *Not* I and *Xba* I sites, respectively. The mouse semaohorin3F insert was ligated into the p3xFLAG-CMV-8 vector in frame, between *Not* I and *Xba* I sites. The mouse semaphorin3F-FLAG was verified by sequencing and by transfection of cells.

Cell culture and transfection

HEK297 and GN11 cells were maintained in DMEM with 10% FBS, 2 mM L-glutamine and antibiotics. Transfections were performed using a calcium phosphate precipitation method (Clontech), as described in chapter 4C. Expression of the chicken Sema3A-myc and mouse Sema3F-FLAG plasmids was confirmed by anti-myc and anti-FLAG immunocytochemistry, respectively.

RESULTS

Several studies have shown abnormalities in axon pathfinding in *p35*- or *Cdk5*-deficient mice (Chae et al., 1997e;Gilmore et al., 1998h;Kwon et al., 1999d). I sought to study in more detail the development of cortical connections with the thalamus in *p35* -/- mice, specifically the topography of the projections and relationship between TCAs and the SP.

Early corticofugal and corticopetal projections are not affected in *p35* mutants

To compare the early course of CF and TC axons in *p35* +/- and *p35* -/-, I placed one crystal of DiA into the prospective somatosensory cortex and one crystal of DiI into the dorsal thalamus at E14.5. The appearance of the projections from the cortex and from the thalamus were basically identical between *p35* +/- and *p35* -/- mice (Fig.5-1A,B). Outgrowth of CF and TC axons progressed to the same extent, appropriate for the developmental stage, and these axons established first contact in the ventral telencephalon.

To assess the topography of both early TC and corticothalamic (CT) projections in *p35* +/- and *p35* -/- mice, I placed multiple carbocyanine crystals into the future somatosensory cortex, parasagittally, along the rostrocaudal axis (DiI in rostral, DiA in middle, and DiI in caudal cortex), at E16.5 and E18.5. By anterograde (from the cortex) and retrograde (from the thalamus) diffusion of the dyes along the axons, I was able to identify both fibre systems, CT and TC. The bundles of axons labelled by the different dyes remained separate from each other along their whole journey, indicating highly precise and ordered projection to and from the cortex in control and *p35* mutant mice (Fig.5-1C-F).

_p35_-deficient subplate/cortical neurons are abnormally branched

Placement of a DiI crystal into the IC revealed the morphology and distribution of backlabelled cells in the cortex. These cells could be the SP or projection neurons (Auladell et al., 2000; del Rio et al., 2000). Backlabelled cells in the cortex of *p35* +/- mice at E16.5 and E18.5 mainly exhibited a pyramidal shape, and a vertically-oriented and moderately branched apical dendrite that typically made a contact with layer I (Fig.5-1G,I). In contrast, the backlabelled cells in *p35* -/- mice had pyramidal somata, but 'crooked' and highly branched apical dendrites (Fig.5-1H,J). Furthermore, the apical dendrites were often not attached to the pial surface, especially in older animals (E18.5), and these apical dendrites showed more elaborate branching and random orientation (Fig.5-1J); these 'detached' cells were very often horizontally positioned. It should be mentioned that similar morphology of early generated cortical cells in *p35* -/- has previously been described in the study of Gupta et al. (2003).

Prenatal thalamic axons cross over the entire cortical plate in _p35_ mutants

I next placed a DiI crystal in the dorsal thalamus to label thalamocortical fibres, at E16.5 and E18.5. In *p35* +/- and *p35* -/- animals, labelled TCAs were present in the IZ and accumulated within the SP (Fig.5-1K-N). In *p35* +/- mice, TCAs appeared to run tangentially within the upper IZ as a thick, compact band, without dispersion (Fig.5-1K). A slow radial growth of these axons towards the CP was observed at E16.5 (Fig.5-1K), and was more substantial two days later (Fig.5-1M). In *p35* mutant mice, growth of

TCAs in the cortex was considerably different than in their heterozygous littermates. First, the TCAs were rather scattered within the IZ (Fig.5-1L). Second, and most striking, many TCAs appeared to leave the SP and coursed obliquely through the CP and streamed towards the pial surface (Fig.5-1L,N). This 'overshooting' of thalamic axons was first observed at E16.5, became more evident at E18.5, and disappeared after birth, around P3 (data not shown). I and others (Molnar et al., 1998b) rarely observed such behaviour of TCAs in normal mice.

To determine the exact position of the DiI labelled TCAs in relation to specific cortical layers of *p35* +/- and *p35* -/- mice, I counterstained DiI labelled sections with a nuclear marker, bisbenzimide, that clearly reveals cortical cytoarchitecture. At E18.5, all developing cortical layers were present in both genotypes. However, in comparison to *p35* heterozygous mice, *p35* mutants showed a thinner CP, and layer I and IZ that were wider and more cellular (Fig.5-2A,B). It was clear that DiI labelled thalamic axons were tightly bundled and tangentially oriented within the IZ/SP zones in *p35* heterozygous mice. A small number of thalamic axonal branches radially ascending from the SP were observed in the CP (Fig.5-2C). In contrast, in *p35* mutants, labelled TCAs were widely spread in IZ/SP zones, and did not respect the border between the SP and CP layers. Instead, they massively and prematurely entered into a relatively non-permissive CP, coursed across it at an angle, and clearly entered into layer I (Fig.5-2D).

I used CalR immunohistochemistry to confirm that thalamic axons and neurons that derived from PPL cells are misplaced in *p35* -/- mice. At E15.5, CalR labelled thalamic axons were present in the IZ/SP in both *p35* +/- and *p35* -/- mice (Fig.5-3A,B). However, they were more dispersed in the *p35* mutants, and a few entered the CP prematurely streaming in the direction of the pia (Fig.5-3B). The trajectory of $CalR^+$ thalamic axons in both genotypes at E17.5 had a similar pattern to that at E15.5 (Fig.5-3G-L). However, the 'overshooting' of $CalR^+$ thalamic axons in *p35* -/- animals was more prominent at this developmental stage (Fig.5-3G-L), particularly in rostral cortical regions (Fig.5-3K,L). While only less than 10% of *p35* +/- forebrain sections showed this 'overshooting' phenomenon, it was noted in all *p35* -/- sections (Fig.5-3M). The distribution of CalR+ labelled cells in *p35* +/- was more confined to layers I and SP, with a few vertically oriented neurons in the CP (Fig.5-3C,M). On the contrary, CalR stained cells in *p35* -/- populated heavily the CP, in addition to layers I and SP (Fig.5-3D,N).

I also used another axonal marker, an antibody against Nogo-A, to study the distribution of cortical axons (Fig.5-3E,F). While in *p35* +/- mice, Nogo-A$^+$ axons located in the IZ/SP, ran as an uninterrupted bundle (Fig.5-3E), in *p35* -/- mice there was a compartment within the IZ, just below the SP, devoid of Nogo-A immunoreactivity (Fig.5-3F).

In conclusion, in *p35* -/- mice a portion of the developing thalamocortical fibres (DiI- or CalR-labelled) enter the CP prematurely (E16.5-E18.5) without stopping at the SP and streaming obliquely towards layer I. Two hypotheses may be suggested from this observation: (i) PPL does not split properly in *p35* mutants (incomplete *reeler* or *reeler*-like phenotype) resulting in mispositioned SP cells and, thus, misguided TC axons, or/and (ii) TCAs do not respond adequately to molecular cues (such as secreted semaphorins class III), repulsive or attractive, present in the SP and CP.

Defective splitting of the preplate in *p35* mutants

To test the first hypothesis, that the overshooting of thalamocortical fibres is due to defective PPL splitting, I labelled with BrdU the neurons of this layer at the time of their birth and studied their distribution after its supposed splitting. Preplate neurons in mice are born between E10.5-12.5. I injected pregnant females, carrying *p35* heterozygous and homozygous embryos, with two pulses of BrdU, three hours apart, at E11.5 to label PPL neurons during their final DNA synthesis (S) phase of the cell cycle. The distribution of BrdU labelled cells in layer I, CP, and SP was studied at E15.5 and E18.5 (Fig.5-4A).

BrdU$^+$ cells were located mainly above and below the CP in *p35* +/- and *p35* -/- mice, indicating splitting of the PPL. However, the organization of the PPL derivatives and accuracy of its splitting were different in the two genotypes. BrdU$^+$ cells in *p35* +/- mice at E15.5 were aligned in two well-separated, parallel layers, layer I and SP (Fig.5-4B). In contrast, in *p35* -/- mice, BrdU$^+$ cells had a more random distribution and appeared disorganized (Fig.5-4C). I then performed triple immunolabelling, using antibodies to BrdU and CalR (markers of prenatal PPL cells), and bisbenizmide (to label layers), at E17.5, with the view to examine the positions of cells in relation to the specific layers. In *p35* +/- mice, BrdU$^+$ cells were mostly located in layer I and SP, and a

few in the CP (Fig.5-4D). In *p35* -/- mice, many more $BrdU^+$ cells were observed in LI and CP and fewer in the SP compared to their heterozygous littermates (Fig5-4E).

I next examined the relative distribution of $BrdU^+$ cells in layer I, CP, and SP, of both genotypes, by counting labelled cells in each layer in rostral (septum level), medial (anterior commissural level), and caudal (hippocampus level) regions of the brain (n = 6 brains for each genotype). The relative distribution of $BrdU^+$ cells in each layer (LI, CP, or SP) was calculated as a percentage of the total number of $BrdU^+$ cells in all three layers. There was a significant shift in distribution of $BrdU^+$ cells in *p35* -/- compared to *p35* +/-; regardless of the region examined, there was a significant increase of $BrdU^+$ cells present in layer I and CP, and a significant decrease of $BrdU^+$ cells located in the SP (Fig.5-3F-H). The difference in distribution of labelled cells between the two genotypes was more prominent in the rostral region and that is in accord with the findings on $CalR^+$ fibre distribution (Fig.5-3 L).

Surprisingly, I found $CalR^+$ thalamic axons (Fig.5-5A) growing over $BrdU^+$ cells (Fig.5-5B) located in the SP (Fig.5-5C) in *p35* -/- mice at E18.5 (Fig.5-5D). Because Fig.5-5D was a result of maximal projections of numerous z-stack confocal planes (each 2 μm apart), there was a possibility that the cells and axon growing over them were not in the same plane. Therefore, I carefully examined each z-plane to confirm co-localization of single $CalR^+$ axons coursing over $BrdU^+$ cells in the SP (Fig.5-5E-J).

DISCUSSION

The major findings in this chapter are: (i) in *p35*-deficient mice, prenatal thalamocortical fibres run beyond the SP towards layer I; (ii) this phenomenon could be explained by improper splitting of the PPL. Therefore, Cdk5 can be added to the list of molecules, such as Reelin, involved in the proper formation and partition of the PPL.

Overshooting phenomenon

First, I described the 'overshooting' phenomenon of developing thalamic axons in prenatal *p35* -/- forebrain. In normal mice, TCAs were mainly associated with the SP during early development. If these axons access the CP, they do so by radial ascendance

of short branches, and confine themselves to the lower part of the CP. In contrast, in *p35* mutants, numerous thalamic axons entered the CP from early on, ran obliquely, and made contact with layer I. In agreement with other studies (Molnar et al., 1998b), I rarely observed this 'overshooting' phenomenon in normal animals. However, by labelling TCAs in two different ways, either with carbocyanine dye placement in the thalamus or antibody against CalR, I observed that TCA 'overshooting' was common in *p35* -/- mice. This was not fully recognized in previous studies on the development of thalamic axons in *p35* -/- (Kwon et al., 1999) or *Cdk5* -/- (Gilmore et al., 1998) mice, although Gilmore et al. (1998) observed LI^{+} thalamic fibres crossing over the entire CP, but omitted to include this finding in their final model of neuronal cytoarchitecture in *Cdk5* -/- mutants.

Incomplete preplate splitting

I hypothesized that incomplete PPL splitting, which results in misplaced SP neurons, underlay the overshooting phenomenon in *p35* -/- mice. The hypothesis was confirmed primarily by a BrdU birthdating study, in addition to CalR staining, which indicated a shift in the distribution of cells derived from the PPL towards the superficial locations. I also found backlabelled cells at different levels of the cortex after carbocyanine dye placement in the IC, but mostly superficially and close to the pia (Fig.5-1H,J). These labelled cells could be either SP or CP neurons, but the finding fits perfectly with the notion of SP cell misplacement in the *p35* -/- mutant. In future, in order to exclusively label SP cells, I should place the carbocyanine crystal in the IC at E13.5 or early E14, before the migrating or migrated CP cells begin to project axons.

The idea that the PPL might not be properly split in *Cdk5*-like mutants is not completely novel. Studies by Tsai and coworkers showed (i) that layer I and SP, identified histologically and by CalR staining, are markedly less distinct in *p35* -/-/p39 -/- double mutants (*Cdk5*-like) when compared with normal cortices (Ko et al., 2001), and (ii) that migration of early born, PPL destined neurons was defective in *p35* -/- mutants as observed in an *in vitro* time lapse study (Gupta et al., 2003). Thus, Cdk5 emerges as an important participant in the early compartmentalization of the cerebral cortex. Interestingly, in *reeler* mice that express Reelin in proliferative zones under the nestin promoter, a *Cdk5*-like phenotype was observed (Magdaleno et al., 2002). These

mice had a thin CP and ectopic SP, with most of the projection neurons beneath it. Although ectopically expressed Reelin did induce splitting of the PPL in these transgenic *reeler* mice, the splitting was not correct. Thus, the correct amount and position of Reelin are important for proper PPL splitting (see below).

How does preplate splitting occur?

Preplate splitting is an evolutionary adaptation, and although the PPL exists in amphibians, it is not split before the reptile evolutionary level. The multilayer cortex, formed in ascending order, appeared with the evolution of mammals (from review Marin-Padilla, 1998). The partition of the PPL in mammalian cortex is an extremely accurate process and probably requires a programmed interaction between the host environment (PPL cells and extracellular matrix) and guests (emerging glial fibres and migrating projection neurons). The molecular mechanisms that control PPL formation and its splitting are yet to be defined. Real-time imaging of this event, using e.g. EGFP under control of PPL cell specific marker promoter (such as Golli), would be a very useful tool in future studies.

So far, inadequate amounts of Reelin, such as lack of Reelin (*reeler*; Caviness, Jr., 1982; Golli/preplate ablation model, Xie et al., 2002), decreased level of Reelin (*Tbr1* mutant; Hevner et al., 2001; *Reeler*/Reelin transgenic; Magdaleno et al., 2002), increased level of Reelin (*Pax6* mutant; Stoykova et al., 2003), or absence of Reelin pathway molecules (*VLDLR/ApoER2* mutant; Trommsdorff et al., 1999; *Dab1* mutants; Howell et al., 1997; Sheldon et al., 1997), have been considered to explain the incorrect splitting of this layer. This study adds the p35/Cdk5 complex into this molecular group. Cdk5 regulates N-cadherin-mediated adhesion, and lack of Cdk5 increases cell adhesion (Kwon et al., 2000). Thus, Cdk5 might be involved in proper segregation of LI and SP neurons prior to arrival of the CP.

Is PPL splitting important for proper layering of the cortex?

If PPL splitting does not occur or is defective, cortical layers are not properly formed. This has been confirmed in all mice models described to be important for PPL splitting (see above). However, even if the PPL does completely split, as in e.g *EMX1/2* (Shinozaki et al., 2002) and *p73* (Meyer et al., 2004) mutants, late projection neurons fail to migrate in an inside-out fashion, probably due to a lack of Reelin at later stages.

This suggests a level of independence in proper cortical (II-VI) layering, and the importance of Reelin throughout the entire neuron migratory period.

Are CR cells necessary for PPL splitting and cortical lamination?

If the CR cells are eliminated by local application of domoic acid in newborn mice the migration of late born neurons is affected (Super et al., 2000), indicating an important role for CR cells in neuronal migration and corticogenesis. However, in the *Wnt3a* mutant, the cortical hem does not develop and almost all CR cells are missing. Despite this, there is a slight Reelin expression and, strikingly, this mutant does not show disruption in lamination of the cortex. Similarly, in the *p73* mutant, p73-expressing CR cells are lost, although Reelin is faintly expressed in layer I. The partition of PPL and early CP formation are not disturbed (Meyer et al., 2004).

In conclusion, Reelin is essential for PPL splitting. Furthermore, CR cells – which constitute the major source of Reelin within the developing cortex – are, by association, also necessary for this process to occur. There may be other sources of Reelin. In contrast, the p35/Cdk5 complex and other molecules, that are likely to be involved in the process of PPL splitting, are probably functionally redundant.

More than defect in PPL splitting in the *p35* mutants

The results described in Fig.5-5 prompted me to consider whether the 'overshooting' phenomenon in *p35* -/- mice is axon-autonomous (primary defect in axons due to a lack of *p35*) or axon-non-autonomous (secondary response to a primary, *p35*-dependent neuron migration defect, such as improper PPL splitting). As I have already discussed in relation to the second possibility, I would like to consider in future the idea that the position of thalamic axons in *p35* -/- mice might be due to their defective responsiveness to chemotropic or contact guidance cues, especially semaphorins, in the SP/CP region,. Semaphorins are a family of membrane-bound or secreted molecules implicated in neuron and axon guidance in the developing forebrain (Polleux et al., 1998b; Polleux et al., 2000; Marin et al., 2001; Tamamaki et al., 2003). Secreted semaphorins of family III are found to be expressed in the cortical region- or layer-specific territories (Tamamaki et al., 2003), and can act as attractive or repulsive guidance cues. Cdk5 is has been

shown to be expressed in bundles of developing cortical fibres (Tsai et al., 1993). It has also been found that semaphorin 3A signals through the Cdk5 pathway in the cerebral cortex (Sasaki et al., 2002).

In future studies, I plan to investigate whether thalamic axons respond to semaphorin 3A and 3F molecules, and to assess whether Cdk5 mediates this process. In preliminary studies using a co-culture collagen gel assay of rat E17 brain tissue, I have observed a repulsive effect of LGE on the outgrowth of thalamic axons (Fig.5-6A,B). LGE is found to express semaphorins 3A and 3F and to be a repulsive region for migrating cortical interneurons (Marin et al., 2001). I shall next study the direct effect of semaphorin 3A and 3F on the outgrowth of thalamic axons in wild-type and *p35* mutant mice (Fig.5-6C,D).

Fasciculation in *p35* mutants

It has been hypothesised that fasciculation of early cortical axon systems is impaired in *p35* -/- mice (Kwon et al., 1999b). This phenomenon could be secondary to accumulation of projection neurons in the IZ. In Nissl sections of *p35* -/- cortex at E16.5, there was a clear accumulation of cells beneath the ectopic SP (Fig.3-1D). At the same time, Nogo-A^+ axons avoid this sub-SP cell-rich region (Fig.5-3F). Therefore, it seems that fibres in the *p35* mutant are widely spread in the IZ as they have to navigate through numerous cells that could be acting as a physical barrier for their outgrowth.

Postnatal thalamocortical projections in *p35* mutants

The 'barrels' are smaller and indistinguishable in the somatosensory cortex, and the corpus callosum is very often diminished in adult *p35* mutants (Kwon et al., 1999). Further studies on the development of mature cortical connections in *p35* -/- mice are needed. I have done a preliminary study by placing a DiI crystal in the thalamus at P8, and observed three interesting things. In normal mice, backlabelled cells in the cortex were nicely positioned within the layer V only (Fig.5-7A), while in the *p35* mutant they were randomly and unevenly distributed in a wide, superficial cortical region (Fig.5-7B). This confirmed the absence/inversion of layers in *p35* mutants as I observed in Nissl-stained sections and in the BrdU birthdating study (chapter 3). The adult cortex projects

axons to the thalamus from layer VI. The backlabelling of layer V cells in control mice in my study could be due to either normal position of CTAs at that age as described by Clasca and colleagues in ferrets (Clasca et al., 1995), or the placement of the crystal was in the in the cerebral peduncle and, therefore, corticospinal or corticopontine axons were labelled. However, by looking at the DiI injection site, it seems that the thalamus has been targeted (Fig.5-7A,B insets). Next, I found that backlabelled projection neurons in *p35* mutants had thicker and abnormally branched apical dendrites (Fig.5-7D,E), compared to their control littermates (Fig.5-7C), confirming the importance of Cdk5 in neuritogenesis (Nikolic et al., 1996c). And lastly, I observed in *p35* +/- and *p35* -/- mice, that the TCAs, before contacting the target cells, ran tangentially in the white matter and obliquely in the cortex, respectively. However, when the TCAs approached closely their targets, they turned sharply towards them in both genotypes (Fig.5-7F,G). This indicates that proper branching of TCAs is not affected in *p35* mutants and is, therefore, a Cdk5 independent process.

Figure 5-1. CF and TC projections and SP/CP neurons in control and *p35* mutant mice

(A,B) CFAs and TCAs meet in the ventral telencephalon at E14.5.

(C-D, E-F) Ordered projections of CTAs and TCAs were maintained in *p35* +/- and *p35* -/- mice at E16.5 (C-D) and E18.5 (E-F).

(G-H, I-J) Morphology and position of backlabelled cells in the cortex after DiI injections in the internal capsule at E16.5 (G-H) and E18.5 (I-J); Cells in *p35* -/- mice (H-J) were more branched, located at different levels, and very often detached from the pial surface compared to control cells (G-I).

(K-N) Position of TCAs in the cortex after DiI injections in the thalamus at E16.5 (K-L) and E18.5 (M-N); TCAs in *p35* +/- (K-M) ran in a tight bundle and entered the CP by radial growth (arrowheads). TCAs in *p35* -/- (L-N) were spread widely and cross over the CP obliquely as they course towards the pial surface (arrows).

Cx – cortex; GE – ganglionic eminence; cfa – corticofugal axons; tca- thalamocortical axons; TE – thalamic eminence; Th – thalamus; LI – layer I; CP – cortical plate; SP – subplate; IZ – intermediate zone. Scale bars, 300 μm (A-B,E-F); 400 μm (C-D); 100 μm (G-I); 50 μm (H-J); 200 μm (K-N).

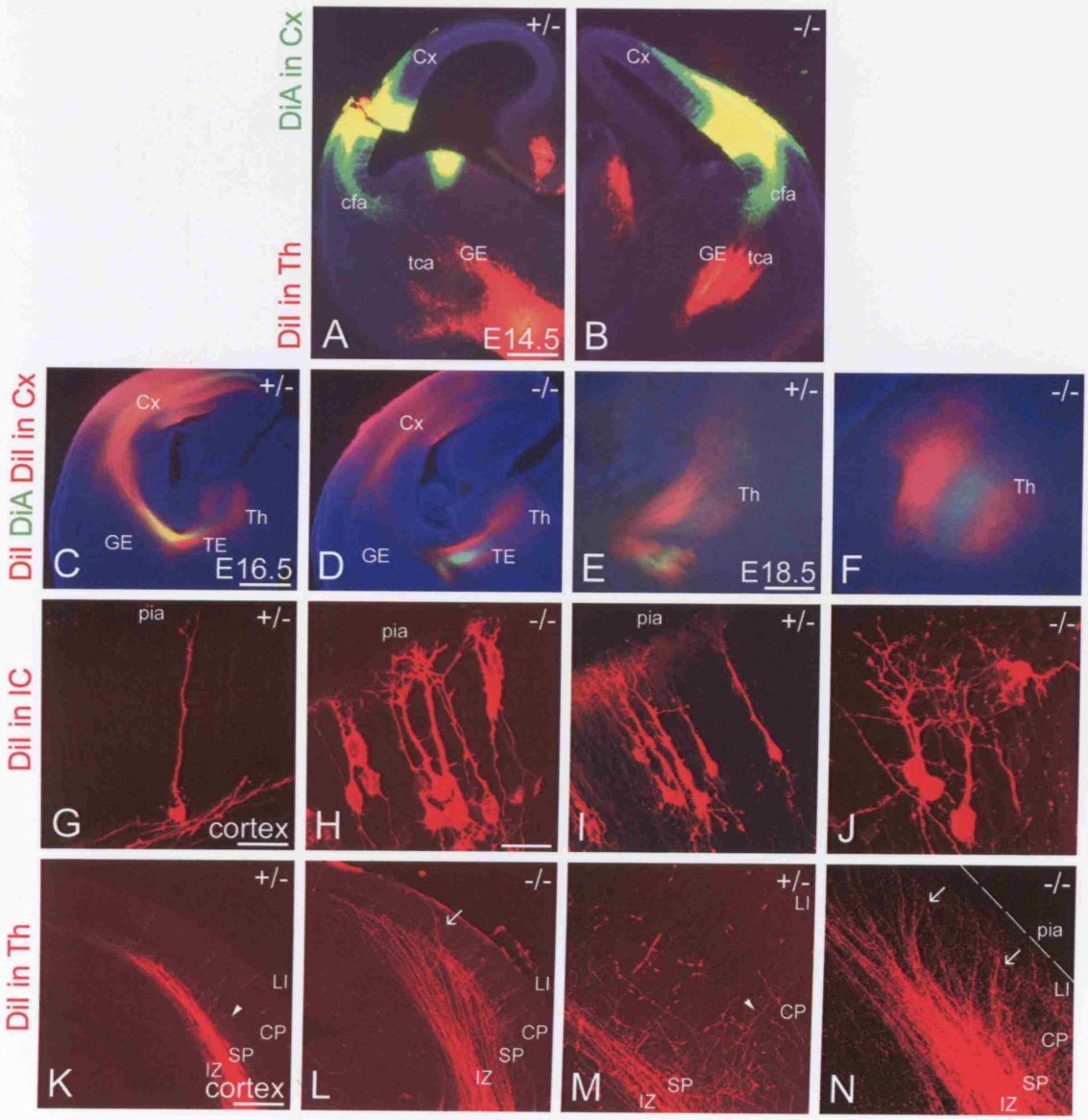
DiA in Cx
DiI in Th
+/-
-/-
Cx
cfa
tca
GE
A
E14.5
B
DiI DiA DiI in Cx
Th
TE
C
D
E
E16.5
E18.5
F
DiI in IC
pia
G
cortex
H
I
J
DiI in Th
LI
CP
SP
IZ
K
L
M
N

Figure 5-2. Position of the TCAs within the developing cortical layers

(A-B) Cortical layers, at E18.5, labelled with the nuclear marker bisbenzimide. Note a thin CP, ectopic SP, and wider LI and IZ in *p35* mutants (B) compared to control cortex (A).

(C-D) Cortex, at E18.5, after DiI crystal placement in the thalamus (Th). Thalamic axons entered the lower CP radially in *p35* +/- mice (C). TCAs reached layer I in an oblique trajectory in *p35* -/- mice (D).

LI – layer I; CP – cortical plate; SP – subplate; IZ – intermediate zone. Scale bar, 200 μm.

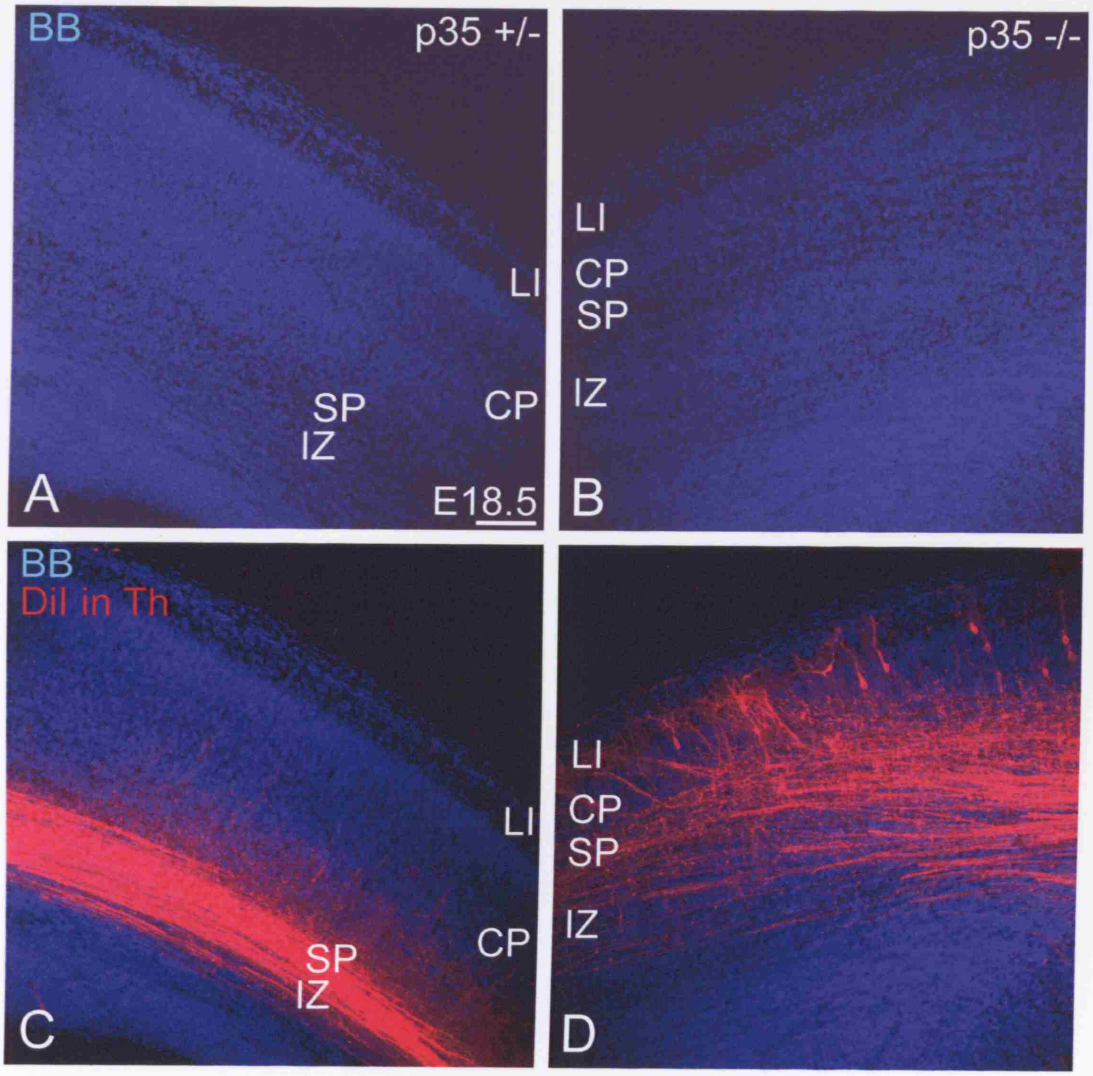
BB
p35 +/-
LI
SP
CP
IZ
A
E18.5
p35 -/-
LI
CP
SP
IZ
B
BB
DiI in Th
LI
CP
SP
IZ
C
LI
CP
SP
IZ
D

Figure 5-3. CalR$^+$ axons and cells are misplaced in *p35* -/- cortex

(A-F) E15.5; (G-O) E17.5

(A,B) CalR$^+$ axons and cells in the middle regions of the cortex at E15.5.

(C-D) CalR$^+$ axons and cells in the caudal cortex at E15.5

(E-F) Nogo-A$^+$ fibres in the cortex at E15.5. (F) Note a space bellow SP, in *p35* -/-, devoid of Nogo-A$^+$ axons (white vertical line).

(G-M) CalR$^+$ axons in middle (G-J) and rostral (K-L) cortex at E17.5. Fibres that run obliquely over the entire width of the CP in *p35* mutants are labelled with white arrows. (M) Percentage of sections that showed 'overshooting' in the two groups of animals.

(N-O) CalR$^+$ cells in the cortex at E17.5.

LI – layer I; CP – cortical plate; SP – subplate; IZ – intermediate zone. Scale bars, 200 μm (A-B); 300 μm (C-F); 400 μm (G-L, N-O).

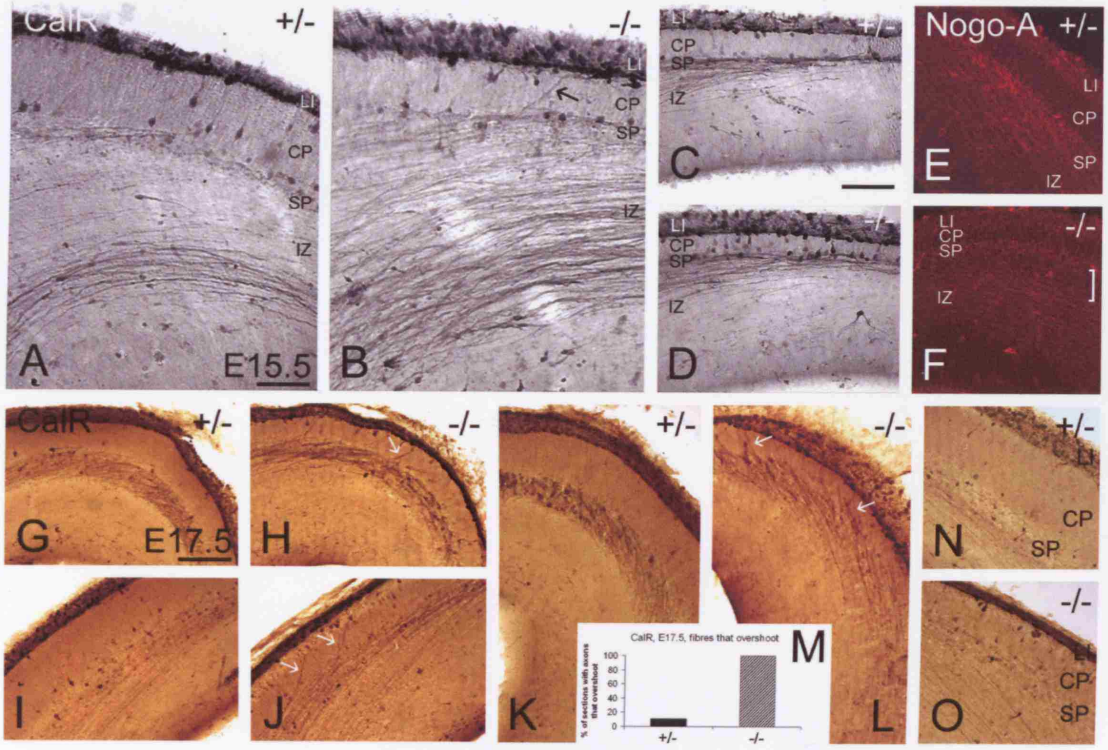
CalR
+/-
LI
CP
SP
IZ
A
E15.5
B
-/-
C
D
Nogo-A
E
F
]
G
E17.5
H
I
J
K
L
M
CalR, E17.5, fibres that overshoot
% of sections with axons that overshoot
100
80
60
40
20
0
N
O

Figure 5-4. *p35-deficiency* affects proper splitting of the preplate

(A) Pregnant dams were injected with the S phase cell cycle marker, BrdU, at E11.5, and sacrificed at E15.5 and E18.5.

(B-C) BrdU labelled preplate derivatives at E15.5.

(D-E) BrdU labelled preplate derivatives at E18.5

(F-H) Relative distribution of BrdU (E11.5) labelled cells at E18.5 in layers I, CP, SP, at different brain levels: (F) rostral, (G) middle, (H) caudal. Data in the graph represent mean percentage of $BrdU^+$ cells per layer ± SEM (standard error of the mean) from six brains for each genotype. Error bars represent SEM. * $p<0.05$, ** $p<0.01$, *** <0.005; Student *t*-test.

LI – layer I; CP – cortical plate; SP – subplate layer. Scale bar, 50 μm.

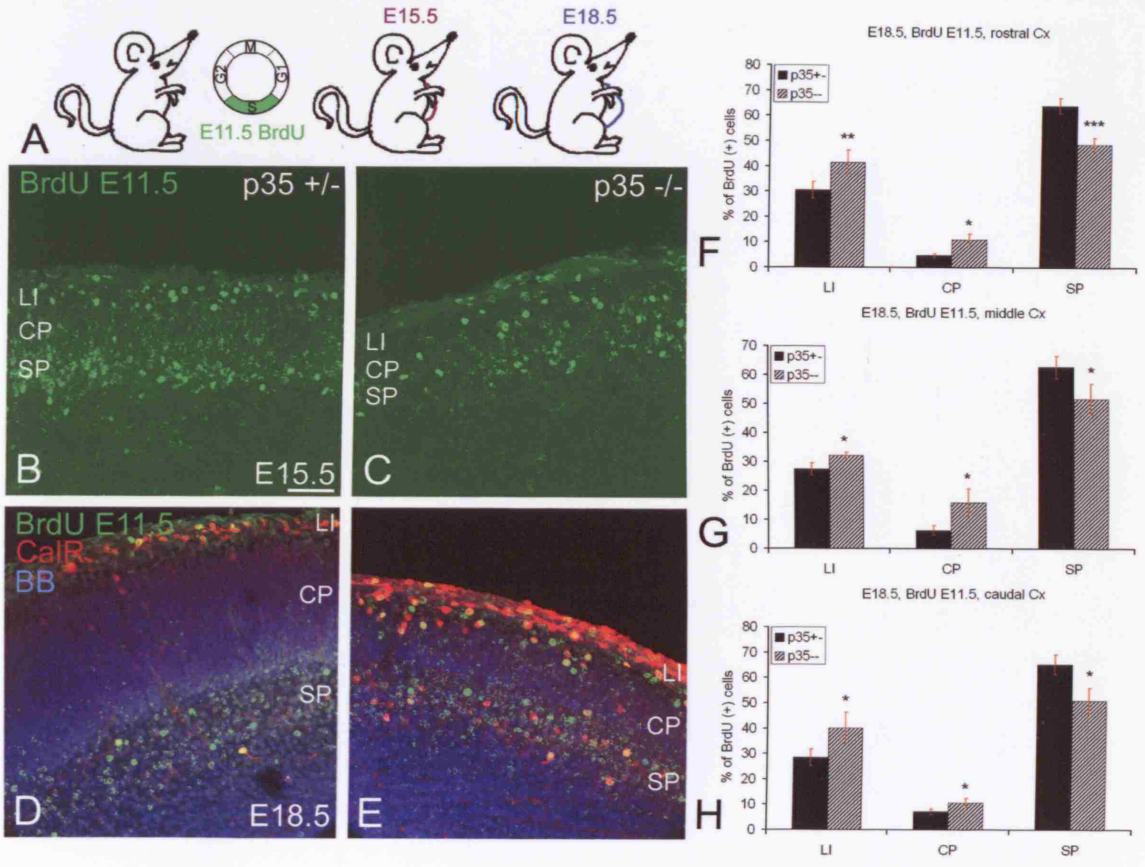
A
E15.5
E18.5
E11.5 BrdU
M
G2
G1
S
BrdU E11.5
p35 +/-
LI
CP
SP
B
E15.5
p35 -/-
C
BrdU E11.5
CalR
BB
D
E18.5
E
F
E18.5, BrdU E11.5, rostral Cx
p35+-
p35--
% of BrdU (+) cells
LI
CP
SP
G
E18.5, BrdU E11.5, middle Cx
H
E18.5, BrdU E11.5, caudal Cx

Figure 5-5. Thalamic axons run over cells in the SP of *p35* mutants

(A-D) Maximal projection of the confocal microscope z-stack of E18.5 cortical sections labelled with CalR (A), BrdU (injection E11.5; B), and bisbenzimide (BB; C). (D) An overlay of A,B,C; (E-J) Z optical planes, each 2 μm apart, of the confocal image D. Note a $CalR^+$ fibre that ran over $BrdU^+/BB^+$, presumably SP cell (all marked with white arrows).

LI – layer I; CP – cortical plate; SP – subplate. Scale bars, 50 μm (A-C), 25 μm (D), 75 μm (E-J).

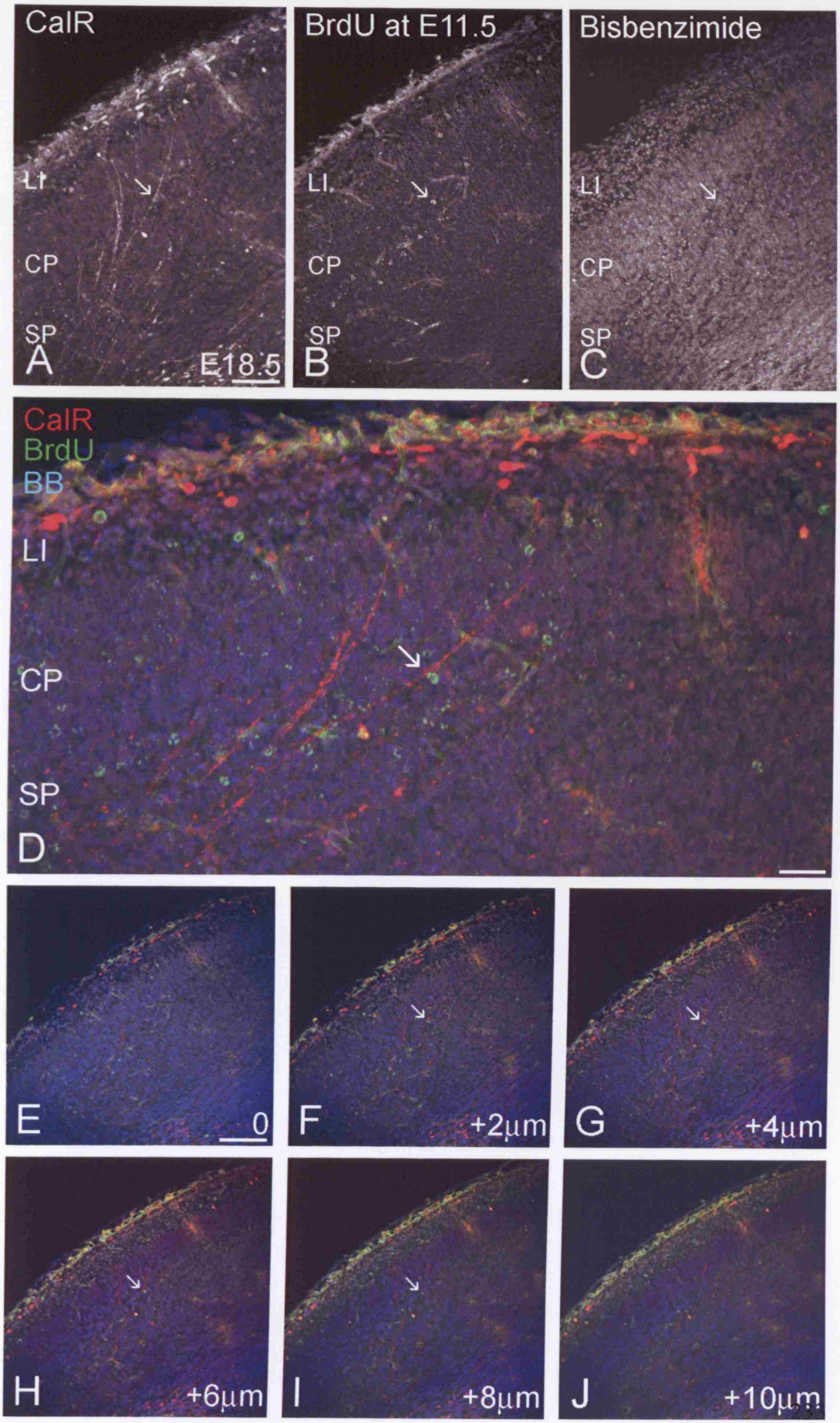
CalR
BrdU at E11.5
Bisbenzimide
LI
CP
SP
A
E18.5
B
C
CalR
BrdU
BB
D
E
0
F
+2μm
G
+4μm
H
+6μm
I
+8μm
J
+10μm

Figure 5-6. Future work: Response of TCAs to guidance cues in *p35* mutants

(A-B) Rat E17 thalamic axons from thalamic explants grow away from the LGE explants in a collagen matrix, after 3 days in culture. Axons were stained with the antibody to β-III-tubulin.

(C-D) Cultured HEK293 and GN11 cells were transfected with the myc-tagged chicken Semaphorin3A (C) and FLAG-tagged mouse Semaphorin3F (D) plasmids and visualized by c-myc and FLAG immunofluorescence, respectively. Bisbenizimide (BB) was used to label nuclei.

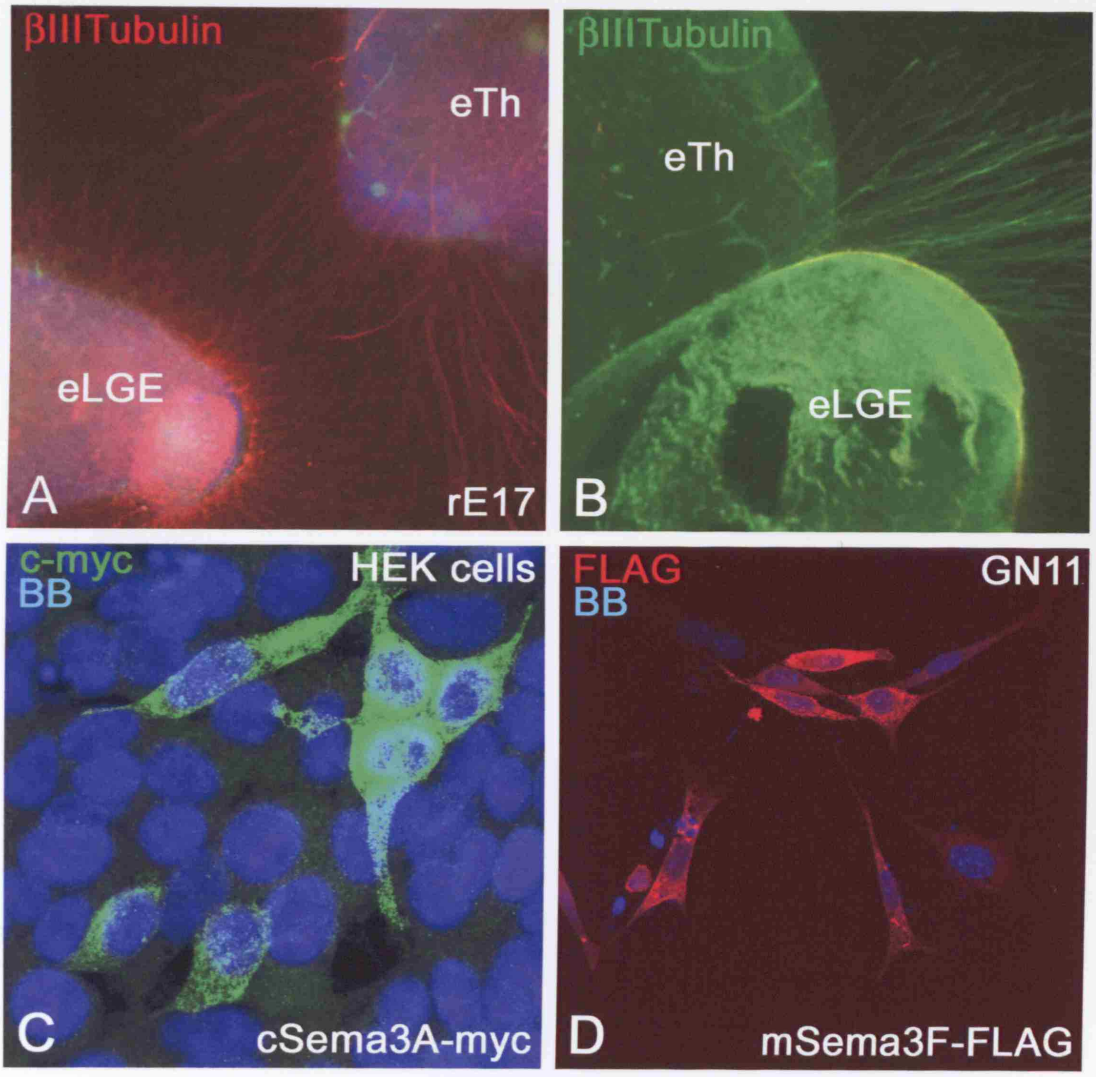
βIIITubulin
eTh
eLGE
A
rE17
βIIITubulin
eTh
eLGE
B
c-myc
BB
HEK cells
C
cSema3A-myc
FLAG
BB
GN11
D
mSema3F-FLAG

Figure 5-7. Future work: Postnatal TC projections in *p35* mutants

DiI crystal was placed in the thalamus at P8, and labelled cells and fibres were assessed.

(A-B) Backlabelled cells were found in layer V in *p35* +/- mice (A) and in the superficial part of the cortex in *p35* -/- mice (B). Cells in *p35* mutants were also aligned unevenly. Note the absence of white matter beneath the cortex in *p35* -/- mice. Instead, the labelled fibres were found within the cortex. Sites of DiI placements in the thalamus are shown in insets (A-B).

(C-E) Morphology of backlabelled cells in *p35* +/- (C) and *p35*-/- mice (D,E).

(F-G) Fibres turned at an angle (white angled lines) in both *p35* +/- (F) and *p35* -/- (G) mice. However, the fibre turn occurs at different cortical levels, a border between white matter and cortex in *p35* +/- and within the upper cortex in *p35* -/- animals. Turning angle is smaller (in *p35* +/-) or greater (in *p35* -/-) than 90°.

Cx - cortex; WM – white matter; Th – thalamus; BG – basal ganglia; hipp – hippocampus. Scale bars, 500 μm (A-B), 100 μm (C-G).

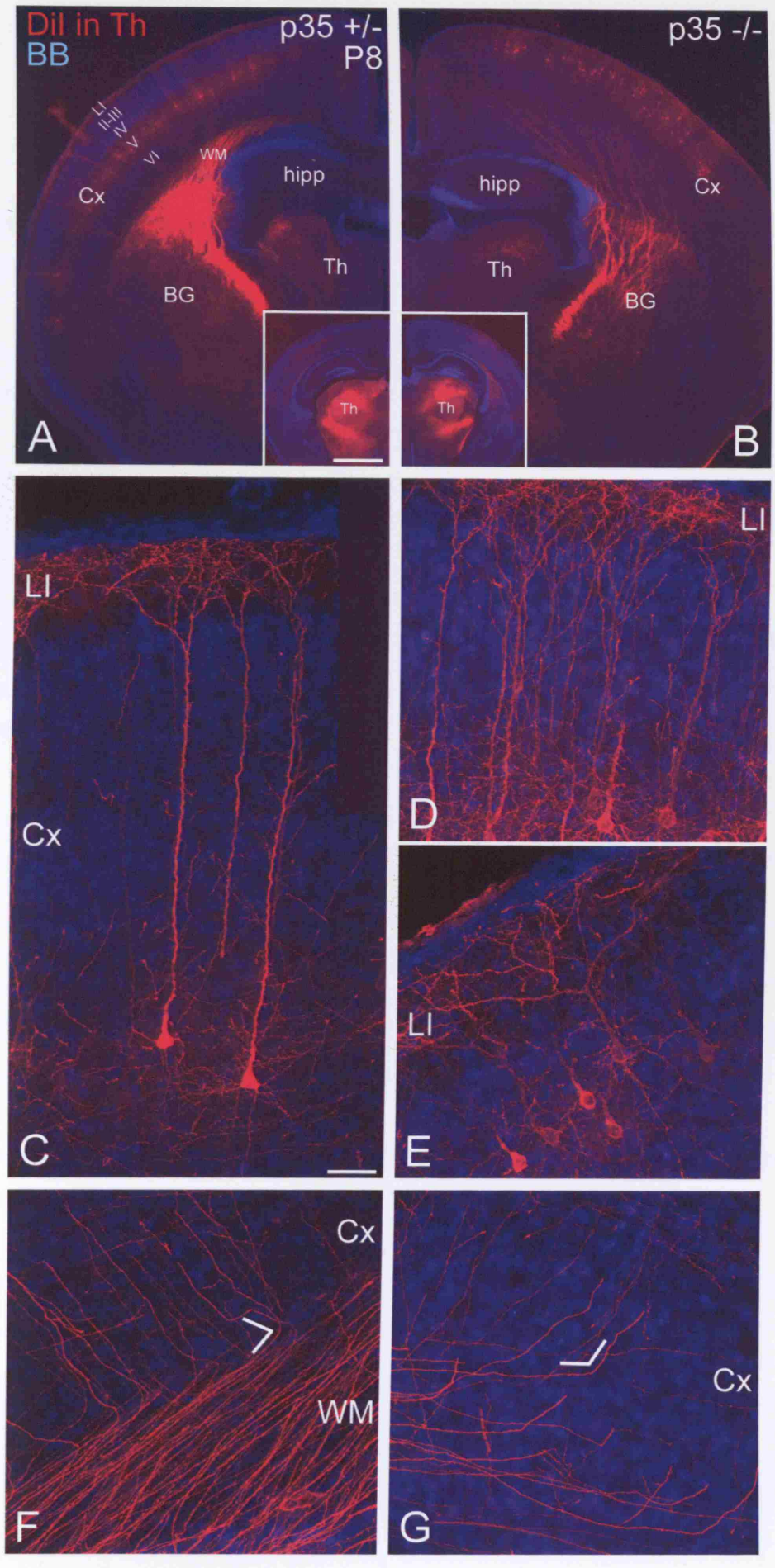
DiI in Th
BB
p35 +/-
P8
LI
II-III
IV
V
VI
WM
hipp
Cx
Th
BG
Th
A
p35 -/-
hipp
Cx
Th
BG
Th
B
LI
Cx
C
LI
D
LI
E
Cx
WM
F
Cx
G

REFERENCES

(1970) Embryonic vertebrate central nervous system: revised terminology. The Boulder Committee. Anat Rec 166:257-261.

Adams NC, Lozsadi DA, Guillery RW (1997) Complexities in the thalamocortical and corticothalamic pathways. Eur J Neurosci 9:204-209.

Alifragis P, Liapi A, Parnavelas JG (2004) Lhx6 regulates the migration of cortical interneurons from the ventral telencephalon but does not specify their GABA phenotype. J Neurosci 24:5643-5648.

Alifragis P, Parnavelas JG, Nadarajah B (2002) A novel method of labeling and characterizing migrating neurons in the developing central nervous system. Exp Neurol 174:259-265.

Allendoerfer KL, Shatz CJ (1994) The subplate, a transient neocortical structure: its role in the development of connections between thalamus and cortex. Annu Rev Neurosci 17:185-218.

Anderson S, Mione M, Yun K, Rubenstein JL (1999) Differential origins of neocortical projection and local circuit neurons: role of Dlx genes in neocortical interneuronogenesis. Cereb Cortex 9:646-654.

Anderson SA, Eisenstat DD, Shi L, Rubenstein JL (1997) Interneuron migration from basal forebrain to neocortex: dependence on Dlx genes. Science 278:474-476.

Anderson SA, Kaznowski CE, Horn C, Rubenstein JL, McConnell SK (2002) Distinct origins of neocortical projection neurons and interneurons in vivo. Cereb Cortex 12:702-709.

Anderson SA, Marin O, Horn C, Jennings K, Rubenstein JL (2001) Distinct cortical migrations from the medial and lateral ganglionic eminences. Development 128:353-363.

Ang ES, Jr., Haydar TF, Gluncic V, Rakic P (2003) Four-dimensional migratory coordinates of GABAergic interneurons in the developing mouse cortex. J Neurosci 23:5805-5815.

Angevine J.B., Sidman R.L (1961) Autoradiographic study of cell migration during histogenesis of the cerebral cortex in the mouse. pp 766-768.

Anton ES, Ghashghaei HT, Weber JL, McCann C, Fischer TM, Cheung ID, Gassmann M, Messing A, Klein R, Schwab MH, Lloyd KC, Lai C (2004) Receptor tyrosine kinase ErbB4 modulates neuroblast migration and placement in the adult forebrain. Nat Neurosci 7:1319-1328.

Anton ES, Marchionni MA, Lee KF, Rakic P (1997) Role of GGF/neuregulin signaling in interactions between migrating neurons and radial glia in the developing cerebral cortex. Development 124:3501-3510.

Arnaud L, Ballif BA, Forster E, Cooper JA (2003) Fyn tyrosine kinase is a critical regulator of disabled-1 during brain development. Curr Biol 13:9-17.

Assimacopoulos S, Grove EA, Ragsdale CW (2003) Identification of a Pax6-dependent epidermal growth factor family signaling source at the lateral edge of the embryonic cerebral cortex. J Neurosci 23:6399-6403.

Auladell C, Perez-Sust P, Super H, Soriano E (2000) The early development of thalamocortical and corticothalamic projections in the mouse. Anat Embryol (Berl) 201:169-179.

Bai J, Ramos RL, Ackman JB, Thomas AM, Lee RV, LoTurco JJ (2003) RNAi reveals doublecortin is required for radial migration in rat neocortex. Nat Neurosci 6:1277-1283.

Beffert U, Weeber EJ, Morfini G, Ko J, Brady ST, Tsai LH, Sweatt JD, Herz J (2004) Reelin and cyclin-dependent kinase 5-dependent signals cooperate in regulating neuronal migration and synaptic transmission. J Neurosci 24:1897-1906.

Behar TN, Dugich-Djordjevic MM, Li YX, Ma W, Somogyi R, Wen X, Brown E, Scott C, McKay RD, Barker JL (1997) Neurotrophins stimulate chemotaxis of embryonic cortical neurons. Eur J Neurosci 9:2561-2570.

Behar TN, Li YX, Tran HT, Ma W, Dunlap V, Scott C, Barker JL (1996) GABA stimulates chemotaxis and chemokinesis of embryonic cortical neurons via calcium-dependent mechanisms. J Neurosci 16:1808-1818.

Behar TN, Scott CA, Greene CL, Wen X, Smith SV, Maric D, Liu QY, Colton CA, Barker JL (1999) Glutamate acting at NMDA receptors stimulates embryonic cortical neuronal migration. J Neurosci 19:4449-4461.

Bellion A, Baudoin JP, Alvarez C, Bornens M, Metin C (2005) Nucleokinesis in tangentially migrating neurons comprises two alternating phases: forward migration of the Golgi/centrosome associated with centrosome splitting and myosin contraction at the rear. J Neurosci 25:5691-5699.

Bermingham-McDonogh O, McCabe KL, Reh TA (1996) Effects of GGF/neuregulins on neuronal survival and neurite outgrowth correlate with erbB2/neu expression in developing rat retina. Development 122:1427-1438.

Bertrand N, Castro DS, Guillemot F (2002) Proneural genes and the specification of neural cell types. Nat Rev Neurosci 3:517-530.

Bibb JA, Chen J, Taylor JR, Svenningsson P, Nishi A, Snyder GL, Yan Z, Sagawa ZK, Ouimet CC, Nairn AC, Nestler EJ, Greengard P (2001) Effects of chronic exposure to cocaine are regulated by the neuronal protein Cdk5. Nature 410:376-380.

Bibb JA, Snyder GL, Nishi A, Yan Z, Meijer L, Fienberg AA, Tsai LH, Kwon YT, Girault JA, Czernik AJ, Huganir RL, Hemmings HC, Jr., Nairn AC, Greengard P (1999)

Phosphorylation of DARPP-32 by Cdk5 modulates dopamine signalling in neurons. Nature 402:669-671.

Bicknese AR, Sheppard AM, O'Leary DD, Pearlman AL (1994) Thalamocortical axons extend along a chondroitin sulfate proteoglycan-enriched pathway coincident with the neocortical subplate and distinct from the efferent path. J Neurosci 14:3500-3510.

Birnboim HC, Doly J (1979) A rapid alkaline extraction procedure for screening recombinant plasmid DNA. Nucleic Acids Res 7:1513-1523.

Bishop KM, Goudreau G, O'Leary DD (2000) Regulation of area identity in the mammalian neocortex by Emx2 and Pax6. Science 288:344-349.

Blaschke AJ, Weiner JA, Chun J (1998) Programmed cell death is a universal feature of embryonic and postnatal neuroproliferative regions throughout the central nervous system. J Comp Neurol 396:39-50.

Bock HH, Herz J (2003) Reelin activates SRC family tyrosine kinases in neurons. Curr Biol 13:18-26.

Boyden (1962) The chemotactic effect of mixtures of antibody and antigen on polymorphonuclear leucocytes. J Exp Med 115:453-466.

Braisted JE, Catalano SM, Stimac R, Kennedy TE, Tessier-Lavigne M, Shatz CJ, O'Leary DD (2000) Netrin-1 promotes thalamic axon growth and is required for proper development of the thalamocortical projection. J Neurosci 20:5792-5801.

Braisted JE, Tuttle R, O'Leary DD (1999) Thalamocortical axons are influenced by chemorepellent and chemoattractant activities localized to decision points along their path. Dev Biol 208:430-440.

Brodmann K (1909) Vergleichende Lokalisationslehre der Grosshirnrinde. Leipzig: Johann Ambrosius Barth.

Brun A (1965) The subpial granular layer of the foetal cerebral cortex in man. Its ontogeny and significance in congenital cortical malformations. Acta Pathol Microbiol ScandSuppl-98.

Bu B, Li J, Davies P, Vincent I (2002) Deregulation of cdk5, hyperphosphorylation, and cytoskeletal pathology in the Niemann-Pick type C murine model. J Neurosci 22:6515-6525.

Buonanno A, Fischbach GD (2001) Neuregulin and ErbB receptor signaling pathways in the nervous system. Curr Opin Neurobiol 11:287-296.

Burden S, Yarden Y (1997) Neuregulins and their receptors: a versatile signaling module in organogenesis and oncogenesis. Neuron 18:847-855.

Cai XH, Tomizawa K, Tang D, Lu YF, Moriwaki A, Tokuda M, Nagahata S, Hatase O, Matsui H (1997) Changes in the expression of novel Cdk5 activator messenger RNA (p39nck5ai mRNA) during rat brain development. Neurosci Res 28:355-360.

Calaora V, Rogister B, Bismuth K, Murray K, Brandt H, Leprince P, Marchionni M, Dubois-Dalcq M (2001) Neuregulin signaling regulates neural precursor growth and the generation of oligodendrocytes in vitro. J Neurosci 21:4740-4751.

Caric D, Raphael H, Viti J, Feathers A, Wancio D, Lillien L (2001) EGFRs mediate chemotactic migration in the developing telencephalon. Development 128:4203-4216.

Casarosa S, Fode C, Guillemot F (1999) Mash1 regulates neurogenesis in the ventral telencephalon. Development 126:525-534.

Catalano SM, Robertson RT, Killackey HP (1991) Early ingrowth of thalamocortical afferents to the neocortex of the prenatal rat. Proc Natl Acad Sci U S A 88:2999-3003.

Caviness VS, Jr. (1982) Neocortical histogenesis in normal and reeler mice: a developmental study based upon [3H]thymidine autoradiography. Brain Res 256:293-302.

Caviness VS, Jr., Sidman RL (1973) Time of origin or corresponding cell classes in the cerebral cortex of normal and reeler mutant mice: an autoradiographic analysis. J Comp Neurol 148:141-151.

Chae T, Kwon YT, Bronson R, Dikkes P, Li E, Tsai LH (1997) Mice lacking p35, a neuronal specific activator of Cdk5, display cortical lamination defects, seizures, and adult lethality. Neuron 18:29-42.

Cheng K, Ip NY (2003) Cdk5: a new player at synapses. Neurosignals 12:180-190.

Cheung ZH, Ip NY (2004) Cdk5: mediator of neuronal death and survival. Neurosci Lett 361:47-51.

Ching YP, Pang AS, Lam WH, Qi RZ, Wang JH (2002) Identification of a neuronal Cdk5 activator-binding protein as Cdk5 inhibitor. J Biol Chem 277:15237-15240.

Church SM, Cotter D, Bramon E, Murray RM (2002) Does schizophrenia result from developmental or degenerative processes? J Neural Transm Suppl129-147.

Clasca F, Angelucci A, Sur M (1995) Layer-specific programs of development in neocortical projection neurons. Proc Natl Acad Sci U S A 92:11145-11149.

Cohen S, Levi-Montalcini R (1957) Purification and properties of a nerve growth-promoting factor isolated from mouse sarcoma 180. Cancer Res 17:15-20.

Colamarino SA, Tessier-Lavigne M (1995) The axonal chemoattractant netrin-1 is also a chemorepellent for trochlear motor axons. Cell 81:621-629.

Corbin JG, Nery S, Fishell G (2001) Telencephalic cells take a tangent: non-radial migration in the mammalian forebrain. Nat Neurosci 4 Suppl:1177-1182.

Corfas G, Roy K, Buxbaum JD (2004) Neuregulin 1-erbB signaling and the molecular/cellular basis of schizophrenia. Nat Neurosci 7:575-580.

Cruz JC, Tsai LH (2004) A Jekyll and Hyde kinase: roles for Cdk5 in brain development and disease. Curr Opin Neurobiol 14:390-394.

D'Arcangelo G, Miao GG, Chen SC, Soares HD, Morgan JI, Curran T (1995) A protein related to extracellular matrix proteins deleted in the mouse mutant reeler. Nature 374:719-723.

De Azevedo WF, Leclerc S, Meijer L, Havlicek L, Strnad M, Kim SH (1997) Inhibition of cyclin-dependent kinases by purine analogues: crystal structure of human cdk2 complexed with roscovitine. Eur J Biochem 243:518-526.

de Carlos JA, Lopez-Mascaraque L, Valverde F (1996) Dynamics of cell migration from the lateral ganglionic eminence in the rat. J Neurosci 16:6146-6156.

de Carlos JA, O'Leary DD (1992) Growth and targeting of subplate axons and establishment of major cortical pathways. J Neurosci 12:1194-1211.

DeDiego I, Smith-Fernandez A, Fairen A (1994) Cortical cells that migrate beyond area boundaries: characterization of an early neuronal population in the lower intermediate zone of prenatal rats. Eur J Neurosci 6:983-997.

del Rio JA, Martinez A, Auladell C, Soriano E (2000) Developmental history of the subplate and developing white matter in the murine neocortex. Neuronal organization and relationship with the main afferent systems at embryonic and perinatal stages. Cereb Cortex 10:784-801.

del Rio JA, Martinez A, Fonseca M, Auladell C, Soriano E (1995) Glutamate-like immunoreactivity and fate of Cajal-Retzius cells in the murine cortex as identified with calretinin antibody. Cereb Cortex 5:13-21.

del Rio JA, Soriano E, Ferrer I (1992) Development of GABA-immunoreactivity in the neocortex of the mouse. J Comp Neurol 326:501-526.

Delalle I, Bhide PG, Caviness VS, Jr., Tsai LH (1997) Temporal and spatial patterns of expression of p35, a regulatory subunit of cyclin-dependent kinase 5, in the nervous system of the mouse. J Neurocytol 26:283-296.

Demetrick DJ, Zhang H, Beach DH (1994) Chromosomal mapping of human CDK2, CDK4, and CDK5 cell cycle kinase genes. Cytogenet Cell Genet 66:72-74.

Denaxa M, Chan CH, Schachner M, Parnavelas JG, Karagogeos D (2001) The adhesion molecule TAG-1 mediates the migration of cortical interneurons from the ganglionic eminence along the corticofugal fiber system. Development 128:4635-4644.

Dhavan R, Tsai LH (2001) A decade of CDK5. Nat Rev Mol Cell Biol 2:749-759.

Dufour A, Seibt J, Passante L, Depaepe V, Ciossek T, Frisen J, Kullander K, Flanagan JG, Polleux F, Vanderhaeghen P (2003) Area specificity and topography of thalamocortical projections are controlled by ephrin/Eph genes. Neuron 39:453-465.

Dulabon L, Olson EC, Taglienti MG, Eisenhuth S, McGrath B, Walsh CA, Kreidberg JA, Anton ES (2000) Reelin binds alpha3beta1 integrin and inhibits neuronal migration. Neuron 27:33-44.

Edmondson JC, Hatten ME (1987) Glial-guided granule neuron migration in vitro: a high-resolution time-lapse video microscopic study. J Neurosci 7:1928-1934.

Elenius K, Choi CJ, Paul S, Santiestevan E, Nishi E, Klagsbrun M (1999) Characterization of a naturally occurring ErbB4 isoform that does not bind or activate phosphatidyl inositol 3-kinase. Oncogene 18:2607-2615.

Elenius K, Corfas G, Paul S, Choi CJ, Rio C, Plowman GD, Klagsbrun M (1997a) A novel juxtamembrane domain isoform of HER4/ErbB4. Isoform-specific tissue distribution and differential processing in response to phorbol ester. J Biol Chem 272:26761-26768.

Elenius K, Paul S, Allison G, Sun J, Klagsbrun M (1997b) Activation of HER4 by heparin-binding EGF-like growth factor stimulates chemotaxis but not proliferation. EMBO J 16:1268-1278.

Fairen A, Cobas A, Fonseca M (1986) Times of generation of glutamic acid decarboxylase immunoreactive neurons in mouse somatosensory cortex. J Comp Neurol 251:67-83.

Falconer DS (1951) The two mutants, *Trembler* and *Reeler*, with neurological actions in the house mouse. pp 192-201.

Falls DL (2003) Neuregulins: functions, forms, and signaling strategies. Exp Cell Res 284:14-30.

Falls DL, Rosen KM, Corfas G, Lane WS, Fischbach GD (1993) ARIA, a protein that stimulates acetylcholine receptor synthesis, is a member of the neu ligand family. Cell 72:801-815.

Fatemi SH (2005) Reelin glycoprotein: structure, biology and roles in health and disease. Mol Psychiatry 10:251-257.

Feldman ML, Peters A (1978) The forms of non-pyramidal neurons in the visual cortex of the rat. J Comp Neurol 179:761-793.

Fischbach GD, Rosen KM (1997) ARIA: a neuromuscular junction neuregulin. Annu Rev Neurosci 20:429-458.

Flames N, Long JE, Garratt AN, Fischer TM, Gassmann M, Birchmeier C, Lai C, Rubenstein JL, Marin O (2004) Short- and long-range attraction of cortical GABAergic interneurons by neuregulin-1. Neuron 44:251-261.

Flanagan JG, Vanderhaeghen P (1998) The ephrins and Eph receptors in neural development. Annu Rev Neurosci 21:309-345.

Floyd SR, Porro EB, Slepnev VI, Ochoa GC, Tsai LH, De CP (2001) Amphiphysin 1 binds the cyclin-dependent kinase (cdk) 5 regulatory subunit p35 and is phosphorylated by cdk5 and cdc2. J Biol Chem 276:8104-8110.

Fonseca M, Soriano E (1995) Calretinin-immunoreactive neurons in the normal human temporal cortex and in Alzheimer's disease. Brain Res 691:83-91.

Fox IJ, Kornblum HI (2005) Developmental profile of ErbB receptors in murine central nervous system: implications for functional interactions. J Neurosci Res 79:584-597.

Fox JW, Lamperti ED, Eksioglu YZ, Hong SE, Feng Y, Graham DA, Scheffer IE, Dobyns WB, Hirsch BA, Radtke RA, Berkovic SF, Huttenlocher PR, Walsh CA (1998) Mutations in filamin 1 prevent migration of cerebral cortical neurons in human periventricular heterotopia. Neuron 21:1315-1325.

Francis F, Koulakoff A, Boucher D, Chafey P, Schaar B, Vinet MC, Friocourt G, McDonnell N, Reiner O, Kahn A, McConnell SK, Berwald-Netter Y, Denoulet P, Chelly J (1999) Doublecortin is a developmentally regulated, microtubule-associated protein expressed in migrating and differentiating neurons. Neuron 23:247-256.

Fu AK, Fu WY, Cheung J, Tsim KW, Ip FC, Wang JH, Ip NY (2001) Cdk5 is involved in neuregulin-induced AChR expression at the neuromuscular junction. Nat Neurosci 4:374-381.

Fu AK, Fu WY, Ng AK, Chien WW, Ng YP, Wang JH, Ip NY (2004) Cyclin-dependent kinase 5 phosphorylates signal transducer and activator of transcription 3 and regulates its transcriptional activity. Proc Natl Acad Sci U S A 101:6728-6733.

Fukuchi-Shimogori T, Grove EA (2001) Neocortex patterning by the secreted signaling molecule FGF8. Science 294:1071-1074.

Furuta Y, Piston DW, Hogan BL (1997) Bone morphogenetic proteins (BMPs) as regulators of dorsal forebrain development. Development 124:2203-2212.

Galceran J, Miyashita-Lin EM, Devaney E, Rubenstein JL, Grosschedl R (2000) Hippocampus development and generation of dentate gyrus granule cells is regulated by LEF1. Development 127:469-482.

Gambarotta G, Garzotto D, Destro E, Mautino B, Giampietro C, Cutrupi S, Dati C, Cattaneo E, Fasolo A, Perroteau I (2004) ErbB4 expression in neural progenitor cells (ST14A) is necessary to mediate neuregulin-1beta1-induced migration. J Biol Chem 279:48808-48816.

Gao PP, Yue Y, Zhang JH, Cerretti DP, Levitt P, Zhou R (1998) Regulation of thalamic neurite outgrowth by the Eph ligand ephrin-A5: implications in the development of thalamocortical projections. Proc Natl Acad Sci U S A 95:5329-5334.

Garel S, Rubenstein JL (2004) Intermediate targets in formation of topographic projections: inputs from the thalamocortical system. Trends Neurosci 27:533-539.

Garel S, Yun K, Grosschedl R, Rubenstein JL (2002) The early topography of thalamocortical projections is shifted in Ebf1 and Dlx1/2 mutant mice. Development 129:5621-5634.

Gassmann M, Casagranda F, Orioli D, Simon H, Lai C, Klein R, Lemke G (1995) Aberrant neural and cardiac development in mice lacking the ErbB4 neuregulin receptor. Nature 378:390-394.

Gassmann M, Lemke G (1997) Neuregulins and neuregulin receptors in neural development. Curr Opin Neurobiol 7:87-92.

Gerecke KM, Wyss JM, Carroll SL (2004) Neuregulin-1beta induces neurite extension and arborization in cultured hippocampal neurons. Mol Cell Neurosci 27:379-393.

Ghosh A, Antonini A, McConnell SK, Shatz CJ (1990) Requirement for subplate neurons in the formation of thalamocortical connections. Nature 347:179-181.

Ghosh A, Shatz CJ (1992) Involvement of subplate neurons in the formation of ocular dominance columns. Science 255:1441-1443.

Ghosh A, Shatz CJ (1994) Segregation of geniculocortical afferents during the critical period: a role for subplate neurons. J Neurosci 14:3862-3880.

Gilmore EC, Herrup K (2001) Neocortical cell migration: GABAergic neurons and cells in layers I and VI move in a cyclin-dependent kinase 5-independent manner. J Neurosci 21:9690-9700.

Gilmore EC, Ohshima T, Goffinet AM, Kulkarni AB, Herrup K (1998) Cyclin-dependent kinase 5-deficient mice demonstrate novel developmental arrest in cerebral cortex. J Neurosci 18:6370-6377.

Gleeson JG, Allen KM, Fox JW, Lamperti ED, Berkovic S, Scheffer I, Cooper EC, Dobyns WB, Minnerath SR, Ross ME, Walsh CA (1998) Doublecortin, a brain-specific gene mutated in human X-linked lissencephaly and double cortex syndrome, encodes a putative signaling protein. Cell 92:63-72.

Gleeson JG, Lin PT, Flanagan LA, Walsh CA (1999) Doublecortin is a microtubule-associated protein and is expressed widely by migrating neurons. Neuron 23:257-271.

Gleeson JG, Walsh CA (2000) Neuronal migration disorders: from genetic diseases to developmental mechanisms. Trends Neurosci 23:352-359.

Godement P, Vanselow J, Thanos S, Bonhoeffer F (1987) A study in developing visual systems with a new method of staining neurones and their processes in fixed tissue. Development 101:697-713.

Golding JP, Sobieszczuk D, Dixon M, Coles E, Christiansen J, Wilkinson D, Gassmann M (2004) Roles of erbB4, rhombomere-specific, and rhombomere-independent cues in maintaining neural crest-free zones in the embryonic head. Dev Biol 266:361-372.

Golding JP, Trainor P, Krumlauf R, Gassmann M (2000) Defects in pathfinding by cranial neural crest cells in mice lacking the neuregulin receptor ErbB4. Nat Cell Biol 2:103-109.

Goldman JE (2004) Astrocyte Lineage. In: Myelin Biology and Disorders pp 311-328. Elsevier.

Gong X, Tang X, Wiedmann M, Wang X, Peng J, Zheng D, Blair LA, Marshall J, Mao Z (2003) Cdk5-mediated inhibition of the protective effects of transcription factor MEF2 in neurotoxicity-induced apoptosis. Neuron 38:33-46.

Gotz M, Novak N, Bastmayer M, Bonhoeffer F (1992) Membrane-bound molecules in rat cerebral cortex regulate thalamic innervation. Development 116:507-519.

Graham ME, Ruma-Haynes P, Capes-Davis AG, Dunn JM, Tan TC, Valova VA, Robinson PJ, Jeffrey PL (2004) Multisite phosphorylation of doublecortin by cyclin-dependent kinase 5. Biochem J 381:471-481.

Green SL, Kulp KS, Vulliet R (1997) Cyclin-dependent protein kinase 5 activity increases in rat brain following ischemia. Neurochem Int 31:617-623.

Grobin AC, Heenan EJ, Lieberman JA, Morrow AL (2003) Perinatal neurosteroid levels influence GABAergic interneuron localization in adult rat prefrontal cortex. J Neurosci 23:1832-1839.

Grove EA, Fukuchi-Shimogori T (2003) Generating the cerebral cortical area map. Annu Rev Neurosci 26:355-380.

Grove EA, Tole S, Limon J, Yip L, Ragsdale CW (1998) The hem of the embryonic cerebral cortex is defined by the expression of multiple Wnt genes and is compromised in Gli3-deficient mice. Development 125:2315-2325.

Gu Y, Rosenblatt J, Morgan DO (1992) Cell cycle regulation of CDK2 activity by phosphorylation of Thr160 and Tyr15. EMBO J 11:3995-4005.

Guillemot F, Lo LC, Johnson JE, Auerbach A, Anderson DJ, Joyner AL (1993) Mammalian achaete-scute homolog 1 is required for the early development of olfactory and autonomic neurons. Cell 75:463-476.

Gullick WJ (2001) The Type 1 growth factor receptors and their ligands considered as a complex system. Endocr Relat Cancer 8:75-82.

Gupta A, Sanada K, Miyamoto DT, Rovelstad S, Nadarajah B, Pearlman AL, Brunstrom J, Tsai LH (2003) Layering defect in p35 deficiency is linked to improper neuronal-glial interaction in radial migration. Nat Neurosci 6:1284-1291.

Gupta A, Tsai LH (2003) Cyclin-dependent kinase 5 and neuronal migration in the neocortex. Neurosignals 12:173-179.

Gupta A, Tsai LH (2001) Neuroscience. A kinase to dampen the effects of cociane? Science 292:236-237.

Gupta A, Tsai LH, Wynshaw-Boris A (2002) Life is a journey: a genetic look at neocortical development. Nat Rev Genet 3:342-355.

Hamasaki T, Goto S, Nishikawa S, Ushio Y (2001) Early-generated preplate neurons in the developing telencephalon: inward migration into the developing striatum. Cereb Cortex 11:474-484.

Hammond V, Tsai LH, Tan SS (2004) Control of cortical neuron migration and layering: cell and non cell-autonomous effects of p35. J Neurosci 24:576-587.

Harada T, Morooka T, Ogawa S, Nishida E (2001) ERK induces p35, a neuron-specific activator of Cdk5, through induction of Egr1. Nat Cell Biol 3:453-459.

Hebert JM, Mishina Y, McConnell SK (2002) BMP signaling is required locally to pattern the dorsal telencephalic midline. Neuron 35:1029-1041.

Hellmich MR, Pant HC, Wada E, Battey JF (1992) Neuronal cdc2-like kinase: a cdc2-related protein kinase with predominantly neuronal expression. Proc Natl Acad Sci U S A 89:10867-10871.

Hendry SH, Schwark HD, Jones EG, Yan J (1987) Numbers and proportions of GABA-immunoreactive neurons in different areas of monkey cerebral cortex. J Neurosci 7:1503-1519.

Henke-Fahle S, Mann F, Gotz M, Wild K, Bolz J (1996) Dual action of a carbohydrate epitope on afferent and efferent axons in cortical development. J Neurosci 16:4195-4206.

Hevner RF, Daza RA, Englund C, Kohtz J, Fink A (2004) Postnatal shifts of interneuron position in the neocortex of normal and reeler mice: evidence for inward radial migration. Neuroscience 124:605-618.

Hevner RF, Daza RA, Rubenstein JL, Stunnenberg H, Olavarria JF, Englund C (2003a) Beyond laminar fate: toward a molecular classification of cortical projection/pyramidal neurons. Dev Neurosci 25:139-151.

Hevner RF, Miyashita-Lin E, Rubenstein JL (2002) Cortical and thalamic axon pathfinding defects in Tbr1, Gbx2, and Pax6 mutant mice: evidence that cortical and thalamic axons interact and guide each other. J Comp Neurol 447:8-17.

Hevner RF, Neogi T, Englund C, Daza RA, Fink A (2003b) Cajal-Retzius cells in the mouse: transcription factors, neurotransmitters, and birthdays suggest a pallial origin. Brain Res Dev Brain Res 141:39-53.

Hevner RF, Shi L, Justice N, Hsueh Y, Sheng M, Smiga S, Bulfone A, Goffinet AM, Campagnoni AT, Rubenstein JL (2001) Tbr1 regulates differentiation of the preplate and layer 6. Neuron 29:353-366.

Hiesberger T, Trommsdorff M, Howell BW, Goffinet A, Mumby MC, Cooper JA, Herz J (1999) Direct binding of Reelin to VLDL receptor and ApoE receptor 2 induces

tyrosine phosphorylation of disabled-1 and modulates tau phosphorylation. Neuron 24:481-489.

His W (1889) Die Neuroblasten und deren Entstehung im embryonalen Mark. pp 249-300.

Hisanaga S, Saito T (2003) The regulation of cyclin-dependent kinase 5 activity through the metabolism of p35 or p39 Cdk5 activator. Neurosignals 12:221-229.

Holmes WE, Sliwkowski MX, Akita RW, Henzel WJ, Lee J, Park JW, Yansura D, Abadi N, Raab H, Lewis GD, . (1992) Identification of heregulin, a specific activator of p185erbB2. Science 256:1205-1210.

Hong SE, Shugart YY, Huang DT, Shahwan SA, Grant PE, Hourihane JO, Martin ND, Walsh CA (2000) Autosomal recessive lissencephaly with cerebellar hypoplasia is associated with human RELN mutations. Nat Genet 26:93-96.

Howell BW, Hawkes R, Soriano P, Cooper JA (1997) Neuronal position in the developing brain is regulated by mouse disabled-1. Nature 389:733-737.

Howell BW, Herrick TM, Cooper JA (1999) Reelin-induced tryosine phosphorylation of disabled 1 during neuronal positioning. Genes Dev 13:643-648.

Humbert S, Lanier LM, Tsai LH (2000) Synaptic localization of p39, a neuronal activator of cdk5. Neuroreport 11:2213-2216.

Hunt D, Coffin RS, Prinjha RK, Campbell G, Anderson PN (2003) Nogo-A expression in the intact and injured nervous system. Mol Cell Neurosci 24:1083-1102.

Ino H, Chiba T (1996) Intracellular localization of cyclin-dependent kinase 5 (CDK5) in mouse neuron: CDK5 is located in both nucleus and cytoplasm. Brain Res 732:179-185.

Ino H, Ishizuka T, Chiba T, Tatibana M (1994) Expression of CDK5 (PSSALRE kinase), a neural cdc2-related protein kinase, in the mature and developing mouse central and peripheral nervous systems. Brain Res 661:196-206.

Ishiguro K, Kobayashi S, Omori A, Takamatsu M, Yonekura S, Anzai K, Imahori K, Uchida T (1994) Identification of the 23 kDa subunit of tau protein kinase II as a putative activator of cdk5 in bovine brain. FEBS Lett 342:203-208.

Ishiguro K, Takamatsu M, Tomizawa K, Omori A, Takahashi M, Arioka M, Uchida T, Imahori K (1992) Tau protein kinase I converts normal tau protein into A68-like component of paired helical filaments. J Biol Chem 267:10897-10901.

Jacobsen CT, Miller RH (2003) Control of astrocyte migration in the developing cerebral cortex. Dev Neurosci 25:207-216.

Jimenez D, Lopez-Mascaraque L, de Carlos JA, Valverde F (2002) Further studies on cortical tangential migration in wild type and Pax-6 mutant mice. J Neurocytol 31:719-728.

Jones FE, Welte T, Fu XY, Stern DF (1999) ErbB4 signaling in the mammary gland is required for lobuloalveolar development and Stat5 activation during lactation. J Cell Biol 147:77-88.

Junttila TT, Sundvall M, Maatta JA, Elenius K (2000) Erbb4 and its isoforms: selective regulation of growth factor responses by naturally occurring receptor variants. Trends Cardiovasc Med 10:304-310.

Kainulainen V, Sundvall M, Maatta JA, Santiestevan E, Klagsbrun M, Elenius K (2000) A natural ErbB4 isoform that does not activate phosphoinositide 3-kinase mediates proliferation but not survival or chemotaxis. J Biol Chem 275:8641-8649.

Kawauchi T, Chihama K, Nishimura YV, Nabeshima Y, Hoshino M (2005) MAP1B phosphorylation is differentially regulated by Cdk5/p35, Cdk5/p25, and JNK. Biochem Biophys Res Commun 331:50-55.

Kesavapany S, Lau KF, McLoughlin DM, Brownlees J, Ackerley S, Leigh PN, Shaw CE, Miller CC (2001) p35/cdk5 binds and phosphorylates beta-catenin and regulates beta-catenin/presenilin-1 interaction. Eur J Neurosci 13:241-247.

Keshvara L, Benhayon D, Magdaleno S, Curran T (2001) Identification of reelin-induced sites of tyrosyl phosphorylation on disabled 1. J Biol Chem 276:16008-16014.

Keshvara L, Magdaleno S, Benhayon D, Curran T (2002) Cyclin-dependent kinase 5 phosphorylates disabled 1 independently of Reelin signaling. J Neurosci 22:4869-4877.

Kim AS, Anderson SA, Rubenstein JL, Lowenstein DH, Pleasure SJ (2001) Pax-6 regulates expression of SFRP-2 and Wnt-7b in the developing CNS. J Neurosci 21:RC132.

Kitamura K, et al. (2002) Mutation of ARX causes abnormal development of forebrain and testes in mice and X-linked lissencephaly with abnormal genitalia in humans. Nat Genet 32:359-369.

Ko J, Humbert S, Bronson RT, Takahashi S, Kulkarni AB, Li E, Tsai LH (2001) p35 and p39 are essential for cyclin-dependent kinase 5 function during neurodevelopment. J Neurosci 21:6758-6771.

Komuro H, Rakic P (1993) Modulation of neuronal migration by NMDA receptors. Science 260:95-97.

Kostovic I, Rakic P (1990) Developmental history of the transient subplate zone in the visual and somatosensory cortex of the macaque monkey and human brain. J Comp Neurol 297:441-470.

Kostovic I, Rakic P (1980) Cytology and time of origin of interstitial neurons in the white matter in infant and adult human and monkey telencephalon. J Neurocytol 9:219-242.

Kramer R, Bucay N, Kane DJ, Martin LE, Tarpley JE, Theill LE (1996) Neuregulins with an Ig-like domain are essential for mouse myocardial and neuronal development. Proc Natl Acad Sci U S A 93:4833-4838.

Kusakawa G, Saito T, Onuki R, Ishiguro K, Kishimoto T, Hisanaga S (2000) Calpain-dependent proteolytic cleavage of the p35 cyclin-dependent kinase 5 activator to p25. J Biol Chem 275:17166-17172.

Kwon YT, Gupta A, Zhou Y, Nikolic M, Tsai LH (2000) Regulation of N-cadherin-mediated adhesion by the p35-Cdk5 kinase. Curr Biol 10:363-372.

Kwon YT, Tsai LH (1998) A novel disruption of cortical development in p35(-/-) mice distinct from reeler. J Comp Neurol 395:510-522.

Kwon YT, Tsai LH, Crandall JE (1999) Callosal axon guidance defects in p35(-/-) mice. J Comp Neurol 415:218-229.

Lambert de RC, Goffinet AM (1998) A new view of early cortical development. Biochem Pharmacol 56:1403-1409.

Lambert de RC, Goffinet AM (2001) Neuronal migration. Mech Dev 105:47-56.

Landry CF, Pribyl TM, Ellison JA, Givogri MI, Kampf K, Campagnoni CW, Campagnoni AT (1998) Embryonic expression of the myelin basic protein gene: identification of a promoter region that targets transgene expression to pioneer neurons. J Neurosci 18:7315-7327.

Lavdas AA, Grigoriou M, Pachnis V, Parnavelas JG (1999) The medial ganglionic eminence gives rise to a population of early neurons in the developing cerebral cortex. J Neurosci 19:7881-7888.

Lazaro JB, Kitzmann M, Poul MA, Vandromme M, Lamb NJ, Fernandez A (1997) Cyclin dependent kinase 5, cdk5, is a positive regulator of myogenesis in mouse C2 cells. J Cell Sci 110 (Pt 10):1251-1260.

Ledda F, Paratcha G, Ibanez CF (2002) Target-derived GFRalpha1 as an attractive guidance signal for developing sensory and sympathetic axons via activation of Cdk5. Neuron 36:387-401.

Lee KF, Simon H, Chen H, Bates B, Hung MC, Hauser C (1995) Requirement for neuregulin receptor erbB2 in neural and cardiac development. Nature 378:394-398.

Lee MH, Nikolic M, Baptista CA, Lai E, Tsai LH, Massague J (1996) The brain-specific activator p35 allows Cdk5 to escape inhibition by p27Kip1 in neurons. Proc Natl Acad Sci U S A 93:3259-3263.

Lee MS, Kwon YT, Li M, Peng J, Friedlander RM, Tsai LH (2000a) Neurotoxicity induces cleavage of p35 to p25 by calpain. Nature 405:360-364.

Lee SM, Tole S, Grove E, McMahon AP (2000b) A local Wnt-3a signal is required for development of the mammalian hippocampus. Development 127:457-467.

Lemke G (1996) Neuregulins in development. Mol Cell Neurosci 7:247-262.

Letinic K, Kostovic I (1996) Transient neuronal population of the internal capsule in the developing human cerebrum. Neuroreport 7:2159-2162.

Levi-Montalcini R, Hamburger V (1951) Selective growth stimulating effects of mouse sarcoma on the sensory and sympathetic nervous system of the chick embryo. J Exp Zool 116:321-361.

Levitt P, Eagleson KL, Powell EM (2004) Regulation of neocortical interneuron development and the implications for neurodevelopmental disorders. Trends Neurosci 27:400-406.

Lew J, Beaudette K, Litwin CM, Wang JH (1992a) Purification and characterization of a novel proline-directed protein kinase from bovine brain. J Biol Chem 267:13383-13390.

Lew J, Huang QQ, Qi Z, Winkfein RJ, Aebersold R, Hunt T, Wang JH (1994) A brain-specific activator of cyclin-dependent kinase 5. Nature 371:423-426.

Lew J, Winkfein RJ, Paudel HK, Wang JH (1992b) Brain proline-directed protein kinase is a neurofilament kinase which displays high sequence homology to p34cdc2. J Biol Chem 267:25922-25926.

Li BS, Ma W, Jaffe H, Zheng Y, Takahashi S, Zhang L, Kulkarni AB, Pant HC (2003) Cyclin-dependent kinase-5 is involved in neuregulin-dependent activation of phosphatidylinositol 3-kinase and Akt activity mediating neuronal survival. J Biol Chem 278:35702-35709.

Li H, Chou S, O'Leary DD (2004) Neuregulin-ErbB4 signaling controls tangential migration of GABAergic interneurons and cortical lamination. Society for Neuroscience Meeting266.18.

Liu Q, Dwyer ND, O'Leary DD (2000) Differential expression of COUP-TFI, CHL1, and two novel genes in developing neocortex identified by differential display PCR. J Neurosci 20:7682-7690.

Lopez-Bendito G, Chan CH, Mallamaci A, Parnavelas J, Molnar Z (2002a) Role of Emx2 in the development of the reciprocal connectivity between cortex and thalamus. J Comp Neurol 451:153-169.

Lopez-Bendito G, Lujan R, Shigemoto R, Ganter P, Paulsen O, Molnar Z (2003) Blockade of GABA(B) receptors alters the tangential migration of cortical neurons. Cereb Cortex 13:932-942.

Lopez-Bendito G, Molnar Z (2003) Thalamocortical development: how are we going to get there? Nat Rev Neurosci 4:276-289.

Lopez-Bendito G, Shigemoto R, Fairen A, Lujan R (2002b) Differential distribution of group I metabotropic glutamate receptors during rat cortical development. Cereb Cortex 12:625-638.

Lopez-Bendito G, Shigemoto R, Kulik A, Paulsen O, Fairen A, Lujan R (2002c) Expression and distribution of metabotropic GABA receptor subtypes GABABR1 and GABABR2 during rat neocortical development. Eur J Neurosci 15:1766-1778.

Luskin MB, Parnavelas JG, Barfield JA (1993) Neurons, astrocytes, and oligodendrocytes of the rat cerebral cortex originate from separate progenitor cells: an ultrastructural analysis of clonally related cells. J Neurosci 13:1730-1750.

Ma YJ, Hill DF, Creswick KE, Costa ME, Cornea A, Lioubin MN, Plowman GD, Ojeda SR (1999) Neuregulins signaling via a glial erbB-2-erbB-4 receptor complex contribute to the neuroendocrine control of mammalian sexual development. J Neurosci 19:9913-9927.

Magdaleno S, Keshvara L, Curran T (2002) Rescue of ataxia and preplate splitting by ectopic expression of Reelin in reeler mice. Neuron 33:573-586.

Maggi R, Pimpinelli F, Molteni L, Milani M, Martini L, Piva F (2000) Immortalized luteinizing hormone-releasing hormone neurons show a different migratory activity in vitro. Endocrinology 141:2105-2112.

Magini G (1888) Sur la neuroglie et les cellules nerveuses cerebrales chez les foetus. pp 59-60.

Malatesta P, Hartfuss E, Gotz M (2000) Isolation of radial glial cells by fluorescent-activated cell sorting reveals a neuronal lineage. Development 127:5253-5263.

Mallamaci A, Mercurio S, Muzio L, Cecchi C, Pardini CL, Gruss P, Boncinelli E (2000a) The lack of Emx2 causes impairment of Reelin signaling and defects of neuronal migration in the developing cerebral cortex. J Neurosci 20:1109-1118.

Mallamaci A, Muzio L, Chan CH, Parnavelas J, Boncinelli E (2000b) Area identity shifts in the early cerebral cortex of Emx2-/- mutant mice. Nat Neurosci 3:679-686.

Manetto V, Sternberger NH, Perry G, Sternberger LA, Gambetti P (1988) Phosphorylation of neurofilaments is altered in amyotrophic lateral sclerosis. J Neuropathol Exp Neurol 47:642-653.

Mann F, Zhukareva V, Pimenta A, Levitt P, Bolz J (1998) Membrane-associated molecules guide limbic and nonlimbic thalamocortical projections. J Neurosci 18:9409-9419.

Marchionni MA, Goodearl AD, Chen MS, Bermingham-McDonogh O, Kirk C, Hendricks M, Danehy F, Misumi D, Sudhalter J, Kobayashi K, . (1993) Glial growth factors are alternatively spliced erbB2 ligands expressed in the nervous system. Nature 362:312-318.

Marin O (2003) Thalamocortical topography reloaded: it's not where you go, but how you get there. Neuron 39:388-391.

Marin O, Plump AS, Flames N, Sanchez-Camacho C, Tessier-Lavigne M, Rubenstein JL (2003) Directional guidance of interneuron migration to the cerebral cortex relies on subcortical Slit1/2-independent repulsion and cortical attraction. Development 130:1889-1901.

Marin O, Rubenstein JL (2001) A long, remarkable journey: tangential migration in the telencephalon. Nat Rev Neurosci 2:780-790.

Marin O, Rubenstein JL (2003) Cell migration in the forebrain. Annu Rev Neurosci 26:441-483.

Marin O, Yaron A, Bagri A, Tessier-Lavigne M, Rubenstein JL (2001) Sorting of striatal and cortical interneurons regulated by semaphorin-neuropilin interactions. Science 293:872-875.

Marin-Padilla M (1998) Cajal-Retzius cells and the development of the neocortex. Trends Neurosci 21:64-71.

Marin-Padilla M (1971) Early prenatal ontogenesis of the cerebral cortex (neocortex) of the cat (Felis domestica). A Golgi study. I. The primordial neocortical organization. Z Anat Entwicklungsgesch 134:117-145.

McConnell SK, Ghosh A, Shatz CJ (1989) Subplate neurons pioneer the first axon pathway from the cerebral cortex. Science 245:978-982.

McConnell SK, Kaznowski CE (1991) Cell cycle dependence of laminar determination in developing neocortex. Science 254:282-285.

McEvilly RJ, de Diaz MO, Schonemann MD, Hooshmand F, Rosenfeld MG (2002) Transcriptional regulation of cortical neuron migration by POU domain factors. Science 295:1528-1532.

Meijer L, Borgne A, Mulner O, Chong JP, Blow JJ, Inagaki N, Inagaki M, Delcros JG, Moulinoux JP (1997) Biochemical and cellular effects of roscovitine, a potent and selective inhibitor of the cyclin-dependent kinases cdc2, cdk2 and cdk5. Eur J Biochem 243:527-536.

Meinecke DL, Peters A (1987) GABA immunoreactive neurons in rat visual cortex. J Comp Neurol 261:388-404.

Metin C, Deleglise D, Serafini T, Kennedy TE, Tessier-Lavigne M (1997) A role for netrin-1 in the guidance of cortical efferents. Development 124:5063-5074.

Metin C, Godement P (1996) The ganglionic eminence may be an intermediate target for corticofugal and thalamocortical axons. J Neurosci 16:3219-3235.

Meyer D, Birchmeier C (1995) Multiple essential functions of neuregulin in development. Nature 378:386-390.

Meyer D, Birchmeier C (1994) Distinct isoforms of neuregulin are expressed in mesenchymal and neuronal cells during mouse development. Proc Natl Acad Sci U S A 91:1064-1068.

Meyer G, Cabrera SA, Perez Garcia CG, Martinez ML, Walker N, Caput D (2004) Developmental roles of p73 in Cajal-Retzius cells and cortical patterning. J Neurosci 24:9878-9887.

Meyer G, Castro R, Soria JM, Fairen A (2000) The subpial granular layer in the developing cerebral cortex of rodents. Results Probl Cell Differ 30:277-291.

Meyer G, Goffinet AM, Fairen A (1999) What is a Cajal-Retzius cell? A reassessment of a classical cell type based on recent observations in the developing neocortex. Cereb Cortex 9:765-775.

Meyer G, Perez-Garcia CG, Abraham H, Caput D (2002) Expression of p73 and Reelin in the developing human cortex. J Neurosci 22:4973-4986.

Meyer G, Soria JM, Martinez-Galan JR, Martin-Clemente B, Fairen A (1998) Different origins and developmental histories of transient neurons in the marginal zone of the fetal and neonatal rat cortex. J Comp Neurol 397:493-518.

Meyerson M, Enders GH, Wu CL, Su LK, Gorka C, Nelson C, Harlow E, Tsai LH (1992) A family of human cdc2-related protein kinases. EMBO J 11:2909-2917.

Meyerson M, Faha B, Su LK, Harlow E, Tsai LH (1991) The cyclin-dependent kinase family. Cold Spring Harb Symp Quant Biol 56:177-186.

Mienville JM (1999) Cajal-Retzius cell physiology: just in time to bridge the 20th century. Cereb Cortex 9:776-782.

Miller MW (1985) Cogeneration of retrogradely labeled corticocortical projection and GABA-immunoreactive local circuit neurons in cerebral cortex. Brain Res 355:187-192.

Miller MW, Nowakowski RS (1988) Use of bromodeoxyuridine-immunohistochemistry to examine the proliferation, migration and time of origin of cells in the central nervous system. Brain Res 457:44-52.

Mione MC, Cavanagh JF, Harris B, Parnavelas JG (1997) Cell fate specification and symmetrical/asymmetrical divisions in the developing cerebral cortex. J Neurosci 17:2018-2029.

Mitrofanis J, Guillery RW (1993) New views of the thalamic reticular nucleus in the adult and the developing brain. Trends Neurosci 16:240-245.

Miyajima M, Nornes HO, Neuman T (1995) Cyclin E is expressed in neurons and forms complexes with cdk5. Neuroreport 6:1130-1132.

Miyashita-Lin EM, Hevner R, Wassarman KM, Martinez S, Rubenstein JL (1999) Early neocortical regionalization in the absence of thalamic innervation. Science 285:906-909.

Miyata T, Kawaguchi A, Okano H, Ogawa M (2001) Asymmetric inheritance of radial glial fibers by cortical neurons. Neuron 31:727-741.

Molnar Z, Adams R, Blakemore C (1998a) Mechanisms underlying the early establishment of thalamocortical connections in the rat. J Neurosci 18:5723-5745.

Molnar Z, Adams R, Goffinet AM, Blakemore C (1998b) The role of the first postmitotic cortical cells in the development of thalamocortical innervation in the reeler mouse. J Neurosci 18:5746-5765.

Molnar Z, Blakemore C (1995) How do thalamic axons find their way to the cortex? Trends Neurosci 18:389-397.

Moorthamer M, Chaudhuri B (1999) Identification of ribosomal protein L34 as a novel Cdk5 inhibitor. Biochem Biophys Res Commun 255:631-638.

Moorthamer M, Zumstein-Mecker S, Chaudhuri B (1999) DNA binding protein dbpA binds Cdk5 and inhibits its activity. FEBS Lett 446:343-350.

Moreno S, Nurse P (1990) Substrates for p34cdc2: in vivo veritas? Cell 61:549-551.

Morest DK (1970) A study of neurogenesis in the forebrain of opossum pouch young. Z Anat Entwicklungsgesch 130:265-305.

Muzio L, Mallamaci A (2003) Emx1, emx2 and pax6 in specification, regionalization and arealization of the cerebral cortex. Cereb Cortex 13:641-647.

Nadarajah B, Alifragis P, Wong RO, Parnavelas JG (2002) Ventricle-directed migration in the developing cerebral cortex. Nat Neurosci 5:218-224.

Nadarajah B, Alifragis P, Wong RO, Parnavelas JG (2003a) Neuronal migration in the developing cerebral cortex: observations based on real-time imaging. Cereb Cortex 13:607-611.

Nadarajah B, Brunstrom JE, Grutzendler J, Wong RO, Pearlman AL (2001) Two modes of radial migration in early development of the cerebral cortex. Nat Neurosci 4:143-150.

Nadarajah B, Liapi A, Parnavelas J (2003b) The role of SDF-1 in the developing cerebral cortex. pp 780.7.

Nadarajah B, Parnavelas JG (2002) Modes of neuronal migration in the developing cerebral cortex. Nat Rev Neurosci 3:423-432.

Nagano T, Yoneda T, Hatanaka Y, Kubota C, Murakami F, Sato M (2002) Filamin A-interacting protein (FILIP) regulates cortical cell migration out of the ventricular zone. Nat Cell Biol 4:495-501.

Nakagawa Y, Johnson JE, O'Leary DD (1999) Graded and areal expression patterns of regulatory genes and cadherins in embryonic neocortex independent of thalamocortical input. J Neurosci 19:10877-10885.

Nery S, Fishell G, Corbin JG (2002) The caudal ganglionic eminence is a source of distinct cortical and subcortical cell populations. Nat Neurosci 5:1279-1287.

Nguyen MD, Lariviere RC, Julien JP (2001) Deregulation of Cdk5 in a mouse model of ALS: toxicity alleviated by perikaryal neurofilament inclusions. Neuron 30:135-147.

Niethammer M, Smith DS, Ayala R, Peng J, Ko J, Lee MS, Morabito M, Tsai LH (2000) NUDEL is a novel Cdk5 substrate that associates with LIS1 and cytoplasmic dynein. Neuron 28:697-711.

Nikolic M, Chou MM, Lu W, Mayer BJ, Tsai LH (1998) The p35/Cdk5 kinase is a neuron-specific Rac effector that inhibits Pak1 activity. Nature 395:194-198.

Nikolic M, Dudek H, Kwon YT, Ramos YF, Tsai LH (1996) The cdk5/p35 kinase is essential for neurite outgrowth during neuronal differentiation. Genes Dev 10:816-825.

Noctor SC, Flint AC, Weissman TA, Dammerman RS, Kriegstein AR (2001) Neurons derived from radial glial cells establish radial units in neocortex. Nature 409:714-720.

Noctor SC, Flint AC, Weissman TA, Wong WS, Clinton BK, Kriegstein AR (2002) Dividing precursor cells of the embryonic cortical ventricular zone have morphological and molecular characteristics of radial glia. J Neurosci 22:3161-3173.

Noctor SC, Martinez-Cerdeno V, Ivic L, Kriegstein AR (2004) Cortical neurons arise in symmetric and asymmetric division zones and migrate through specific phases. Nat Neurosci 7:136-144.

O'Leary DD (1989) Do cortical areas emerge from a protocortex? Trends Neurosci 12:400-406.

O'Leary DD, Nakagawa Y (2002) Patterning centers, regulatory genes and extrinsic mechanisms controlling arealization of the neocortex. Curr Opin Neurobiol 12:14-25.

O'Rourke NA, Dailey ME, Smith SJ, McConnell SK (1992) Diverse migratory pathways in the developing cerebral cortex. Science 258:299-302.

Ogawa M, Miyata T, Nakajima K, Yagyu K, Seike M, Ikenaka K, Yamamoto H, Mikoshiba K (1995) The reeler gene-associated antigen on Cajal-Retzius neurons is a crucial molecule for laminar organization of cortical neurons. Neuron 14:899-912.

Ohshima T, Gilmore EC, Longenecker G, Jacobowitz DM, Brady RO, Herrup K, Kulkarni AB (1999) Migration defects of cdk5(-/-) neurons in the developing cerebellum is cell autonomous. J Neurosci 19:6017-6026.

Ohshima T, Nagle JW, Pant HC, Joshi JB, Kozak CA, Brady RO, Kulkarni AB (1995) Molecular cloning and chromosomal mapping of the mouse cyclin-dependent kinase 5 gene. Genomics 28:585-588.

Ohshima T, Ogawa M, Veeranna, Hirasawa M, Longenecker G, Ishiguro K, Pant HC, Brady RO, Kulkarni AB, Mikoshiba K (2001) Synergistic contributions of cyclin-dependant kinase 5/p35 and Reelin/Dab1 to the positioning of cortical neurons in the developing mouse brain. Proc Natl Acad Sci U S A 98:2764-2769.

Ohshima T, Ogura H, Tomizawa K, Hayashi K, Suzuki H, Saito T, Kamei H, Nishi A, Bibb JA, Hisanaga SI, Matsui H, Mikoshiba K (2005) Impairment of hippocampal long-term depression and defective spatial learning and memory in p35 mice. J Neurochem.

Ohshima T, Ward JM, Huh CG, Longenecker G, Veeranna, Pant HC, Brady RO, Martin LJ, Kulkarni AB (1996) Targeted disruption of the cyclin-dependent kinase 5 gene results in abnormal corticogenesis, neuronal pathology and perinatal death. Proc Natl Acad Sci U S A 93:11173-11178.

Olayioye MA, Neve RM, Lane HA, Hynes NE (2000) The ErbB signaling network: receptor heterodimerization in development and cancer. EMBO J 19:3159-3167.

Paglini G, Pigino G, Kunda P, Morfini G, Maccioni R, Quiroga S, Ferreira A, Caceres A (1998) Evidence for the participation of the neuron-specific CDK5 activator P35 during laminin-enhanced axonal growth. J Neurosci 18:9858-9869.

Parnavelas JG (2000) The origin and migration of cortical neurones: new vistas. Trends Neurosci 23:126-131.

Parnavelas JG, Dinopoulos A, Davies SW (1989) The central visual pathways. In: Handbook of Chemical Neuroanatomy: Integrated systems of the CNS, Part II (Bjorklund A, Hokfelt T, Swanson LW, eds), pp 1-164. Elsevier Science Publishers B.V. (Biomedical Division).

Patrick GN, Zhou P, Kwon YT, Howley PM, Tsai LH (1998) p35, the neuronal-specific activator of cyclin-dependent kinase 5 (Cdk5) is degraded by the ubiquitin-proteasome pathway. J Biol Chem 273:24057-24064.

Patrick GN, Zukerberg L, Nikolic M, de la MS, Dikkes P, Tsai LH (1999) Conversion of p35 to p25 deregulates Cdk5 activity and promotes neurodegeneration. Nature 402:615-622.

Patten BA, Peyrin JM, Weinmaster G, Corfas G (2003) Sequential signaling through Notch1 and erbB receptors mediates radial glia differentiation. J Neurosci 23:6132-6140.

Patzke H, Maddineni U, Ayala R, Morabito M, Volker J, Dikkes P, Ahlijanian MK, Tsai LH (2003) Partial rescue of the p35-/- brain phenotype by low expression of a neuronal-specific enolase p25 transgene. J Neurosci 23:2769-2778.

Patzke H, Tsai LH (2002) Calpain-mediated cleavage of the cyclin-dependent kinase-5 activator p39 to p29. J Biol Chem 277:8054-8060.

Paudel HK, Lew J, Ali Z, Wang JH (1993) Brain proline-directed protein kinase phosphorylates tau on sites that are abnormally phosphorylated in tau associated with Alzheimer's paired helical filaments. J Biol Chem 268:23512-23518.

Paxinos G, Watson C (1982) The Rat Brain in Stereotaxic Coordinates. New York: Academic Press.

Pearlman AL, Sheppard AM (1996) Extracellular matrix in early cortical development. Prog Brain Res 108:117-134.

Peduzzi JD (1988) Genesis of GABA-immunoreactive neurons in the ferret visual cortex. J Neurosci 8:920-931.

Peles E, Bacus SS, Koski RA, Lu HS, Wen D, Ogden SG, Levy RB, Yarden Y (1992) Isolation of the neu/HER-2 stimulatory ligand: a 44 kd glycoprotein that induces differentiation of mammary tumor cells. Cell 69:205-216.

Peterson BS (1995) Neuroimaging in child and adolescent neuropsychiatric disorders. J Am Acad Child Adolesc Psychiatry 34:1560-1576.

Philpott A, Porro EB, Kirschner MW, Tsai LH (1997) The role of cyclin-dependent kinase 5 and a novel regulatory subunit in regulating muscle differentiation and patterning. Genes Dev 11:1409-1421.

Pigino G, Paglini G, Ulloa L, Avila J, Caceres A (1997) Analysis of the expression, distribution and function of cyclin dependent kinase 5 (cdk5) in developing cerebellar macroneurons. J Cell Sci 110 (Pt 2):257-270.

Pleasure SJ, Anderson S, Hevner R, Bagri A, Marin O, Lowenstein DH, Rubenstein JL (2000) Cell migration from the ganglionic eminences is required for the development of hippocampal GABAergic interneurons. Neuron 28:727-740.

Plowman GD, Culouscou JM, Whitney GS, Green JM, Carlton GW, Foy L, Neubauer MG, Shoyab M (1993) Ligand-specific activation of HER4/p180erbB4, a fourth member of the epidermal growth factor receptor family. Proc Natl Acad Sci U S A 90:1746-1750.

Polleux F, Dehay C, Kennedy H (1998a) Neurogenesis and commitment of corticospinal neurons in reeler. J Neurosci 18:9910-9923.

Polleux F, Giger RJ, Ginty DD, Kolodkin AL, Ghosh A (1998b) Patterning of cortical efferent projections by semaphorin-neuropilin interactions. Science 282:1904-1906.

Polleux F, Morrow T, Ghosh A (2000) Semaphorin 3A is a chemoattractant for cortical apical dendrites. Nature 404:567-573.

Polleux F, Whitford KL, Dijkhuizen PA, Vitalis T, Ghosh A (2002) Control of cortical interneuron migration by neurotrophins and PI3-kinase signaling. Development 129:3147-3160.

Poon RY, Lew J, Hunter T (1997) Identification of functional domains in the neuronal Cdk5 activator protein. J Biol Chem 272:5703-5708.

Powell EM, Mars WM, Levitt P (2001) Hepatocyte growth factor/scatter factor is a motogen for interneurons migrating from the ventral to dorsal telencephalon. Neuron 30:79-89.

Pozas E, Ibanez CF (2005) GDNF and GFRalpha1 Promote Differentiation and Tangential Migration of Cortical GABAergic Neurons. Neuron 45:701-713.

Price DJ, Aslam S, Tasker L, Gillies K (1997) Fates of the earliest generated cells in the developing murine neocortex. J Comp Neurol 377:414-422.

Price DJ, Willshaw DJ (2000) Mechanisms of Cortical development. Oxford University Press.

Puelles L, Rubenstein JL (1993) Expression patterns of homeobox and other putative regulatory genes in the embryonic mouse forebrain suggest a neuromeric organization. Trends Neurosci 16:472-479.

Qi Z, Huang QQ, Lee KY, Lew J, Wang JH (1995) Reconstitution of neuronal Cdc2-like kinase from bacteria-expressed Cdk5 and an active fragment of the brain-specific activator. Kinase activation in the absence of Cdk5 phosphorylation. J Biol Chem 270:10847-10854.

Radovick S, Wray S, Lee E, Nicols DK, Nakayama Y, Weintraub BD, Westphal H, Cutler GB, Jr., Wondisford FE (1991) Migratory arrest of gonadotropin-releasing hormone neurons in transgenic mice. Proc Natl Acad Sci U S A 88:3402-3406.

Ragsdale CW, Grove EA (2001) Patterning the mammalian cerebral cortex. Curr Opin Neurobiol 11:50-58.

Rakic P (1974) Neurons in rhesus monkey visual cortex: systematic relation between time of origin and eventual disposition. Science 183:425-427.

Rakic P (1971) Guidance of neurons migrating to the fetal monkey neocortex. Brain Res 33:471-476.

Rakic P (1972) Mode of cell migration to the superficial layers of fetal monkey neocortex. J Comp Neurol 145:61-83.

Rakic P (1978) Neuronal migration and contact guidance in the primate telencephalon. Postgrad Med J 54 Suppl 1:25-40.

Rakic P (1988) Specification of cerebral cortical areas. Science 241:170-176.

Rakic S, Zecevic N (2003) Emerging complexity of layer I in human cerebral cortex. Cereb Cortex 13:1072-1083.

Ramon y Cajal S (1891) Sur la structure de l'ecorce cerebrale de quelques mammiferes. La Cellule 7:176.

Ramon y Cajal S (1911) Histologie du Systeme Nerveux de l'Homme et des Vertebres. Paris: Maloine.

Raper JA (2000) Semaphorins and their receptors in vertebrates and invertebrates. Curr Opin Neurobiol 10:88-94.

Rashid T, Banerjee M, Nikolic M (2001) Phosphorylation of Pak1 by the p35/Cdk5 kinase affects neuronal morphology. J Biol Chem 276:49043-49052.

Reiner O, Albrecht U, Gordon M, Chianese KA, Wong C, Gal-Gerber O, Sapir T, Siracusa LD, Buchberg AM, Caskey CT, . (1995) Lissencephaly gene (LIS1) expression in the CNS suggests a role in neuronal migration. J Neurosci 15:3730-3738.

Retzius G (1893) Die Cajal'schen Zellen der Grosshirnrinde beim Menschen und bei Saugetieren. Biologische Untersuchungen, Neue Folge 5:8.

Rickmann M, Chronwall BM, Wolff JR (1977) On the development of non-pyramidal neurons and axons outside the cortical plate: the early marginal zone as a pallial anlage. Anat Embryol (Berl) 151:285-307.

Rickmann M, Wolff JR (1981) Differentiation of 'preplate' neurons in the pallium of the rat. Bibl Anat142-146.

Rieff HI, Raetzman LT, Sapp DW, Yeh HH, Siegel RE, Corfas G (1999) Neuregulin induces GABA(A) receptor subunit expression and neurite outgrowth in cerebellar granule cells. J Neurosci 19:10757-10766.

Riese DJ, Stern DF (1998) Specificity within the EGF family/ErbB receptor family signaling network. Bioessays 20:41-48.

Rio C, Rieff HI, Qi P, Khurana TS, Corfas G (1997) Neuregulin and erbB receptors play a critical role in neuronal migration. Neuron 19:39-50.

Rodgers EE, Theibert AB (2002) Functions of PI 3-kinase in development of the nervous system. Int J Dev Neurosci 20:187-197.

Rougon G, Hobert O (2003) New insights into the diversity and function of neuronal immunoglobulin superfamily molecules. Annu Rev Neurosci 26:207-238.

Rubenstein JL, Anderson S, Shi L, Miyashita-Lin E, Bulfone A, Hevner R (1999) Genetic control of cortical regionalization and connectivity. Cereb Cortex 9:524-532.

Rubenstein JL, Beachy PA (1998) Patterning of the embryonic forebrain. Curr Opin Neurobiol 8:18-26.

Saito T, Ishiguro K, Onuki R, Nagai Y, Kishimoto T, Hisanaga S (1998) Okadaic acid-stimulated degradation of p35, an activator of CDK5, by proteasome in cultured neurons. Biochem Biophys Res Commun 252:775-778.

Saito T, Onuki R, Fujita Y, Kusakawa G, Ishiguro K, Bibb JA, Kishimoto T, Hisanaga S (2003) Developmental regulation of the proteolysis of the p35 cyclin-dependent kinase 5 activator by phosphorylation. J Neurosci 23:1189-1197.

Sambrook J, Russel D (2001) Molecular cloning: A Laboratory manual. New York: Cold Spring Harbour Laboratory Press.

Sanada K, Gupta A, Tsai LH (2004) Disabled-1-regulated adhesion of migrating neurons to radial glial fiber contributes to neuronal positioning during early corticogenesis. Neuron 42:197-211.

Sarker KP, Lee KY (2004) L6 myoblast differentiation is modulated by Cdk5 via the PI3K-AKT-p70S6K signaling pathway. Oncogene 23:6064-6070.

Sasaki S, Shionoya A, Ishida M, Gambello MJ, Yingling J, Wynshaw-Boris A, Hirotsune S (2000) A LIS1/NUDEL/cytoplasmic dynein heavy chain complex in the developing and adult nervous system. Neuron 28:681-696.

Sasaki Y, Cheng C, Uchida Y, Nakajima O, Ohshima T, Yagi T, Taniguchi M, Nakayama T, Kishida R, Kudo Y, Ohno S, Nakamura F, Goshima Y (2002) Fyn and Cdk5 mediate semaphorin-3A signaling, which is involved in regulation of dendrite orientation in cerebral cortex. Neuron 35:907-920.

Sausville EA (2002) Complexities in the development of cyclin-dependent kinase inhibitor drugs. Trends Mol Med 8:S32-S37.

Schmahl W, Knoedlseder M, Favor J, Davidson D (1993) Defects of neuronal migration and the pathogenesis of cortical malformations are associated with Small eye (Sey) in the mouse, a point mutation at the Pax-6-locus. Acta Neuropathol (Berl) 86:126-135.

Schmechel DE, Rakic P (1979) A Golgi study of radial glial cells in developing monkey telencephalon: morphogenesis and transformation into astrocytes. Anat Embryol (Berl) 156:115-152.

Schmid RS, Anton ES (2003) Role of integrins in the development of the cerebral cortex. Cereb Cortex 13:219-224.

Schmid RS, Jo R, Shelton S, Kreidberg JA, Anton ES (2005) Reelin, Integrin and Dab1 Interactions during Embryonic Cerebral Cortical Development. Cereb Cortex.

Schmid RS, McGrath B, Berechid BE, Boyles B, Marchionni M, Sestan N, Anton ES (2003) Neuregulin 1-erbB2 signaling is required for the establishment of radial glia and their transformation into astrocytes in cerebral cortex. Proc Natl Acad Sci U S A 100:4251-4256.

Seibt J, Schuurmans C, Gradwhol G, Dehay C, Vanderhaeghen P, Guillemot F, Polleux F (2003) Neurogenin2 specifies the connectivity of thalamic neurons by controlling axon responsiveness to intermediate target cues. Neuron 39:439-452.

Senzaki K, Ogawa M, Yagi T (1999) Proteins of the CNR family are multiple receptors for Reelin. Cell 99:635-647.

Sharma P, Veeranna, Sharma M, Amin ND, Sihag RK, Grant P, Ahn N, Kulkarni AB, Pant HC (2002) Phosphorylation of MEK1 by cdk5/p35 down-regulates the mitogen-activated protein kinase pathway. J Biol Chem 277:528-534.

Sheldon M, Rice DS, D'Arcangelo G, Yoneshima H, Nakajima K, Mikoshiba K, Howell BW, Cooper JA, Goldowitz D, Curran T (1997) Scrambler and yotari disrupt the disabled gene and produce a reeler-like phenotype in mice. Nature 389:730-733.

Sheppard AM, Pearlman AL (1997) Abnormal reorganization of preplate neurons and their associated extracellular matrix: an early manifestation of altered neocortical development in the reeler mutant mouse. J Comp Neurol 378:173-179.

Shinozaki K, Miyagi T, Yoshida M, Miyata T, Ogawa M, Aizawa S, Suda Y (2002) Absence of Cajal-Retzius cells and subplate neurons associated with defects of tangential cell migration from ganglionic eminence in Emx1/2 double mutant cerebral cortex. Development 129:3479-3492.

Shu T, Ayala R, Nguyen MD, Xie Z, Gleeson JG, Tsai LH (2004) Ndel1 operates in a common pathway with LIS1 and cytoplasmic dynein to regulate cortical neuronal positioning. Neuron 44:263-277.

Smith PD, Crocker SJ, Jackson-Lewis V, Jordan-Sciutto KL, Hayley S, Mount MP, O'Hare MJ, Callaghan S, Slack RS, Przedborski S, Anisman H, Park DS (2003) Cyclin-dependent kinase 5 is a mediator of dopaminergic neuron loss in a mouse model of Parkinson's disease. Proc Natl Acad Sci U S A 100:13650-13655.

Sobue K, garwal-Mawal A, Li W, Sun W, Miura Y, Paudel HK (2000) Interaction of neuronal Cdc2-like protein kinase with microtubule-associated protein tau. J Biol Chem 275:16673-16680.

Solecki DJ, Model L, Gaetz J, Kapoor TM, Hatten ME (2004) Par6alpha signaling controls glial-guided neuronal migration. Nat Neurosci 7:1195-1203.

Soriano E, del Rio JA (2005) The cells of cajal-retzius: still a mystery one century after. Neuron 46:389-394.

Srinivasan R, Poulsom R, Hurst HC, Gullick WJ (1998) Expression of the c-erbB-4/HER4 protein and mRNA in normal human fetal and adult tissues and in a survey of nine solid tumour types. J Pathol 185:236-245.

Stefansson H, et al. (2002) Neuregulin 1 and susceptibility to schizophrenia. Am J Hum Genet 71:877-892.

Stewart GR, Pearlman AL (1987) Fibronectin-like immunoreactivity in the developing cerebral cortex. J Neurosci 7:3325-3333.

Stoykova A, Fritsch R, Walther C, Gruss P (1996) Forebrain patterning defects in Small eye mutant mice. Development 122:3453-3465.

Stoykova A, Hatano O, Gruss P, Gotz M (2003) Increase in reelin-positive cells in the marginal zone of Pax6 mutant mouse cortex. Cereb Cortex 13:560-571.

Stumm RK, Zhou C, Ara T, Lazarini F, Dubois-Dalcq M, Nagasawa T, Hollt V, Schulz S (2003) CXCR4 regulates interneuron migration in the developing neocortex. J Neurosci 23:5123-5130.

Sugitani Y, Nakai S, Minowa O, Nishi M, Jishage K, Kawano H, Mori K, Ogawa M, Noda T (2002) Brn-1 and Brn-2 share crucial roles in the production and positioning of mouse neocortical neurons. Genes Dev 16:1760-1765.

Super H, del Rio JA, Martinez A, Perez-Sust P, Soriano E (2000) Disruption of neuronal migration and radial glia in the developing cerebral cortex following ablation of Cajal-Retzius cells. Cereb Cortex 10:602-613.

Sussel L, Marin O, Kimura S, Rubenstein JL (1999) Loss of Nkx2.1 homeobox gene function results in a ventral to dorsal molecular respecification within the basal telencephalon: evidence for a transformation of the pallidum into the striatum. Development 126:3359-3370.

Tabata H, Nakajima K (2003) Multipolar migration: the third mode of radial neuronal migration in the developing cerebral cortex. J Neurosci 23:9996-10001.

Taglialatela P, Soria JM, Caironi V, Moiana A, Bertuzzi S (2004) Compromised generation of GABAergic interneurons in the brains of Vax1-/- mice. Development 131:4239-4249.

Tamamaki N, Fujimori K, Nojyo Y, Kaneko T, Takauji R (2003) Evidence that Sema3A and Sema3F regulate the migration of GABAergic neurons in the developing neocortex. J Comp Neurol 455:238-248.

Tamamaki N, Fujimori KE, Takauji R (1997) Origin and route of tangentially migrating neurons in the developing neocortical intermediate zone. J Neurosci 17:8313-8323.

Tamamaki N, Nakamura K, Okamoto K, Kaneko T (2001) Radial glia is a progenitor of neocortical neurons in the developing cerebral cortex. Neurosci Res 41:51-60.

Tan SS, Breen S (1993) Radial mosaicism and tangential cell dispersion both contribute to mouse neocortical development. Nature 362:638-640.

Tan SS, Faulkner-Jones B, Breen SJ, Walsh M, Bertram JF, Reese BE (1995) Cell dispersion patterns in different cortical regions studied with an X-inactivated transgenic marker. Development 121:1029-1039.

Tan SS, Kalloniatis M, Sturm K, Tam PP, Reese BE, Faulkner-Jones B (1998) Separate progenitors for radial and tangential cell dispersion during development of the cerebral neocortex. Neuron 21:295-304.

Tan TC, Valova VA, Malladi CS, Graham ME, Berven LA, Jupp OJ, Hansra G, McClure SJ, Sarcevic B, Boadle RA, Larsen MR, Cousin MA, Robinson PJ (2003) Cdk5 is essential for synaptic vesicle endocytosis. Nat Cell Biol 5:701-710.

Tanaka D, Nakaya Y, Yanagawa Y, Obata K, Murakami F (2003) Multimodal tangential migration of neocortical GABAergic neurons independent of GPI-anchored proteins. Development 130:5803-5813.

Tanaka T, Serneo FF, Higgins C, Gambello MJ, Wynshaw-Boris A, Gleeson JG (2004a) Lis1 and doublecortin function with dynein to mediate coupling of the nucleus to the centrosome in neuronal migration. J Cell Biol 165:709-721.

Tanaka T, Serneo FF, Tseng HC, Kulkarni AB, Tsai LH, Gleeson JG (2004b) Cdk5 phosphorylation of doublecortin ser297 regulates its effect on neuronal migration. Neuron 41:215-227.

Tanaka T, Veeranna, Ohshima T, Rajan P, Amin ND, Cho A, Sreenath T, Pant HC, Brady RO, Kulkarni AB (2001) Neuronal cyclin-dependent kinase 5 activity is critical for survival. J Neurosci 21:550-558.

Tang D, Chun AC, Zhang M, Wang JH (1997) Cyclin-dependent kinase 5 (Cdk5) activation domain of neuronal Cdk5 activator. Evidence of the existence of cyclin fold in neuronal Cdk5a activator. J Biol Chem 272:12318-12327.

Tang D, Yeung J, Lee KY, Matsushita M, Matsui H, Tomizawa K, Hatase O, Wang JH (1995) An isoform of the neuronal cyclin-dependent kinase 5 (Cdk5) activator. J Biol Chem 270:26897-26903.

Tarabykin V, Stoykova A, Usman N, Gruss P (2001) Cortical upper layer neurons derive from the subventricular zone as indicated by Svet1 gene expression. Development 128:1983-1993.

Tarricone C, Dhavan R, Peng J, Areces LB, Tsai LH, Musacchio A (2001) Structure and regulation of the CDK5-p25(nck5a) complex. Mol Cell 8:657-669.

Threadgill DW, Dlugosz AA, Hansen LA, Tennenbaum T, Lichti U, Yee D, LaMantia C, Mourton T, Herrup K, Harris RC, . (1995) Targeted disruption of mouse EGF receptor: effect of genetic background on mutant phenotype. Science 269:230-234.

Tidcombe H, Jackson-Fisher A, Mathers K, Stern DF, Gassmann M, Golding JP (2003) Neural and mammary gland defects in ErbB4 knockout mice genetically rescued from embryonic lethality. Proc Natl Acad Sci U S A 100:8281-8286.

Tissir F, Goffinet AM (2003) Reelin and brain development. Nat Rev Neurosci 4:496-505.

Tomizawa K, Matsui H, Matsushita M, Lew J, Tokuda M, Itano T, Konishi R, Wang JH, Hatase O (1996) Localization and developmental changes in the neuron-specific cyclin-dependent kinase 5 activator (p35nck5a) in the rat brain. Neuroscience 74:519-529.

Tomizawa K, Sunada S, Lu YF, Oda Y, Kinuta M, Ohshima T, Saito T, Wei FY, Matsushita M, Li ST, Tsutsui K, Hisanaga S, Mikoshiba K, Takei K, Matsui H (2003) Cophosphorylation of amphiphysin I and dynamin I by Cdk5 regulates clathrin-mediated endocytosis of synaptic vesicles. J Cell Biol 163:813-824.

Tosic M, Rakic S, Matthieu JM, Zecevic N (2002) Identification of Golli and myelin basic proteins in human brain during early development. Glia 37:219-228.

Towbin H, Staehelin T, Gordon J (1992) Electrophoretic transfer of proteins from polyacrylamide gels to nitrocellulose sheets: procedure and some applications. 1979. Biotechnology 24:145-149.

Tozaki H, Kawasaki T, Takagi Y, Hirata T (2002) Expression of Nogo protein by growing axons in the developing nervous system. Brain Res Mol Brain Res 104:111-119.

Tripodi M, Filosa A, Armentano M, Studer M (2004) The COUP-TF nuclear receptors regulate cell migration in the mammalian basal forebrain. Development 131:6119-6129.

Trommsdorff M, Gotthardt M, Hiesberger T, Shelton J, Stockinger W, Nimpf J, Hammer RE, Richardson JA, Herz J (1999) Reeler/Disabled-like disruption of neuronal migration in knockout mice lacking the VLDL receptor and ApoE receptor 2. Cell 97:689-701.

Tsai LH, Delalle I, Caviness VS, Jr., Chae T, Harlow E (1994) p35 is a neural-specific regulatory subunit of cyclin-dependent kinase 5. Nature 371:419-423.

Tsai LH, Gleeson JG (2005) Nucleokinesis in neuronal migration. Neuron 46:383-388.

Tsai LH, Takahashi T, Caviness VS, Jr., Harlow E (1993) Activity and expression pattern of cyclin-dependent kinase 5 in the embryonic mouse nervous system. Development 119:1029-1040.

Tuttle R, Nakagawa Y, Johnson JE, O'Leary DD (1999) Defects in thalamocortical axon pathfinding correlate with altered cell domains in Mash-1-deficient mice. Development 126:1903-1916.

Tuttle R, Schlaggar BL, Braisted JE, O'Leary DD (1995) Maturation-dependent upregulation of growth-promoting molecules in developing cortical plate controls thalamic and cortical neurite growth. J Neurosci 15:3039-3052.

Valcanis H, Tan SS (2003) Layer specification of transplanted interneurons in developing mouse neocortex. J Neurosci 23:5113-5122.

Valverde F, Facal-Valverde MV, Santacana M, Heredia M (1989) Development and differentiation of early generated cells of sublayer VIb in the somatosensory cortex of the rat: a correlated Golgi and autoradiographic study. J Comp Neurol 290:118-140.

Van Eden CG, Mrzljak L, Voorn P, Uylings HB (1989) Prenatal development of GABA-ergic neurons in the neocortex of the rat. J Comp Neurol 289:213-227.

Vecchi M, Baulida J, Carpenter G (1996) Selective cleavage of the heregulin receptor ErbB-4 by protein kinase C activation. J Biol Chem 271:18989-18995.

Wang J, Liu S, Fu Y, Wang JH, Lu Y (2003) Cdk5 activation induces hippocampal CA1 cell death by directly phosphorylating NMDA receptors. Nat Neurosci 6:1039-1047.

Ware ML, Fox JW, Gonzalez JL, Davis NM, Lambert de RC, Russo CJ, Chua SC, Jr., Goffinet AM, Walsh CA (1997) Aberrant splicing of a mouse disabled homolog, mdab1, in the scrambler mouse. Neuron 19:239-249.

Wassarman KM, Lewandoski M, Campbell K, Joyner AL, Rubenstein JL, Martinez S, Martin GR (1997) Specification of the anterior hindbrain and establishment of a normal mid/hindbrain organizer is dependent on Gbx2 gene function. Development 124:2923-2934.

Weishaupt JH, Kussmaul L, Grotsch P, Heckel A, Rohde G, Romig H, Bahr M, Gillardon F (2003) Inhibition of CDK5 is protective in necrotic and apoptotic paradigms of neuronal cell death and prevents mitochondrial dysfunction. Mol Cell Neurosci 24:489-502.

Wenzel HJ, Robbins CA, Tsai LH, Schwartzkroin PA (2001) Abnormal morphological and functional organization of the hippocampus in a p35 mutant model of cortical dysplasia associated with spontaneous seizures. J Neurosci 21:983-998.

Wichterle H, Garcia-Verdugo JM, Herrera DG, Alvarez-Buylla A (1999) Young neurons from medial ganglionic eminence disperse in adult and embryonic brain. Nat Neurosci 2:461-466.

Wichterle H, Turnbull DH, Nery S, Fishell G, Alvarez-Buylla A (2001) In utero fate mapping reveals distinct migratory pathways and fates of neurons born in the mammalian basal forebrain. Development 128:3759-3771.

Wichterle H, varez-Dolado M, Erskine L, Alvarez-Buylla A (2003) Permissive corridor and diffusible gradients direct medial ganglionic eminence cell migration to the neocortex. Proc Natl Acad Sci U S A 100:727-732.

Wilson SW, Rubenstein JL (2000) Induction and dorsoventral patterning of the telencephalon. Neuron 28:641-651.

Wong K, Park HT, Wu JY, Rao Y (2002) Slit proteins: molecular guidance cues for cells ranging from neurons to leukocytes. Curr Opin Genet Dev 12:583-591.

Woolsey TA, Van der LH (1970) The structural organization of layer IV in the somatosensory region (SI) of mouse cerebral cortex. The description of a cortical field composed of discrete cytoarchitectonic units. Brain Res 17:205-242.

Xie Y, Skinner E, Landry C, Handley V, Schonmann V, Jacobs E, Fisher R, Campagnoni A (2002) Influence of the embryonic preplate on the organization of the cerebral cortex: a targeted ablation model. J Neurosci 22:8981-8991.

Xie Z, Sanada K, Samuels BA, Shih H, Tsai LH (2003) Serine 732 phosphorylation of FAK by Cdk5 is important for microtubule organization, nuclear movement, and neuronal migration. Cell 114:469-482.

Xie Z, Tsai LH (2004) Cdk5 phosphorylation of FAK regulates centrosome-associated miocrotubules and neuronal migration. Cell Cycle 3:108-110.

Xiong Y, Zhang H, Beach D (1992) D type cyclins associate with multiple protein kinases and the DNA replication and repair factor PCNA. Cell 71:505-514.

Xu Q, Cobos I, De La CE, Rubenstein JL, Anderson SA (2004) Origins of cortical interneuron subtypes. J Neurosci 24:2612-2622.

Yau HJ, Wang HF, Lai C, Liu FC (2003) Neural development of the neuregulin receptor ErbB4 in the cerebral cortex and the hippocampus: preferential expression by interneurons tangentially migrating from the ganglionic eminences. Cereb Cortex 13:252-264.

Yozu M, Tabata H, Nakajima K (2004) Birth-date dependent alignment of GABAergic neurons occurs in a different pattern from that of non-GABAergic neurons in the developing mouse visual cortex. Neurosci Res 49:395-403.

Zhang Q, Ahuja HS, Zakeri ZF, Wolgemuth DJ (1997) Cyclin-dependent kinase 5 is associated with apoptotic cell death during development and tissue remodeling. Dev Biol 183:222-233.

Zheng M, Leung CL, Liem RK (1998) Region-specific expression of cyclin-dependent kinase 5 (cdk5) and its activators, p35 and p39, in the developing and adult rat central nervous system. J Neurobiol 35:141-159.

Zhou C, Qiu Y, Pereira FA, Crair MC, Tsai SY, Tsai MJ (1999) The nuclear orphan receptor COUP-TFI is required for differentiation of subplate neurons and guidance of thalamocortical axons. Neuron 24:847-859.

Zhu Y, Li H, Zhou L, Wu JY, Rao Y (1999) Cellular and molecular guidance of GABAergic neuronal migration from an extracortical origin to the neocortex. Neuron 23:473-485.

Zukerberg LR, Patrick GN, Nikolic M, Humbert S, Wu CL, Lanier LM, Gertler FB, Vidal M, Van Etten RA, Tsai LH (2000) Cables links Cdk5 and c-Abl and facilitates Cdk5 tyrosine phosphorylation, kinase upregulation, and neurite outgrowth. Neuron 26:633-646.